

Examining the Gas-Phase Fragmentation of Select Metal β -diketonate Complexes Using
Computational Methods

by

Kyle G. Kemats

Submitted in Partial Fulfillment of the Requirements

for the Degree of

Master of Science

in the

Chemistry

Program

YOUNGSTOWN STATE UNIVERSITY

August, 2014

Examining the Gas-Phase Fragmentation of Select Metal β -diketonate Complexes Using
Computational Methods

Kyle G. Kemats

I hereby release this thesis to the public. I understand that this thesis will be made available from the OhioLINK ETD Center and the Maag Library Circulation Desk for public access. I also authorize the University or other individuals to make copies of this thesis as needed for scholarly research.

Signature:

Kyle G. Kemats, Student

Date

Approvals:

Dr. Brian D. Leskiw, Thesis Advisor

Date

Dr. Howard D. Mettee, Committee Member

Date

Dr. Ganesaratnam K. Balendiran, Committee Member

Date

Dr. Salvatore A. Sanders, Associate Dean of Graduate Studies

Date

Abstract

The fragmentation and stability of various copper, nickel, and zinc β -diketonate compounds were observed using mass spectrometry and were modeled using Spartan '04. Rate constants of dissociation of terminal groups and ligands, as well as transition state energies were calculated in an effort to explain the patterns of fragmentation and stability that were experimentally observed.

Acknowledgements

First and foremost, I would like to thank my family for their love and support throughout my academic pursuits. I would especially like to thank my mother, who has always been more than helpful along the way.

Next, I would like to thank Dr. Brian Leskiw for taking me on as a graduate student and providing guidance throughout this project. Dr. Leskiw was able to assist me with any issues I encountered in my research and also in my work as a teaching assistant. I thank Dr. Leskiw for providing me with these opportunities to succeed.

Special thanks go out to the YSU Chemistry Department, Graduate School of Studies, and the Leslie H. Cochran University Scholars program for all of the financial support, both a graduate and undergraduate student. The education I have received at YSU has been priceless. I would specifically like to thank Dr. Howard D. Mettee and Dr. Ganesaratnam K. Balendiran for serving on my thesis committee. A special thanks goes out to Dr. Mettee for helping me learn how to use Spartan '04 and for his assistance in furthering my understanding of physical and computational chemistry.

Finally, special thanks go out to all of my colleagues in the YSU Chemistry Department. Jennifer Pekar and Dominic Silvistri were my group-mates throughout this time in graduate school and they have been good people to talk to about both chemistry and non-chemistry topics. Caleb Tatebe has been a friend and colleague throughout both my undergraduate and graduate career at YSU and deserves special thanks for his help and support.

Table of Contents

Abstract.....	iii
Acknowledgements.....	iv
List of Tables	vi
List of Equations.....	viii
List of Figures	x
Chapter One: Introduction	1
1.1 Metal β -diketonates.....	1
1.2 Applications of Metal β -diketonate Complexes.....	4
1.3 Computational Chemistry and Parameterized Model 3	6
1.4 Transition State Theory and RRKM Theory.....	8
Chapter 2: Computational Methods and Calculations.....	12
2.1 Molecular Modeling.....	12
2.2 Determination of Transition State	13
2.3 Calculation of Rate Constant	13
Chapter 3: Results and Discussion	18
3.1 Single Ligand β -diketonates	18
3.1.1 Loss of Terminal Group From <i>bis</i> Complex	21
3.1.2 Loss of Ligand	23
3.1.3 Loss of terminal group from mono ligand complexes.....	27
3.2 Fluorine Migration	29
3.2.1 Fluorine Migration in <i>hfac</i> Complexes.....	29
3.2.2 Fluorine Migration in <i>tftm</i> Complexes	34
3.3 Mixed Ligand β -diketonates	38
3.4 Future Work.....	42
References	43
Appendix A: Example Rate Constant Calculation.....	45
Appendix B: Bond Length vs. Heat of Formation Data	57
Appendix C: Vibrational Frequency Tables	78
Appendix D: RRKM Calculated Data.....	117
Appendix E: NMR Data.....	159

List of Tables

	Page	
Table 3.1	Relative positive ion intensities (% abundance) of metal species to their respective base peaks for the loss of a terminal group from a <i>bis</i> complex.	21
Table 3.2	Calculated rate constants for loss of a terminal group.	22
Table 3.3	Relative positive ion intensities (% abundance) of metal species to their respective base peak for loss of a ligand from a <i>bis</i> complex.	24
Table 3.4	Calculated rate constants for the loss of an intact ligand.	24
Table 3.5	Calculated rate constants for the loss of <i>hfac</i> from $[M(\text{hfac})(\text{hfac-CF}_3)]^+$.	25
Table 3.6	Calculated rate constants for loss of ligand after loss of terminal group.	27
Table 3.7	Relative positive ion intensities (% abundance) for loss of terminal group from single ligand metal species to their respective base peaks.	28
Table 3.8	Calculated rate constants for the loss of a terminal group for <i>mono</i> ligand species.	28
Table 3.9	Relative positive ion intensities (% abundance) for the loss of CF_2 in <i>hfac</i> species to their respective base peaks.	30
Table 3.10	Heats of formations of <i>hfac</i> complexes after fluorine migration.	33
Table 3.11	Relative positive ion intensities (% abundance) for the loss of CF_2 in <i>tftm</i> species to their respective base peaks.	34
Table 3.12	Heats of formation of <i>tftm</i> complexes after the loss of CF_2 .	38

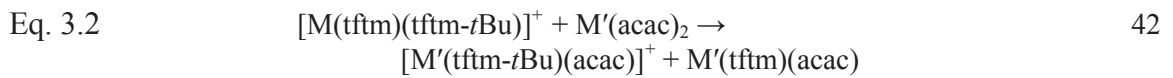
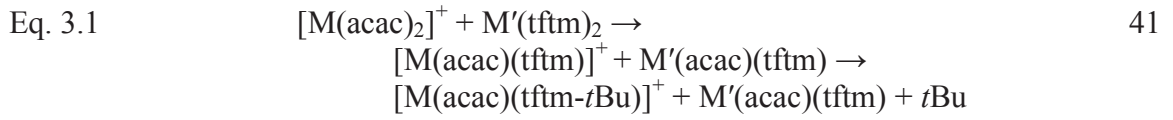
Table 3.13	Relative Positive ion intensities (% abundance) for formation of M(acac)(tftm- <i>t</i> Bu) from homo and hetero-metal species to their respective base peaks.	41
Table 3.14	Calculated rate constants for the loss of <i>t</i> Bu from mixed ligand M(acac)(tftm) species.	41

List of Equations

		Page
Eq. 1.1	$A \rightleftharpoons A^\ddagger \rightleftharpoons \text{Products}$	8
Eq. 1.2	$A \rightleftharpoons A^* \rightleftharpoons A^\ddagger \rightleftharpoons \text{Products}$	9
Eq. 1.3	$k(E^*) = \frac{1}{h} \frac{P(E^\ddagger)}{N(E^*)}$	10
Eq. 2.1	$k(E)_{WR} = \frac{1}{s \cdot h} \cdot \frac{\sum_{i=1}^s v_i}{\sum_{i=1}^s v_i^\ddagger} \cdot \frac{(E^\ddagger + a^\ddagger E_Z^\ddagger)^s}{(E + aE_Z)^{s-1}} \cdot \frac{1}{[1 - \beta \frac{dw}{dE'}]}$	14
Eq. 2.2	$E = (H_f^\ddagger - \Delta H^\ddagger) - (H_f - \Delta H)$	14
Eq. 2.3	$E' = \frac{E}{E_Z}$	14
Eq. 2.4	$E'^\ddagger = \frac{E}{E_Z^\ddagger}$	14
Eq. 2.5	$w(E') = [5.00E' + 2.73(E')^{0.5} + 3.51]^{-1}$	15
Eq. 2.6	$\frac{dw(E')}{dE'} = - \frac{5.00 + \frac{1.3650}{(E')^{0.50}}}{[5.00E' + 2.73(E')^{0.5} + 3.51]^2}$	15
Eq. 2.7	$w(E') = e^{-2.4191(E')^{0.25}}$	15
Eq. 2.8	$\frac{dw(E')}{dE'} = - \frac{0.604775e^{-24191(E')^{0.25}}}{(E')^{0.75}}$	15
Eq. 2.9	$\beta = \frac{s-1}{s} \cdot \frac{v^2}{v^2}$	16

$$\text{Eq. 2.10} \quad a = 1 - \beta w E' \quad 16$$

$$\text{Eq. 2.11} \quad k_{uni} = \frac{i k_i e^{-E_i / RT}}{i e^{-E_i / RT}} \quad 16$$



List of Figures

	Page
Fig. 1.1	1
Fig. 1.2	2
Fig. 1.3	2
Fig. 1.4	3
Fig. 1.5	9
Fig. 1.6	11
Fig. 3.1	18
Fig. 3.2	18
Fig. 3.3	19
Fig. 3.4	19
Fig. 3.5	19
Fig. 3.6	20
Fig. 3.7	20
Fig. 3.8	20
Fig. 3.9	21
Fig. 3.10	26
Fig. 3.11	26
Fig. 3.12	30
Fig. 3.13	31

Fig. 3.14	Model of $[\text{Ni}(\text{hfac})_2]^+$ with a C-CF ₃ bond stretched to 5.0 Å.	31
Fig. 3.15	Model of $[\text{Zn}(\text{hfac})_2]^+$ with a C-CF ₃ bond stretched to 5.0 Å.	32
Fig. 3.16	Scheme of fluorine realigning along bond axis.	32
Fig. 3.17	General <i>hfac</i> β-diketonate complex after loss of CF ₂ .	34
Fig. 3.18	Model of $[\text{Ni}(\text{tfm})]^+$ with the C-CF ₃ bond stretched to 4.0 Å.	36
Fig. 3.19	Model of $[\text{Zn}(\text{tfm})]^+$ with the C-CF ₃ bond stretched to 4.0 Å.	36
Fig. 3.20	Model of $[\text{Ni}(\text{tfm})]^+$ with the C-CF ₃ bond stretched to 5.0 Å.	37
Fig. 3.21	Model of $[\text{Zn}(\text{tfm})]^+$ with the C-CF ₃ bond stretched to 5.0 Å.	37
Fig. 3.22	Proposed structure of $[\text{M}(\text{tfm}-\text{CF}_2)]^+$.	38
Fig. 3.23	Mass Spectra of gas-phase reaction of Cu(acac) ₂ and Cu(tfm) ₂ .	39
Fig. 3.24	Mass Spectra of the gas-phase reaction of Ni(acac) ₂ and Ni(tfm) ₂ .	39
Fig. 3.25	Mass Spectra of the gas-phase reaction of Cu(acac) ₂ and Ni(tfm) ₂ .	40
Fig. 3.26	Mass Spectra of the gas-phase reaction of Zn(acac) ₂ and Zn(tfm) ₂ .	40
Fig. 3.27	Mass Spectra of the gas-phase reaction of Co(acac) ₂ and Zn(tfm) ₂ .	40

Chapter One: Introduction

1.1 Metal β -diketonates

Metal β -diketonates are classified as coordination compounds and contain metal ions that are bound to ligands, which can be other molecules or ions. The ligands act as Lewis bases, or electron donors, while the metal centers act as Lewis acids, or electron acceptors¹.

As illustrated in Figure 1.1, the beta-diketone ligands coordinated to the metal exist as keto-enol tautomers before they are ionized. In the keto form of the molecule, both oxygens are double bonded to carbon. However, in the enol form, a double bond exists between the α and β carbon, with the oxygen bound to the β carbon existing as an alcohol².

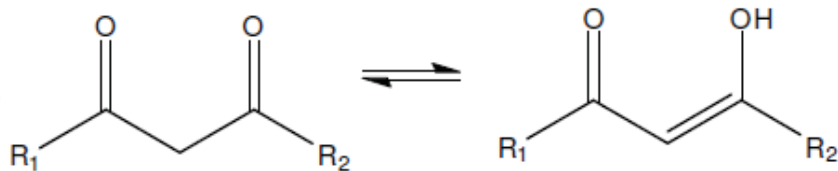


Figure 1.1: The keto-enol tautomerism of a β -diketone.

When the ligands are subjected to a basic media, the acidic alpha proton of the molecule is removed. The resulting negatively charged ion is stabilized by resonance. Delocalization of the negative charge, described in Figure 1.2, allows for bidentate coordination to the metal center even though the charge of the anion is -1 (Figure 1.2).

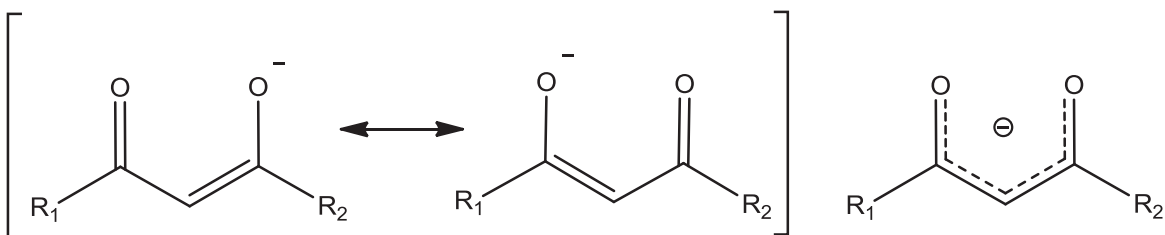


Figure 1.2: Charge delocalization of β -diketone anion.

In this study, the gas-phase dissociation of bis β -diketonates containing metal centers of nickel, copper, and zinc will be examined using computational methods. The ligands coordinated to these metal centers, which are presented in Figure 1.3, include acetylacetonate (acac), hexafluoroacetylacetonate (hfac), and trifluorotrimethylacetylacetonate (tfm).

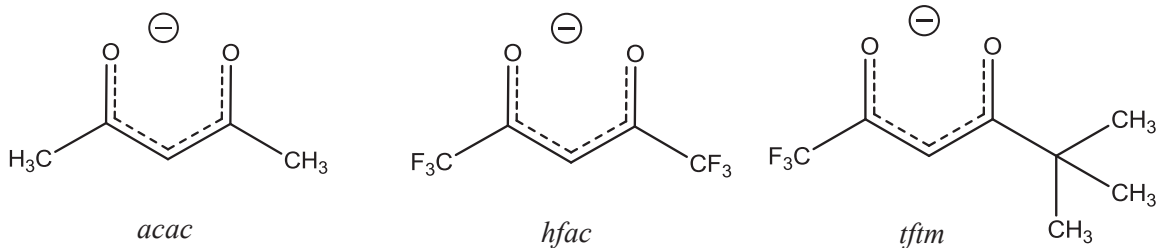


Figure 1.3: The β -diketonate ligands investigated herein.

The volatility of these compounds plays a key role in the study of them as many acetylacetonate complexes readily sublime in moderate temperatures and low pressures, making them ideal for study via mass spectrometry^{1,3}. When metal β -diketonates, are introduced to the conditions of the mass spectrometer, they are ionized and are either detected as is intact, or undergo a series of dissociation events where the stability and fragmentation pathways depend on the metal center and the ligand attached. For example, a metal β -diketonate with two ligands may lose one of its ligands entirely or the

complex could also lose the terminal group of the ligand, such as a CH₃, CF₃, or *t*-butyl group as illustrated in Figure 1.4.

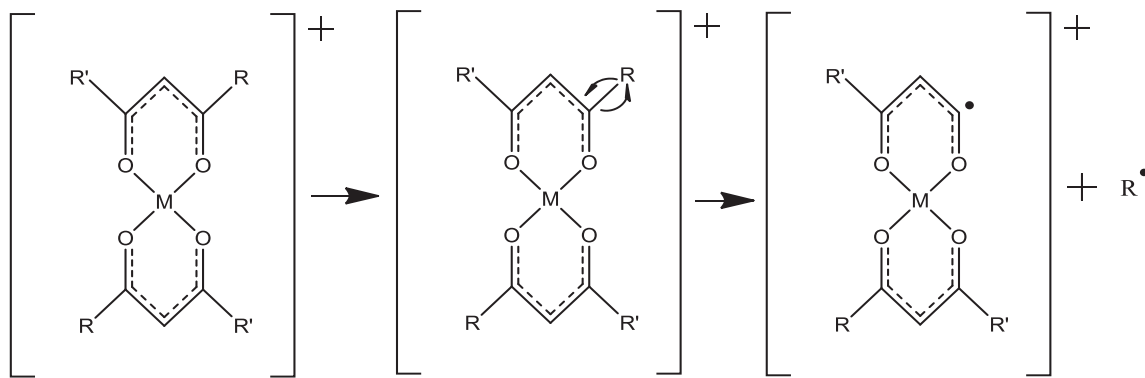


Figure 1.4: Proposed gas-phase β -diketonate dissociation for the loss of terminal group.

The gas phase dissociation of several complexes has been previously observed, as well as ligand exchange reactions between different species^{4,5}. Hunter and Leskiw reported gas phase ligand exchange between cobalt and zinc *acac*, *hfac*, and *tftm* species, and Hunter, Lerach, Lockso and Leskiw reported ligand exchange between copper and nickel *acac*, *hfac*, and *tftm* species^{6,7}.

While ligand exchange reactions involving different species has been an area of great interest, the explanation of how and why certain species undergo particular fragmentation pathways has not been explored yet. For example, in the mass spectrum of Cu(acac)₂, the loss of what amounts to two CH₃ groups is observed, while only the loss of a single CH₃ group is observed in the mass spectra Ni(acac)₂ and Zn(acac)₂^{6,7}. A thorough investigation is needed to shed light on these processes.

A common observation in reactions involving fluorinated β -diketonates is the loss of CF₂, which is also known as fluorine migration or fluorine rearrangement. Morris and

Koob, attempted to apply hard/soft acid/base theory to explain why this occurs⁸. Hard acids and bases are compact species, with electrons being held tightly to the nucleus. A hard acid is generally a metal ion with a high charge density, meaning it has a high ionic charge and a small ionic radius. If metal ions carry the same charge, they become softer acids as the atomic radius increases. The β -diketone ions of interest are considered soft bases because they are large polarizable ions. According to hard/soft acid/base theory, hard acids are likely to bind to hard bases, while soft acids tend to bind to soft bases^{9,10}.

Morris and Koob proposed that one fluorine atom of a CF_3 migrates to the metal center while CF_2 is lost. Furthermore they suggested that fluorine rearrangement depends on the acidity of the metal center, with migration being more likely when the metal is a harder acid. According to hard/soft acid/base theory, because F^- is considered a hard base due to its small ionic radius, it is likely to bind to a metal that is a hard acid. However, Morris and Koob do note that hard/soft acid/base theory may not be sufficient to fully explain this rearrangement and further investigation is necessary⁸.

1.2 Applications of Metal β -diketonate Complexes

One of the many applications of metal β -diketonate complexes is their use in catalysis. Ford and Mcclain developed a process in which metal β -diketonate complexes are used as catalysts in lactone polymerization reactions. In this process, the catalysts have the formula of MZ_3 , where M is scandium, yttrium, bismuth, or a lanthanide series rare earth metal, and the ligands, Z, are beta-diketones, beta-ketoesters, and malonate anions. The results of the study showed that catalysis was especially preferred when beta-diketone ligands were used¹¹. Lanthanum beta-diketonate complexes have also been

used as catalysts in trans-esterification processes¹². Nickel, iron, and cobalt *acac* complexes have been shown to have uses as catalysts in the synthesis of carbon nanotubes¹³. Finally, Cu(acac)₂ has been demonstrated to serve as a useful catalyst in organic synthesis, catalyzing reactions such as the benzylation of alcohols, reduction of aromatic nitro compounds, and cyclopropanation¹⁴.

Another application of metal β -diketonate complexes is their role in the vapor deposition of thin films¹. This application of metal β -diketonates dates as far back as 1975. Dismukes, Kane, and Albis invented a device and method which uses metal β -diketonates as precursors for thin films. In this method, vanadium containing metal β -diketonates are vaporized and moved by a non-reactive carrier gas such as nitrogen, krypton, neon, or argon. At the deposition site, the temperature is increased to 500 °C, which causes the β -diketonate complexes to decompose and deposit the desired luminescent oxides¹⁵. Lanthanum and palladium β -diketonate complexes have also been shown to be precursors for thin films using this method of vaporization and decomposition^{16, 17}.

Metal β -diketonate complexes have also been demonstrated to serve as optically active thin films, not just as precursors. Metal β -diketonate complexes consisting of Tb³⁺ and Al³⁺ metal centers have been shown to exhibit the optical properties that would make them useful in organic light emitting devices (OLEDs). OLEDs, which can be made from a variety of organic materials including metal complexes, have been explored as possible options for use in flat panel displays and backlighting systems¹⁸. Luminescent properties have also been observed in Eu³⁺ β -diketonate complexes in which a polymer chain has been synthesized on one of the ligands¹⁹.

1.3 Computational Chemistry and Parameterized Model 3

In the field of theoretical chemistry, computational methods are commonly used to create models and predict the behavior of species in real chemical systems. Computational chemistry has been used to estimate pKa values, electrostatic potentials, and reactivity indexes²⁰⁻²². Programs such as Spartan '04 are used in computational chemistry to carry out these simulations. The molecules are first created atom by atom with positions being determined by both program and the modeler. The calculation method, overall charge, and desired properties to be computed are selected, and the calculation is started. Once the energy minimization and convergence is complete, the software is able to calculate other properties of interest. The results are given in an output page and can be further analyzed.

The computer software is able to calculate information such as heats of formation, equilibrium and transition state geometries, as well as vibrational frequencies for the system in question. The calculations are based on either ab initio or semiempirical methods. Ab initio methods are based solely on using quantum mechanics to solve the Schrödinger equation for the chemical system. Semiempirical methods on the other hand, use information obtained through empirical parameterization as well as quantum mechanics. Two of the most common semiempirical methods are Austin Model 1 (AM1) and Parameterized Model 3 (PM3).

Semiempirical methods have been used to predict and model a variety of chemical systems. For example, AM1 and PM3 methods have been used to predict intermolecular interactions in biomolecules²³. Semiempirical methods have also been used to study hydrogen bonding in both inorganic molecules such as ammonia and water as well as

organic biomolecules such as DNA bases and amino acids²⁴. In addition to the modeling and study of the intermolecular behavior of molecules, semiempirical methods have also been used to study electrostatic potentials and partial charges in quantum mechanical systems²⁵.

Semiempirical calculations only take into account the valence electrons of a molecule. The molecule's inner shell electrons are considered part of a fixed core, and are thus ignored in calculations, which is one of the major approximations of the semiempirical approach. The other major approximation for semiempirical calculation is the neglect of diatomic differential overlap (NDDO) approximation. With the NDDO approximation, atomic orbitals associated with specific atoms do not overlap. This approximation reduces the number of electron-electron interactions and does not consider atomic basis functions on adjacent atoms and dramatically reduces the overall computation times. Calculations using semiempirical methods take only minutes on basic computers while other methods may require hours and even supercomputer use.

The AM1 and PM3 methods are based on the Modified Neglect of Diatomic Overlap (MNDO) method. In the MNDO method, diatomic overlap takes place at only adjacent atomic centers. The diatomic overlap is accounted for using basis sets that are parameterized using empirical data. The AM1 method is only parameterized for hydrogen, carbon, nitrogen, and oxygen, making it useful for only organic molecules. The PM3 method has been parameterized for row 3, 4, 5, and 6 elements, including the transition metals. Both AM1 and PM3 methods are parameterized to calculate the standard enthalpy of formation for the given molecule at 298 K and 1 bar^{26,27}.

1.4 Transition State Theory and RRKM Theory

Transition state theory, was developed by Henry Eyring in 1935 in an attempt to explain the kinetics of reacting molecules. According to transition state theory, the transition state complex is defined as a saddle point of a potential energy surface. The theory assumes an equilibrium between reactants and transition state as presented in Equation 1.1.



Because the transition state is converted to products, statistical mechanics can be used to calculate the transition state concentration based on the concentration of reactants, and from this, chemical kinetics can be used to calculate the rate of this conversion²⁸.

Though transition state theory serves as a basis for modern theory, it does have some drawbacks and limitations. For example, transition state theory assumes that atomic nuclei behave according to classical mechanics while it is now known that atomic nuclei follow quantum mechanics²⁹. Also, transition state theory suggests that the energy of the reactant is the only variable responsible for the formation of the transition state. Even though energy does play a role in the formation of the transition state from the reactants, other factors such as the geometrical orientation of the reacting molecule are now believed to play a role in transition state formation³⁰.

Rice-Ramsperger-Kassel-Marcus (RRKM) theory is an extension of transition state theory. Similar to transition state theory, RRKM theory attempts to explain the kinetics of reacting molecules. However, RRKM theory takes into account the way molecular vibrations, molecular rotations, and zero-point energies contribute to the reaction rate. Also according to this theory, an energized molecule is described as being

either active or inactive, with only active molecules having the ability to be converted to products as described in Equation 1.2.



The excited molecule A^* , has the total energy required to be converted to products, but it lacks the proper orientation. The activated molecule, A^\ddagger , has both the energy and orientation to be converted to products, and is considered to be the transition state. The activated complex can either be considered “rigid” or “loose.” Rigid activated complexes do not have internal rotations that are not present in the reactant, while loose activated complexes have a degree of free internal rotation which was not initially present in the reactant molecule. The difference between rigid and loose activated complexes can be seen in their respective potential energy profiles. For rigid activated complexes, the potential energy reaches a maximum value and then decreases as the activated complex is converted to products. For loose activated products, the potential energy reaches a maximum and then levels off as it is converted to products as shown in Figure 1.5¹¹.

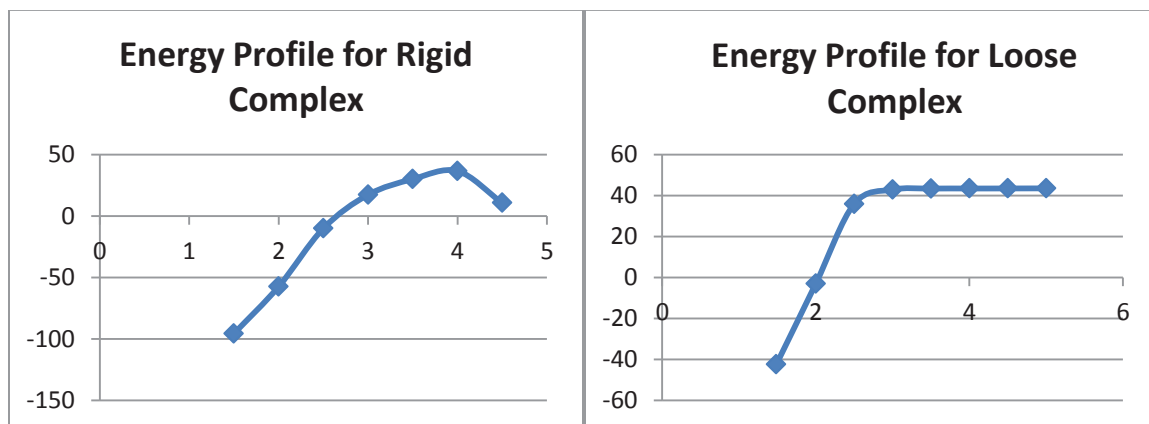


Figure 1.5: Potential Energy curves for rigid and loose activated complexes.

According to RRKM theory, the rate of the reaction is dependent on the ratio of the sum of active quantum states of the activated complex, $P(E^+)$, to the density of states, $N(E^*)$. The sum of states is the number of vibrational states between zero and the total energy, E^* . The density of states is the number of vibrational states in an energy interval that varies from E^* to $E+dE^*$. An energy dependent rate constant can then be calculated using Equation 1.3^{30,31}.

$$k(E^*) = \frac{1}{h} \frac{P(E^\ddagger)}{N(E^*)} \quad [1.3]$$

As represented in Figure 1.6, the potential energy of complex A increases as the number of energetic states becomes more dense. As more energy is added, complex A eventually has enough energy to be converted to products and is described as A^* . Finally, when A^* is oriented so that its potential energy is maximized, it becomes the activated complex A^\ddagger , which is the transition state. Using the density of energetic states for the energized complex and the sum of energetic starts for the activated complex, a rate constant can be calculated for the conversion of the original molecule to products.

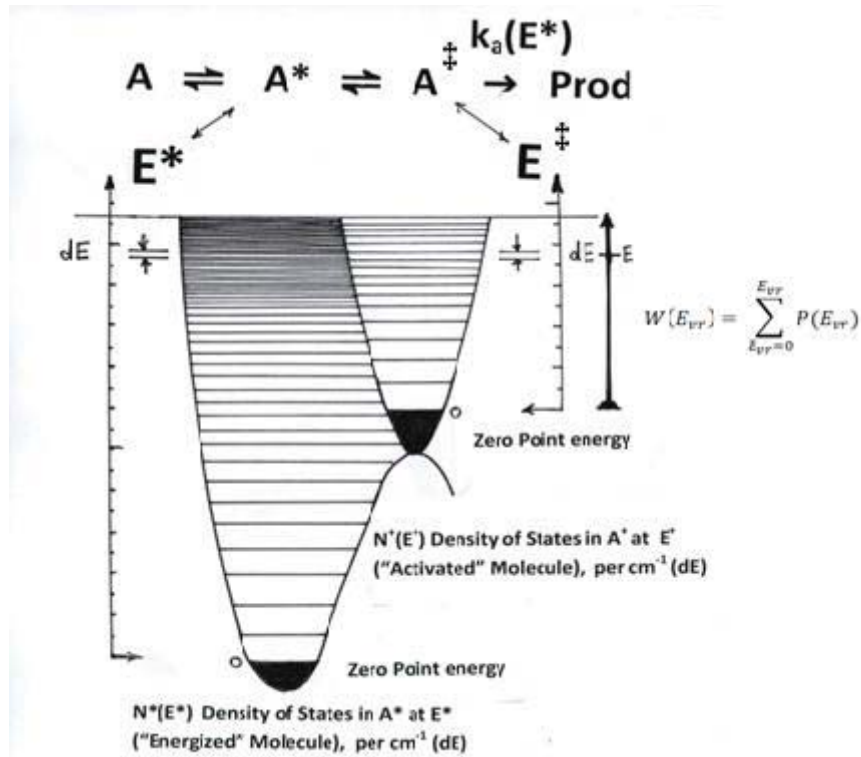


Figure 1.6: Summary of RRKM theory as interpreted from reference 30 by Dr. Howard Mettee.

Chapter 2: Computational Methods and Calculations

2.1 Molecular Modeling

In Spartan '04, each molecule to be analyzed is first built atom by atom using the tools of the software. Once the molecule is completely built, the program's energy minimization button is pressed to clean up the structure and better prepare the molecule for calculations. A molecular mechanics calculation is then run to ensure that the modeled molecule has the correct geometry that will be used in subsequent calculations. The molecular mechanics calculation does not provide information about the complex in the form of data, but its use makes the PM3 equilibrium geometry calculation more reliable.

In the setup box for the calculations, there are several parameters that can be adjusted. The first step determines what type of calculation will be run. In the case of the molecules in this study, all calculations were done for the equilibrium geometry in the ground state of the molecule. The level of theory at which the calculation is run can be changed as well, but again, for this study, all calculations were run at the PM3 level of theory due to the speed of the calculation and the strength of the computer on which the calculation is run.

Once all of the parameters are set, the calculation can commence. The time that the program takes to complete the calculation varies based on the size of the molecule, but in general, PM3 calculations do not take longer than 10 to 15 minutes. Once the calculation is complete, results can be viewed on the output page in Spartan '04. The output page gives the calculated heat of formation, list of vibrational frequencies, and

thermodynamic data such as zero point energy, enthalpy, and entropy for the complex. This data is useful for calculating rate constants of dissociation.

2.2 Determination of Transition State

Once the reacting molecule is modeled, the next step in calculating a rate constant, based on RRKM theory, is to determine a reasonable transition state. This can be done by using the computer software to stretch and constrain the bond of the fragment that is dissociating from the original molecule. At each stretch length, an equilibrium geometry calculation is performed in order to determine the heat of formation of the species. As the bond is stretched, the heat of formation increases until a maximum value is reached. The heats of formation vs. bond length can be plotted to give an energy profile for the reacting molecule. This energy profile can be used to determine a transition state whether the complex is loose or rigid. At the bond length associated with the maximum heat of formation, an imaginary frequency is calculated and presented in the list of vibrational frequencies provided by the program. This imaginary frequency is a characteristic of a modeled transition state complex.

2.3 Calculation of Rate Constant

Once a transition state is determined, a dissociation rate constant can be calculated using data from both the reacting molecule and its transition state. Equation 2.1 represents Whitten-Rabinovitch approximation of the RRKM calculation of unimolecular rate constants.

$$k(E)_{WR} = \frac{1}{s \cdot h} \cdot \frac{\sum_{i=1}^s v_i}{\sum_{i=1}^s v_i^\ddagger} \cdot \frac{(E^\ddagger + \alpha^\ddagger E_z^\ddagger)^s}{(E + \alpha E_z)^{s-1}} \cdot \frac{1}{[1 - \beta \frac{dw(E')}{dE'}]} \quad [2.1]$$

In Equation 2.1, s is the number of vibrational modes, h is Planck's constant, and v_i corresponds to the vibrational frequency of starting material. The vibrational frequency of transition state is designated by v_i^\ddagger , E' refers to the energy of reactant, and E^\ddagger is energy of transition state. The zero point energy of the reactant is E_z in the above equation, while α is the molecule dependent function of internal energy for reactant, α^\ddagger is the molecule dependent function of internal energy for transition state, $w(E')$ is the sum of states, and finally, β is the modified frequency dispersion parameter.³⁰

Vibrational modes are obtained from the equilibrium geometry calculations in Spartan '04. The software also calculates heat of formation values, enthalpy values, and zero point energy values for each molecule. The heat of formation (ΔH_f) and enthalpy values (ΔH) for both the reactant and the transition state can be used to calculate the energy for the reaction according to Equation 2.2.

$$E = (\Delta H_f^\ddagger - \Delta H^\ddagger) - (\Delta H_f - \Delta H) \quad [2.2]$$

The calculation of the rate constant is based on the fractions of the approximate zero point energies of the reactant and transition state and are presented in Equation 2.3 and Equation 2.4

$$E' = \frac{E}{E_z} \quad [2.3]$$

$$E'^\ddagger = \frac{E}{E_z^\ddagger} \quad [2.4]$$

The value of E' can be used to calculate the sum of states, $w(E)$, and the derivative of the sum of states with respect to E' using Equations 2.5-2.8. The equation for $w(E')$, formulated by Whitten and Rabinovitch to approximate the sum of states for the molecule of interest is a stepwise function, with an equation for E' values going from 0.1 to 1.0 and another equation for E' values from 1.0 to 8.0³⁰.

For ($0.1 < E' < 1.0$):

$$w(E') = [5.00E' + 2.73(E')^{0.5} + 3.51]^{-1} \quad [2.5]$$

$$\frac{dw(E')}{dE'} = -\frac{5.00 + \frac{1.3650}{(E')^{0.50}}}{[5.00E' + 2.73(E')^{0.5} + 3.51]^2} \quad [2.6]$$

For ($1.0 < E' < 8.0$):

$$w(E') = e^{-2.4191(E')^{0.25}} \quad [2.7]$$

$$\frac{dw(E')}{dE'} = -\frac{0.604775e^{-2.4191(E')^{0.25}}}{(E')^{0.75}} \quad [2.8]$$

The value of β for each molecule represents the dispersion in vibrational frequencies, and is measured by their standard deviation. This value is calculated using Equation 2.9 and is based on both the vibrational frequencies and the number of vibrational frequencies.

$$\beta = \frac{s-1}{s} \cdot \frac{\nu^2}{\nu^2} \quad [2.9]$$

Using the calculated values of β and $\frac{dw(E')}{dE'}$, the value of α can be determined using Equation 2.10.

$$a = 1 - \beta w E' \quad [2.10]$$

Once all of these variables are determined, the rate constant, k , can be calculated using the Whitten-Rabinovitch method³⁰. As the value for the total energy increases, subsequent k values can be calculated using the same method. Using a Boltzmann distribution, an average rate constant for the reaction can be determined using Equation 2.11.

$$k_{uni} = \frac{\sum_i k_i e^{-E_i / RT}}{\sum_i e^{-E_i / RT}} \quad [2.11]$$

The calculated rate constants are expressed in the units of s^{-1} . By taking the reciprocal of these values, approximate times for dissociation can be easily calculated based on the rate constants. By comparing calculated values to previously reported experimental data, some inferences can be drawn regarding the mechanism and reaction pathways for these dissociating β -diketonate complexes.

A step-by-step example of transition state determination and rate constant calculation can be found in Appendix A.

Chapter 3: Results and Discussion

3.1 Single Ligand β -diketonates

Several rate constants of dissociation for β -diketonate complexes containing Cu, Ni, and Zn were calculated in an attempt to explain their gas phase fragmentation patterns. The calculated rate constants will serve as a guide to help qualitatively determine how these complexes dissociate when subjected to the energy and conditions of the mass spectrometer. The experimental mass spectra for the β -diketonate complexes of formula ML_2 , where M = Cu, Ni, or Zn, and L= *acac*, *hfac*, or *tftm* are presented in Figures 3.1-3.9 and are reproduced from references 6 and 7.

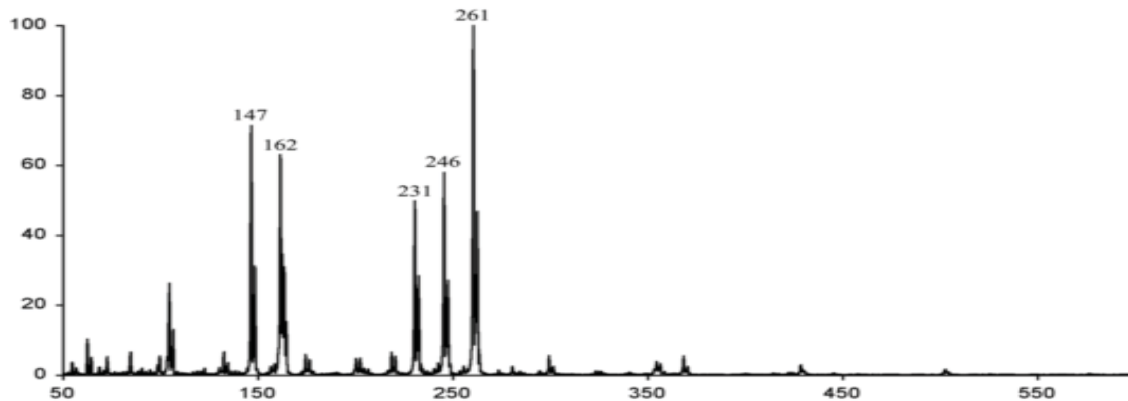


Figure 3.1: Mass Spectrum of $Cu(acac)_2$.

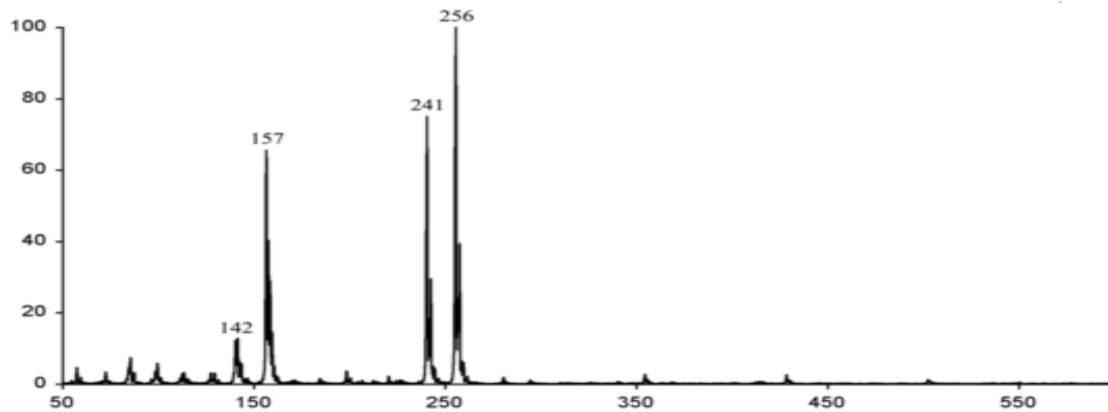


Figure 3.2: Mass Spectrum of $Ni(acac)_2$.

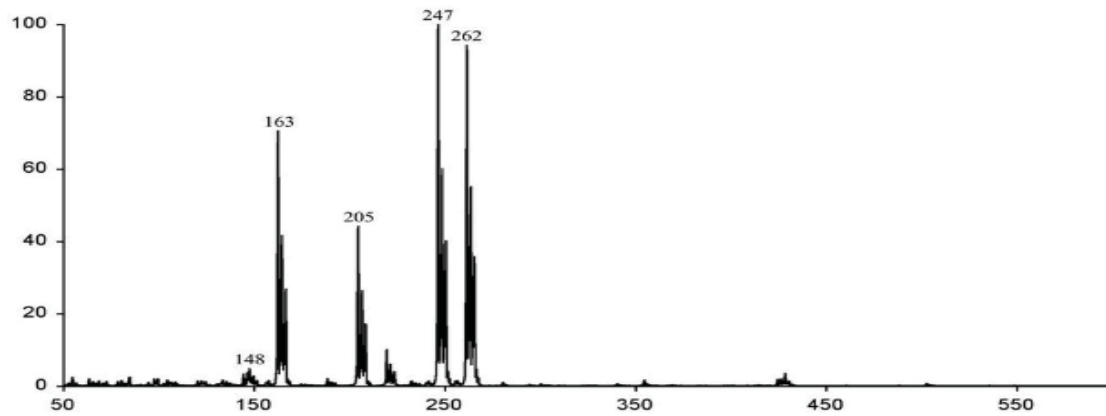


Figure 3.3: Mass Spectrum of $\text{Zn}(\text{acac})_2$.

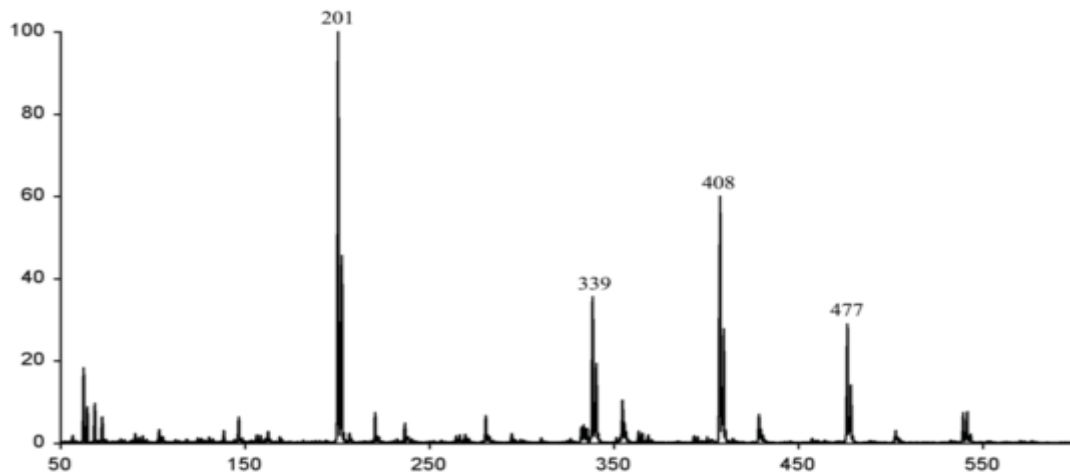


Figure 3.4: Mass Spectrum of $\text{Cu}(\text{hfac})_2$.

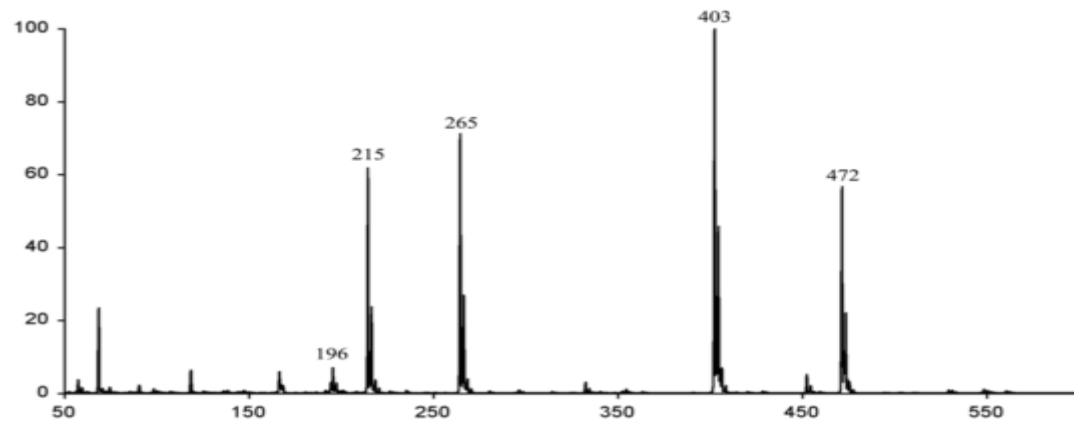


Figure 3.5: Mass Spectrum of $\text{Ni}(\text{hfac})_2$.

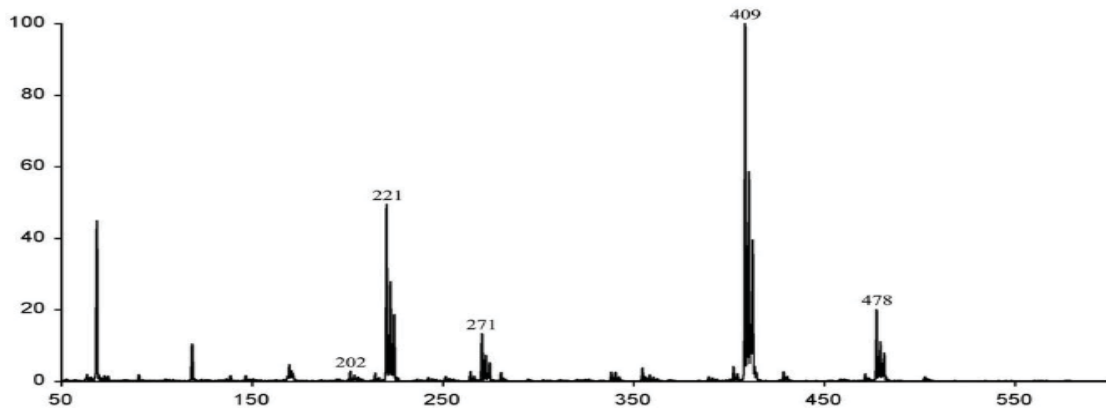


Figure 3.6: Mass Spectrum of $\text{Zn}(\text{hfac})_2$.

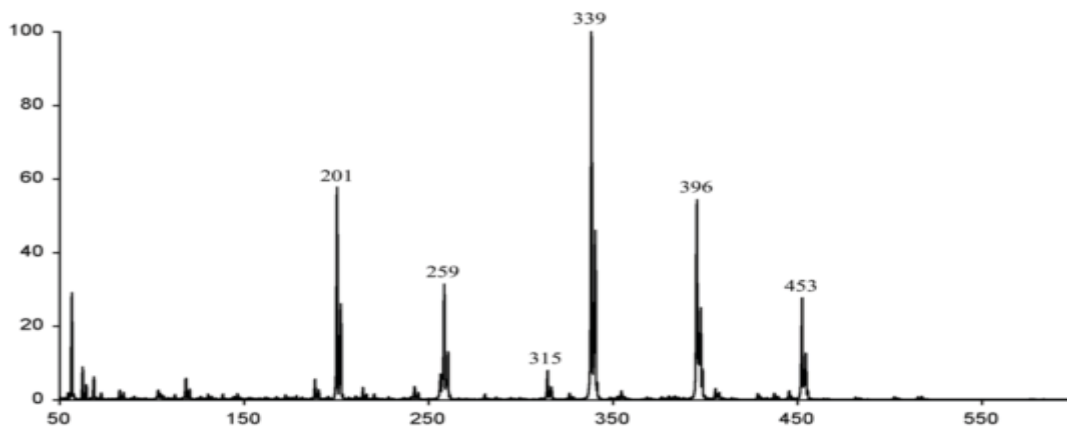


Figure 3.7: Mass Spectrum of $\text{Cu}(\text{tftm})_2$.

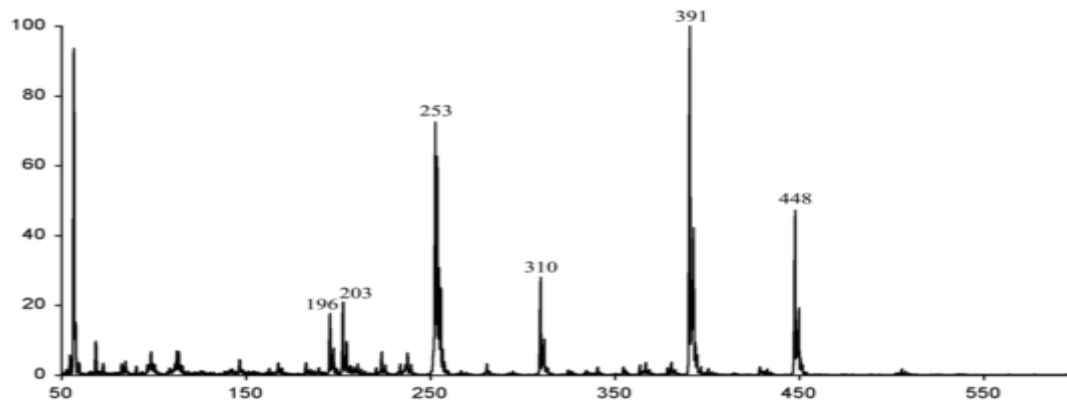


Figure 3.8: Mass Spectrum of $\text{Ni}(\text{tftm})_2$.

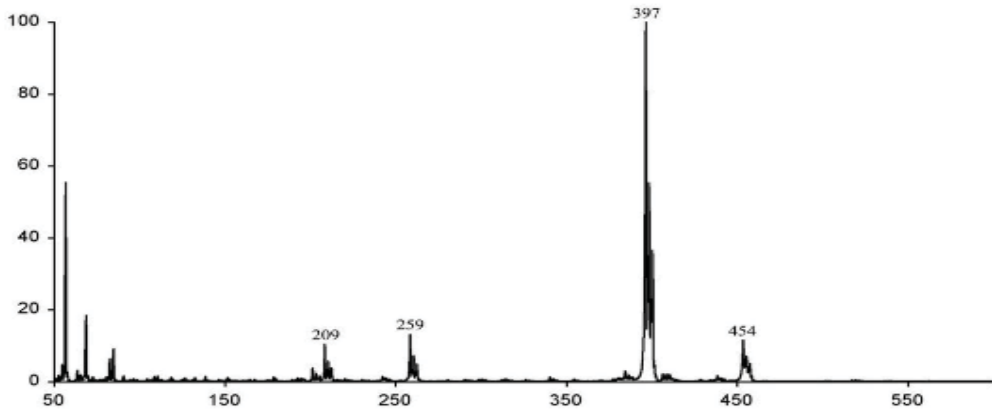


Figure 3.9: Mass Spectrum of $\text{Zn}(\text{tftm})_2$.

3.1.1 Loss of Terminal Group From *bis* Complex

The loss of a terminal group is a common event that occurs as these complexes are ionized within the mass spectrometer. Table 3.1 reports the relative abundance of ions from references 6 and 7 where many of the ions observed are fragments formed as a result of the loss of a terminal group.

Species	Mass Cu	Mass Ni	Mass Zn	Intensity Cu	Intensity Ni	Intensity Zn
$[\text{M}(\text{acac})_2]^+$	261	256	262	100	100	94
$[\text{M}(\text{acac})(\text{acac}-\text{CH}_3)]^+$	246	241	247	58	75	100
$[\text{M}(\text{acac}-\text{CH}_3)_2]^+$	231	226	232	50	0	0
$[\text{M}(\text{hfac})_2]^+$	477	472	478	29	56	20
$[\text{M}(\text{hfac})(\text{hfac}-\text{CF}_3)]^+$	408	403	409	60	100	100
$[\text{M}(\text{hfac}-\text{CF}_3)_2]^+$	339	334	340	35	0	0
$[\text{M}(\text{tftm})_2]^+$	453	448	454	28	47	11
$[\text{M}(\text{tftm})(\text{tftm}-t\text{Bu})]^+$	396	391	397	54	100	100
$[\text{M}(\text{tftm}-t\text{Bu})_2]^+$	339	334	340	100	0	0

Table 3.1: Relative positive ion intensities (% abundance) of metal species to their respective base peaks for the loss of a terminal group from a *bis* complex.^{6,7}

Some peaks of interest are very apparent in the spectra of the copper-containing complexes. For example, the copper *acac*, *hfac*, and *tftm* complexes are often observed to lose terminal groups, while the nickel and zinc complexes only undergo the loss of one

terminal group. In an attempt to explain this, rate constants were calculated and presented in Table 3.2 for the dissociation of CH₃ groups from M(acac)₂ complexes, CF₃ groups from M(hfac)₂ complexes, and *t*-butyl groups from M(tftm)₂ complexes.

Reaction	Species	Rate Constant (s ⁻¹)	Time (s)
Loss of 1 st CH ₃	[Cu(acac) ₂] ⁺	2.36*10 ²⁵	4.24*10 ⁻²⁶
	[Ni(acac) ₂] ⁺	4.78*10 ²⁸	2.09*10 ⁻²⁹
	[Zn(acac) ₂] ⁺	5.72*10 ²⁷	1.75*10 ⁻²⁸
Loss of 2 nd CH ₃	[Cu(acac)(acac-CH ₃)] ⁺	4.32*10 ³¹	2.31*10 ⁻³²
Loss of 1 st CF ₃	[Cu(hfac) ₂] ⁺	1.23*10 ²⁷	8.15*10 ⁻²⁸
	[Ni(hfac) ₂] ⁺	1.11*10 ³²	8.97*10 ⁻³³
	[Zn(hfac) ₂] ⁺	2.07*10 ³⁰	4.83*10 ⁻³¹
Loss of 2 nd CF ₃	[Cu(hfac)(hfac-CF ₃)] ⁺	1.12*10 ³³	8.93*10 ⁻³⁴
Loss of 1 st <i>t</i> Bu	[Cu(tftm) ₂] ⁺	8.40*10 ²⁸	1.19*10 ⁻²⁹
	[Ni(tftm) ₂] ⁺	1.30*10 ¹²	7.70*10 ⁻¹³
	[Zn(tftm) ₂] ⁺	1.64*10 ³¹	6.09*10 ⁻³²
Loss of 2 nd <i>t</i> Bu	[Cu(tftm)(tftm- <i>t</i> Bu)] ⁺	3.51*10 ³²	2.84*10 ⁻³³

Table 3.2: Calculated rate constants for loss of a terminal group.

The intact *acac* and *hfac* species all have 81 vibrational states, while the intact *tftm* species have 135 vibrational states due to the *tftm* ligand containing more atoms than both the *acac* and *hfac* ligands. The copper *acac* and *hfac* species, after the loss of either CH₃ or CF₃, have 69 vibrational states, while [Cu(tftm)(tftm-*t*Bu)]⁺ has 96 vibrational states. A full list of vibrational frequencies for each of these calculations can be found in the Appendix C.

The transition states for the first dissociation in the copper *acac* and *hfac* complexes were found when the bond of interest was stretched to 4.0 Å. For nickel *acac* and *hfac* complexes, the transition states were found at 3.0 Å, and for the zinc *acac* and *hfac* complexes, the transition states were found at 2.5 Å. Interestingly, the transition states for the loss of a *t*-butyl group in all of the intact *tftm* complexes were found at 2.5 Å. For the second dissociation calculated in the copper complexes, the transition states

were between 2.5 and 3.0 Å for each case. Plots of bond length vs. heat of formation for each of these transition state determinations can be found in Appendix B.

In only the copper complexes was the loss of a second terminal group observed experimentally. For the *acac* and *hfac* complexes, the calculations show that the nickel-containing and zinc-containing complexes lose CH₃ or CF₃ groups more rapidly than the copper-containing complexes. Interestingly, the loss of a second CH₃ or CF₃ group from the copper complexes is predicted to occur much more rapidly than the loss of the first. The loss of a second group is consistent with what is experimentally observed. A second dissociation event is not observed experimentally for the nickel and zinc complexes, and may be due in part to a difference in stability or the timescale associated with ionization.

For the *tftm* complexes, copper-containing complexes are predicted to lose a *t*-butyl group more rapidly than the nickel-containing compounds, yet slower than the zinc-containing compounds. Experimentally, the loss of one *t*-butyl group is the preferred pathway for both [Ni(tftm)₂]⁺ and [Zn(tftm)₂]⁺, so the large difference in the calculated rate constants provides little insight into what happens in reality. However, for [Cu(tftm)₂]⁺, the loss of the second *t*-butyl group is predicted to occur more rapidly than the loss of the first, which is consistent with the experimentally observed loss of a second CH₃ or CF₃ group in the copper-containing *acac* and *hfac* complexes.

3.1.2 Loss of Ligand

Another common dissociation event that is observed to readily occur in these *bis*- β -diketonate complexes is the loss of what amounts to an intact ligand. Table 3.3 shows

the relative positive ion intensities for fragments experimentally observed after the loss of a ligand.

	Mass	Mass	Mass	Intensity	Intensity	Intensity
Species	Cu	Ni	Zn	Cu	Ni	Zn
$[M(acac)]^+$	162	157	163	63	65	70
$[M(hfac)]^+$	270	265	271	0	71	13
$[M(tftm)]^+$	258	253	259	31	72	13

Table 3.3: Relative positive ion intensities (% abundance) of metal species to their respective base peak for loss of a ligand from a *bis* complex^{6,7}.

The loss of a ligand from an intact complex is observed in all of the species except for $Cu(hfac)_2$. Rate constants for the dissociation of a ligand from the intact complex were calculated for all the complexes of interest.

Reaction	Species	Rate Constant (s^{-1})	Time (s)
Loss of <i>acac</i> ligand	$[Cu(acac)_2]^+$	3.96×10^{22}	2.5258×10^{-23}
	$[Ni(acac)_2]^+$	5.89×10^{18}	1.69704×10^{-19}
	$[Zn(acac)_2]^+$	4.99×10^{26}	2.00415×10^{-27}
Loss of <i>hfac</i> ligand	$[Cu(hfac)_2]^+$	7.60×10^{18}	1.316×10^{-19}
	$[Ni(hfac)_2]^+$	7.63×10^{18}	1.31007×10^{-19}
	$[Zn(hfac)_2]^+$	1.49×10^{26}	6.73335×10^{-27}
Loss of <i>tftm</i> ligand	$[Cu(tftm)_2]^+$	6.62×10^{11}	1.50993×10^{-12}
	$[Ni(tftm)_2]^+$	3.12×10^{14}	3.20918×10^{-15}
	$[Zn(tftm)_2]^+$	5.19×10^{21}	1.92749×10^{-22}

Table 3.4: Calculated rate constants for the loss of an intact ligand.

In order for a bidentate ligand to fragment away, two metal-oxygen bonds had to be stretched in Spartan '04, which produced transition states with two imaginary frequencies. Similar to the loss of a terminal group from an intact ligand, the *acac* and *hfac* complexes only have 81 vibrational frequencies, while the *tftm* complexes have 135.

For each of the copper-containing species, the transition state was found when both of Cu-O bonds were stretched to 2.5 Å. Conversely, each of the nickel- and zinc-containing species, the transition state was found when both metal-oxygen bonds were stretched to 3.0 Å.

Upon a comparison of Table 3.4 with experimental data, there does not appear to be any correlation between the calculated rate constants and the experimental intensities observed for the intact ligand loss reactions. In all of the cases presented above, the loss of what amounts to an intact ligand is predicted to occur more quickly in the zinc complexes than it is in the copper and nickel complexes. Experimentally, however, only $\text{Zn}(\text{acac})^+$ has a greater intensity than its copper and nickel analogs.

Though $[\text{Cu}(\text{hfac})]^+$ is not observed experimentally, $[\text{Cu}(\text{hfac-CF}_3)]^+$ is observed with appreciable intensity⁶. The loss of CF_3 from $[\text{Cu}(\text{hfac})_2]^+$ is predicted to occur more rapidly, given the calculated rate constant of $1.23 \times 10^{27} \text{ s}^{-1}$, than the loss of one of an *hfac* ligand from $[\text{Cu}(\text{hfac})_2]^+$. $[\text{Cu}(\text{hfac})_2]^+$ is not experimentally observed to lose an *hfac* ligand even though it has a predicted rate constant of $7.60 \times 10^{18} \text{ s}^{-1}$. Furthermore, the loss of an *hfac* ligand after a CF_3 group has been lost from the opposing side is predicted to occur more rapidly than the loss of *hfac* from an intact complex. Calculated rate constants for this dissociation are included in Table 3.5. Each of these complexes has 69 vibrational states. For the copper and zinc complexes, the transition state was found at 2.5 Å, while for the nickel complex, it was found at 3.0 Å.

Reaction	Species	Rate Constant (s^{-1})	Time (s)
Loss of <i>hfac</i> ligand	$[\text{Cu}(\text{hfac})(\text{hfac-CF}_3)]^+$	9.84×10^{27}	1.01651×10^{-28}
	$[\text{Ni}(\text{hfac})(\text{hfac-CF}_3)]^+$	3.70×10^{25}	2.69992×10^{-26}
	$[\text{Zn}(\text{hfac})(\text{hfac-CF}_3)]^+$	4.18×10^{27}	2.39169×10^{-28}

Table 3.5: Calculated rate constants for the loss of *hfac* from $[\text{M}(\text{hfac})(\text{hfac-CF}_3)]^+$.

Based on these calculated rate constants, it seems as though the *hfac* ligand more easily dissociates from the complex once the terminal group from the opposing ligand is lost. From this, it is reasonable to infer that $[\text{Cu}(\text{hfac})_2]^+$ first loses a CF_3 group and then

the opposing ligand dissociates from the complex. Figure 3.10 shows a possible dissociation scheme.

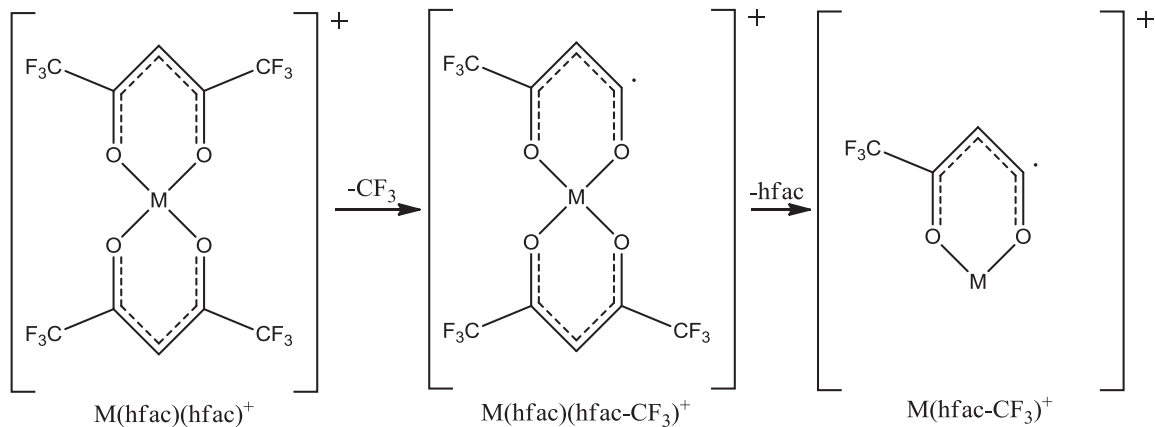


Figure 3.10: Proposed dissociation of *hfac*-containing complexes in mass spectrometer.

It is also possible, in the case of $[\text{Cu}(\text{hfac})_2]^+$ that two CF_3 groups, one from each *hfac* ligand, are lost before the ligand dissociates from the metal as described in Figure 3.11.

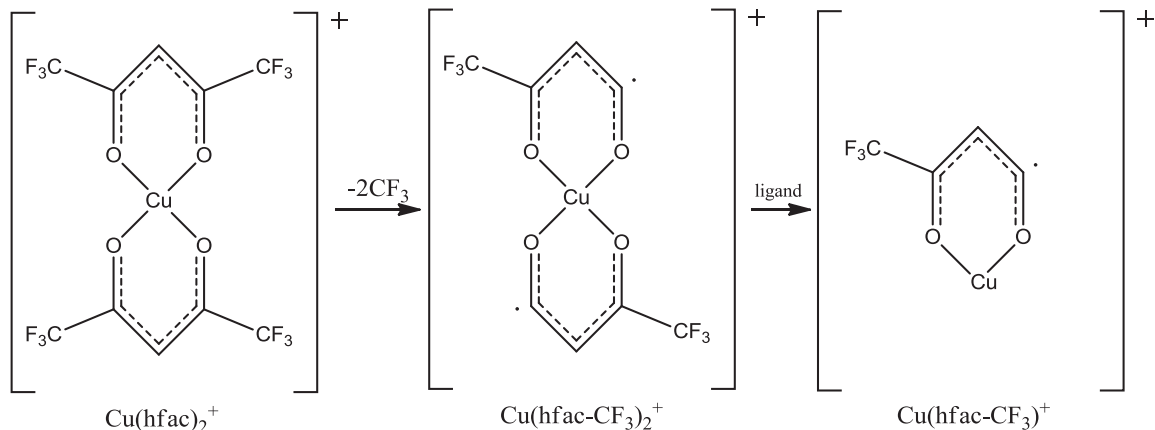


Figure 3.11: Proposed dissociation of $[\text{Cu}(\text{hfac})_2]^+$

In the *acac*- and *tftm*-containing species, the loss of ligand is also predicted to occur at a greater rate once a terminal group is lost from the initial complex as presented in Table 3.6.

Reaction	Species	Rate Constant (s^{-1})	Time (s)
Loss of <i>acac</i> ligand	$[Cu(acac)(acac-CH_3)]^+$	7.91×10^{30}	1.26465×10^{-31}
	$[Ni(acac)(acac-CH_3)]^+$	1.34×10^{24}	7.45774×10^{-25}
	$[Zn(acac)(acac-CH_3)]^+$	8.65×10^{29}	1.15659×10^{-30}
Loss of <i>tftm</i> ligand	$[Cu(tftm)(tftm-tBu)]^+$	5.41×10^{25}	1.8468×10^{-26}
	$[Ni(tftm)(tftm-tBu)]^+$	2.66×10^{25}	3.76429×10^{-26}
	$[Zn(tftm)(tftm-tBu)]^+$	2.67×10^{24}	3.74253×10^{-25}

Table 3.6: Calculated rate constants for loss of ligand after loss of terminal group.

Similar to the $[M(hfac)(hfac-CF_3)]^+$ complexes, the $[M(acac)(acac-CH_3)]^+$ have 69 vibrational states, while $[M(tftm)(tftm-tBu)]^+$ have 96 vibrational states. In the nickel- and copper-containing complexes, the transition states for the dissociation of an intact ligand were found when the two metal-oxygen bonds were stretched to 3.0 Å. In the case of the zinc-containing complexes, the transition states were found when the metal-oxygen bonds were stretched to 2.5 Å.

The calculated rate constants presented in Table 3.6 suggest that the ligand can dissociate from the complex more easily once a terminal group is lost. Based on both experimental data and calculated rate constants, it is possible that nickel and zinc *hfac* species, as well as any of the *acac* and *tftm* species can lose a terminal group before or after a ligand is lost from the initial complex. For the $Cu(hfac)_2$ complex however, there seems to be only one route for the formation of the $[Cu(hfac-CF_3)]^+$ fragment, which is that the terminal group must be lost before the ligand dissociates from the complex.

3.1.3 Loss of terminal group from mono ligand complexes

These aforementioned ligand loss pathways are predicted to occur quickly enough so that further dissociations can occur once a ligand is lost. The mono ligand metal β-diketonates that have lost a terminal group is another common fragment experimentally

observed in the mass spectra of these complexes and is presented in Table 3.7. The corresponding calculated rate constants for these dissociations are shown presented in Table 3.8.

	Mass	Mass	Mass	Intensity	Intensity	Intensity
Species	Cu	Ni	Zn	Cu	Ni	Zn
$[M(acac-CH_3)]^+$	147	142	148	71	13	5
$[M(hfac-CF_3)]^+$	201	196	202	100	7	3
$[M(tftm-tBu)]^+$	201	196	202	58	17	4

Table 3.7: Relative positive ion intensities (% abundance) for loss of terminal group from single ligand metal species to their respective base peaks^{6,7}

Reaction	Species	Rate Constant (s^{-1})	Time (s)
Loss of CH_3	$[Cu(acac)]^+$	9.91×10^{33}	1.00932×10^{-34}
	$[Ni(acac)]^+$	8.46×10^{31}	1.18249×10^{-32}
	$[Zn(acac)]^+$	1.72×10^{31}	5.82251×10^{-32}
Loss of CF_3	$[Cu(hfac)]^+$	2.00×10^{33}	5.00272×10^{-34}
	$[Ni(hfac)]^+$	4.22×10^{32}	2.36775×10^{-33}
	$[Zn(hfac)]^+$	2.23×10^{32}	4.49012×10^{-33}
Loss of $t\text{-}Bu$	$[Cu(tftm)]^+$	4.79×10^{35}	2.08693×10^{-36}
	$[Ni(tftm)]^+$	2.25×10^{33}	4.44793×10^{-34}
	$[Zn(tftm)]^+$	2.47×10^{25}	4.05605×10^{-26}

Table 3.8: Calculated rate constants for the loss of a terminal group for *mono* ligand species.

Because these complexes have fewer atoms than the *bis* complexes, they have a fewer number of vibrational frequencies, with the *acac* and *hfac* complexes having 39 vibrational frequencies and the *tftm* complexes having 66. Generally, for these *mono* ligand complexes, transition states were found when the bond to be broken was stretched to 2.5 or 3.0 Å, with the exception of $[Ni(acac)]^+$, for which the transition state for loss of CH_3 was found when the C- CH_3 bond was stretched to 4.0 Angstroms.

One reason that the loss of a terminal group from *mono* ligand complexes is predicted to occur more rapidly than from *bis* ligand complexes could be because of a smaller difference in energies from the initial state to transition state. Since these

complexes already acquired a sufficient amount of energy to lose one of their ligands, only a slight addition of energy would be necessary to form the transition state and subsequently lose a terminal group. Also, the smaller *mono* ligand complexes may dissociate faster due to the energy being less spread out than it is in the *bis* ligand complex. This smaller energy gap between initial state and transition state yields higher calculated rate constants according to RRKM theory³⁰.

For each of these reactions, the copper-containing species are predicted to lose their terminal group faster than the nickel- and zinc-containing species. This is consistent with experimental data, as the reported mass spectrum peak intensity corresponding to these reactions is highest in the copper-containing species⁶. The rate of the reaction may also explain why copper complexes are more readily observed experimentally than both nickel and zinc complexes.

3.2 Fluorine Migration

The loss of CF₂ is a commonly observed peak in the mass spectra of many metal β -diketonates that contain CF₃ groups. The exact mechanism and position of the remaining fluorine requires additional work, both experimental and theoretical.

3.2.1 Fluorine Migration in *hfac* Complexes

Experimentally, the loss of CF₂ has been observed in the mass spectra of both Ni(hfac)₂ and Zn(hfac)₂. However, the loss of CF₂ is not observed in the mass spectra of Cu(hfac)₂ as illustrated by the corresponding intensities presented in Table 3.9.

	Mass	Mass	Mass	Intensity	Intensity	Intensity
Species	Cu	Ni	Zn	Cu	Ni	Zn
$[M(hfac-CF_2)]^+$	220	215	221	0	62	49
$[M(hfac-CF_3)]^+$	201	196	202	100	7	3

Table 3.9: Relative positive ion intensities (% abundance) for the loss of CF_2 in *hfac* species to their respective base peaks^{6,7}.

In the *hfac* complexes, the loss of CF_2 is experimentally observed in the nickel and zinc complexes but interestingly, not in the copper complexes. This observation was investigated by using Spartan '04 to stretch the C- CF_3 bond of these fluorinated metal β -diketonates complexes. While constraining one of the C- CF_3 bonds to various lengths and running equilibrium geometry calculations, a realignment of the CF_3 was observed in both $[Ni(hfac)_2]^+$ and $[Zn(hfac)_2]^+$. The final geometry of the modeled molecule, after the calculation was complete, showed one of the fluorine atoms of the CF_3 group being parallel to the axis of the C- CF_3 bond. As shown in figures 3.12 and 3.13 a fluorine atom begins to line up along the axis of the C- CF_3 bond. As the bond is stretched, the fluorine is predicted to orient closer to the bond axis.

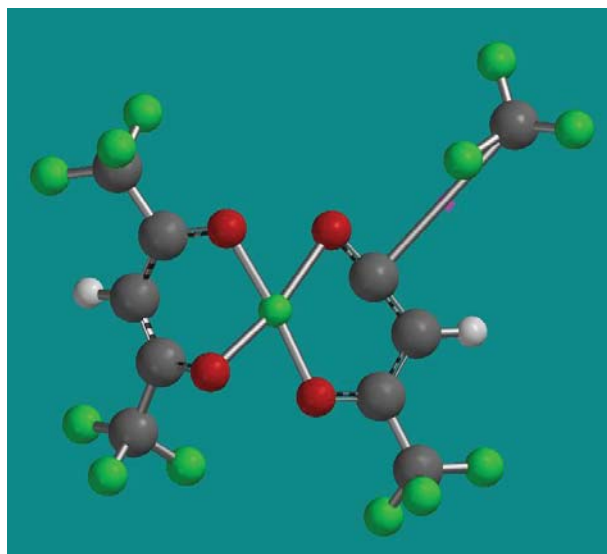


Figure 3.12: Model of $[Ni(hfac)_2]^+$ with a C- CF_3 bond stretched to 4.0 Å.

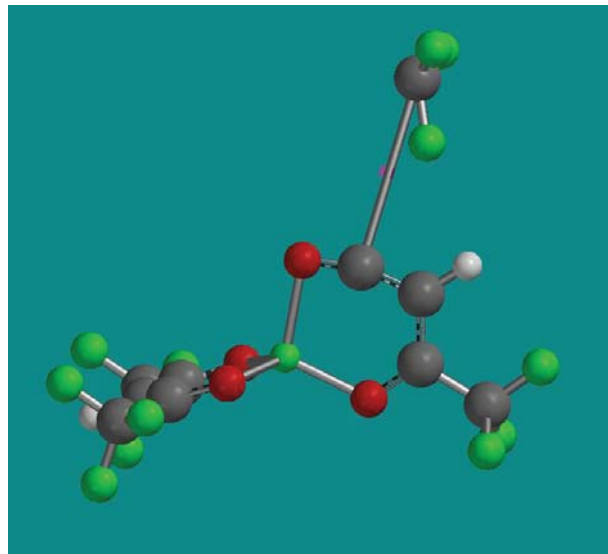


Figure 3.13: Model of $[\text{Zn}(\text{hfac})_2]^+$ with a C-CF₃ bond stretched to 4.0 Å.

The realignment in the predicted equilibrium geometry of $[\text{Ni}(\text{hfac})_2]^+$ and $[\text{Zn}(\text{hfac})_2]^+$ is presented in Figures 3.14 and 3.15 and gives insight into how these species may behave in the gas phase. It seems as though the fluorine atom aligns along the bond axis to provide electron density to the stretched bond. At some point, the CF₂ portion of the group breaks off and the remaining fluorine is coordinated to the complex as illustrated in Figure 3.16.

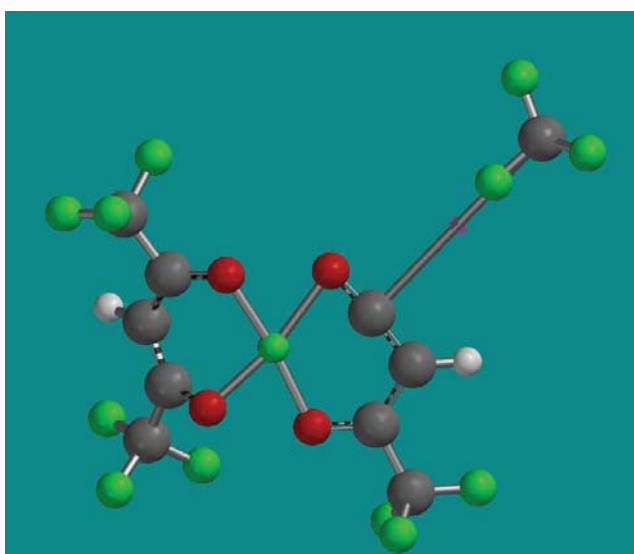


Figure 3.14: Model of $[\text{Ni}(\text{hfac})_2]^+$ with a C-CF₃ bond stretched to 5.0 Å.

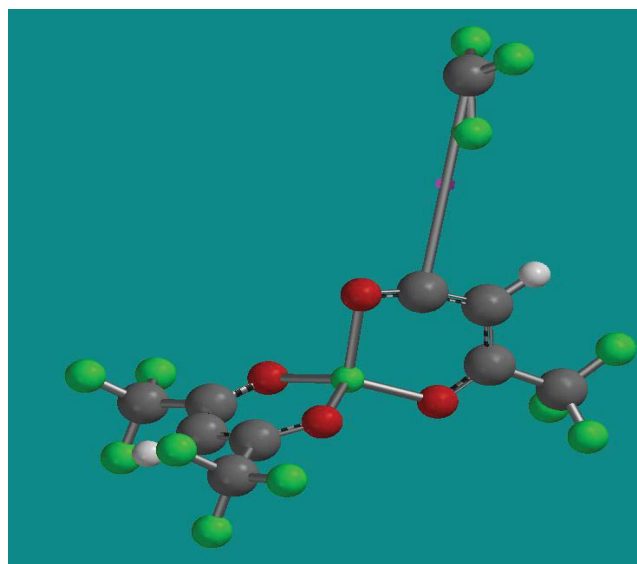


Figure 3.15: Model of $[\text{Zn}(\text{hfac})_2]^+$ with a C-CF₃ bond stretched to 5.0 Å.

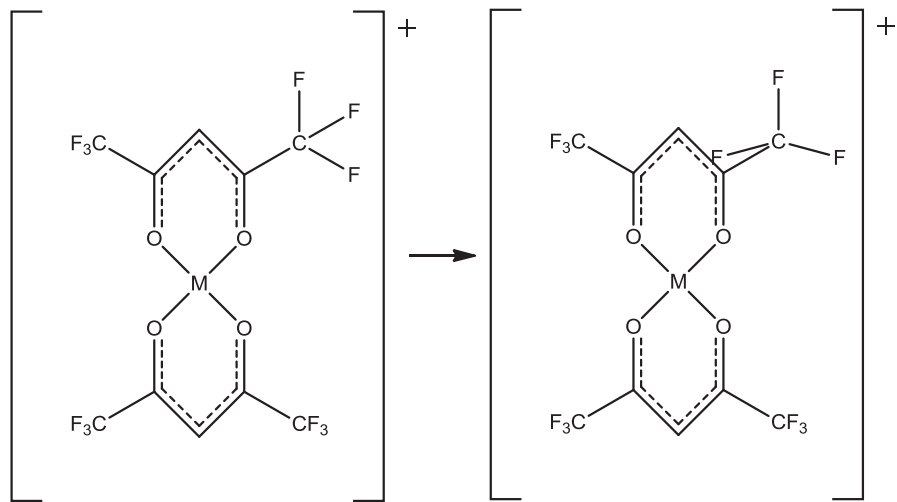


Figure 3.16: Scheme of fluorine realigning along bond axis.

In experimental data, the loss of CF₂ is only observed in mono ligand fragments, but, in the computer model, the fluorine realignment is predicted to occur in *bis* complexes as well. For $[\text{Cu}(\text{hfac})]^+$, the computer model undergoes this fluorine realignment, but experimentally, the loss of CF₂ is not observed in copper *hfac* complexes. Conversely, fluorine realignment is not observed in the simulated $[\text{Ni}(\text{hfac})]^+$

and $[\text{Zn}(\text{hfac})^+]$. However, in $[\text{Cu}(\text{hfac})_2]^+$, the fluorine realignment is not observed in the modeling as it is with $[\text{Ni}(\text{hfac})_2]^+$ and $[\text{Zn}(\text{hfac})_2]^+$.

Upon comparing the model to experimental results, a pattern begins to emerge where a fluorine atom first realigns itself with the aforementioned bond before the opposing ligand is lost. Following the loss of a ligand, CF_2 is also lost, leaving a $[\text{M}(\text{hfac}-\text{CF}_2)^+]$ species that is detected in the mass spectrometer. It is difficult to say whether the ligand and the CF_2 group are lost in a concerted fashion or if one loss occurs before the other. In either case, it appears that the two dissociations are closely related.

The location of the migrated fluorine within the complex still remains somewhat uncertain. Previous speculation suggested that the fluorine remaining with the complex migrated to the metal, but the fluorine could also have migrated to the former position of the CF_3 group. Both scenarios were modeled in Spartan '04 with equilibrium geometries calculated in order to establish which of the two pathways is predicted to be more stable. Heats of formation were also calculated and are summarized in Table 3.10.

Species	Poistion of Migrated Fluorine	Heat of Formation (kcal/mol)
$[\text{Ni}(\text{hfac}-\text{CF}_2)]^+$	Metal	-373.381
	Terminal	-328.495
$[\text{Zn}(\text{hfac}-\text{CF}_2)]^+$	Metal	-71.747
	Terminal	-90.617

Table 3.10: Heats of Formations of *hfac* Complexes after fluorine migration.

Unfortunately, these heats of formation do not provide a clear answer regarding the final position of the migrated fluorine. In the case of the nickel complex, the modeled molecule is predicted to be more stable with the fluorine bound to the metal, but in the case of the zinc complex, the more stable arrangement has the fluorine at the former position of the CF_3 group. It is also possible that the remaining fluorine migrates to

neither of these positions, but is coordinated to the complex in another way. A more general depiction of the complex after CF_2 is lost, such as that displayed in Figure 3.17, may be more useful in describing experimental results than assigning the migrated fluorine to a specific location.

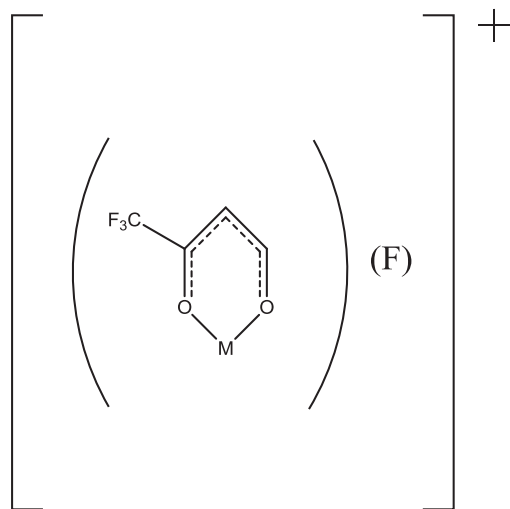


Figure 3.17: General *hfac* β -diketonate complex after loss of CF_2 .

3.2.2 Fluorine Migration in *tftm* Complexes

Fluorine migration is also experimentally observed in the mass spectra of $\text{M}(\text{tftm})_2$ complexes. The loss of CF_2 is observed in the mass spectra of $\text{Ni}(\text{tftm})_2$ and $\text{Zn}(\text{tftm})_2$, but similar to the *hfac* compounds, the loss is not observed for $\text{Cu}(\text{tftm})_2$, as presented in Table 3.11.

	Mass	Mass	Mass	Intensity	Intensity	Intensity
Species	Cu	Ni	Zn	Cu	Ni	Zn
$[\text{M}(\text{tftm}-\text{CF}_2)]^+$	209	203	209	0	21	10

Table 3.11: Relative positive ion intensities (% abundance) for the loss of CF_2 in *tftm* species to their respective base peaks^{6,7}

The intensity of the peaks corresponding to the loss of CF_2 are lower for the nickel and zinc *tftm* complexes in comparison to the intensity of *hfac* complexes. This is

likely due to the fact that the *hfac* complexes simply have more CF₃ groups that can undergo this rearrangement than the *tftm* complexes do. While stretching the C-CF₃ bond of the *tftm* complexes in Spartan '04, fluorine rearrangement, similar to what was seen in *hfac* species, was observed. However, in the case of the *tftm* complexes, the realignment of fluorine was only seen in species containing a single ligand and not in the intact [M(tftm)₂]⁺ complexes.

Though [Cu(tftm-CF₂)]⁺ is not observed experimentally, fluorine rearrangement is predicted to occur during the simulation. This may suggest that the timescale and parameters of the mass spectrometry experiment do not allow for the formation of this fragment, even though its formation may in fact be possible. Further investigation may be required to determine which of the possibilities is true.

In the cases of the nickel and zinc *tftm* complexes, the rearrangement of one of the fluorine atoms of the CF₃ is very similar to that seen in the *hfac* complexes. As the C-CF₃ bond is stretched to greater and greater lengths, the fluorine atom is more closely aligned with the bond axis. With a bond length of 4.0 Å, the fluorine is just beginning to align itself along the axis of the C-CF₃ bond, as illustrated in Figures 3.18 and 3.19.

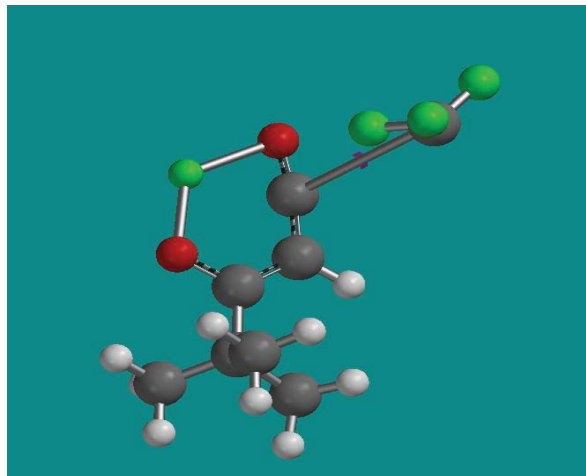


Figure 3.18: Model of $[\text{Ni}(\text{tftm})]^+$ with the C-CF₃ bond stretched to 4.0 Å.

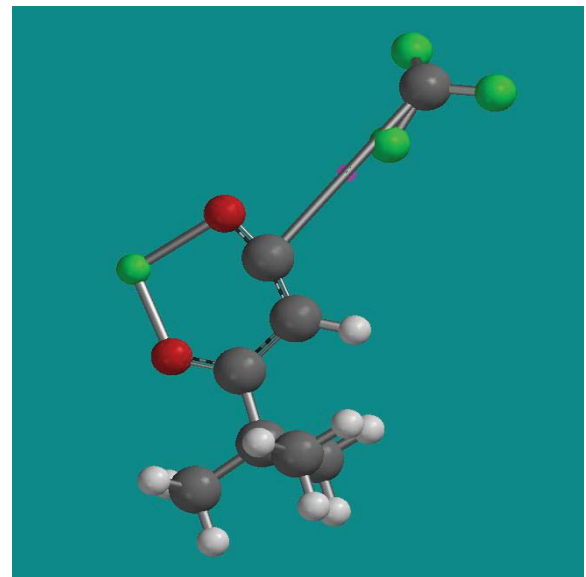


Figure 3.19: Model of $[\text{Zn}(\text{tftm})]^+$ with the C-CF₃ bond stretched to 4.0 Å.

As the bond is stretched to 5.0 Å and an equilibrium geometry calculation is complete, a fluorine atom becomes more in line with the bond axis as illustrated in Figures 3.20 and 3.21.

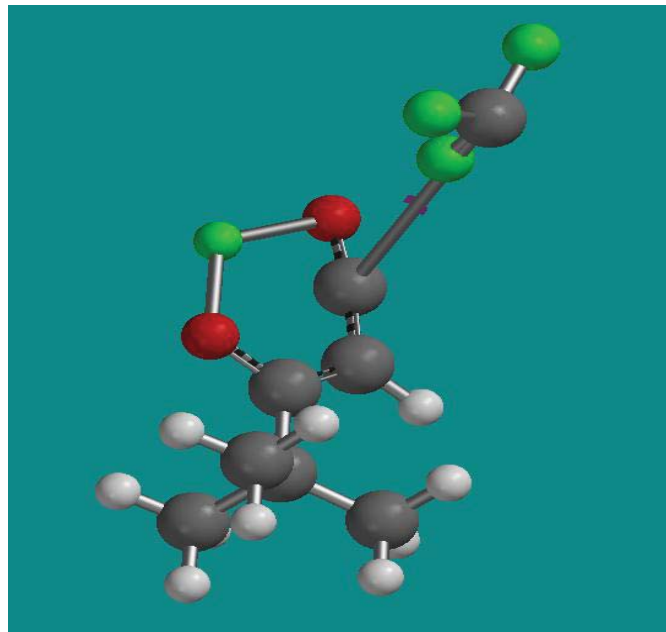


Figure 3.20: Model of $[\text{Ni}(\text{tftm})]^+$ with the C-CF₃ bond stretched to 5.0 Å.

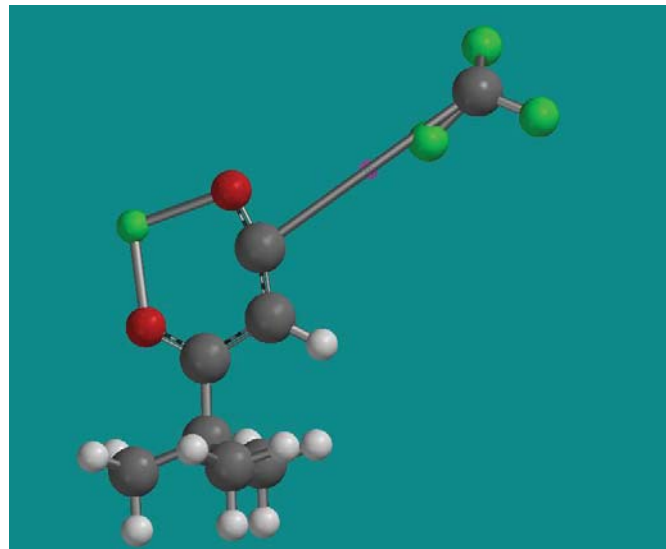


Figure 3.21: Model of $[\text{Zn}(\text{tftm})]^+$ with the C-CF₃ bond stretched to 5.0 Å.

Similar to the *hfac* complexes, the position of the migrated fluorine remains somewhat elusive. Equilibrium geometry calculations were completed for each of the complexes that experience the loss of CF₂, with the fluorine migrated to the metal and the fluorine migrated to the terminal position. Heats of formation were calculated in an

attempt to determine which of the scenarios is more stable and are presented in Table 3.12.

Species	Position of Migrated Fluorine	Heat of Formation (kcal/mol)
$[\text{Ni}(\text{tfm}-\text{CF}_2)]^+$	Metal	-203.533
	Terminal	-220.159
$[\text{Zn}(\text{tfm}-\text{CF}_2)]^+$	Metal	52.992
	Terminal	22.402

Table 3.12: Heats of formation of *tfm* complexes after the loss of CF_2 .

In the case of the *tfm* complexes, the more negative heats of formation correspond to the fluorine migrating to the terminal position and not to the metal. These results suggest that, at least in *tfm*-containing complexes, the molecule is predicted to be more stable after the loss of CF_2 with the fluorine bound to the former position of the CF_3 group as shown in Figure 3.22.

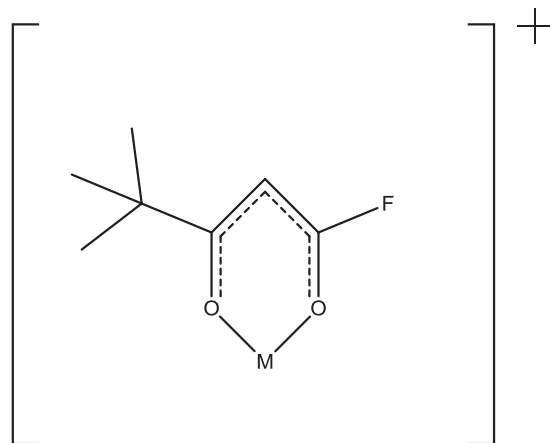


Figure 3.22: Proposed structure of $[\text{M}(\text{tfm}-\text{CF}_2)]^+$.

3.3 Mixed Ligand β -diketonates

Mixed ligand metal β -diketonate complexes have also been observed experimentally in mass spectra. Mixed ligand species are the result of the co-sublimation

of two different metal metal β -diketonate species. In the mass spectra, the dissociation patterns for the mixed ligand complexes contain similar features when compared to single ligand species. For example, both mixed ligand and single ligand species experience the loss of terminal groups.

Nickel, copper, and zinc *acac* complexes have been observed to undergo ligand exchange with *tftm* containing complexes. A common fragmentation that is experimentally observed is the loss of the terminal *t*-butyl group from the *tftm* ligand. Mass spectra for these mixed ligands reactions can be seen in Figures 3.23-3.27 and the results are summarized in Table 3.13 and are reproduced from references 6 and 7. Rate constants for this dissociation have been calculated and are presented in Table 3.14.

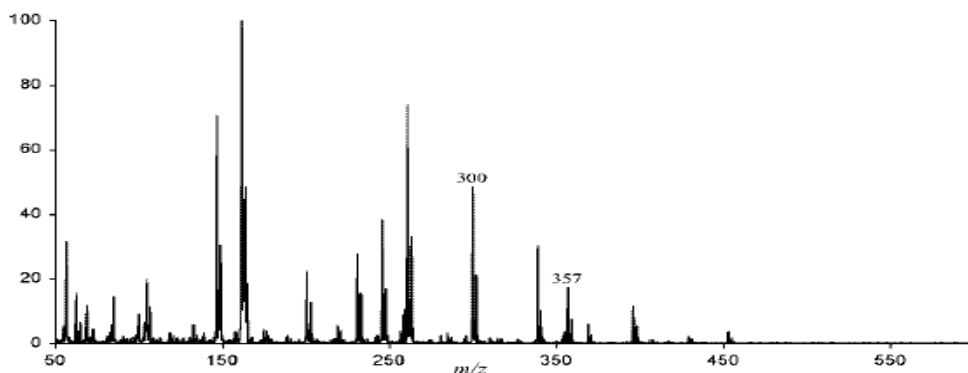


Figure 3.23: Mass Spectra of gas-phase reaction of $\text{Cu}(\text{acac})_2$ and $\text{Cu}(\text{tftm})_2$.

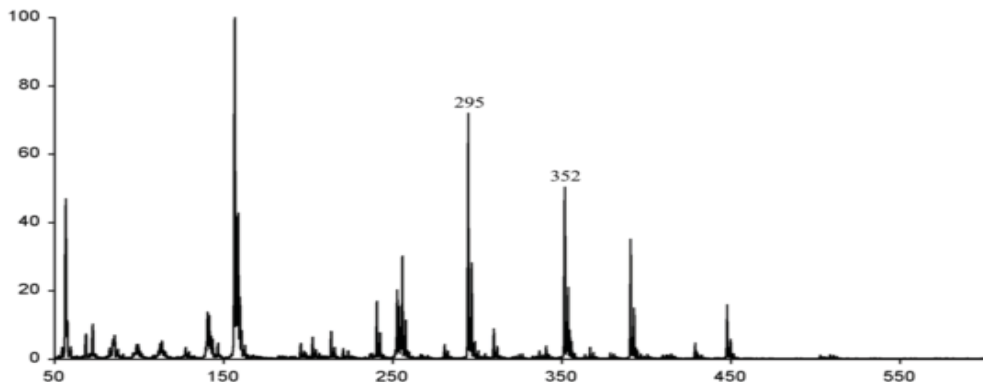


Figure 3.24: Mass Spectra of the gas-phase reaction of $\text{Ni}(\text{acac})_2$ and $\text{Ni}(\text{tftm})_2$.

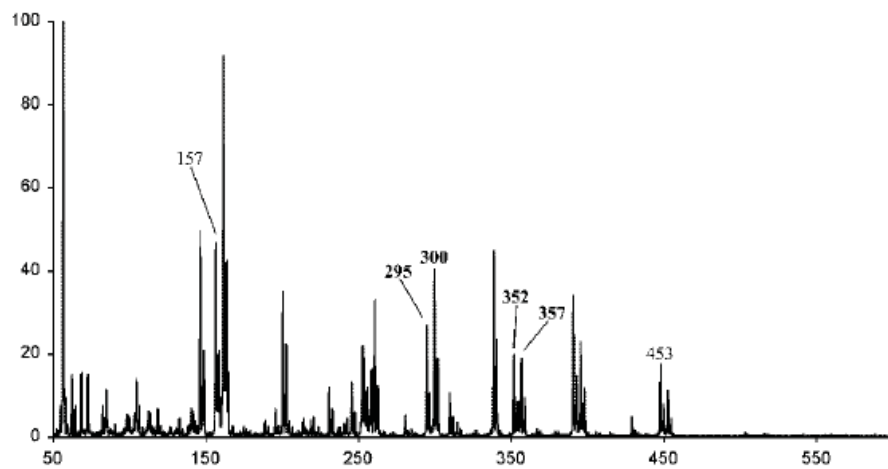


Figure 3.25: Mass Spectra of the gas-phase reaction of $\text{Cu}(\text{acac})_2$ and $\text{Ni}(\text{tftm})_2$.

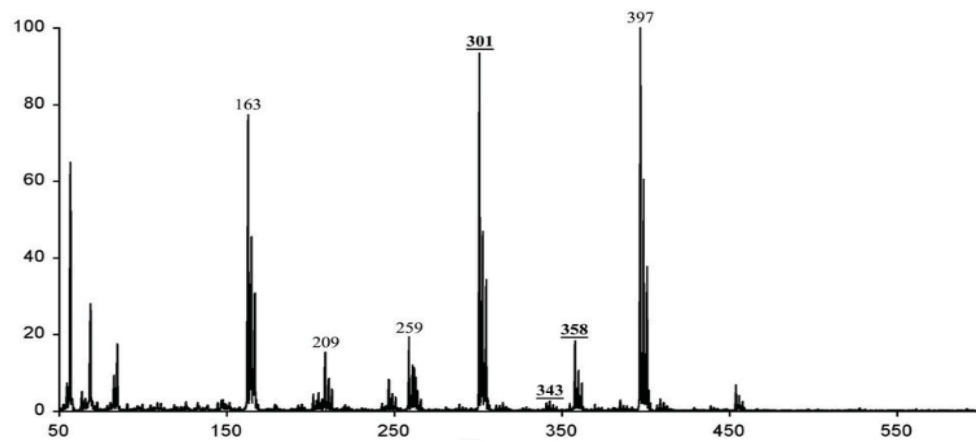


Figure 3.26: Mass Spectra of the gas-phase reaction of $\text{Zn}(\text{acac})_2$ and $\text{Zn}(\text{tftm})_2$.

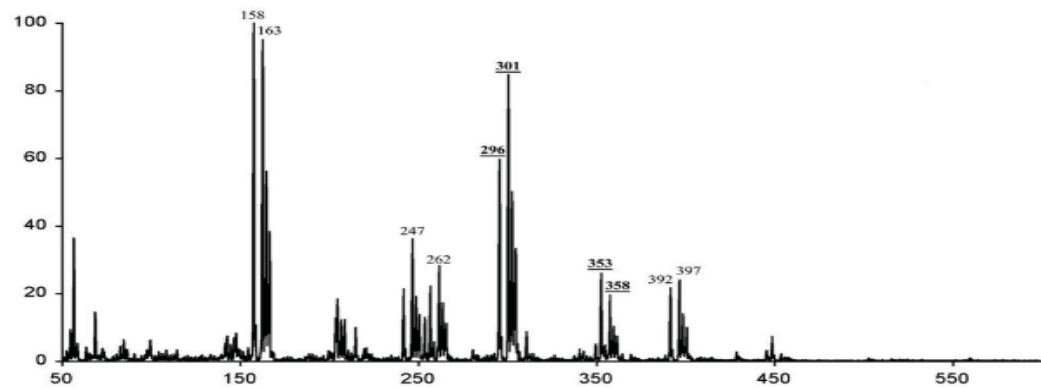


Figure 3.27: Mass Spectra of the gas-phase reaction of $\text{Co}(\text{acac})_2$ and $\text{Zn}(\text{tftm})_2$.

$[M(acac)(tftm-tBu)]^+$	Reaction				
	Cu(acac) ₂ & Cu(tftm) ₂	Ni(acac) ₂ & Ni(tftm) ₂	Cu(acac) ₂ & Ni(tftm) ₂	Zn(acac) ₂ & Zn(tftm) ₂	Co(acac) ₂ & Zn(tftm) ₂
Species	Cu	Ni	Cu	Ni	Zn
Mass	300	295	300	295	301
Intensity	48	72	40	27	93
					85

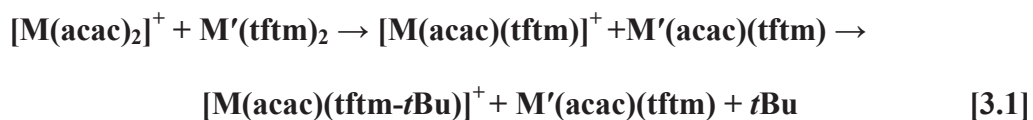
Table 3.13: Relative Positive ion intensities (% abundance) for formation of $M(acac)(tftm-tBu)$ from homo and hetero-metal species to their respective base peaks.

Species	Rate Constant (s^{-1})	Time (s)
$[Cu(acac)(tftm)]^+$	4.11×10^{-29}	2.4346×10^{-30}
$[Ni(acac)(tftm)]^+$	7.49×10^{-28}	1.33429×10^{-29}
$[Zn(acac)(tftm)]^+$	5.10×10^{-29}	1.96162×10^{-30}

Table 3.14: Calculated rate constants for the loss of *t*Bu from mixed ligand $M(acac)(tftm)$ species.

Each of these mixed ligand complexes has 108 vibrational frequencies. Also, for each complex, the transition state was found when the C-*t*Bu bond was stretched to 2.5 Å. Similar to the *mono* ligand complexes, it is likely that these mixed ligand complexes have large rate constants of dissociation because of a small energy gap between the reacting species and the transition state.

While the calculated rate constants do not vary greatly as the metal is changed, when compared the loss of *t*-butyl in single ligand species, the rates suggest that the loss occurs more quickly in the mixed ligands, except in the case of $[Zn(acac)(tftm)]^+$. In all cases involving the mixed ligands, the loss of *t*-butyl is predicted to occur very fast, which leaves open the possibility that an intact mixed ligand complex is able to form before it fragments and dissociates further as seen in Equation 3.1.



It is also possible that the *t*-butyl group is lost from the *tftm* group before the mixed ligand complex is formed, as seen in Equation 3.2.



It is likely that, in reality, both of these pathways can occur given the applicable energies and the fact that fragmentation readily occurs.

3.4 Future Work

There is still much to be explored in this area of metal β -diketonate chemistry. Complexes containing cadmium and cobalt have been recently synthesized and analyzed via mass spectrometry. The combinations of ligands that are coordinated to these metal centers are also vast.

More computational work can also be done to study the fragmentation of mixed ligand species. Due to time constraints and focus on homo ligand complexes and fluorine migration, the majority of mixed ligand fragmentation reactions observed experimentally remained largely unexplored in this study.

These same calculations described herein can also be carried out at higher levels of theory to test the results presented. Higher levels of theory can provide more accurate rate constants and provide a better understanding of how and why these complexes fragment and exchange. The interesting observation of fluorine migration can also be investigated at these higher levels of theory in order to provide a more definitive understanding of this rearrangement.

References

1. Condorelli, G.G., Malandrino, G., Fragalà, I.L. *Coordination Chemistry Reviews* **2007** 251, 1931-1950
2. Sloop, J.C., Bumgardner, C.L., Washington, G., Loehle, W.D., Sankar, S. S., Lewis, A.B. *Journal of Fluorine Chemistry* **2006** 127, 780-786
3. Fahlman, B.D., Barron, A.R. *Adv. Mater. Opt. Electron* **2000** 10, 223-232
4. Majer, J.R., Perry, R. *Chemical Communications* **1969** 297, 454-455
5. Westmore, J.B. *Chemical Review* **1976** 6, 695-715
6. Hunter, G.O., Lerach, J.O., Lockso, T.R., Leskiw, B.D., *Rapid Commun. Mass Spectrom.* **2010** 24, 129-137
7. Hunter, G.O., Leskiw, B.D., *Rapid Commun. Mass Spectrom.* **2012** 26, 369-376
8. Morris, M.L., Koob, R.D., *Inorg. Chem.* **1980** 20, 2737-2738
9. Pearson, R.G., *J. Am. Chem. Soc.* **1963** 85, 3533-3539
10. Pearson R.G. *J. Chem. Educ.* **1968** 45, 581-587
11. Ford, T. M., McLain, S.J., United States Patent 5,208,297 **1993**
12. Kurian, J.V., Liang, Y., United States Patent 5,840,957 **1998**
13. Katok, K.V., Tertykh, V.A., Brichka, S.Y., Prikohod ko, G.P., *J. Therm. Anal. Cal.* **2006** 86 109-114
14. Burtuloso, A.C.B., *Synlett* **2005** 18, 2859-2860
15. Dismukes, J.P., Kane, J., United States Patent 3,894,164 **1975**
16. Nieminen, M., Putkonen, M., Niinistö, L., *Applied Surface Science* **2001** 174, 155-165
17. Bhaskaran, V., Antanasova, P., Hampden-Smith, M.J., Kodas, T.T. *Chem. Mater.* **1997** 9 2822-2829

18. Zheng, Y., Lin, J., Liang, Y., Lin, Q., Yu, Y., Guo, C., Wang, S., Zhang, H.
Materials Letters **2002** 54 424-429
19. Wang, L.H., Wang, W., Zhang, W.G., Kang, E.T., Huang, W. *Chem. Mater.*
2000 12 2212-2218
20. Citra, M.J. *Chemosphere* **1999** 38 191-206
21. Schaftenaar, G., Noordik, J.H., *Journal of Computer-Aided Molecular Design*
2000 14 123-134
22. Chermette, H. *Journal of Computational Chemistry* **1999** 20 129-154
23. Hillier, I.H., McNamara, J.P. *Phys. Chem. Chem. Phys.* **2007** 9 2362-2370
24. Rezac, J., Fanfrlik, J., Salahub, D., Hobza., P. *J. Chem. Theory Comput.* **2009** 5 1749-1760
25. Bakowies, D., Thiel, W. *Journal of Computational Chemistry* **1996** 17 87-108
26. Wavefunction, Inc., Spartan '04 AWindows: Tutorial and User's Guide. USA:
2004
27. Stewart, J.P.J., *Computational Chem.* **1989** 10, 209-220
28. Laidier, K.J, and King, M.C., *J.Phys. Chem.* **1983**, 87, 2657-2664
29. Eyring, H. *J. Chem. Phys.* **1935** 3 (2): 107–115
30. Robinson, P.J., and Holbrook, K.A. Unimolecular Reactions. Wiley-Interscience
London: 1972
31. IUPAC. Compendium of Chemical Terminology, 2nd ed. (the "Gold Book").
Compiled by A. D. McNaught and A. Wilkinson. Blackwell Scientific
Publications, Oxford (1997)

Appendix A: Example Rate Constant Calculation

The following is a step by step example of the calculation of the rate constant for the dissociation of a methyl group from $[\text{Zn}(\text{acac})_2]^+$. The first thing that is done is a PM3 calculation of the equilibrium geometry of $[\text{Zn}(\text{acac})_2]^+$. The charge was set to positive, and the spin multiplicity was set to doublet. The resulting calculation gives the following relevant information about the reactant molecule (Table A.1).

Heat of formation (kcal/mol)	-119.826
Enthalpy (kJ/mol)	33.2169
Zero Point Energy (kJ/mol)	598.2555

Table A.1: Energetic Information for $[\text{Zn}(\text{acac})_2]^+$.

Because the heat of formation is listed in kcal/mol and the enthalpy and zero point energy are listed in kJ/mol, a conversion must be made, as shown in Equation A.1.

$$-119.826 \text{ kcal} * 4.184 \frac{\text{kJ}}{\text{kcal}} = -501.352 \text{ kJ} \quad [\text{A.1}]$$

In addition to the energetic information that the PM3 calculation provides, a list of vibrational frequencies for the molecule is also determined and is presented in Table A.2.

$[\text{Zn}(\text{acac})_2]^+$		
84.269	736.72	1373.148
25.808	864.163	1374.795
21.916	917.394	1374.953
31.646	945.007	1375.664
36.284	952.911	1393.323
58.346	957.677	1402.603
104.859	975.355	1444.131
176.697	978.889	1470.604
179.343	982.626	1511.591
181.389	992.805	1626.876
185.604	996.283	1714.372
205.556	1024.227	1774.616
210.089	1032.063	1827.24
216.578	1070.853	3005.369
264.284	1082.974	3036.283
290.308	1115.679	3036.454
339.134	1120.533	3046.663
375.823	1131.649	3062.487
405.214	1160.542	3062.634
427.287	1175.598	3079.887
441.67	1313.303	3080.102
456.674	1334.355	3087.358
523.693	1342.884	3087.629
561.518	1350.188	3139.082
579.295	1352.046	3139.7
626.622	1356.622	3169.407
633.327	1356.888	3170.176

Table A.2: $[\text{Zn}(\text{acac})_2]^+$ vibrational frequencies (cm^{-1}).

After the information is gathered about the reactant, a transition state can be determined. To determine the transition state, an equilibrium geometry calculation is performed with the C-CH₃ bond of interest being stretched and constrained to various lengths, until a maximum heat of formation is determined, as shown in Table A.3 and Figure A.1

Bond Length (Å)	Heat of formation (kcal/mol)
1.5	-119.862
1.8	-103.177
2.2	-62.895
2.5	-48.236
2.8	-52.83
3	-52.908
3.3	-53.046
3.7	-52.973

Table A.3: C-CH₃ bond stretching of [Zn(acac)₂]⁺.

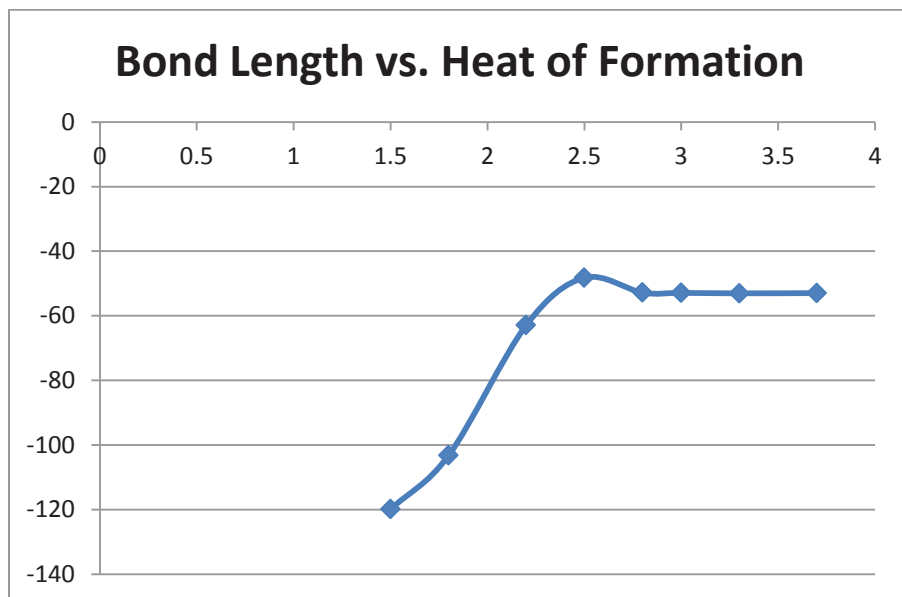


Figure A.1: Bond length vs. heat of formation plot for the C-CH₃ bond stretching of [Zn(acac)₂]⁺.

Based on the above information, the transition state for the dissociation of CH₃ from [Zn(acac)₂]⁺ is determined to be at a C-CH₃ bond length of 2.5 Å, with a corresponding heat of formation of -48.236 kcal/mol. The enthalpy and zero point energy of this transition state complex, as well as the vibrational frequencies are also necessary for the rate constant calculations and are presented in Tables A.4 and A.5

Heat of formation (kcal/mol)	-48.236
Enthalpy (kJ/mol)	39.770
Zero Point Energy (kJ/mol)	582.0349

Table A.4: Energetic Information for transition state, loss of CH₃, [Zn(acac)₂][‡].

[[Zn(acac) ₂] ⁺] [‡]		
-162.702	596.051	1360.989
45.767	629.303	1375.259
51.935	634.522	1375.505
53.373	672.385	1378.456
80.036	827.755	1381.243
83.209	863.338	1393.192
105.345	923.859	1456.634
126.781	943.444	1461.475
137.915	966.113	1479.272
143.644	978.905	1656.331
144.153	985.783	1657.82
155.279	987.009	1713.208
164.604	992.347	2104.661
195.112	993.325	3016.508
195.687	1025.203	3052.462
208.895	1074.474	3052.713
287.912	1079.753	3063.444
313.309	1084.382	3063.551
316.46	1121.779	3066.418
345.465	1129.501	3075.522
353.083	1178.344	3075.691
404.392	1263.342	3148.809
441.002	1270.639	3161.524
441.879	1310.073	3161.605
479.133	1343.135	3162.232
533.533	1344.25	3237.716
558.096	1351.17	3240.246

Table A.5: [[Zn(acac)₂]⁺][‡] loss of first CH₃, transition state vibrational frequencies (cm⁻¹).

Similar to the reacting species, the heat of formation of the transition state must also be converted from kcal/mol to kJ/mol as seen in Equation A.2.

$$-48.236 * 4.184 \frac{\text{kJ}}{\text{kcal}} = -201.932 \quad [\text{A.2}]$$

After all of the information is collected from the calculations in Spartan '04, the rate constant can be calculated. The initial energy of the reaction must first be calculated using the heats of formation and enthalpies of the reactant and transition state, as shown in Equation A.3.

$$E = (\Delta H_f^\ddagger - \Delta H^\ddagger) - (\Delta H_f - \Delta H) \quad [A.3]$$

$$E_0 = (-201.932 - 39.770) - (-501.352 - 33.2169)$$

$$E = 292.867 \text{ kJ}$$

In the following calculations, the total energies from which the rate constant will be calculated will be increased by 25 kJ for forty increments. These increments will be the same for all reactions, to allow for comparison between average rate constants. The maximum total energy in this example will be increased to 1267.867 kJ.

Once the initial total energy, E_0 , is calculated, the quantities of E' and E'^\ddagger for each energy increment, E , can be calculated as shown in Equation A.4 and A.5

For $E = 317.867$

$$E' = \frac{E}{E_z} \quad [A.4]$$

$$E' = \frac{317.867}{598.2555} = 0.5313$$

$$E'^\ddagger = \frac{E}{E_z^\ddagger} \quad [A.5]$$

$$E'^\ddagger = \frac{317.867}{582.0349} = 0.5461$$

Next, using these E' values, the sum of states, $w(E)$, and the derivative of the sum of states can be calculated. The following calculations are for the reactant, with the same methods being used for the transition state as demonstrated with Equations A.6-A.9.

For E = 317.867, E' = 0.5313

$$w(E') = [5.00E' + 2.73(E')^{0.5} + 3.51]^{-1} \quad [\text{A.6}]$$

$$w(E') = [5.00 * 0.5313 + 2.73(0.5313)^{0.5} + 3.51]^{-1} = 0.1226$$

$$\frac{dw(E')}{dE'} = -\frac{5.00 + \frac{1.3650}{(E')^{0.50}}}{[5.00E' + 2.73(E')^{0.5} + 3.51]^2} \quad [\text{A.7}]$$

$$\frac{dw(E')}{dE'} = -\frac{5.00 + \frac{1.3650}{0.5313^{0.50}}}{[5.00 * 0.5313 + 2.73(0.5313)^{0.5} + 3.51]^2} = 0.1033$$

For E = 692.867, E' = 1.1581

$$w(E') = e^{-2.4191(E')^{0.25}} \quad [\text{A.8}]$$

$$w(E') = e^{-2.4191(1.1581)^{0.25}} = 0.0813$$

$$\frac{dw(E')}{dE'} = -\frac{0.604775e^{-2.4191(E')^{0.25}}}{(E')^{0.75}} \quad [\text{A.9}]$$

$$\frac{dw(E')}{dE'} = -\frac{0.604775e^{-2.4191(1.1581)^{0.25}}}{1.1581^{0.75}} = 0.044044$$

The value of β is calculated using the vibrational frequencies. A β value can be calculated for both the reactant and the transition state using Equation A.10.

Since $\text{Zn}(\text{acac})_2^+$ has 81 vibrational modes s is 81.

$$\beta = \frac{s-1}{s} \cdot \frac{\nu^2}{\nu^2} \quad [\text{A.10}]$$

$$\beta = \frac{81-1}{81} \cdot \frac{\frac{84.269^2 + 25.808^2 + \dots + 3170.176^2}{81}}{\frac{(84.269 + 25.808 + \dots + 3170.176)^2}{81}} = 1.602$$

Similarly, for the transition state,

$$\beta^\ddagger = 1.679$$

Using the values for β and $w(E')$, the value of α can be calculated using Equation A.11.

For $E = 317.867$

$$\alpha = 1 - \beta w(E') \quad [\text{A.11}]$$

$$\alpha = 1 - 1.602 * 0.1226 = 0.8956$$

For the transition state

$$\alpha^\ddagger = 0.8890$$

These values can then be used in the Whitten-Rabinovitch version of the RRKM rate constant equation to determine the rate constant for that specific value of E using Equation A.12

For $E = 317.867$

$$k(E)_{WR} = \frac{1}{s \cdot h} \cdot \frac{\sum_{i=1}^s v_i}{\sum_{i=1}^s v_i^\ddagger} \cdot \frac{(E^\ddagger + a^\ddagger E_Z^\ddagger)^s}{(E + aE_Z)^{s-1}} \cdot \frac{1}{[1 - \beta \frac{dw(E')}{dE'}]} \quad [\text{A.12}]$$

The value of $\frac{\prod_{i=1}^s \nu_i}{\prod_{i=1}^s \nu_i^\ddagger}$ is found by multiplying the vibrational frequencies together.

s

$$\nu_i = 84,269 * 25.808 * \dots * 3170.176 = 9.69 * 10^{233} \text{ cm}^{-1}$$

i=1

s

$$\nu_i^\ddagger = 45.676 * 51.935 \dots * 3240.246 = 6.36 * 10^{232} \text{ cm}^{-1}$$

i=1

$$\frac{\prod_{i=1}^s \nu_i}{\prod_{i=1}^s \nu_i^\ddagger} = \frac{9.69 * 10^{233} \text{ cm}^{-1}}{6.36 * 10^{232} \text{ cm}^{-1}} = 15.241$$

$$k(E)_{WR} = \frac{1}{81 \cdot h} \cdot 15.241 \cdot \frac{(25 + 0.8890 * 582.0349)^{81}}{(317.867 + 0.8956 * 598.2555)^{81-1}}$$

$$\cdot \frac{1}{[1 - 1.602 * 0.1033]}$$

$$k(E)_{WR} = 3.16 * 10^{19}$$

Table A.6 shows the values calculated for all forty values of E, from E=292.876 to E=1267.876.

E(kJ)	E'	E'^\ddagger	w	α	α^\ddagger	$\frac{(E^\ddagger + a^\ddagger E_z^\ddagger)^s}{(E + aE_z)^{s-1}}$	$\frac{1}{[1 - \beta \frac{dw}{dE'}]}$	k(E) (sec ⁻¹)
292.867	0.4895	0.5032	0.1271	0.9003	0.8939	2.67E-14	1.1929	9.05E+18
317.867	0.5313	0.5461	0.1226	0.8956	0.8890	9.48E-14	1.1747	3.16E+19
342.867	0.5731	0.5891	0.1185	0.8912	0.8843	3.13E-13	1.1593	1.03E+20
367.867	0.6149	0.6320	0.1146	0.8871	0.8800	9.68E-13	1.1461	3.15E+20
392.867	0.6567	0.6750	0.1110	0.8832	0.8759	2.81E-12	1.1346	9.06E+20
417.867	0.6985	0.7179	0.1077	0.8795	0.8720	7.73E-12	1.1246	2.47E+21
442.867	0.7403	0.7609	0.1046	0.8760	0.8683	2.01E-11	1.1158	6.37E+21
467.867	0.7821	0.8038	0.1028	0.8712	0.8634	4.87E-11	1.1206	1.55E+22
492.867	0.8238	0.8468	0.0998	0.8683	0.8604	1.16E-10	1.1117	3.67E+22
517.867	0.8656	0.8898	0.0970	0.8655	0.8575	2.66E-10	1.1039	8.33E+22
542.867	0.9074	0.9327	0.0943	0.8629	0.8547	5.84E-10	1.0969	1.82E+23
567.867	0.9492	0.9757	0.0918	0.8604	0.8520	1.23E-09	1.0907	3.82E+23
592.867	0.9910	1.0186	0.0895	0.8579	0.8495	2.51E-09	1.0851	7.74E+23
617.867	1.0328	1.0616	0.0873	0.8556	0.8471	4.96E-09	1.0801	1.52E+24
642.867	1.0746	1.1045	0.0852	0.8534	0.8447	9.5E-09	1.0756	2.90E+24
667.867	1.1164	1.1475	0.0832	0.8512	0.8425	1.77E-08	1.0715	5.37E+24
692.867	1.1581	1.1904	0.0813	0.8492	0.8403	3.2E-08	1.0677	9.68E+24
717.867	1.1999	1.2334	0.0795	0.8472	0.8382	5.64E-08	1.0643	1.70E+25
742.867	1.2417	1.2763	0.0778	0.8452	0.8362	9.72E-08	1.0611	2.93E+25
767.867	1.2835	1.3193	0.0762	0.8434	0.8343	1.64E-07	1.0582	4.92E+25
792.867	1.3253	1.3622	0.0746	0.8416	0.8324	2.71E-07	1.0555	8.10E+25
817.867	1.3671	1.4052	0.0731	0.8399	0.8306	4.38E-07	1.0530	1.31E+26
842.867	1.4089	1.4481	0.0717	0.8382	0.8289	6.96E-07	1.0507	2.07E+26
867.867	1.4507	1.4911	0.0703	0.8366	0.8272	1.09E-06	1.0486	3.23E+26
892.867	1.4925	1.5340	0.0690	0.8351	0.8256	1.67E-06	1.0466	4.95E+26
917.867	1.5342	1.5770	0.0677	0.8335	0.8240	2.52E-06	1.0447	7.47E+26
942.867	1.5760	1.6199	0.0665	0.8321	0.8225	3.75E-06	1.0429	1.11E+27
967.867	1.6178	1.6629	0.0653	0.8307	0.8210	5.51E-06	1.0413	1.63E+27
992.867	1.6596	1.7059	0.0642	0.8293	0.8196	7.98E-06	1.0398	2.36E+27
1017.867	1.7014	1.7488	0.0631	0.8280	0.8182	1.14E-05	1.0383	3.37E+27
1042.867	1.7432	1.7918	0.0621	0.8267	0.8169	1.61E-05	1.0369	4.75E+27
1067.867	1.7850	1.8347	0.0610	0.8254	0.8156	2.26E-05	1.0356	6.63E+27
1092.867	1.8268	1.8777	0.0601	0.8242	0.8143	3.12E-05	1.0344	9.16E+27
1117.867	1.8685	1.9206	0.0591	0.8231	0.8131	4.27E-05	1.0333	1.25E+28
1142.867	1.9103	1.9636	0.0582	0.8219	0.8119	5.78E-05	1.0322	1.69E+28
1167.867	1.9521	2.0065	0.0573	0.8208	0.8108	7.76E-05	1.0312	2.27E+28
1192.867	1.9939	2.0495	0.0564	0.8197	0.8096	1.03E-04	1.0302	3.02E+28
1217.867	2.0357	2.0924	0.0556	0.8187	0.8085	1.36E-04	1.0292	3.98E+28
1242.867	2.0775	2.1354	0.0548	0.8177	0.8075	1.78E-04	1.0284	5.20E+28

Table A.6: Calculated values for the loss of CH₃ from [Zn(acac)₂]⁺.

An average rate constant can then be calculated using a Boltzmann distribution shown in Equation A.13

$$k_{uni} = \frac{\sum_i k_i e^{-E_i / RT}}{\sum_i e^{-E_i / RT}} \quad [A.13]$$

For E=317.867

Numerator term:

$$3.16 * 10^{19} * e^{-317.867 / 8.314 * 298} = 2.78 * 10^{19}$$

Denominator term:

$$e^{-317.867 / 8.314 * 298} = 0.879591$$

These numerator and denominator terms are calculated for each value of E. The terms are then summed together and divided to determine the average rate constant. The numerator and denominator terms for each value of E are summarized below in Table A.7.

Energy (kJ)	Rate constant (s^{-1})	Numerator term	Denominator term
292.867	9.05E+18	8.04E+18	0.888512
317.867	3.16E+19	2.78E+19	0.879591
342.867	1.03E+20	8.97E+19	0.870761
367.867	3.15E+20	2.71E+20	0.862018
392.867	9.06E+20	7.73E+20	0.853364
417.867	2.47E+21	2.08E+21	0.844796
442.867	6.37E+21	5.33E+21	0.836315
467.867	1.55E+22	1.28E+22	0.827918
492.867	3.67E+22	3.01E+22	0.819606
517.867	8.33E+22	6.76E+22	0.811377
542.867	1.82E+23	1.46E+23	0.803231
567.867	3.82E+23	3.03E+23	0.795167
592.867	7.74E+23	6.1E+23	0.787184
617.867	1.52E+24	1.19E+24	0.779281
642.867	2.90E+24	2.24E+24	0.771457
667.867	5.37E+24	4.1E+24	0.763712
692.867	9.68E+24	7.32E+24	0.756044
717.867	1.70E+25	1.28E+25	0.748454
742.867	2.93E+25	2.17E+25	0.740939
767.867	4.92E+25	3.61E+25	0.7335
792.867	8.10E+25	5.88E+25	0.726136
817.867	1.31E+26	9.41E+25	0.718846
842.867	2.07E+26	1.48E+26	0.711629
867.867	3.23E+26	2.28E+26	0.704484
892.867	4.95E+26	3.45E+26	0.697411
917.867	7.47E+26	5.16E+26	0.69041
942.867	1.11E+27	7.59E+26	0.683478
967.867	1.63E+27	1.1E+27	0.676616
992.867	2.36E+27	1.58E+27	0.669823
1017.867	3.37E+27	2.23E+27	0.663098
1042.867	4.75E+27	3.12E+27	0.656441
1067.867	6.63E+27	4.31E+27	0.64985
1092.867	9.16E+27	5.89E+27	0.643326
1117.867	1.25E+28	7.97E+27	0.636867
1142.867	1.69E+28	1.07E+28	0.630473
1167.867	2.27E+28	1.42E+28	0.624143
1192.867	3.02E+28	1.86E+28	0.617877
1217.867	3.98E+28	2.43E+28	0.611673
1242.867	5.20E+28	3.15E+28	0.605532
1267.867	6.74E+28	4.04E+28	0.599453

Table A.7: Determination of Average Rate Constant for loss of CH_3 from $[\text{Zn}(\text{acac})_2]^+$.

Numerator sum=1.68E+29, Denominator sum = 29.39079

Average rate constant

$$k_{any} = \frac{1.68 * 10^{29}}{29.39079} = 5.1937 * 10^{27} s^{-1}$$

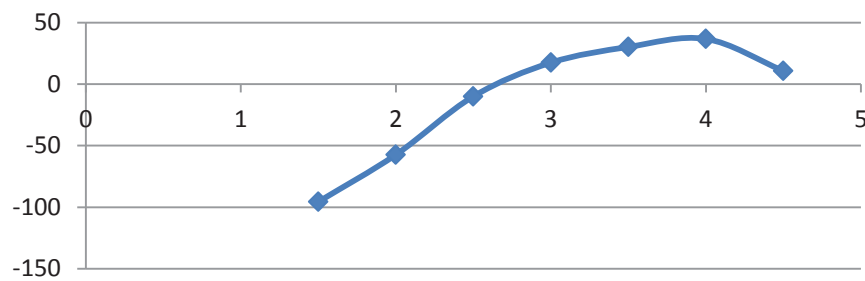
This same method is applied for all rate constant determinations discussed in this study.

Appendix B: Bond Length vs. Heat of Formation Data

B.1 C-CH₃ stretch for [Cu(acac)₂]⁺.

Bond Length (Å)	Heat of Formation (kcal/mol)
1.5	-95.622
2	-57.361
2.5	-9.993
3	17.422
3.5	30.17
4	36.701
4.5	10.769

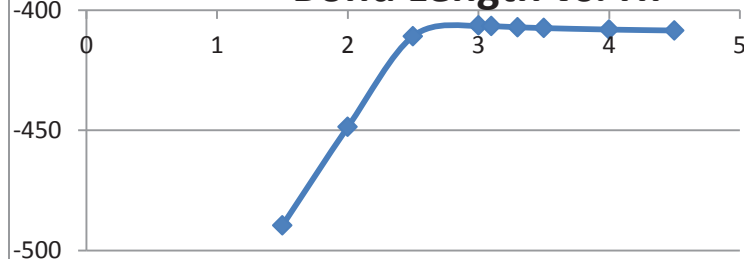
Bond length vs. Hf



B.2 C-CH₃ stretch for [Ni(acac)₂]⁺.

Bond Length (Å)	Heat of Formation (kcal/mol)
1.5	-489.56
2	-448.6
2.5	-410.754
3	-406.339
3.1	-406.564
3.3	-407.027
3.5	-407.395
4	-408.006
4.5	-408.404

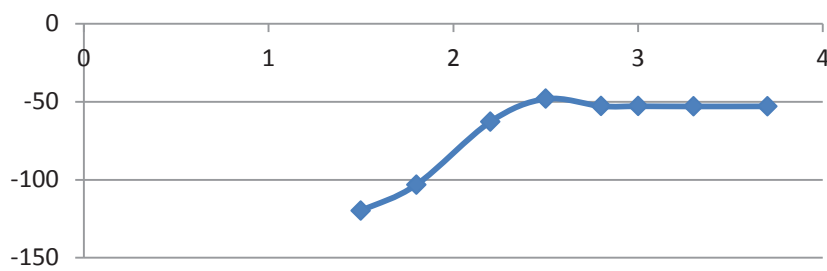
Bond Length vs. Hf



B.3 C-CH₃ Stretch for [Zn(acac)₂]⁺

Bond Length (Å)	Heat of Formation (kcal/mol)
1.5	-119.862
1.8	-103.177
2.2	-62.895
2.5	-48.236
2.8	-52.83
3	-52.908
3.3	-53.046
3.7	-52.973

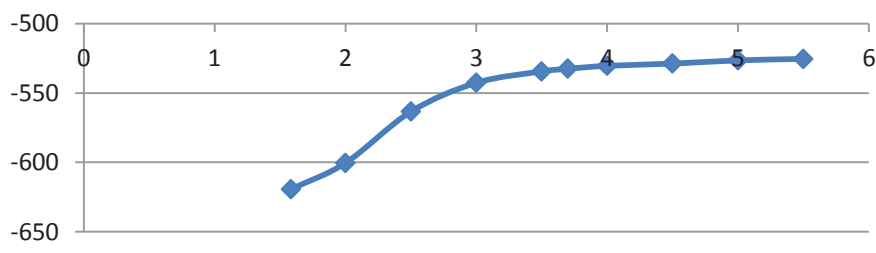
Bond Length vs. Hf



B.4 C-CF₃ stretch for [Cu(hfac)₂]⁺.

Bond Length (Å)	Heat of Formation (kcal/mol)
1.584	-619.344
2	-600.441
2.5	-563.459
3	-542.701
3.5	-534.472
3.7	-532.575
4	-530.462
4.5	-528.87
5	-526.528
5.5	-525.448

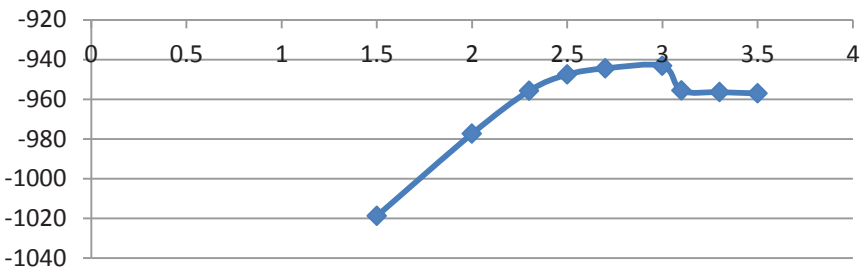
Bond Length vs. Hf



B.5 C-CF₃ stretch for [Ni(hfac)₂]⁺.

Bond Length (Å)	Heat of Formation (kcal/mol)
1.5	-1018.79
2	-977.34
2.3	-955.733
2.5	-947.575
2.7	-944.457
3	-943.203
3.1	-955.622
3.3	-956.415
3.5	-957.036
4	-961.281

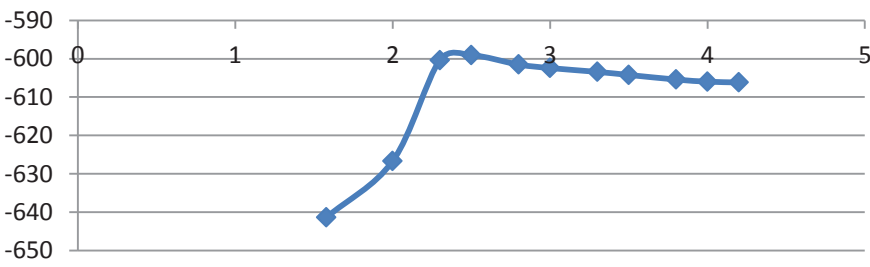
Bond Length vs. Hf



B.6 C-CF₃ stretch for [Zn(hfac)₂]⁺.

Bond Length (Å)	Heat of Formation (kcal/mol)
1.578	-641.406
2	-626.704
2.3	-600.385
2.5	-599.049
2.8	-601.511
3	-602.434
3.3	-603.433
3.5	-604.232
3.8	-605.429
4	-605.982

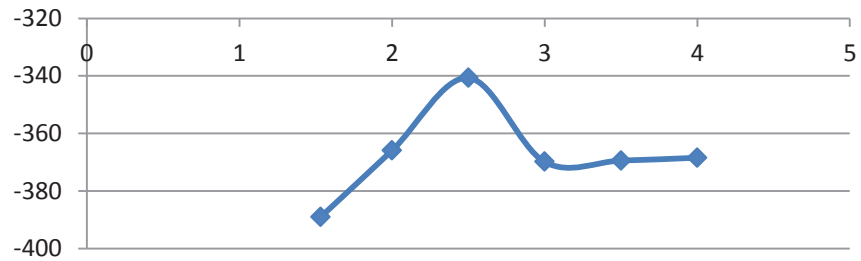
Bond Length vs. Hf



B.7 C-*t*Bu stretch for $[\text{Cu}(\text{tfm})_2]^+$.

Bond Length (Å)	Heat of Formation (kcal/mol)
1.532	-389.026
2	-365.928
2.5	-340.657
3	-369.86
3.5	-369.42
4	-368.425

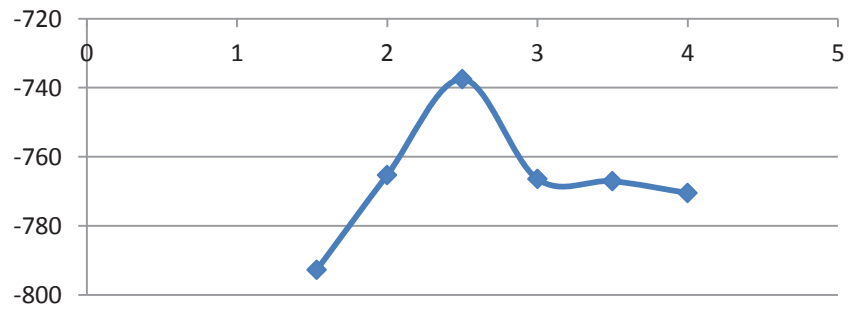
Bond Length vs. Hf



B.8 C-*t*Bu stretch for $[\text{Ni}(\text{tfm})_2]^+$.

Bond Length (Å)	Heat of Formation (kcal/mol)
1.531	-792.765
2	-765.283
2.5	-737.464
3	-766.446
3.5	-767.088
4	-770.497

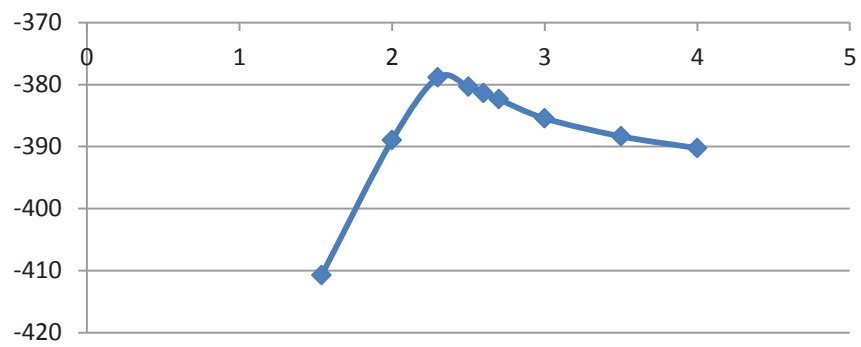
Bond Length vs. Hf



B.9 C-*t*Bu stretch for $[\text{Ni}(\text{tftm})_2]^+$.

Bond Length (Å)	Heat of Formation (kcal/mol)
1.539	-411.405
2	-388.983
2.3	-378.88
2.5	-380.376
3	-385.445
3.5	-388.347
4	-390.254

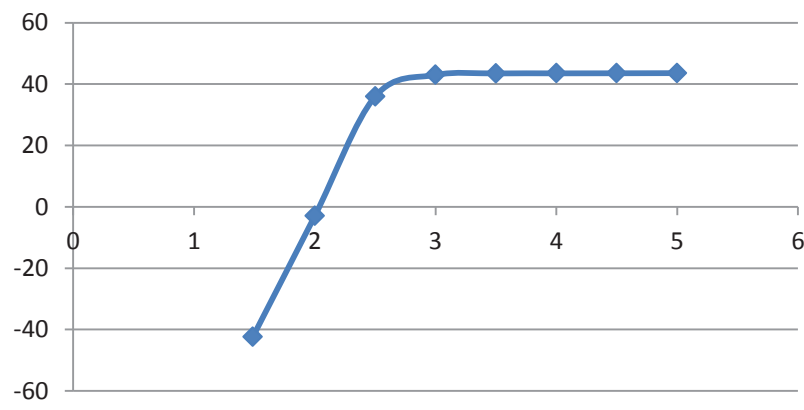
Bond Length vs. Hf



B.10 C-CH₃ stretch for $[\text{Cu}(\text{acac})(\text{acac-CH}_3)]^+$.

Bond Length (Å)	Heat of Formation (kcal/mol)
1.486	-42.433
2	-2.95
2.5	35.973
3	42.99
3.5	43.481
4	43.507
4.5	43.54
5	43.577

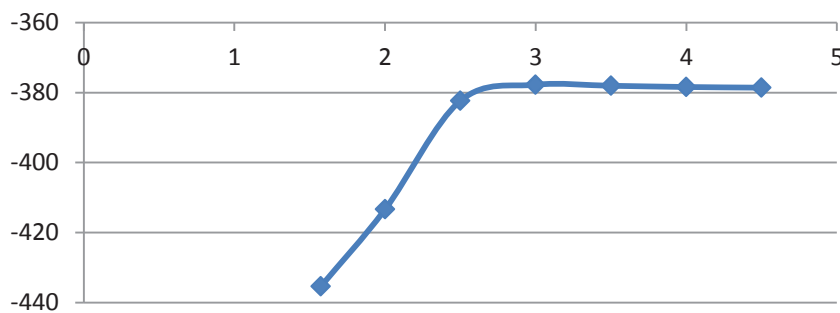
Bond Length vs Hf



B.11 C-CF₃ stretch for [Cu(hfac)(hfac-CF₃)]⁺.

Bond Length (Å)	Heat of Formation (kcal/mol)
1.573	-435.396
2	-413.37
2.5	-382.356
3	-377.765
3.5	-378.065
4	-378.413
4.5	-378.602

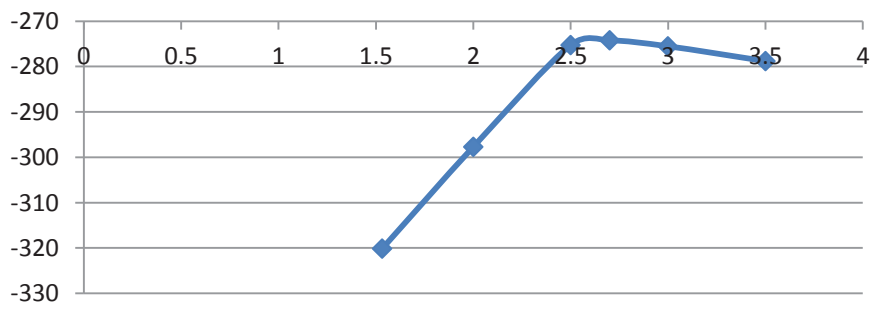
Bond Length vs. Hf



B.12 C-tBu stretch for [Cu(tftm)(tftm-tBu)]⁺.

Bond Length (Å)	Heat of Formation (kcal/mol)
1.532	-320.12
2	-297.686
2.5	-275.25
2.7	-274.226
3	-275.53
3.5	-278.802

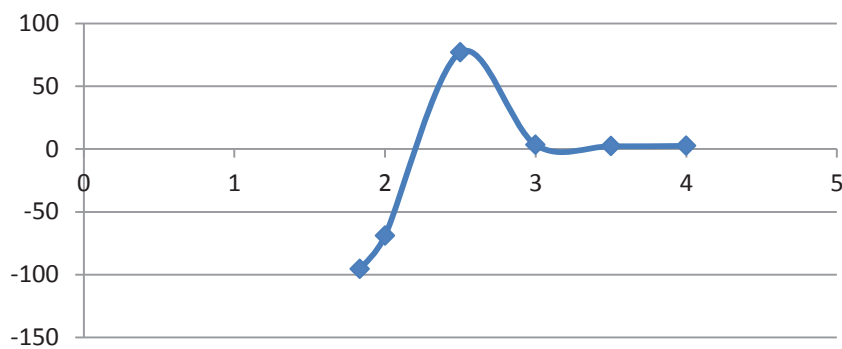
Bond Length vs. hf



B.13 Ligand stretch for $[\text{Cu}(\text{acac})_2]^+$.

Bond Length (Å)	Heat of Formation (kcal/mol)
1.833	-95.624
2	-68.945
2.5	76.976
3	3.352
3.5	2.228
4	2.534

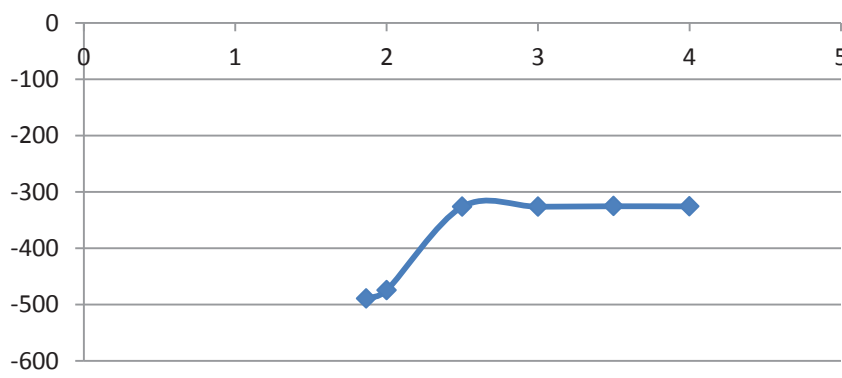
Bond Length vs. Hf



B.14 Ligand stretch for $[\text{Ni}(\text{acac})_2]^+$.

Bond Length (Å)	Heat of Formation (kcal/mol)
1.866	-489.56
2	-474.651
2.5	-326.249
3	-326.249
3.5	-325.425
4	-325.643

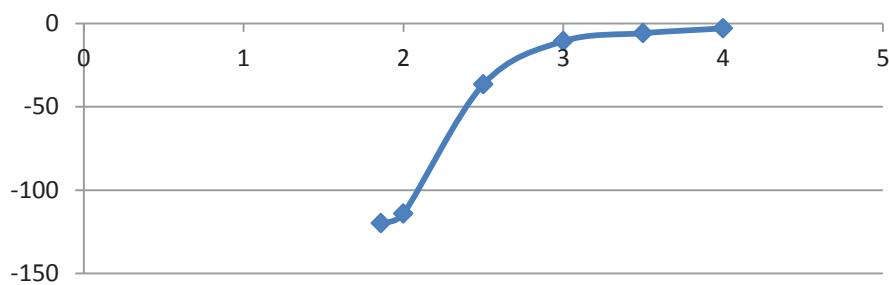
Bond Length Vs. Hf



B.15 Ligand stretch for $[\text{Zn}(\text{acac})_2]^+$.

Bond Length (\AA)	Heat of Formation (kcal/mol)
1.86	-119.861
2	-114.057
2.5	-36.541
3	-10.698
3.5	-5.862
4	-3.000

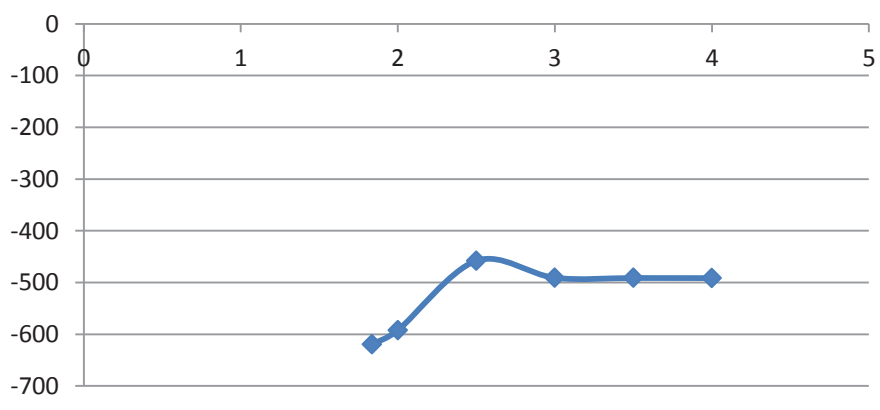
Bond Length vs. Hf



B.16 Ligand stretch for $[\text{Cu}(\text{hfac})_2]^+$.

Bond Length (\AA)	Heat of Formation (kcal/mol)
1.835	-619.344
2	-592.308
2.5	-457.914
3	-490.873
3.5	-491.213
4	-491.421

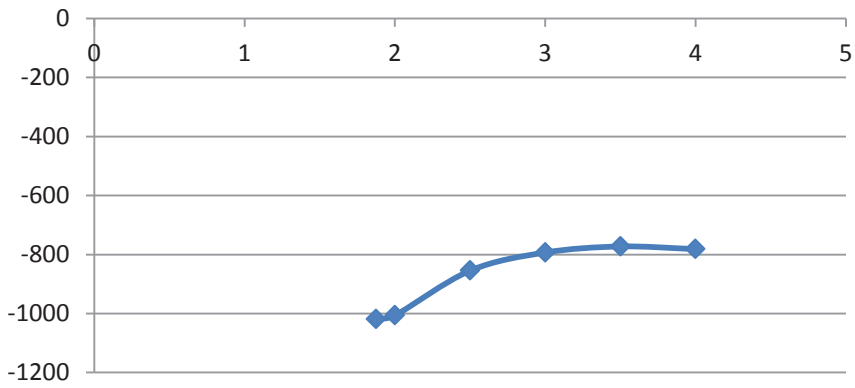
Bond Length vs. Hf



B.17 Ligand stretch for $[\text{Ni}(\text{hfac})_2]^+$.

Bond Length (\AA)	Heat of Formation (kcal/mol)
1.875	-1018.78
2	-1006.35
2.5	-854.624
3	-793.142
3.5	-772.738
4	-781.622

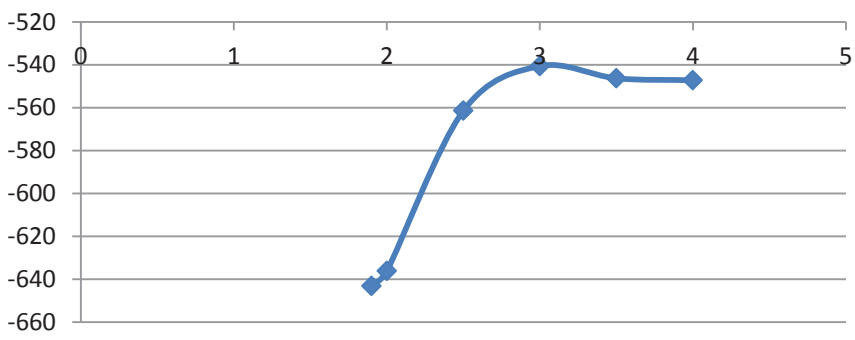
Bond Length vs. Hf



B.18 Ligand stretch for $[\text{Zn}(\text{hfac})_2]^+$.

Bond Length (\AA)	Heat of Formation (kcal/mol)
1.9	-643.258
2	-636.267
2.5	-561.508
3	-540.651
3.5	-546.336
4	-547.225

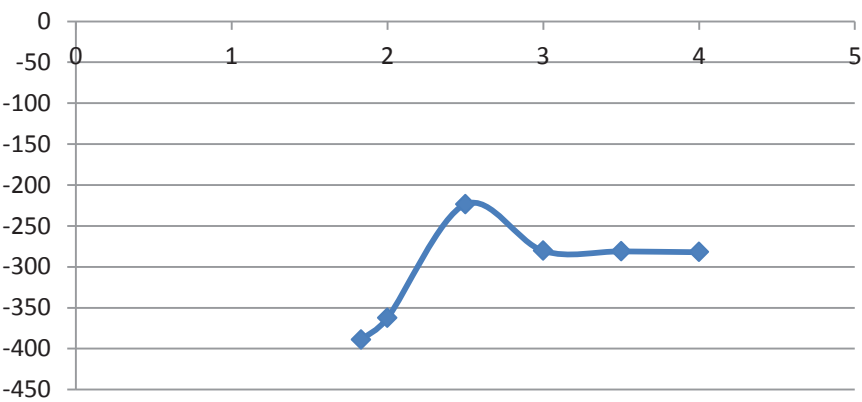
Bond Length vs. Hf



B.19 Ligand stretch for $[\text{Cu}(\text{tftm})_2]^+$.

Bond Length (\AA)	Heat of Formation (kcal/mol)
1.9	-643.258
2	-636.267
2.5	-561.508
3	-540.651
3.5	-546.336
4	-547.225

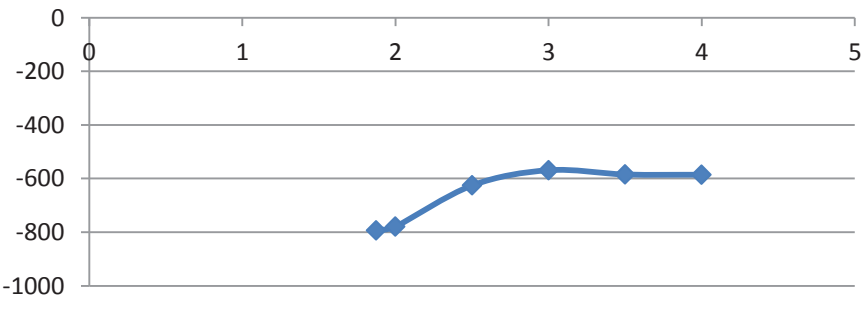
Bond Length vs. Hf



B.20 Ligand stretch for $[\text{Ni}(\text{tftm})_2]^+$.

Bond Length (\AA)	Heat of Formation (kcal/mol)
1.9	-643.258
2	-636.267
2.5	-561.508
3	-540.651
3.5	-546.336
4	-547.225

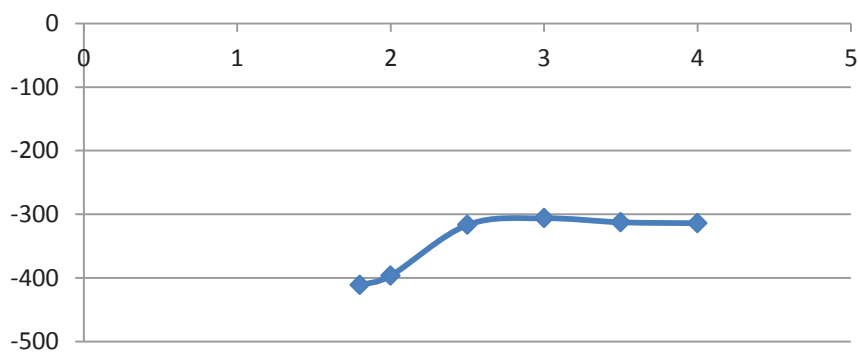
Bond Length vs. Hf



B.21 Ligand stretch for $[\text{Zn}(\text{tftm})_2]^+$.

Bond Length (\AA)	Heat of Formation (kcal/mol)
1.8	-411.405
2	-396.614
2.5	-316.714
3	-306.246
3.5	-312.529
4	-314.021

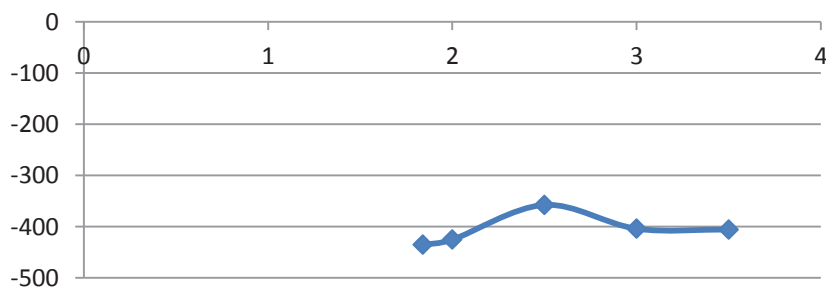
Bond Length vs. Hf



B.22 Hfac stretch for $[\text{Cu}(\text{hfac})(\text{hfac-CF}_3)]^+$.

Bond Length (\AA)	Heat of Formation (kcal/mol)
1.8	-411.405
2	-396.614
2.5	-316.714
3	-306.246
3.5	-312.529
4	-314.021

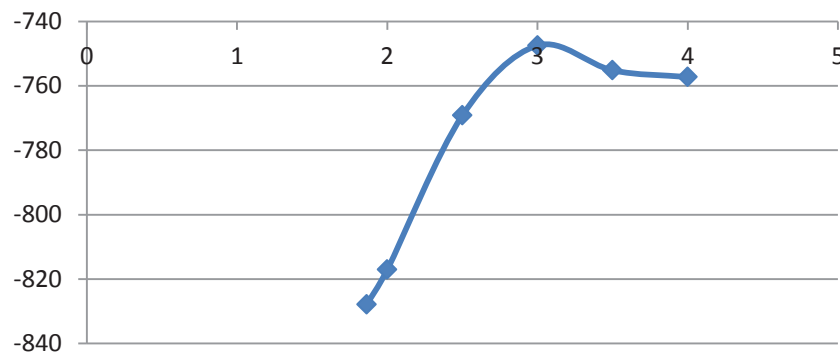
Bond Length vs. Hf



B.23 Hfac stretch for $[\text{Ni}(\text{hfac})(\text{hfac-CF}_3)]^+$.

Bond Length (\AA)	Heat of Formation (kcal/mol)
1.863	-827.863
2	-817.083
2.5	-769.211
3	-747.498
3.5	-755.182
4	-757.277

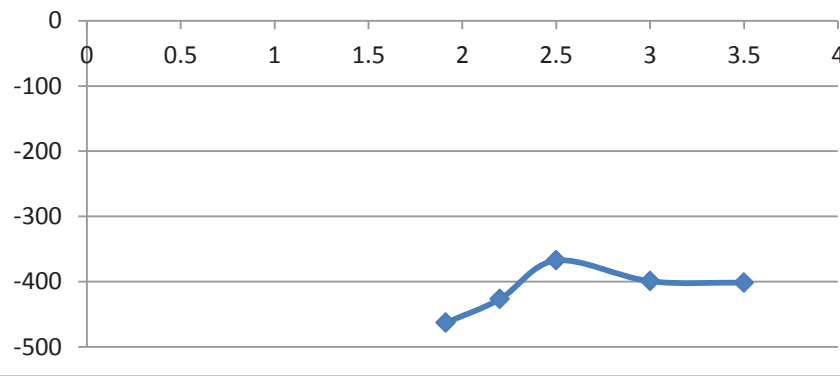
Bond Length vs. Hf



B.24 Hfac stretch for $[\text{Zn}(\text{hfac})(\text{hfac-CF}_3)]^+$.

Bond Length (\AA)	Heat of Formation (kcal/mol)
1.911	-463.165
2.2	-426.684
2.5	-367.563
3	-399.352
3.5	-401.555

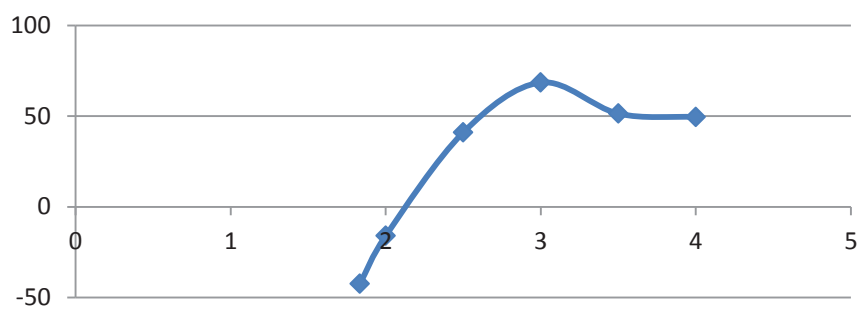
Bond Length vs. Hf



B.25 Acac stretch for $[\text{Cu}(\text{acac})(\text{acac-CH}_3)]^+$.

Bond Length (\AA)	Heat of Formation (kcal/mol)
1.833	-42.432
2	-15.9587
2.5	41.005
3	68.516
3.5	51.3807
4	49.489

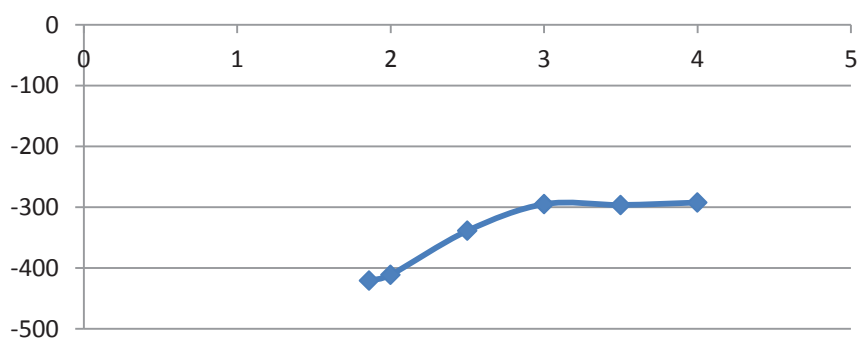
Bond Length vs. Hf



B.26 Acac stretch for $[\text{Ni}(\text{acac})(\text{acac-CH}_3)]^+$.

Bond Length (\AA)	Heat of Formation (kcal/mol)
1.86	-420.797
2	-411.19
2.5	-338.786
3	-295.043
3.5	-296.341
4	-292.341

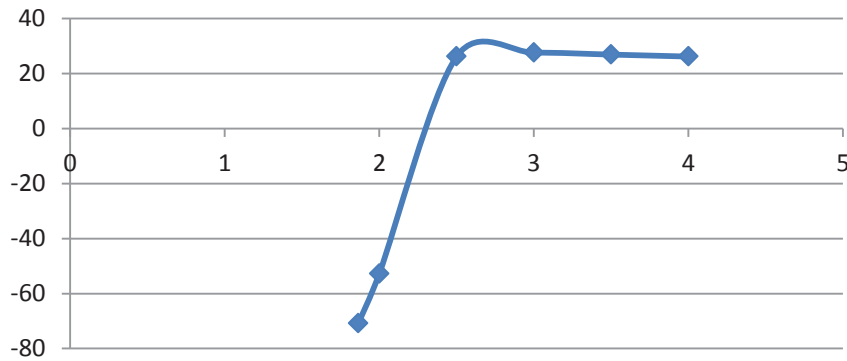
Bond Length vs. Hf



B.27 Acac stretch for $[\text{Zn}(\text{acac})(\text{acac-CH}_3)]^+$.

Bond Length (\AA)	Heat of Formation (kcal/mol)
1.864	-70.841
2	-52.731
2.5	26.122
3	27.519
3.5	26.845
4	26.128

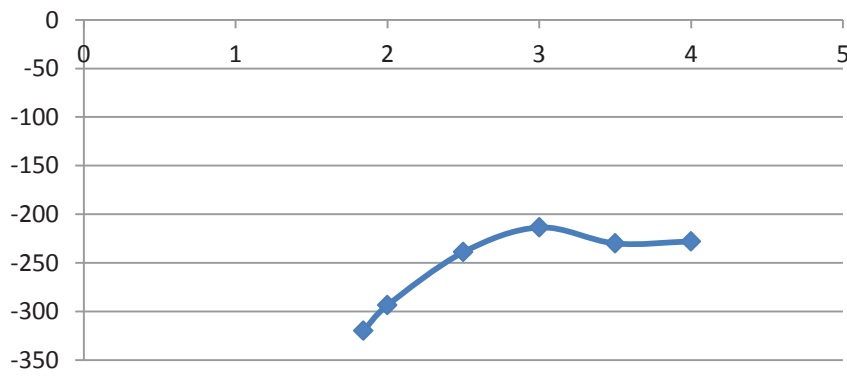
Bond Length vs. Hf



B.28 Tfpm stretch for $[\text{Cu}(\text{tfpm})(\text{tfpm-}t\text{Bu})]^+$.

Bond Length (\AA)	Heat of Formation (kcal/mol)
1.842	-320.119
2	-293.713
2.5	-239.056
3	-213.607
3.5	-230.02
4	-227.981

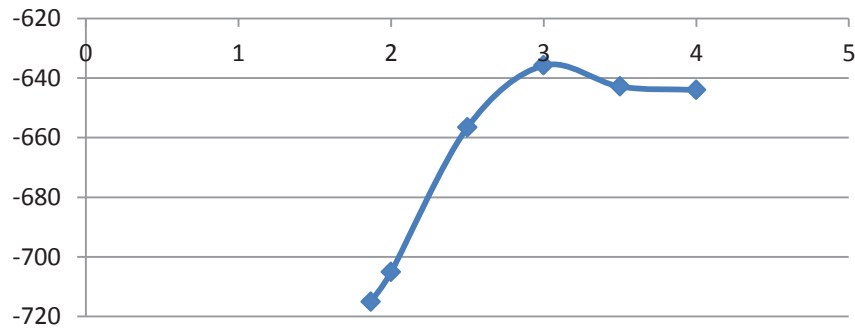
Bond Length vs. Hf



B.29 Tf_{tm} stretch for [Ni(tftm)(tftm-tBu)]⁺.

Bond Length (Å)	Heat of Formation (kcal/mol)
1.867	-715.091
2	-705.105
2.5	-656.598
3	-635.812
3.5	-642.855
4	-643.992

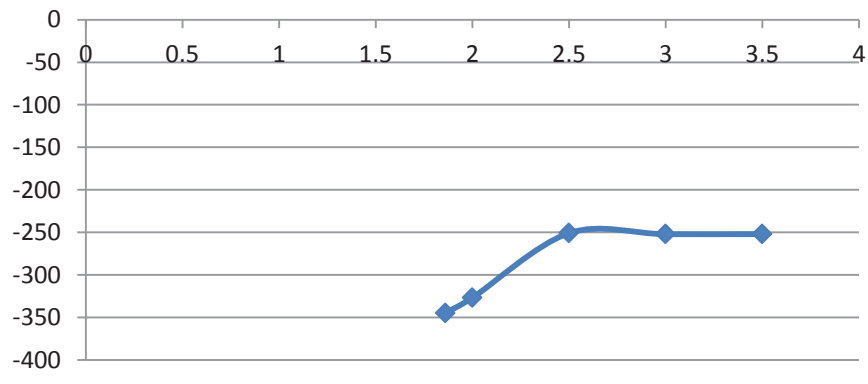
Bond Length vs. Hf



B.30 Tf_{tm} stretch for [Zn(tftm)(tftm-tBu)]⁺.

Bond Length (Å)	Heat of Formation (kcal/mol)
1.86	-344.95
2	-326.967
2.5	-250.929
3	-252.191
3.5	-252.089

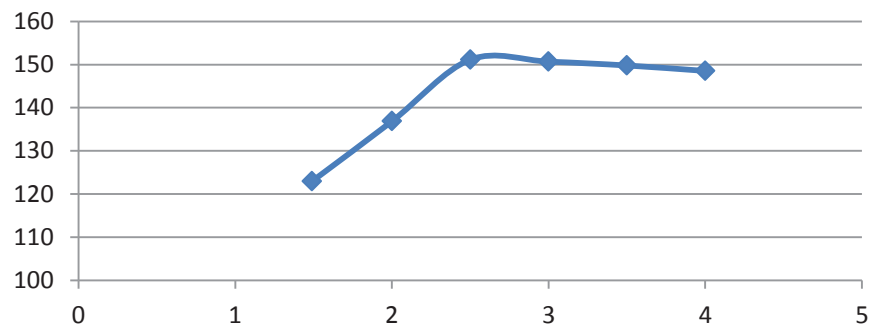
Bond Length vs. Hf



B.31 C-CH₃ stretching for [Cu(acac)]⁺.

Bond Length (Å)	Heat of Formation (kcal/mol)
1.49	122.963
2	136.855
2.5	151.136
3	150.674
3.5	149.7854
4	148.524

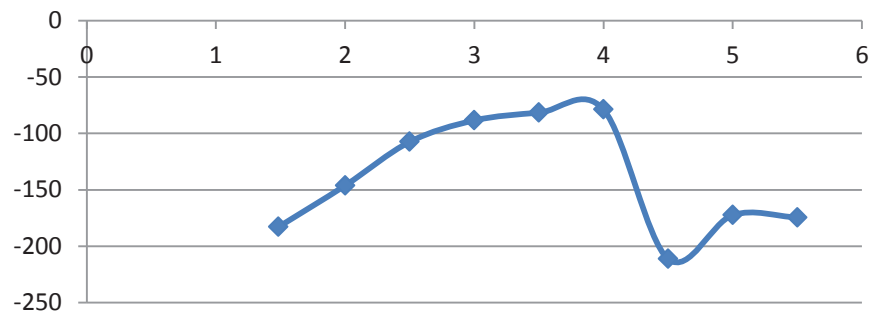
Bond Length vs. Heat of Formation



B.32 C-CH₃ stretching for [Ni(acac)]⁺.

Bond Length (Å)	Heat of Formation (kcal/mol)
1.483	-182.907
2	-146.138
2.5	-107.458
3	-88.471
3.5	-81.631
4	-78.908
4.5	-211.187
5	-172.386
5.5	-174.462

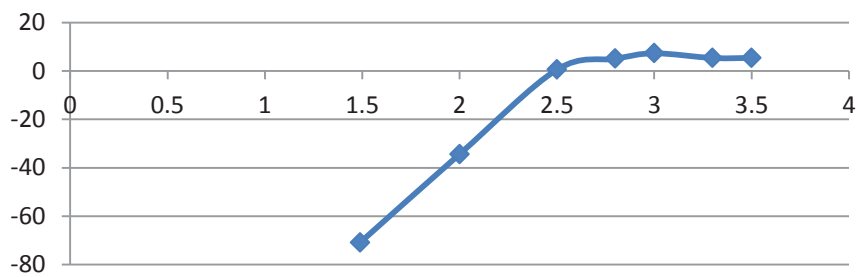
Bond length vs. Heat of Formation



B.33 C-CH₃ stretching for [Zn(acac)]⁺.

Bond Length (Å)	Heat of Formation (kcal/mol)
1.489	-70.841
2	-34.353
2.5	0.557
2.8	5.034
3	7.295
3.3	5.355
3.5	5.402

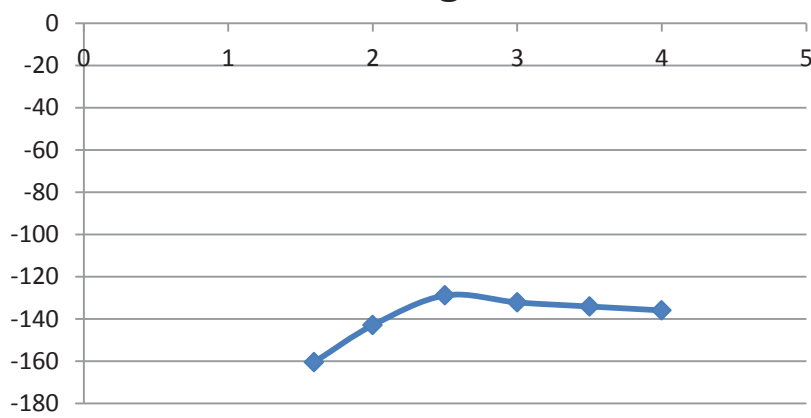
Bond Length vs. Hf



B.34 C-CF₃ stretching for [Cu(hfac)]⁺.

Bond Length (Å)	Heat of Formation (kcal/mol)
1.593	-160.569
2	-143.011
2.5	-128.917
3	-132.222
3.5	-134.143
4	-135.985

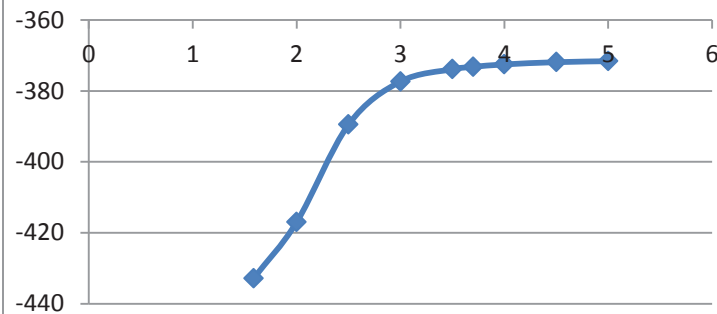
Bond Length vs. Hf



B.35 C-CF₃ stretching for [Ni(hfac)]⁺.

Bond Length (Å)	Heat of Formation (kcal/mol)
1.586	-432.845
2	-417.007
2.5	-389.463
3	-377.328
3.5	-373.869
3.7	-373.194
4	-372.505
4.5	-371.873
5	-371.601

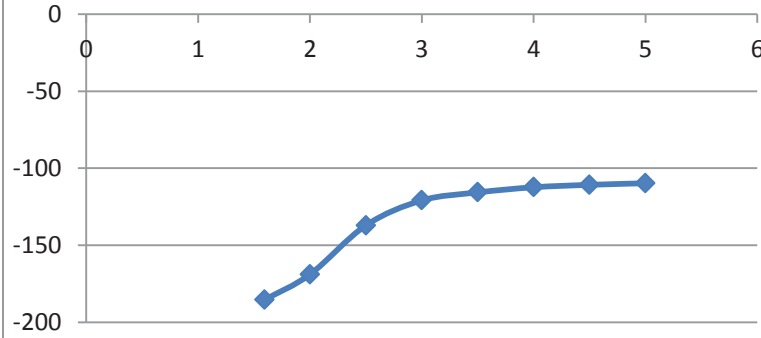
Bond Length vs. Hf



B.36 C-CF₃ stretching for [Zn(hfac)]⁺.

Bond Length (Å)	Heat of Formation (kcal/mol)
1.593	-185.476
2	-168.932
2.5	-137.119
3	-120.899
3.5	-115.709
4	-112.359
4.5	-110.776
5	-109.753

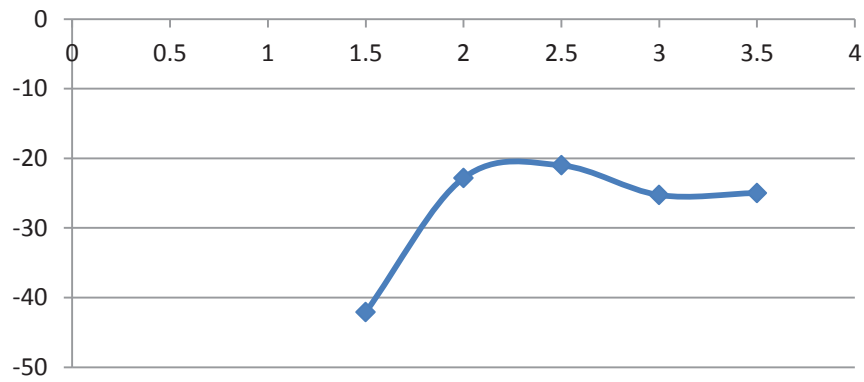
Bond Length vs. Hf



B.37 C-*t*Bu stretching for $[\text{Cu}(\text{tftm})]^+$.

Bond Length (\AA)	Heat of Formation (kcal/mol)
1.5	-42.079
2	-22.8217
2.5	-21.012
3	-25.267
3.5	-24.971

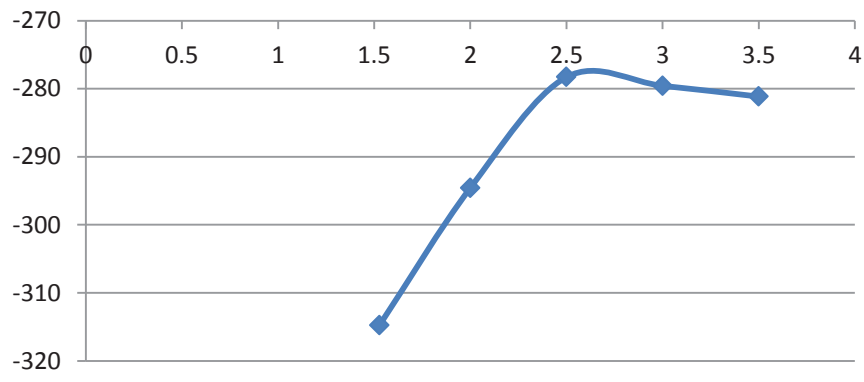
Bond Length vs. Hf



B.38 C-*t*Bu stretching for $[\text{Ni}(\text{tftm})]^+$.

Bond Length (\AA)	Heat of Formation (kcal/mol)
1.527	-314.774
2	-294.575
2.5	-278.29
3	-279.568
3.5	-281.152

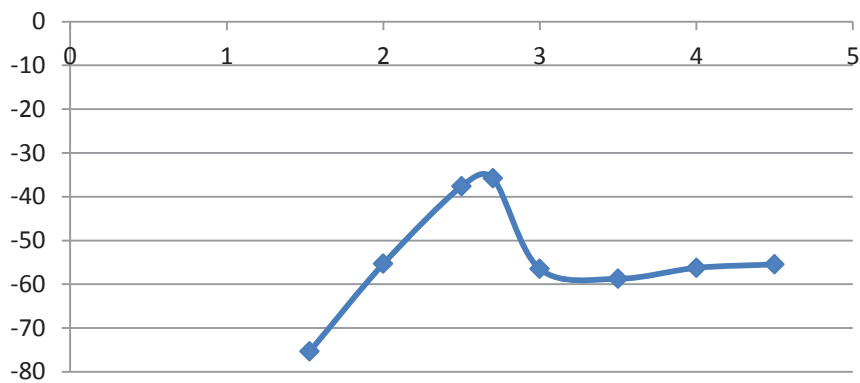
Bond Length vs. Hf



B.39 C-*t*Bu stretching for $[\text{Zn}(\text{tfm})]^+$.

Bond Length (\AA)	Heat of Formation (kcal/mol)
1.53	-75.339
2	-55.339
2.5	-37.613
2.7	-35.772
3	-56.5038
3.5	-58.753
4	-56.255
4.5	-55.452

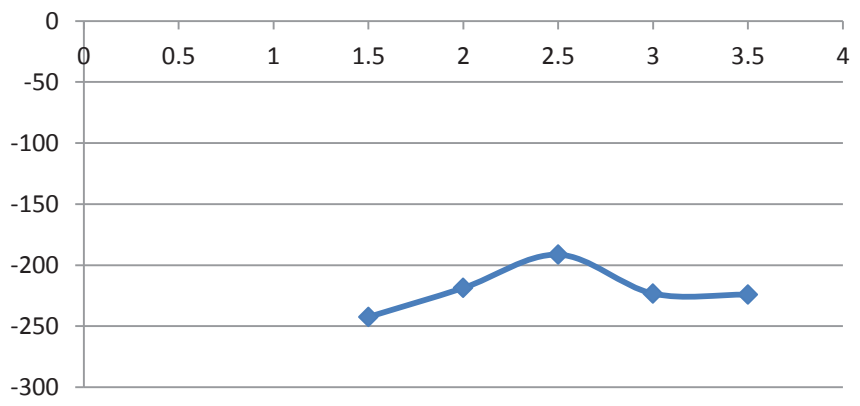
Bond Length vs. Hf



B.40 C-*t*Bu stretching for $[\text{Cu}(\text{acac})(\text{tfm})]^+$.

Bond Length (\AA)	Heat of Formation (kcal/mol)
1.5	-242.477
2	-218.699
2.5	-191.43
3	-223.327
3.5	-224.148

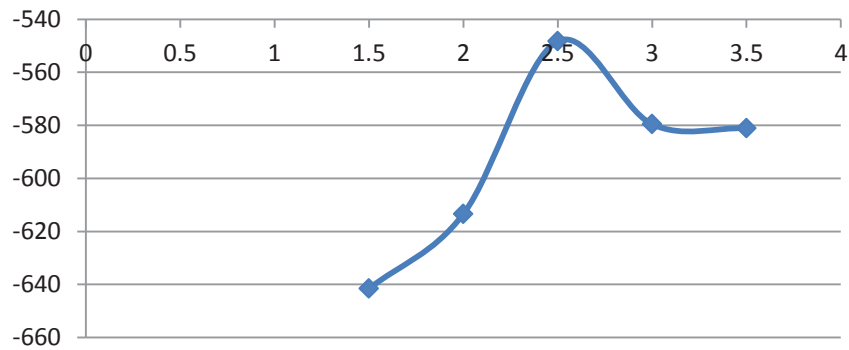
Bond Length vs. Hf



B.41 C-*t*Bu stretching for $[\text{Ni}(\text{acac})(\text{tfm})]^+$.

Bond Length (Å)	Heat of Formation (kcal/mol)
1.5	-641.616
2	-613.451
2.5	-548.258
3	-579.566
3.5	-581.111

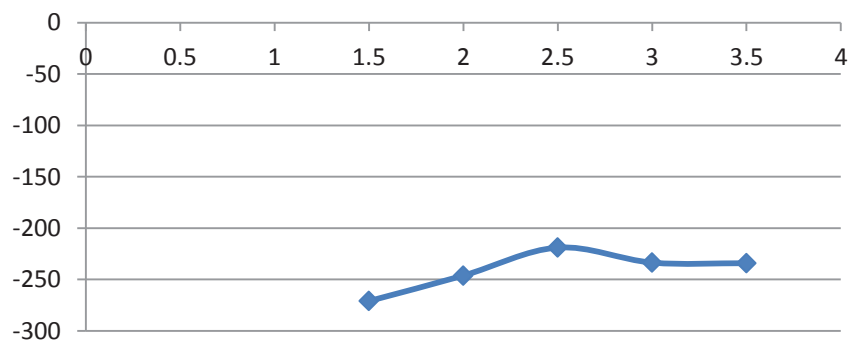
Bond Length vs. Hf



B.42 C-*t*Bu stretching for $[\text{Zn}(\text{acac})(\text{tfm})]^+$.

Bond Length (Å)	Heat of Formation (kcal/mol)
1.5	-271.026
2	-246.228
2.5	-218.964
3	-233.604
3.5	-234.188

Bond Length vs. Hf



Appendix C: Vibrational Frequency Tables

Table C.1: Vibrational frequencies (cm^{-1}) for the loss of CH_3 from $[\text{Ni}(\text{acac})_2]^+$.

$[\text{Ni}(\text{acac})_2]^+$			$[[\text{Ni}(\text{acac})_2]^+]^\ddagger$		
67.03	875.368	1360.989	-127.372	614.463	1358.949
97.315	881.841	1374.02	57.784	667.017	1359.747
115.615	914.094	1375.759	69.941	759.489	1360.216
120.572	929.855	1383.066	103.792	790.674	1366.038
123.542	947.652	1385.787	108.447	855.375	1376.273
124.723	963.126	1423.268	111.094	865.135	1378.942
130.512	967.255	1438.146	118.121	888.346	1425.781
132.91	975.064	1460.547	122.578	932.955	1439.869
135.291	977.395	1474.186	129.854	947.018	1476.017
187.609	981.808	1570.101	131.495	954.307	1564.573
222.345	988.707	1598.983	153.904	968.688	1573.081
252.333	1005.571	1601.373	184.254	977.066	1621.161
300.929	1015.152	1608.14	225.314	985.579	1683.786
318.772	1020.455	2974.45	265.351	998.105	2974.572
359.953	1034.44	2975.61	273.167	1001.076	2990.32
371.176	1047.716	3056.91	296.313	1013.75	3050.809
394.135	1054.303	3057.12	336.246	1031.82	3056.951
420.369	1125.386	3057.795	338.567	1052.69	3058.463
450.329	1175.786	3057.989	350.41	1073.451	3073.815
376.785	1178.916	3079.402	380.147	1117.702	3078.447
506.842	1331.572	3079.533	394.397	1170.508	3078.971
557.315	1333.348	3079.649	406.557	1266.821	3150.575
566.884	1340.657	3079.766	455.313	1278.228	3155.907
580.561	1341.867	3156.49	466.475	1311.478	3156.521
628.962	1359.247	3156.962	522.77	1331.559	3171.661
656.693	1359.648	3157.042	563.491	1339.247	3255.312
700.726	1360.214	3157.951	574.477	1346.483	3258.448

Table C.2: Vibrational frequencies (cm^{-1}) for the loss of CH_3 from $[\text{Cu}(\text{acac})_2]^+$.

$[\text{Cu}(\text{acac})_2]^+$			$[[\text{Cu}(\text{acac})_2]^+]^\ddagger$		
46.362	865.899	1368.726	-93.529	615.964	1375.573
58.52	866.528	1376.958	43.759	630.505	1377.51
68.781	916.636	1378.472	49.22	693.629	1377.677
105.507	961.186	1390.615	55.091	838.377	1380.635
113.351	964.913	1390.96	74.944	860.035	1395.297
118.719	980.854	1445.351	79.128	905.511	1408.708
120.239	985.18	1451.37	81.222	942.64	1451.208
123.842	985.311	1451.464	118.131	974.946	1469.913
133.042	998.724	1453.163	124.153	991.441	1484.707
158.308	1004.95	1630.134	131.06	992.803	1611.177
169.711	1017.296	1642.346	142.633	1002.428	1637.206
183.679	1018.882	1718.29	143.655	1005.547	1730.459
219.552	1028.364	1723.802	162.226	1019.483	1761.216
280.277	1085.135	3042.924	185.059	1020.264	3056.454
281.68	1106.496	3043.445	200.058	1075.255	3067.025
304.408	1118.166	3057.547	205.683	1086.352	3068.047
348.585	1145.519	3057.548	224.595	1113.864	3069.332
392.07	1163.391	3057.686	271.634	1142.488	3077.917
407.562	1176.143	3057.734	280.697	1156.971	3078.114
416.716	1275.087	3072.481	329.389	1174.579	3081.128
434.827	1341.549	3072.618	382.31	1239.155	3094.714
541.223	1344.077	3072.662	393.672	1257.408	3103.135
542.047	1346.188	3072.849	407.167	1257.527	3164.546
587.386	1347.45	3156.64	437.492	1263.988	3165.017
624.749	1368.24	3156.822	456.275	1348.725	3168.124
629.057	1368.28	3157.249	544.421	1356.013	3213.211
632.672	1368.642	3157.793	601.419	1365.699	3214.019

Table C.3: Vibrational frequencies (cm^{-1}) for the loss of CH_3 from $[\text{Zn}(\text{acac})_2]^+$.

$[\text{Zn}(\text{acac})_2]^+$			$[[\text{Zn}(\text{acac})_2]^+]^\ddagger$		
84.269	736.72	1373.148	-162.702	596.051	1360.989
25.808	864.163	1374.795	45.767	629.303	1375.259
21.916	917.394	1374.953	51.935	634.522	1375.505
31.646	945.007	1375.664	53.373	672.385	1378.456
36.284	952.911	1393.323	80.036	827.755	1381.243
58.346	957.677	1402.603	83.209	863.338	1393.192
104.859	975.355	1444.131	105.345	923.859	1456.634
176.697	978.889	1470.604	126.781	943.444	1461.475
179.343	982.626	1511.591	137.915	966.113	1479.272
181.389	992.805	1626.876	143.644	978.905	1656.331
185.604	996.283	1714.372	144.153	985.783	1657.82
205.556	1024.227	1774.616	155.279	987.009	1713.208
210.089	1032.063	1827.24	164.604	992.347	2104.661
216.578	1070.853	3005.369	195.112	993.325	3016.508
264.284	1082.974	3036.283	195.687	1025.203	3052.462
290.308	1115.679	3036.454	208.895	1074.474	3052.713
339.134	1120.533	3046.663	287.912	1079.753	3063.444
375.823	1131.649	3062.487	313.309	1084.382	3063.551
405.214	1160.542	3062.634	316.46	1121.779	3066.418
427.287	1175.598	3079.887	345.465	1129.501	3075.522
441.67	1313.303	3080.102	353.083	1178.344	3075.691
456.674	1334.355	3087.358	404.392	1263.342	3148.809
523.693	1342.884	3087.629	441.002	1270.639	3161.524
561.518	1350.188	3139.082	441.879	1310.073	3161.605
579.295	1352.046	3139.7	479.133	1343.135	3162.232
626.622	1356.622	3169.407	533.533	1344.25	3237.716
633.327	1356.888	3170.176	558.096	1351.17	3240.246

Tabel C.4: Vibrational frequencies (cm^{-1}) for the loss of CF_3 from $[\text{Ni(hfac)}_2]^+$.

$[\text{Ni(hfac)}_2]^+$			$[[\text{Ni(hfac)}_2]^+]^\ddagger$		
34.38	408.195	939.206	-53.023	364.336	965.944
37.455	416.481	991.065	14.307	370.705	1061.936
40.373	464.691	1077.136	16.265	392.165	1088.312
42.548	466.18	1149.178	22.086	402.952	1140.797
45.597	469.963	1161.691	23.48	416.772	1187.045
73.72	469.963	1317.944	30.164	427.514	1200.142
98.215	474.119	1319.164	33.424	428.037	1214.938
102.607	508.843	1321.019	42.941	463.507	1311.357
108.114	533.334	1324.924	44.111	470.924	1330.98
110.867	543.756	1378.284	47.133	492.829	1338.986
122.053	556.197	1385.98	77.875	524.192	1366.877
200.382	556.67	1417.406	95.129	533.08	1391.079
218.22	607.736	1436.051	100.71	545.414	1459.194
225.161	621.965	1545.618	108.057	555.958	1571.245
227.106	697.196	1555.729	129.308	587.017	1572.872
232.784	701.456	1563.726	137.357	618.772	1585.316
243.425	723.313	1570.191	144.698	664.572	1588.966
261.658	723.844	1586.467	215.192	686.776	1590.46
266.581	741.896	1589.097	221.872	693.664	1604.204
293.178	744.896	1592.962	226.846	699.715	1640.369
315.669	821.861	1600.854	243.158	706.279	1652.766
323.419	829.96	1601.062	250.013	783.837	1697.446
324.707	860.147	1602.004	264.679	819.397	1706.253
365.877	884.695	1605.432	277.536	866.387	1791.001
368.869	902.659	1609.31	300.693	891.385	1841.771
394.839	916.021	2938.553	334.937	916.341	2999.657
399.18	932.921	2941.148	339.069	936.714	3031.066

Tabel C.5: Vibrational frequencies (cm^{-1}) for the loss of CF_3 from $[\text{Cu(hfac)}_2]^+$.

$[\text{Cu(hfac)}_2]^+$			$[[\text{Cu(hfac)}_2]^+]^\ddagger$		
19.379	361.387	999.366	-48.15	359.208	980.274
19.833	383.607	1094.341	19.294	374.75	1054.537
19.947	395.362	1117.023	24.045	391.434	1079.051
20.124	414.983	1162.254	24.693	395.329	1108.972
20.355	463.679	1264.14	28.17	440.248	1160.575
34.387	463.991	1320.709	28.86	440.394	1209.746
39.799	489.97	1324.447	30.504	463.978	1245.576
86.858	493.623	1325.355	33.517	470.942	1323.703
89.682	522.213	1325.596	41.548	496.63	1352.773
91.145	523.023	1353.545	42.231	528.542	1378.469
98.015	535.934	1363.643	46.053	536.965	1378.723
104.554	546.628	1432.265	68.317	545.05	1475.523
137.161	601.987	1443.808	85.559	548.201	1483.525
155.527	612.82	1573.511	106.674	551.813	1560.826
156.524	684.118	1573.841	111.628	590.265	1562.894
180.111	687.651	1574.005	127.699	608.208	1568.599
221.385	694.756	1575.316	152.993	692.415	1570.148
229.056	695.315	1590.785	155.225	693.438	1581.016
244.614	706.946	1592.185	199.852	696.793	1582.907
252.478	708.267	1593.204	225.291	701.496	1621.307
273.952	854.335	1593.721	250.299	723.716	1678.294
276.015	863.827	1617.351	264.211	863.503	1747.765
279.194	939.036	1629.893	269.454	886.145	1789.834
279.896	940.153	1763.374	274.788	913.745	1797.703
329.085	974.031	1765.114	294.885	923.245	1797.879
344.486	976.655	3004.496	316.481	959.438	3018.904
355.038	981.719	3005.431	337.703	976.34	3083.396

Table C.6: Vibrational frequencies (cm^{-1}) for the loss of CF_3 from $[\text{Zn(hfac)}_2]^+$.

$[\text{Zn(hfac)}_2]^+$			$[[\text{Zn(hfac)}_2]^+]^\ddagger$		
22.537	352.28	966.17	-244.473	330.222	966.375
25.056	368.051	1045.658	24.008	353.588	1043.517
26.949	385.207	1061.362	25.519	366.641	1060.587
27.879	394.16	1163.146	26.017	393.029	1072.689
29.144	458.646	1184.669	27.185	399.288	1156.754
30.357	463.275	1203.39	28.142	425.256	1167.36
31.761	470.576	1307.44	30.884	432.117	1184.694
59.022	492.431	1309.753	32.522	444.138	1310.673
88.067	515.331	1316.494	48.398	463.912	1314.336
96.532	525.795	1342.893	66.806	470.606	1343.993
100.58	536.654	1368.848	87.067	492.407	1369.897
102.997	547.999	1452.741	96.079	524.63	1389.907
150.616	591.523	1456.443	97.775	526.145	1454.358
156.142	610.959	1569.822	107.654	548.239	1569.165
169.304	623.173	1570.156	117.671	567.809	1569.509
170.22	671.46	1577.539	151.203	622.256	1579.976
212.382	687.271	1579.273	153.283	623.193	1585.763
215.323	694.551	1586.322	165.797	668.036	1587.135
255.963	704.798	1587.204	182.373	694.206	1599.436
258.039	706.269	1605.712	212.343	704.716	1646.145
264.618	829.665	1607.591	214.399	706.478	1705.184
267.827	842.289	1646.335	257.843	793.768	1714.568
269.125	881.887	1764.27	262.076	872.512	1766.448
283.866	916.592	1767.548	271.866	881.98	1776.467
295.318	929.259	1828.915	283.863	887.277	1888.376
330.333	936.845	2962.484	293.236	919.17	2988.979
333.629	950.915	2988.326	321.889	936.902	2989.783

Table C.7: Vibrational frequencies (cm^{-1}) for the loss of *t*Bu from $[\text{Ni}(\text{tftm})_2]^+$.

$[\text{Ni}(\text{tftm})_2]^+$			$[[\text{Ni}(\text{tftm})_2]^+]$		
33.733	570.174	1387.718	-241.342	545.143	1359.184
42.2	591.314	1389.221	34.183	557.088	1374.773
43.162	677.103	1389.649	34.449	575.296	1377.771
51.242	687.401	1392.699	38.604	599.635	1387.983
59.7	722.89	1396.663	43.483	683.074	1390.319
76.534	730.753	1403.941	52.394	712.51	1393.255
83.048	740.974	1404.071	61.895	730.21	1397.376
91.361	768.298	1406.801	72.318	740.536	1401.582
105.851	845.53	1407.26	86.856	764.161	1406.337
109.959	853.63	1410.106	97.452	836.153	1409.659
127.328	894.772	1410.272	100.177	843.983	1412.665
189.558	895.026	1423.112	115.556	847.788	1425.1
193.533	925.8557	1423.21	129.587	876.3	1435.604
202.326	928.38	1435.582	137.199	899.948	1437.389
221.67	931.441	1435.814	157.094	900.886	1475.146
226.346	933.396	1465.37	166.549	909.543	1482.2
229.963	943.192	1472.664	180.513	920.188	1484.961
243.836	951.333	1537.185	186.592	928.321	1549.079
248.396	961.913	1544.314	196.865	939.6	1569.406
255.936	962.703	1577.914	210.379	953.193	1571.985
260.585	967.026	1579.86	225.331	965.141	1585.403
269.471	968.135	1593.641	237.041	967.629	1587.652
278.43	980.15	1594.673	248.559	975.039	1613.408
302.953	980.571	1607.043	252.31	977.778	1640.192
306.03	1003.356	1622.834	258.124	980.097	1680.886
311.464	1010.964	2953.828	283.227	982.003	2969.201
313.853	1013.126	2954.775	293.568	1001.302	2993.67
319.575	1020.841	3071.069	300.864	1013.065	3017.07
324.139	1022.582	3071.594	313.683	1021.817	3021.378
336.113	1102.396	3071.769	327.361	1026.351	3024.741
367.001	1176.903	3071.984	333.116	1080.872	3058.62
367.137	1179.125	3076.425	339.374	1099.949	3062.489
373.286	1222.803	3076.729	363.327	1192.83	3066.685
389.651	1233.172	3077.469	367.899	1220.797	3074.396
410.528	1272.82	3077.562	383.497	1241.851	3074.884
412.549	1276.525	3086.183	397.822	1282.26	3077.539
418.729	1302.238	3086.683	404.815	1295.501	3080.451
422.702	1302.553	3087.785	414.981	1302.175	3088.272
472.531	1348.502	3088.487	421.784	1302.822	3089.185
473.98	1349.122	3166.854	423.622	1330.655	3140.518
488.361	1362.924	3167.168	436.675	1342.985	3143.519
494.212	1376.983	3175.228	469.772	1344.869	3146.781
531.745	1384.498	3175.324	479.181	1346.517	3169.953
543.211	1384.761	3175.978	492.082	1352.579	3177.936
556.905	1387.612	3176.882	518.649	1355.098	3178.954

Table C.8: Vibrational frequencies (cm^{-1}) for the loss of *t*Bu from $[\text{Cu}(\text{tftm})_2]^+$.

$[\text{Cu}(\text{tftm})_2]^+$			$[[\text{Cu}(\text{tftm})_2]^+]^\ddagger$		
21.341	549.206	1389.546	-237.711	544.451	1360.113
25.072	561.747	1389.853	23.76	550.802	1369.875
27.859	665.876	1390.01	25.674	556.897	1378.443
37.98	674.212	1395.193	27.761	567.346	1387.164
38.836	694.507	1395.444	40.047	671.553	1391.119
52.257	695.404	1401.378	41.097	695.459	1391.622
57.633	714.713	1401.586	46.55	698.863	1397.199
80.56	716.025	1408.093	57.101	714.516	1402.791
89.705	870.377	1408.255	73.88	724.892	1410.664
100.187	876.256	1411.025	79.013	831.237	1411.137
103.899	926.514	1411.174	86.281	847.295	1416.437
119.329	930.382	1428.545	98.751	874.336	1429.803
145.05	942.37	1428.798	111.037	893.979	1434.101
157.314	943.353	1432.122	118.78	913.567	1479.593
172.54	959.695	1432.488	141.713	925.903	1483.174
184.159	959.753	1473.594	142.544	937.22	1489.861
185.239	960.395	1475.866	151.938	939.059	1497.369
188.145	960.944	1565.761	159.875	943.174	1554.521
217.134	967.697	1566.335	161.605	962.06	1562.149
220.326	981.925	1584.451	164.888	962.441	1576.939
243.451	983.014	1585.251	184.706	972.667	1578.979
245.898	983.439	1613.471	187.443	982.672	1616.036
254.716	988.265	1622.632	190.874	983.154	1665.034
260.568	1007.251	1750.855	219.275	984.918	1754.305
273.325	1010.272	1754.743	235.634	988.484	1770.097
274.92	1010.631	3016.753	252.412	995.492	3023.98
281.074	1027.285	3017.54	259.427	1011.54	3025.28
291.894	1027.356	3073.826	277.053	1022.28	3026.55
298.786	1090.381	3074.093	290.876	1029.224	3029.509
300.105	1147.864	3074.266	292.784	1069.621	3059.159
328.792	1201.353	3074.471	293.982	1109.126	3062.427
343.907	1236.385	3075.096	300.993	1172.866	3063.605
358.128	1241.685	3075.51	323.795	1222.281	3065.133
366.745	1274.153	3086.253	339.613	1250.374	3075.578
392.297	1281.137	3086.667	361.583	1256.201	3076.003
403.73	1281.246	3087.417	375.325	1283.13	3076.034
417.563	1288.54	3088.272	400.482	1293.477	3086.301
424.805	1296.497	3088.283	408.496	1297.557	3087.382
426.887	1349.916	3089.194	426.499	1310.722	3088.002
483.864	1351.683	3176.434	428.787	1338.573	3143.78
485.539	1357.148	3176.622	442.015	1340.079	3146.811
486.092	1358.059	3177.482	468.027	1348.791	3149.228
490.013	1384.32	3178.005	486.811	1350.192	3177.258
535.817	1384.477	3178.226	489.682	1350.963	3178.554
544.321	1389.407	3179.303	537.302	1358.17	3178.79

Table C.9: Vibrational frequencies (cm^{-1}) for the loss of *t*Bu from $[\text{Zn}(\text{tfm})_2]^+$.

$[\text{Zn}(\text{tfm})_2]^+$			$[[\text{Zn}(\text{tfm})_2]^+]^\ddagger$		
27.071	566.953	1386.918	-51.097	536.688	1352.766
17.199	575.854	1388.209	16.258	545.84	1364.195
9.769	581.406	1390.68	27.444	571.851	1378.181
17.345	660.79	1393.323	28.765	584.061	1389.254
22.041	680.519	1396.78	30.62	671.7	1393.081
29.097	685.39	1398.127	33.687	678.193	1393.591
50.002	704.321	1402.554	46.827	703.648	1395.601
68.143	709.802	1405.251	54.698	713.196	1399.148
80.916	838.544	1407.992	65.469	717.845	1404.9
94.991	877.557	1409.024	69.861	808.664	1413.318
99.909	883.717	1412.342	94.168	832.239	1413.988
110.48	917.492	1424.177	99.478	864.027	1434.885
146.345	932.263	1427.906	113.999	866.588	1441.171
152.27	934.225	1438.107	144.453	885.067	1466.078
166.894	936.078	1440.738	154.38	916.422	1472.38
173.44	953.814	1477.846	156.201	933.526	1497.347
188.987	955.438	1490.44	161.605	934.265	1544.726
195.594	964.428	1568.046	165.76	948.077	1556.384
203.291	966.634	1574.243	15.594	949.834	1558.451
220.658	968.957	1581.132	185.025	959.66	1577.915
231.051	972.043	1601.096	191.564	964.862	1590.021
233.107	983.792	1623.721	205.633	965.361	1601.21
255.23	984.458	1754.494	212.212	971.083	1638.042
260.098	1007.402	1762.657	219.044	975.976	1766.399
265.732	1013.762	1822.108	223.699	984.745	1910.193
267.898	1015.305	2996.289	238.278	988.985	2992.741
288.528	1022.633	3017.579	266.919	1013.414	2998.72
293.493	1026.005	3071.09	268.657	1025.299	3002.385
299.515	1070.067	3072.785	286.535	1035.529	3008.85
312.183	1092.833	3074.985	291.006	1045.088	3049.445
322.296	1183.231	3075.394	292.839	1057.322	3050.717
329.03	1188.468	3078.108	298.894	1139.71	3052.987
338.517	1189.75	3079.01	326.856	1218.666	3055.931
352.707	1233.759	3082.652	354.263	1244.792	3076.101
360.842	1287.068	3085.465	357.638	1276.544	3076.428
387.385	1289.923	3085.841	362.884	1284.929	3076.68
393.464	1293.291	3087.99	392.121	1293.492	3086.285
422.657	1294.76	3088.689	401.936	1296.362	3087.431
436.323	1311.739	3093.83	415.443	1304.075	3088.161
460.519	1337.501	3167.781	428.642	1322.483	3125.921
485.515	1344.909	3170.685	434.911	1334.324	3129.395
488.145	1369.53	3174.562	463.535	1335.313	3134.911
488.864	1376.737	3179.29	487.999	1340.517	3177.822
529.448	1382.951	3179.322	494.38	1345.382	3179.519
542.268	1386.767	3185.008	524.825	1349.816	3180.54

Table C.10: Vibrational frequencies (cm^{-1}) for the loss of CH_3 from $[\text{Cu}(\text{acac}-\text{CH}_3)(\text{acac})]^+$.

$[\text{Cu}(\text{acac}-\text{CH}_3)(\text{acac})]^+$			$[\text{Cu}(\text{acac}-\text{CH}_3)(\text{acac})]^{+ \ddagger}$		
54.774	702.019	1368.115	-113.514	597.259	1342.183
67.177	846.159	1368.606	31.645	600.31	1342.908
79.573	868.938	1374.249	34.811	673.471	1362.371
117.973	912.393	1386.67	54.348	690.582	1362.632
128.883	945.5	1387.693	56.703	735.474	1383.838
137.036	970.247	1441.709	72.775	846.745	1384.842
141.336	984.931	1448.612	77.119	848.385	1448.417
146.27	993.819	1457.647	122.783	888.658	1457.952
165.675	996.358	1575.14	131.896	912.333	1554.982
181.227	1003.649	1634.79	135.763	956.106	1556.036
231.63	1013.809	1715.715	147.599	992.353	1808.638
280.1	1018.321	1834.071	165.748	992.911	1848.212
291.932	1050.893	3042.78	181.35	996.925	3051.644
318.601	1073.299	3053.487	200.364	1012.507	3052.132
381.769	1107.153	3056.614	222.189	1049.953	3065.161
393.377	1147.506	3056.922	273.288	1052.472	3065.763
406.693	1162.038	3066.695	309.456	1087.636	3068.568
420.667	1254.702	3069.853	330.356	1114.272	3068.788
445.243	1297.25	3070.408	387.037	1209.786	3150.888
542.383	1341.942	3071.181	393.478	1264.257	3151.233
598.329	1344.942	3153.031	426.244	1265.593	3180.894
601.842	1345.936	3154.658	428.496	1267.04	3265.639
631.165	1364.054	3155.99	441.262	1292.373	3265.831

Table C.11: Vibrational frequencies (cm^{-1}) for the loss of CF_3 from $[\text{Cu(hfac-CF}_3\text{)(hfac)}]^+$.

$[\text{Cu(hfac-CF}_3\text{)(hfac)}]^+$			$[[\text{Cu(hfac-CF}_3\text{)(hfac)}]^+]^\ddagger$		
26.574	389.754	1076.118	-46.252	359.668	1056.733
28.477	405.475	1083.385	16.852	390.657	1076.002
28.618	436.874	1167.082	23.362	427.83	1083.685
29.703	466.094	1234.499	23.599	428.208	1174.787
45.324	493.753	1264.8	29.304	437.646	1188.084
59.683	514.996	1321.165	32.845	439.25	1209.036
89.807	523.654	1327.487	33.977	514.02	1250.595
105.277	529.162	1343.376	40.918	518.621	1339.802
111.055	541.345	1358.384	44.462	519.161	1342.359
138.473	545.007	1433.668	50.933	526.627	1454.652
146.871	609.021	1449.845	80.812	532.916	1458.595
152.89	683.974	1575.522	91.966	534.681	1572.532
204.917	685.259	1577.253	135.105	587.252	1574.188
227.81	696.677	1578.046	136.059	681.502	1574.709
260.246	706.399	1585.153	142.697	683.829	1574.812
264.167	706.952	1591.201	196.429	699.928	1588.816
267.82	851.974	1591.293	202.455	704.231	1590.369
274.253	899.205	1597.149	254.491	875.022	1696.312
276.386	937.475	1622.688	267.624	896.712	1705.281
308.3	939.712	1760.086	279.076	900.262	1804.532
343.206	953.59	1829.509	288.647	933.773	1850.159
356.86	977.33	2990.97	306.248	943.465	3022.246
370.399	981.323	3029.752	358.913	967.164	3032.281

Table C.12: Vibrational frequencies (cm^{-1}) for the loss of *t*Bu from $[\text{Cu}(\text{tftm-}t\text{Bu})(\text{tftm})]^+$.

$[\text{Cu}(\text{tftm-}t\text{bu})(\text{tftm})]^+$			$[[\text{Cu}(\text{hfac-}t\text{bu})(\text{tftm})]^+]^\ddagger$		
25.437	513.659	1350.596	-50.827	461.556	1310.241
26.822	530.993	1352.001	21.386	513.267	1320.179
32.247	539.438	1383.252	24.554	518.348	1323.837
46.49	543.929	1388.736	26.09	526.434	1326.036
52.35	558.014	1389.158	27.657	534.249	1330.9
64.556	668.031	1394.296	34.348	535.348	1333.845
88.157	683.925	1400.721	41.539	542.101	1368.226
99.106	694.963	1407.045	57.754	685.74	1384.333
110.15	710.539	1410.756	68.26	691.567	1391.215
134.832	716.302	1428.186	93.392	708.299	1474.267
155.096	871.474	1431.437	108.518	710.842	1500.283
157.92	895.8	1454.205	125.741	782.387	1501.034
189.402	923.937	1463.857	135.66	784.663	1531.047
200.544	941.507	1567.705	139.579	807.493	1553.547
211.172	945.224	1570.439	141.988	862.966	1559.584
234.622	956.841	1584.97	144.411	882.378	1569.541
254.176	959.455	1588.181	170.856	908.949	1573.329
257.195	960.35	1605.184	183.339	918.406	1577.383
265.994	981.939	1613.592	189.853	950.101	1649.707
279.621	983.389	1745.58	210.389	962.248	1907.61
292.387	984.273	1838.64	232.488	965.199	1926.068
294.329	1010.001	3010.865	277.825	966.333	2952.261
305.353	1026.748	3036.676	283.925	979.505	2965.74
336.162	1078.145	3073.313	293.589	982.747	2981.418
361.296	1083.294	3073.714	305.057	1050.193	3044.076
361.554	1159.583	3073.921	327.191	1065.645	3044.572
398.627	1224.32	3086.43	360.009	1110.752	3052.841
404.845	1247.629	3087.617	365.851	1154.531	3067.828
424.896	1263.293	3088.03	408.544	1231.987	3082.315
436.399	1280.267	3176.104	430.683	1260.107	3115.416
483.745	1289.543	3177.192	432.476	1280.685	3117.347
487.119	1347.587	3177.317	440.991	1284.768	3123.735

Table C.13: Vibrational frequencies (cm^{-1}) for the loss of CH_3 from $[\text{Ni(acac)}^+]$.

$[\text{Ni(acac)}]^+$			$[[\text{Ni(acac)}]^+]^\ddagger$		
58.526	944.249	1364.653	-65.969	622.012	1353.351
64.637	970.259	1373.069	36.861	695.329	1373.779
89.32	975.296	1409.453	44.322	826.641	1388.268
98.705	990.319	1454.543	72.879	889.655	1451.456
169.796	1009.191	1618.624	113.824	956.371	1596.831
264.085	1060.138	1695.787	133.088	996.731	1889.441
341.289	1158.408	3008.68	176.522	1001.12	3049.227
369.712	1185.081	3036.162	193.632	1095.09	3066.255
440.085	1215.208	3036.414	202.276	1124.713	3075.325
528.264	1323.748	3054.755	290.859	1248.57	3106.185
609.068	1325.208	3055.174	317.671	1249.203	3161.152
627.523	1351.344	3136.732	399.291	1266.704	3166.599
872.53	1351.352	3138.169	477.706	1320.24	3168.293

Table C.14: Vibrational frequencies (cm^{-1}) for the loss of CH_3 from $[\text{Cu(acac)}^+]$.

$[\text{Cu(acac)}]^+$			$[[\text{Cu(acac)}]^+]^\ddagger$		
-1065.05	761.143	1356.029	-80.145	552.626	1335.487
-178.693	928.137	1363.344	39.974	659.259	1355.315
-66.597	951.143	1448.074	84.214	703.657	1377.547
-43.668	954.752	1541.397	93.197	852.588	1472.815
54.663	972.673	1559.298	120.287	923.082	1615.356
84.873	981.166	2249.903	142.63	966.346	2048.697
96.146	1115.605	3004.123	189.344	972.942	3007.358
285.382	1115.763	3044.705	229.932	994.78	3039.757
397.544	1144.791	3045.08	292.875	1077.083	3059.047
407.961	1223.235	3064.018	302.901	1089.229	3142.214
494.493	1332.045	3094.524	348.376	1266.089	3171.229
548.776	1343.077	3146.557	441.812	1270.934	3245.382
573.561	1355.84	3190.336	499.313	1286.881	3246.273

Table C.15: Vibrational frequencies (cm^{-1}) for the loss of CH_3 from $[\text{Zn(acac)}^+]$.

$[\text{Zn(acac)}]^+$			$[[\text{Zn(acac)}]^+]^\ddagger$		
77.541	953.989	1359.916	-125.623	589.048	1352.769
90.249	959.075	1366.642	60.665	708.494	1372.285
144.368	974.405	1407.084	75.638	856.088	1389.384
164.651	976.377	1436.887	86.078	956.948	1444.616
169.322	1021.143	1631.149	128.56	995.504	1586.713
282.167	1092.432	1637.891	143.504	1000.879	1704.645
300.342	1122.038	2981.806	192.987	1007.545	3041.471
396.017	1146.928	3040.777	226.539	1064.554	3063.335
436.898	1171.321	3040.987	230.111	1126.731	3071.143
553.903	1323.121	3057.398	286.481	1230.297	3080.042
616.767	1324.884	3057.745	345.437	1253.664	3159.7
617.982	1356.928	3140.772	454.287	1253.882	3193.684
869.091	1356.965	3142.532	479.045	1254.362	3194.599

Table C.16: Vibrational frequencies (cm^{-1}) for the loss of CF_3 from $[\text{Cu(hfac)}^+]$.

$[\text{Cu(hfac)}]^+$			$[[\text{Cu(hfac)}]^+]^\ddagger$		
24.429	399.797	982.154	-195.318	340.364	986.396
26.49	459.07	1142.828	26.993	392.593	1038.817
48.939	463.669	1199.205	28.284	431.594	1144.101
53.421	520.985	1309.012	44.904	432.679	1167.671
142.147	539.875	1319.032	48.977	458.902	1316.369
179.468	603.149	1429.654	76.283	499.542	1403.892
199.638	622.436	1579.983	97.092	530.828	1585.448
236.155	686.999	1588.17	124.107	587.921	1592.916
262.19	708.994	1593.715	149.61	630.221	1700.541
271.482	827.262	1600.715	192.857	713.115	1711.159
291.446	830.194	1756.417	252.143	807.352	1722.578
331.199	875.935	1789.283	279.678	821.867	1830.991
382.301	942.545	2916.888	331.172	883.91	2933.944

Table C.17: Vibrational frequencies (cm^{-1}) for the loss of CF_3 from $[\text{Ni(hfac)}^+]$.

$[\text{Ni(hfac)}]^+$			$[[\text{Ni(hfac)}]^+]^\ddagger$		
-5.651	379.172	1121.226	-25.842	363.149	1036.608
-1.954	454.925	1192.943	20.129	443.408	1095.405
68.278	482.302	1281.397	25.272	443.885	1143.988
89.262	515.264	1308.04	28.037	464.239	1180.397
89.664	533.1	1345.189	30.918	528.238	1365.716
114.421	612.274	1357.259	32.034	535.521	1495.137
172.654	679.527	1583.339	40.099	547.817	1564.196
233.633	686.376	1585.044	72.298	664.396	1567.863
261.109	696.085	1600.204	164.637	694.623	1578.292
263.5	853.158	1601.119	173.173	719.076	1797.876
323.581	944.293	1606.77	273.583	864.188	1798.437
323.693	977.633	1737.296	287.311	888.605	1893.644
368.378	1094.279	2970.126	317.756	969.505	3092.874

Table C.18: Vibrational frequencies (cm^{-1}) for the loss of CF_3 from $[\text{Zn(hfac)}^+]$.

$[\text{Zn(hfac)}]^+$			$[[\text{Zn(hfac)}]^+]^\ddagger$		
16.89	384.614	1102.085	-116.584	365.565	1072.823
28.069	464.362	1162.072	25.355	437.489	1077.241
91.272	482.97	1297.206	27.283	437.619	1121.363
98.019	519.005	1300.871	45.081	466.642	1163.283
101.43	539.45	1319.489	61.09	503.837	1364.127
176.747	616.815	1380.796	81.247	523.177	1434.767
199.455	681.117	1578.393	92.059	537.882	1558.791
256.132	701.472	1578.592	100.502	584.057	1585.108
261.53	703.712	1598.515	176.809	689.087	1657.332
277.442	854.602	1600.294	188.656	727.295	1692.041
283.937	938.339	1635.533	268.672	900.135	1791.639
321.248	953.448	1692.344	285.627	931.064	1792.705
359.974	1062.17	2943.646	313.195	1013.978	3026.823

Table C.19: Vibrational frequencies (cm^{-1}) for the loss of *t*Bu from $[\text{Cu}(\text{tftm})]^+$.

$[\text{Cu}(\text{tftm})]^+$			$[[\text{Cu}(\text{tftm})]^+]^\ddagger$		
27.94	664.327	1383.977	-73.31	539.378	1339.377
45.832	674.121	1385.175	26.039	617.017	1342.974
61.702	701.991	1396.937	30.904	682.766	1350.147
93.939	847.155	1400.99	44.968	729.002	1369.849
115.341	877.104	1412.647	56.888	795.307	1409.599
141.038	915.315	1426.731	72.021	799.51	1479.299
184.632	928.958	1436.856	79.49	837.073	1485.82
198.784	955.599	1444.886	126.71	872.868	1550.859
233.811	956.393	1495.225	140.314	917.066	1554.313
264.362	983.703	1568.69	144.423	926.194	1586.955
284.169	1009.068	1580.035	160.19	936.309	1598.806
286.499	1034.309	1604.818	196.395	985.614	1861.657
310.587	1077.978	2889.36	198.465	994.404	2989.886
319.925	1113.512	3066.345	259.659	1023.059	2990.652
368.742	1195.993	3066.469	268.812	1033.608	2997.171
386.506	1239.719	3070.421	312.074	1161.523	3000.789
422.717	1270.531	3086.15	370.684	1227.578	3046.675
459.768	1272.623	3087.654	415.633	1286.558	3049.973
478.814	1324.15	3088.538	427.83	1295.598	3051.396
525.793	1341.866	3174.903	444.333	1318.299	3126.31
556.072	1376.047	3175.991	448.315	1327.838	3126.596
593.792	1381.348	3176.297	494.133	1335.282	3134.285

Table C.20: Vibrational frequencies (cm^{-1}) for the loss of *t*Bu from $[\text{Ni}(\text{tftm})]^+$.

$[\text{Ni}(\text{tftm})]^+$			$[[\text{Ni}(\text{tftm})]^+]^\ddagger$		
54.979	585.013	1385.479	-250.729	526.845	1342.909
28.254	655.194	1385.857	26.855	535.213	1347.961
44.267	679.364	1394.201	38.341	610.638	1348.295
59.022	841.503	1401.237	39.503	691.955	1351.617
89.543	845.848	1405.964	61.454	789.835	1375.392
104.823	884.018	1426.337	64.504	809.317	1414.37
176.414	922.923	1430.334	76.6	814.146	1481.947
194.511	954.123	1447.735	110.938	815.853	1481.972
209.058	954.788	1573.205	134.082	842.839	1558.97
217.958	979.922	1602.757	144.429	915.743	1593.862
239.505	987.865	1713.823	151.211	922.168	1748.817
253.194	1003.703	1798.384	168.858	938.217	1784.343
262.539	1019.055	2962.658	169.672	989.047	3002.911
289.671	1025.993	3068.235	180.314	989.844	3007.1
323.22	1164.662	3068.253	251.364	1018.027	3011.427
329.328	1205.229	3071.782	268.607	1070.761	3039.256
384.927	1258.745	3082.976	326.743	1144.657	3054.976
407.996	1278.416	3086.541	368.224	1294.825	3058.086
456.807	1307.311	3087.437	397.839	1298.713	3059.073
482.566	1326.318	3172.668	437.292	1327.257	3135.465
527.616	1375.461	3174.576	446.313	1331.298	3136.587
550.245	1381.339	3175.005	458.598	1341.071	3141.543

Table C.21: Vibrational frequencies (cm^{-1}) for the loss of *t*Bu from $[\text{Zn}(\text{ftm})]^+$.

$[\text{Zn}(\text{ftm})]^+$			$[[\text{Zn}(\text{ftm})]^+]^\ddagger$		
28.194	668.827	1385.204	-123.395	438.695	1331.023
55.128	703.032	1387.934	24.505	595.68	1339.525
92.386	712.228	1393.906	39.792	690.709	1343.324
99.583	874.896	1401.589	51.224	732.449	1369.564
116.405	917.456	1410.979	59.138	776.514	1403.756
174.723	942.641	1415.17	95.697	795.598	1443.953
197.267	955.235	1430.206	120.089	896.933	1498.977
220.04	956.669	1437.914	126.875	933.93	1500.422
226.466	957.196	1571.188	163.854	942.59	1555.419
262.644	986.092	1591.641	172.915	944.295	1585.27
264.434	1007.806	1603.926	176.442	974.094	1667.766
277.133	1029.187	1695.509	180.075	994.97	1683.746
281.416	1066.774	2953.676	189.324	1013.368	2966.293
301.922	1124.966	3069.636	268.003	1041.217	2968.857
343.82	1188.919	3069.844	289.278	1089.368	2990.646
358.556	1222.238	3070.718	314.242	1127.489	3021.837
392.762	1273.066	3086.645	361.455	1163.962	3052.142
423.171	1274.343	3088.083	382.44	1283.798	3053.38
479.597	1324.304	3088.877	436.602	1284.99	3056.113
488.063	1331.785	3175.059	443.17	1313.816	3119.884
537.032	1378.109	3176.031	467.248	1321.077	3122.49
566.029	1384.117	3176.26	524.75	1325.031	3127.648

Table C.22: Vibrational frequencies (cm^{-1}) for the loss of *acac* from $[\text{Cu}(\text{acac})_2]^+$.

$[\text{Cu}(\text{acac})_2]^+$			$[[\text{Cu}(\text{acac})_2]^+]^\ddagger$		
46.362	865.899	1368.726	-419.17	628.828	1377.374
58.52	866.528	1376.958	-304.104	660.771	1377.651
68.781	916.636	1378.472	39.599	859.938	1377.931
105.507	961.186	1390.615	48.105	882.597	1380.931
113.351	964.913	1390.96	80.632	940.493	1383.292
118.719	980.854	1445.351	105.268	961.035	1395.445
120.239	985.18	1451.37	123.539	963.101	1433.456
123.842	985.311	1451.464	132.169	985.222	1463.726
133.042	998.724	1453.163	133.194	988.935	1487.079
158.308	1004.95	1630.134	139.28	989.107	1618.626
169.711	1017.296	1642.346	144.465	993.076	1704.586
183.679	1018.882	1718.29	148.05	1021.549	1731.64
219.552	1028.364	1723.802	164.866	1024.592	1741.502
280.277	1085.135	3042.924	166.861	1036.672	2988.993
281.68	1106.496	3043.445	188.36	1056.057	3037.714
304.408	1118.166	3057.547	210.231	1068.969	3064.635
348.585	1145.519	3057.548	244.278	1092.916	3066.732
392.07	1163.391	3057.686	292.259	1120.165	3067.943
407.562	1176.143	3057.734	324.982	1146.776	3068.599
416.716	1275.087	3072.481	377.402	1176.301	3072.091
434.827	1341.549	3072.618	399.918	1283.485	3074.313
541.223	1344.077	3072.662	414.596	1344.067	3076.076
542.047	1346.188	3072.849	511.594	1351.782	3078.342
587.386	1347.45	3156.64	523.857	1353.1	3160.994
624.749	1368.24	3156.822	552.585	1353.952	3161.51
629.057	1368.28	3157.249	569.184	1370.751	3162.268
632.672	1368.642	3157.793	599.825	1374.459	3165.038

Table C.23: Vibrational frequencies (cm^{-1}) for the loss of *acac* from $[\text{Ni}(\text{acac})_2]^+$.

$[\text{Ni}(\text{acac})_2]^+$			$[[\text{Ni}(\text{acac})_2]^+]$		
67.03	875.368	1360.989	-161.792	631.026	1375.048
97.315	881.841	1374.02	-137.686	673.066	1379.135
115.615	914.094	1375.759	41.231	729.498	1379.171
120.572	929.855	1383.066	51.39	870.962	1384.629
123.542	947.652	1385.787	91.358	916.43	1386.29
124.723	963.126	1423.268	101.685	955.313	1393.663
130.512	967.255	1438.146	103.464	972.007	1440.044
132.91	975.064	1460.547	119.093	982.03	1475.942
135.291	977.395	1474.186	136.401	982.354	1475.997
187.609	981.808	1570.101	136.449	986.175	1641.015
222.345	988.707	1598.983	142.276	992.13	1733.104
252.333	1005.571	1601.373	143.948	996.134	1844.234
300.929	1015.152	1608.14	172.617	1013.689	1890.948
318.772	1020.455	2974.45	183.298	1023.537	3031.704
359.953	1034.44	2975.61	235.708	1046.074	3037.369
371.176	1047.716	3056.91	249.658	1069.293	3054.45
394.135	1054.303	3057.12	271.088	1147.274	3054.652
420.369	1125.386	3057.795	330.417	1159.28	3067.553
450.329	1175.786	3057.989	360.125	1179.101	3067.786
376.785	1178.916	3079.402	364.535	1214	3069.883
506.842	1331.572	3079.533	389.025	1292.315	3070.062
557.315	1333.348	3079.649	440.716	1339.374	3080.007
566.884	1340.657	3079.766	485.531	1344.385	3080.13
580.561	1341.867	3156.49	532.632	1356.521	3152.125
628.962	1359.247	3156.962	537.255	1364.597	3153.043
656.693	1359.648	3157.042	549.158	1364.673	3166.507
700.726	1360.214	3157.951	618.856	1365.377	3166.862

Table C.24: Vibrational frequencies (cm^{-1}) for the loss of *acac* from $[\text{Zn}(\text{acac})_2]^+$.

$[\text{Zn}(\text{acac})_2]^+$			$[[\text{Zn}(\text{acac})_2]^+]^\ddagger$		
-84.269	736.72	1373.148	-117.915	740.647	1371.223
-25.808	864.163	1374.795	-77.054	885.084	1371.979
21.916	917.394	1374.953	50.599	923.684	1373.465
31.646	945.007	1375.664	37.354	939.948	1373.685
36.284	952.911	1393.323	69.858	945.537	1386.892
58.346	957.677	1402.603	86.46	965.747	1426.641
104.859	975.355	1444.131	110.744	966.882	1442.276
176.697	978.889	1470.604	171.527	982.149	1459.633
179.343	982.626	1511.591	179.451	985.897	1546.433
181.389	992.805	1626.876	180.894	987.243	1637.356
185.604	996.283	1714.372	191.814	1005.858	1715.97
205.556	1024.227	1774.616	204.66	1028.737	1769.769
210.089	1032.063	1827.24	206.044	1036.179	1822.619
216.578	1070.853	3005.369	212.048	1074.124	2960.176
264.284	1082.974	3036.283	256.567	1075.722	3044.162
290.308	1115.679	3036.454	284.832	1121.733	3044.339
339.134	1120.533	3046.663	339.979	1122.657	3045.306
375.823	1131.649	3062.487	371.316	1125.394	3066.556
405.214	1160.542	3062.634	398.542	1160.627	3067.088
427.287	1175.598	3079.887	425.754	1182.597	3074.091
441.67	1313.303	3080.102	441.26	1311.888	3074.151
456.674	1334.355	3087.358	462.194	1330.99	3086.003
523.693	1342.884	3087.629	522.528	1339.112	3086.053
561.518	1350.188	3139.082	563.724	1347.421	3147.396
579.295	1352.046	3139.7	580.185	1349.925	3147.853
626.622	1356.622	3169.407	625.263	1358.575	3166.823
633.327	1356.888	3170.176	644.208	1358.73	3167.532

Table C.25: Vibrational frequencies (cm^{-1}) for the loss of *hfac* from $[\text{Cu}(\text{hfac})_2]^+$.

$[\text{Cu}(\text{hfac})_2]^+$			$[[\text{Cu}(\text{hfac})_2]^+]^\ddagger$		
19.379	361.387	999.366	-383.861	328.539	973.575
19.833	383.607	1094.341	-265.089	351.841	1006.77
19.947	395.362	1117.023	20.089	370.953	1063.981
20.124	414.983	1162.254	21.006	386.836	1124.509
20.355	463.679	1264.14	24.256	390.644	1165.916
34.387	463.991	1320.709	27.633	393.62	1186.956
39.799	489.97	1324.447	29.704	463.91	1288.41
86.858	493.623	1325.355	31.449	468.91	1310.718
89.682	522.213	1325.596	42.756	472.8	1314.919
91.145	523.023	1353.545	72.608	491.567	1344.017
98.015	535.934	1363.643	83.338	520.993	1358.455
104.554	546.628	1432.265	85.493	525.621	1454.382
137.161	601.987	1443.808	99.289	538.904	1475.063
155.527	612.82	1573.511	101.109	545.819	1568.159
156.524	684.118	1573.841	132.164	601.687	1568.913
180.111	687.651	1574.005	135.038	614.5	1573.119
221.385	694.756	1575.316	165.045	649.262	1575.633
229.056	695.315	1590.785	178.76	667.195	1585.531
244.614	706.946	1592.185	213.447	687.783	1586.531
252.478	708.267	1593.204	238.541	701.074	1602.394
273.952	854.335	1593.721	241.36	705.248	1605.485
276.015	863.827	1617.351	247.767	707.525	1607.712
279.194	939.036	1629.893	250.292	805.935	1760.353
279.896	940.153	1763.374	260.863	853.084	1766.897
329.085	974.031	1765.114	271.98	915.485	1784.698
344.486	976.655	3004.496	284.691	927.656	2941.302
355.038	981.719	3005.431	320.446	942.875	3004.378

Table C.26: Vibrational frequencies (cm^{-1}) for the loss of *hfac* from $[\text{Ni}(\text{hfac})_2]^+$.

$[\text{Ni}(\text{hfac})_2]^+$			$[[\text{Ni}(\text{hfac})_2]^+]^\ddagger$		
34.38	408.195	939.206	-288.078	326.541	979.665
37.455	416.481	991.065	-273.576	346.476	1085.796
40.373	464.691	1077.136	15.044	368.398	1121.292
42.548	466.18	1149.178	23.191	380.298	1127.721
45.597	469.963	1161.691	24.744	383.94	1164.533
73.72	469.963	1317.944	28.817	387.108	1228.533
98.215	474.119	1319.164	29.814	459.472	1294.877
102.607	508.843	1321.019	32.832	466.837	1316.849
108.114	533.334	1324.924	34.046	476.516	1349.007
110.867	543.756	1378.284	65.122	487.286	1354.79
122.053	556.197	1385.98	79.805	517.914	1355.337
200.382	556.67	1417.406	81.773	524.976	1372.49
218.22	607.736	1436.051	101.119	534.886	1428.548
225.161	621.965	1545.618	108.434	535.6	1561.855
227.106	697.196	1555.729	122.332	538.409	1568.558
232.784	701.456	1563.726	140.375	616.152	1582.023
243.425	723.313	1570.191	162.511	623.893	1582.92
261.658	723.844	1586.467	168.403	682.235	1584.689
266.581	741.896	1589.097	194.307	684.474	1589.823
293.178	744.896	1592.962	201.877	690.598	1596.486
315.669	821.861	1600.854	243.406	698.863	1597.492
323.419	829.96	1601.062	249.504	713.688	1615.58
324.707	860.147	1602.004	257.34	758.776	1750.056
365.877	884.695	1605.432	270.273	832.012	1966.639
368.869	902.659	1609.31	272.131	859.211	1995.411
394.839	916.021	2938.553	299.65	887.767	2965.086
399.18	932.921	2941.148	324.085	943.899	3026.476

Table C.27: Vibrational frequencies (cm^{-1}) for the loss of $hfac$ from $[\text{Zn}(hfac)_2]^+$.

$[\text{Zn}(hfac)_2]^+$			$[[\text{Zn}(hfac)_2]^+]^\ddagger$		
22.537	352.28	966.17	-71.687	324.411	953.593
25.056	368.051	1045.658	-61.39	349.418	1058.54
26.949	385.207	1061.362	12.624	361.062	1097.274
27.879	394.16	1163.146	15.873	386.993	1160.591
29.144	458.646	1184.669	16.842	404.924	1167.441
30.357	463.275	1203.39	27.601	409.573	1169.909
31.761	470.576	1307.44	28.749	462.856	1299.385
59.022	492.431	1309.753	29.118	466.503	1310.485
88.067	515.331	1316.494	30.597	468.522	1331.177
96.532	525.795	1342.893	48.194	486.285	1355.526
100.58	536.654	1368.848	62.772	520.771	1362.715
102.997	547.999	1452.741	85.601	533.147	1390.049
150.616	591.523	1456.443	91.982	541.92	1448.006
156.142	610.959	1569.822	93.589	543.89	1561.672
169.304	623.173	1570.156	100.973	587.478	1563.559
170.22	671.46	1577.539	104.492	618.643	1577.24
212.382	687.271	1579.273	182.167	621.79	1577.489
215.323	694.551	1586.322	197.781	685.021	1586.441
255.963	704.798	1587.204	201.718	695.123	1588.516
258.039	706.269	1605.712	226.998	705.087	1596.87
264.618	829.665	1607.591	244.241	705.387	1598.22
267.827	842.289	1646.335	258.487	706.402	1637.077
269.125	881.887	1764.27	262.932	826.122	1703.21
283.866	916.592	1767.548	268.501	830.911	1869.375
295.318	929.259	1828.915	270.639	862.453	1919.686
330.333	936.845	2962.484	282.516	909.04	2951.353
333.629	950.915	2988.326	317.728	942.21	3008.396

Table C.28: Vibrational frequencies (cm^{-1}) for the loss of *tftm* from $[\text{Zn}(\text{tftm})_2]^+$.

$[\text{Zn}(\text{tftm})_2]^+$			$[[\text{Zn}(\text{tftm})_2]^+]^\ddagger$		
27.071	566.953	1386.918	-84.048	535.305	1390.344
17.199	575.854	1388.209	-73.218	539.386	1390.547
9.769	581.406	1390.68	15.239	564.244	1393.455
17.345	660.79	1393.323	19.989	568.273	1395.856
22.041	680.519	1396.78	21.896	600.967	1397.844
29.097	685.39	1398.127	25.966	671.874	1398.113
50.002	704.321	1402.554	29.541	687.517	1403.003
68.143	709.802	1405.251	44.252	701.675	1403.665
80.916	838.544	1407.992	50.262	703.916	1404.486
94.991	877.557	1409.024	53.679	713.201	1411.747
99.909	883.717	1412.342	60.577	791.147	1412.715
110.48	917.492	1424.177	74.529	838.989	1421.615
146.345	932.263	1427.906	92.425	878.614	1425.462
152.27	934.225	1438.107	100.123	902.428	1425.761
166.894	936.078	1440.738	115.961	921.798	1431.535
173.44	953.814	1477.846	158.694	938.494	1441.601
188.987	955.438	1490.44	171.941	946.94	1442.521
195.594	964.428	1568.046	195.952	953.628	1559.65
203.291	966.634	1574.243	198.211	957.432	1567.782
220.658	968.957	1581.132	201.283	959.489	1581.887
231.051	972.043	1601.096	217.203	963.039	1590.728
233.107	983.792	1623.721	227.951	966.386	1610.718
255.23	984.458	1754.494	228.5	976.59	1706.022
260.098	1007.402	1762.657	242.362	985.424	1906.148
265.732	1013.762	1822.108	245.839	1006.687	1945.871
267.898	1015.305	2996.289	262.443	1009.282	2962.845
288.528	1022.633	3017.579	263.871	1019.389	3029.791
293.493	1026.005	3071.09	269.485	1030.93	3070.342
299.515	1070.067	3072.785	272.362	1062.564	3071.243
312.183	1092.833	3074.985	283.228	1118.589	3071.906
322.296	1183.231	3075.394	298.591	1134.744	3072.457
329.03	1188.468	3078.108	302.017	1156.219	3075.968
338.517	1189.75	3079.01	328.327	1195.171	3079.936
352.707	1233.759	3082.652	343.812	1227.822	3081.634
360.842	1287.068	3085.465	345.75	1276.913	3085.874
387.385	1289.923	3085.841	360.081	1278.432	3086.533
393.464	1293.291	3087.99	378.116	1279.279	3086.591
422.657	1294.76	3088.689	394.619	1288.876	3087.72
436.323	1311.739	3093.83	407.587	1310.42	3088.452
460.519	1337.501	3167.781	417.125	1327.799	3172.991
485.515	1344.909	3170.685	424.469	1342.747	3175.724
488.145	1369.53	3174.562	470.161	1366.774	3176.752
488.864	1376.737	3179.29	481.567	1380.73	3177.157
529.448	1382.951	3179.322	483.62	1385.915	3177.224
542.268	1386.767	3185.008	489.572	1386.37	3178.07

Table C.29: Vibrational frequencies (cm^{-1}) for the loss of *tftm* from $[\text{Ni}(\text{tftm})_2]^+$.

$[\text{Ni}(\text{tftm})_2]^+$			$[[\text{Ni}(\text{tftm})_2]^+]$		
33.733	570.174	1387.718	-307.574	525.804	1387.804
42.2	591.314	1389.221	-265.717	535.05	1389.673
43.162	677.103	1389.649	16.41	537.054	1390.769
51.242	687.401	1392.699	28.368	574.368	1393.723
59.7	722.89	1396.663	32.744	592.066	1396.828
76.534	730.753	1403.941	38.665	672.594	1398.145
83.048	740.974	1404.071	44.283	685.215	1401.222
91.361	768.298	1406.801	46.37	692.646	1402.505
105.851	845.53	1407.26	57.463	696.633	1403.037
109.959	853.63	1410.106	62.174	701.521	1403.659
127.328	894.772	1410.272	78.435	768.012	1411.586
189.558	895.026	1423.112	93.14	770.08	1413.11
193.533	925.8557	1423.21	107.457	840.498	1417.934
202.326	928.38	1435.582	118.222	843.161	1418.887
221.67	931.441	1435.814	128.618	884.7	1421.387
226.346	933.396	1465.37	169.997	895.428	1427.62
229.963	943.192	1472.664	188.316	910.67	1441.095
243.836	951.333	1537.185	197.56	930.3	1511.887
248.396	961.913	1544.314	208.573	937.449	1559.937
255.936	962.703	1577.914	212.972	956.643	1578.579
260.585	967.026	1579.86	225.313	963.029	1584.785
269.471	968.135	1593.641	234.555	965.05	1592.122
278.43	980.15	1594.673	239.837	966.689	1603.549
302.953	980.571	1607.043	246.056	975.402	1928.029
306.03	1003.356	1622.834	248.824	979.006	1981.014
311.464	1010.964	2953.828	261.314	1005.894	2929.816
313.853	1013.126	2954.775	266.463	1007.358	3043.139
319.575	1020.841	3071.069	279.159	1011.134	3068.072
324.139	1022.582	3071.594	282.925	1015.742	3068.594
336.113	1102.396	3071.769	293.526	1020.411	3069.748
367.001	1176.903	3071.984	295.956	1111.595	3071.454
367.137	1179.125	3076.425	319.97	1158.765	3076.792
373.286	1222.803	3076.729	337.948	1172.418	3077.082
389.651	1233.172	3077.469	340.276	1197.013	3079.647
410.528	1272.82	3077.562	355.056	1251.684	3080.175
412.549	1276.525	3086.183	365.557	1275.797	3083.555
418.729	1302.238	3086.683	382.96	1292.742	3084.328
422.702	1302.553	3087.785	390.86	1304.571	3085.195
472.531	1348.502	3088.487	399.249	1310.661	3091.079
473.98	1349.122	3166.854	415.458	1316.278	3166.781
488.361	1362.924	3167.168	416.846	1337.201	3170.889
494.212	1376.983	3175.228	467.072	1365.567	3171.403
531.745	1384.498	3175.324	469.697	1380.926	3175.305
543.211	1384.761	3175.978	482.438	1383.59	3176.746
556.905	1387.612	3176.882	488.988	1385.994	3176.155

Table C.30: Vibrational frequencies (cm^{-1}) for the loss of $t\text{ftm}$ from $[\text{Cu}(\text{tftm})_2]^+$.

$[\text{Cu}(\text{tftm})_2]^+$			$[[\text{Cu}(\text{tftm})_2]^+]^\ddagger$		
21.341	549.206	1389.546	-407.244	537.523	1388.349
25.072	561.747	1389.853	-266.925	539.25	1390.286
27.859	665.876	1390.01	22.362	553.16	1392.23
37.98	674.212	1395.193	24.184	574.353	1392.556
38.836	694.507	1395.444	27.645	639.578	1396.077
52.257	695.404	1401.378	30.505	668.785	1396.878
57.633	714.713	1401.586	45.325	673.006	1400.822
80.56	716.025	1408.093	48.632	700.922	1403.799
89.705	870.377	1408.255	56.101	706.166	1406.057
100.187	876.256	1411.025	73.713	714.314	1411.813
103.899	926.514	1411.174	82.195	822.889	1413.245
119.329	930.382	1428.545	91.661	861.614	1422.269
145.05	942.37	1428.798	104.127	913.795	1426.518
157.314	943.353	1432.122	116.379	924.956	1433.203
172.54	959.695	1432.488	137.325	932.021	1438.12
184.159	959.753	1473.594	147.457	932.716	1458.301
185.239	960.395	1475.866	168.153	950.234	1484.779
188.145	960.944	1565.761	176.459	953.575	1560.617
217.134	967.697	1566.335	193.594	955.788	1566.106
220.326	981.925	1584.451	200.913	963.269	1581.345
243.451	983.014	1585.251	216.27	963.687	1595.741
245.898	983.439	1613.471	228.882	968.522	1600.496
254.716	988.265	1622.632	234.091	982.64	1706.274
260.568	1007.251	1750.855	247.232	983.86	1749.877
273.325	1010.272	1754.743	248.604	1002.408	1787.067
274.92	1010.631	3016.753	253.808	1010.029	2962.418
281.074	1027.285	3017.54	258.162	1013.273	3015.374
291.894	1027.356	3073.826	264.963	1015.399	3069.575
298.786	1090.381	3074.093	277.431	1032.781	3070.771
300.105	1147.864	3074.266	285.716	1069.703	3075.26
328.792	1201.353	3074.471	297.966	1144.843	3075.317
343.907	1236.385	3075.096	305.897	1176.021	3075.706
358.128	1241.685	3075.51	320.686	1212.791	3075.747
366.745	1274.153	3086.253	332.667	1223.224	3082.216
392.297	1281.137	3086.667	362.051	1239.546	3085.025
403.73	1281.246	3087.417	365.893	1284.521	3086.286
417.563	1288.54	3088.272	388.4	1288.415	3086.59
424.805	1296.497	3088.283	395.792	1289.365	3087.646
426.887	1349.916	3089.194	409.932	1303.615	3088.317
483.864	1351.683	3176.434	419.696	1334.079	3173.629
485.539	1357.148	3176.622	426.38	1341.118	3174.692
486.092	1358.059	3177.482	474.378	1364.497	3175.748
490.013	1384.32	3178.005	480.8	1380.661	3177.654
535.817	1384.477	3178.226	485.889	1385.641	3179.234
544.321	1389.407	3179.303	490.868	1387.777	3179.875

Tabel C.31: Vibrational frequencies (cm^{-1}) for the loss of *acac* from $[\text{Cu}(\text{acac}-\text{CH}_3)(\text{acac})]^+$.

$[\text{Cu}(\text{acac}-\text{CH}_3)(\text{acac})]^+$			$[[\text{Cu}(\text{acac}-\text{CH}_3)(\text{acac})]^+]^\ddagger$		
54.829	701.988	1368.024	-173.353	552.845	1371.738
67.419	846.112	1368.509	-171.363	620.392	1380.616
80.098	869.095	1374.232	13.49	663.98	1384.825
117.962	912.6	1386.659	32.277	709.881	1384.918
128.109	945.395	1387.553	32.975	765.545	1388.378
135.678	970.681	1441.051	40.022	847.103	1396.098
138.153	985.095	1448.656	40.745	907.23	1467.117
142.396	993.709	1457.551	52.008	967.284	1470.796
165.502	996.285	1574.26	118.877	969.719	1624.182
181.106	1003.822	1634.183	137.593	973.902	1914.687
231.458	1014.248	1715.946	140.331	982.824	1951.453
280.055	1018.47	1834.468	161.949	989.857	2076.604
291.941	1050.638	3042.52	171.887	995.733	3036.107
319.029	1073.247	3053.314	195.083	1025.791	3045.888
381.75	1107.249	3056.757	227.01	1034.358	3057.353
393.359	1147.886	3058.024	325.248	1072.822	3063.743
406.786	1162.008	3066.709	340.267	1086.125	3075.09
420.691	1254.613	3069.927	345.141	1139.976	3076.85
445.153	1296.348	3070.317	439.167	1281.998	3086.329
542.452	1341.948	3072.543	470.309	1288.218	3086.375
598.372	1344.895	3152.812	508.409	1339.643	3147.329
601.901	1346.025	3155.069	517.158	1359.066	3173.58
631.207	1364.034	3157.479	545.347	1362.625	3174.445

Table C.32: Vibrational frequencies (cm^{-1}) for the loss of *acac* from $[\text{Ni}(\text{acac}-\text{CH}_3)(\text{acac})]^+$.

$[\text{Ni}(\text{acac}-\text{CH}_3)(\text{acac})]^+$			$[[\text{Ni}(\text{acac}-\text{CH}_3)(\text{acac})]^+]^\ddagger$		
51.777	641.321	1359.178	-302.712	596.351	1362.505
63.054	682.587	1364.604	-253.24	647.063	1368.002
101.544	808.896	1365.722	37.738	702.746	1370.597
122.173	844.521	1373.661	90.79	760.158	1386.88
124.333	885.833	1380.006	96.276	803.951	1389.677
134.893	926.877	1393.974	118.639	887.969	1393.527
137.842	957.444	1471.028	136.44	927.748	1425.516
155.242	970.889	1474.22	142.892	953.384	1431.862
171.3	972.262	1595.988	146.671	960.28	1580.576
197.454	984.702	1624.287	152.267	971.343	1825.72
212.302	992.958	1679.847	174.883	991.151	1905.175
282.582	998.829	2170.836	187.099	1001.011	2213.111
313.137	1010.509	2983.053	200.048	1015.224	2988.253
334.952	1021.029	3021.479	269.056	1035.582	2994.403
360.902	1037.997	3046.843	342.558	1043.389	3055.195
394.07	1054.405	3065.076	360.846	1057.728	3072.579
446.651	1115.273	3067.729	375.795	1063.074	3072.955
468.766	1162.728	3070.101	395.93	1176.712	3074.144
508.508	1225.644	3079.021	473.81	1185.617	3085.558
540.294	1316.902	3081.92	517.139	1208.083	3088.659
564.539	1344.764	3150.061	537.253	1321.383	3149.034
572.585	1345.538	3159.37	559.778	1336.729	3176.409
617.135	1356.402	3161.069	570.047	1352.362	3178.08

Table C.33: Vibrational frequencies (cm^{-1}) for the loss of *acac* from $[\text{Zn}(\text{acac}-\text{CH}_3)(\text{acac})]^+$.

$[\text{Zn}(\text{acac}-\text{CH}_3)(\text{acac})]^+$			$[[\text{Zn}(\text{acac}-\text{CH}_3)(\text{acac})]^+]^\ddagger$		
46.336	862.466	1372.025	-86.314	535.116	1370.915
54.242	908.026	1375.505	-70.446	547.972	1379.784
61.963	958.533	1375.627	25.587	667.663	1383.857
115.78	965.318	1378.616	35.545	717.334	1384.651
140.551	977.518	1393.861	47.591	731.988	1388.66
147.961	982.061	1442.488	60.075	832.374	1398.057
151.366	986.18	1456.011	66.073	893.641	1466.769
162.917	991.778	1464.742	81.283	915.654	1469.073
163.865	1024.573	1654.992	123.613	972.902	1623.205
197.833	1031.549	1714.251	144.91	975.691	1900.799
199.283	1072.812	1769.826	146.709	984.006	1939.423
207.276	1081.195	1988.194	149.761	990.825	2146.468
287.825	1113.035	3016.757	167.701	993.328	3045.045
315.621	1129.873	3027.398	191.902	1024.131	3048.243
345.644	1180.026	3044.999	261.954	1039.993	3053.565
360.253	1244.131	3062.175	329.588	1067.22	3060.165
405.642	1334.148	3063.894	341.006	1079.781	3073.454
440.384	1343.585	3064.011	345.401	1143.378	3075.979
441.505	1351.094	3076.075	453.031	1285.058	3085.4
519.877	1359.01	3076.25	477.771	1317.642	3087.331
556.689	862.466	3144.232	479.095	1342.275	3142.154
612.845	908.026	3162.192	524.428	1356.119	3173.214
630.12	958.533	3162.838	529.925	1361.054	3174.764

Table C.34: Vibrational frequencies (cm^{-1}) for the loss of *hfac* from $[\text{Cu}(\text{hfac}-\text{CH}_3)(\text{hfac})]^+$.

$[\text{Cu}(\text{hfac}-\text{CF}_3)(\text{hfac})]^+$			$[[\text{Cu}(\text{hfac}-\text{CF}_3)(\text{hfac})]^+]^\ddagger$		
27.291	389.61	1075.789	-214.534	362.883	973.732
29.504	405.382	1083.527	-103.873	373.022	1043.113
30.625	436.848	1166.288	23.633	385.49	1129.479
33.013	466.393	1233.496	26.827	391.915	1159.783
45.367	494.055	1263.782	30.784	453.134	1216.39
60.283	515.131	1321.313	30.987	466.865	1310.824
90.04	523.459	1327.028	48.644	467.793	1327.896
105.433	529.269	1342.888	70.325	492.009	1335.641
111.066	541.401	1358.154	89.851	524.45	1359.131
138.398	545.015	1436.057	104.489	538.374	1371.153
146.911	608.925	1450.957	110.461	452.599	1424.207
152.949	684.176	1574.987	114.174	597.176	1570.445
205.056	684.9	1577.336	135.995	603.703	1570.938
227.814	696.161	1577.957	174.759	671.736	1574.48
259.585	706.546	1584.791	183.897	685.098	1585.942
263.102	706.805	1590.293	214.195	695.801	1586.693
268.986	851.943	1590.576	247.675	704.531	1588.813
273.471	899.77	1596.876	262.601	708.587	1608.248
277.401	937.33	1620.678	264.866	772.786	1765.25
308.099	939.891	1760.16	266.859	853.601	1819.383
343.255	953.61	1829.483	278.213	896.744	1971.162
356.68	977.293	2991.315	325.894	935.113	2999.807
370.092	981.286	3029.909	328.65	951.999	3037.66

Table C.35: Vibrational frequencies (cm^{-1}) for the loss of *hfac* from $[\text{Ni}(\text{hfac}-\text{CH}_3)(\text{hfac})]^+$.

$[\text{Ni}(\text{hfac}-\text{CF}_3)(\text{hfac})]^+$			$[[\text{Ni}(\text{hfac}-\text{CF}_3)(\text{hfac})]^+]^\ddagger$		
9.229	403.204	982.007	-265.698	400.509	941.955
44.357	411.058	1060.438	-170.651	413.635	995.208
46.643	464.62	1078.841	28.941	462.869	1074.857
50.612	468.426	1171.347	32.441	464.405	1093.109
70.884	471.421	1242.452	42.935	475.137	1182.474
92.905	496.893	1316.297	63.711	482.132	1276.66
107.711	534.274	1323.934	72.767	503.74	1295.341
111.656	547.83	1333.551	92.51	529.766	1327.611
181.81	550.948	1371.855	111.171	542.19	1340.157
201.801	588.216	1419.418	124.913	547.366	1358.827
215.015	619.254	1452.962	136.625	548.131	1416.793
27.692	698.453	1536.774	188.258	618.547	1573.651
243.986	715.848	1547.325	208.152	657.524	1577.794
249.577	723.404	1581.662	225.81	690.108	1584.916
269.735	739.696	1586.106	238.272	705.001	1594.665
277.082	760.223	1588.049	245.484	718.023	1596.757
309.577	829.43	1594.788	255.602	723.195	1597.712
314.236	859.665	1598.166	270.044	763.932	1603.866
335.81	878.414	1601.988	277.045	816.455	1685.624
338.093	892.258	1618.438	314.991	850.263	1938.556
345.266	903.306	1746.943	324.909	854.681	2291.451
377.634	916.798	2939.193	357.162	877.271	2954.123
391.749	936.604	2962.462	398.189	904.685	2990.049

Table C.36: Vibrational frequencies (cm^{-1}) for the loss of *hfac* from $[\text{Zn}(\text{hfac}-\text{CH}_3)(\text{hfac})]^+$.

$[\text{Zn}(\text{hfac}-\text{CF}_3)(\text{hfac})]^+$			$[[\text{Zn}(\text{hfac}-\text{CF}_3)(\text{hfac})]^+]^\ddagger$		
24.851	367.33	1044.469	-311.648	341.584	988.654
25.957	375.101	1047.094	-193.566	364.724	1053.635
26.743	394.64	1062.787	22.309	376.162	1088.176
27.887	464.093	1162.27	25.596	384.669	1095.944
34.135	470.291	1183.926	26.551	433.018	1198.508
49.621	492.111	1309.312	27.276	439.567	1249.498
91.117	523.386	1314.048	35.415	465.207	1263.635
95.29	525.786	1342.109	53.559	482.372	1341.773
99.977	547.937	1368.273	65.734	523.826	1342.093
141.856	560.666	1402.82	70.711	537.154	1358.639
152.619	623.063	1450.902	99.395	51.31	1515.168
157.702	630.025	1569.858	103.943	541.795	1557.978
178.036	683.297	1570.2	125.464	571.89	1562.597
205.001	696.39	1578.355	148.467	580.421	1568.698
216.088	704.929	1586.75	152.203	587.913	1592.556
258.373	706.629	1587.469	204.557	657.377	1594.649
265.377	801.487	1605.672	205.215	687.552	1596.121
276.076	854.648	1646.577	215.213	701.2	1685.711
282.54	881.395	1763.945	240.605	834.784	1775.728
283.705	907.303	1774.109	248.112	852.038	1797.665
325.203	921.626	1971.729	262.49	866.51	2242.8
330.01	938.077	2987.617	279.169	911.819	2940.824
356.911	965.94	2996.836	282.819	920.068	2999.012

Table C.37: Vibrational frequencies (cm^{-1}) for the loss of *tftm* from $[\text{Cu}(\text{tftm}-t\text{Bu})(\text{tftm})]^+$.

$[\text{Cu}(\text{tftm}-t\text{Bu})(\text{tftm})]^+$			$[[\text{Cu}(\text{tftm}-t\text{Bu})(\text{tftm})]^+]^\ddagger$		
25.635	513.55	1350.782	-169.653	469.495	1336.539
28.219	531.294	1352.16	-120.615	476.844	1368.79
31.947	539.316	1383.285	47.706	484.717	1391.095
46.152	543.641	1388.727	38.615	53.224	1394.332
50.968	557.573	1389.015	10.475	534.2	1395.569
64.69	667.837	1394.315	21.032	575.686	1398.909
86.015	683.786	1400.605	27.332	601.924	1403.351
97.757	694.797	1406.966	30.782	621.441	1405.688
109.614	710.587	1410.78	39.99	632.953	1413.169
132.839	715.896	1428.113	45.893	678.356	1425.37
153.54	871.453	1431.265	62.464	680.533	1427.21
157.722	896.684	1455.375	89.056	703.743	1447.178
187.038	923.828	1465.235	123.76	744.978	1466.754
199.997	941.35	1567.548	187.213	808.427	1561.577
217.847	945.428	1571.062	187.962	842.141	1578.127
234.308	956.806	1585.013	194.965	891.66	1579.829
253.338	958.843	1855.168	203.817	893.715	1586.013
255.66	960.11	1604.077	214.103	904.143	1624.04
264.978	981.658	1613.664	222.527	939.571	1879.216
277.144	982.655	1745.81	234.688	963.493	1931.544
291.127	984.053	1838.795	237.469	966.575	2073.253
292.245	1009.464	3010.722	263.808	976.938	3000.609
305.241	1026.93	3036.487	274.667	1007.099	3022.62
336.105	1078.255	3073.471	302.577	1020.787	3075.396
360.332	1083.436	3073.842	311.019	1024.932	3076.516
361.421	1159.421	3074.131	317.81	1115.161	3080.234
398.749	1224.65	3086.622	351.351	1148.958	3084.184
404.973	1248.286	3088.115	364.244	1169.665	3085.82
424.78	1263.443	3088.401	371.163	1220.452	3086.471
436.429	1280.184	3176.414	400.411	1281.038	3176.707
483.742	1289.597	3177.351	415.296	1291.561	3178.084
487.308	1347.516	3177.814	452.108	1310.376	3178.442

Table C.38: Vibrational frequencies (cm^{-1}) for the loss of *tftm* from $[\text{Ni}(\text{tftm}-t\text{Bu})(\text{tftm})]^+$.

$[\text{Ni}(\text{tftm}-t\text{Bu})(\text{tftm})]^+$			$[[\text{Ni}(\text{tftm}-t\text{Bu})(\text{tftm})]^+]^\ddagger$		
35.089	515.353	1348.598	-263.029	506.922	1334.571
38.714	540.257	1372.902	-161.529	520.588	1352.642
40.441	550.888	1383.483	27.802	536.585	1356.652
54.583	571.561	1386.319	41.903	541.929	1384.027
74.691	595.84	1388.437	61.232	569.855	1386.549
92.54	679.88	1394.107	68.963	588.83	188.59
99.627	719.834	1402.839	82.145	643.389	1391.282
116.439	729.908	1404.818	84.166	692.919	1403.483
180.674	739.52	1409.741	105.694	694.947	1405.23
191.835	766.381	1423.117	125.427	711.771	1406.349
196.231	845.118	1433.868	135.669	728.827	1412.763
219.593	851.763	1440.656	183.821	759.208	1422.158
223.281	877.032	1443.269	195.621	814.389	1428.82
240.235	892.602	1542.697	208.652	852.723	1567.718
249.266	903.816	1557.066	226.939	85.406	1581.692
255.267	928.4	1570.375	236.051	897.321	1591.935
272.739	934.779	1584.529	247.931	922.953	1595.423
285.423	948.99	1587.915	250.548	923.653	1629.743
299.579	961.01	1596.732	260.485	943.924	1672.797
310.587	965.021	1601.538	277.48	963.039	1941.635
319.568	980.003	1742.68	292.555	964.147	2274.382
326.632	984.652	2942.914	305.053	979.634	2984.463
334.276	1009.922	2976.571	319.356	1007.895	2998.372
355.073	1019.304	3071.526	326.002	1016.658	3072.508
368.456	1071.032	3071.798	348.18	1020.183	3072.778
380.085	1091.149	3077.431	374.723	1087.035	3076.516
398.643	1184.492	3078.856	398.336	1105.885	3078.424
409.415	1226.731	3088.48	414.057	1180.463	3086.581
418.97	1256.348	3089.834	416.976	1213.065	3087.372
467.982	1277.475	3167.859	470.583	1266.287	3168.203
470.134	1299.523	3177.171	475.557	1303.055	3175.398
485.004	1338.774	3177.8	477.863	1310.434	3176.374

Table C.39: Vibrational frequencies (cm^{-1}) for the loss of *tftm* from $[\text{Cu}(\text{tftm}-t\text{Bu})(\text{tftm})]^+$.)

$[\text{Zn}(\text{tftm}-t\text{Bu})(\text{tftm})]^+$			$[[\text{Zn}(\text{tftm}-t\text{Bu})(\text{tftm})]^+]^\ddagger$		
24.767	492.934	1344.092	-185.038	465.135	1323.454
28.371	523.872	1356.729	-166.64	470.212	1357.005
29.76	543.725	1386.492	20.037	483.302	1389.063
34.899	559.108	1390.699	23.84	523.034	1392.252
49.255	570.651	1391.008	26.56	535.468	1395.111
52.289	627.799	1396.362	27.766	540.296	1396.712
87.284	674.127	1402.904	37.529	561.237	1402.444
96.497	689.016	1407.472	57.383	601.491	1403.3
112.06	704.091	1409.956	59.098	625.261	1406.767
140.517	714.656	1414.1	85.392	677.543	1412.101
158.087	799.088	1433.152	95.905	687.879	1421.43
159.127	846.403	1439.78	105.007	697.864	1425.85
179.163	884.54	148.155	124.287	771.766	1439.964
185.21	904.899	1562.648	170.846	788.399	1564.934
21.295	917.556	1583.042	181.107	799.893	1580.033
216.116	931.799	1585.009	191.309	839.623	1584.378
235.561	942.831	1594.626	199.048	856.928	1594.028
264.54	961.378	1634.488	226.439	895.62	1775.657
267.703	961.942	1747.201	233.678	902.965	1882.072
284.398	966.634	1767.639	243.264	937.9	193.715
287.472	983.973	1981.602	252.669	961.818	2007.153
292.034	1010.8	2993.148	265.599	964.769	3003.5
298.3	1033.552	2995.043	268.91	975.755	3023.501
320.909	1050.662	3074.718	291.502	1006.142	3070.175
354.157	1071.956	3075.075	298.747	1018.54	3075.755
355.282	1080.789	3075.432	330.241	1065.287	3078.414
361.435	1173.2	3087.444	340.838	1131.056	3080.67
369.469	1212.278	3088.607	353.095	1159.915	3084.713
400.92	1240.126	3089.233	360.105	1156.826	3087.808
426.525	1283.079	3177.74	368.103	1276.649	312.533
465.633	1291.605	3179.294	398.594	1288.939	3175.6
485.976	1316.536	3180.279	416.748	1309.92	3178.443

Table C.40: Vibrational frequencies (cm^{-1}) for the loss of *t*Bu from $[\text{Cu(acac)}(\text{tftm})]^+$.

$[\text{Cu(acac)}(\text{tftm})]^+$			$[[\text{Cu(acac)}(\text{tftm})]^+]^\ddagger$		
26.086	630.89	1385.605	-240.664	561.821	1360.995
36.623	672.251	1388.041	22.653	604.301	1362.281
47.745	695.529	1390.54	37.192	630.78	1371.86
53.688	715.36	1390.812	42.852	698.988	1374.951
58.196	869.02	1396.732	55.317	725.557	1377.458
95.043	873.783	1402.166	55.972	839.185	1380.844
102.816	925.358	1409.315	79.74	851.574	1392.208
112.368	934.302	1411.52	84.131	864.261	1417.65
135.37	940.949	1429.3	102.589	892.749	1449.237
141.336	961.298	1432.969	119.053	912.292	1462.756
146.158	961.66	1446.981	132.881	919.437	1480.311
166.674	966.492	1449.735	141.579	940.329	1482.96
173.25	980.614	1477.13	145.487	960.821	1492.427
193.235	983.547	1564.588	146.444	971.919	1553.628
199.236	984.86	1585.268	158.661	986.697	1577.546
212.262	999.509	1617.305	161.555	988.784	1637.105
222.347	1010.296	1637.74	163.569	993.917	1663.334
253.355	1015.59	1717.15	171.051	995.07	1727.306
260.086	1018.228	1755.338	182.853	1004.306	1764.538
279.948	1028.596	3020.479	192.998	1019.074	3028.569
282.599	1041.501	3043.089	208.861	1021.183	3029.317
293.681	1093.778	3056.279	280.527	1026.368	3032.483
303.172	1144.28	3057.084	288.573	1089.177	3050.772
337.736	1152.736	3069.167	291.528	1121.295	3061.185
363.625	1189.316	3071.309	294.858	1139.267	3062.077
385.491	1242.336	3074.372	325.338	1150.943	3063.163
399.151	1274.712	3075.038	373.258	1236.854	3063.353
412.52	1281.873	3075.177	393.294	1255.965	3064.25
416.087	1294.191	3086.178	405.59	1299.49	3067.176
426.184	1341.56	3087.931	408.916	1311.976	3072.998
485.322	1345.339	3088.392	429.065	1341.807	3076.283
489.614	1353.529	3153.999	440.645	1343.098	3146.703
540.901	1360.438	3156.209	468.161	1346.179	3148.492
541.92	1367.631	3176.77	539.997	1350.982	3150.768
556.166	1368.834	3177.947	543.289	1351.684	3158.719
605.369	1374.543	3178.448	555.255	1352.732	3162.196

Table C.41: Vibrational frequencies (cm^{-1}) for the loss of $t\text{Bu}$ from $[\text{Ni}(\text{acac})(\text{tftm})]^+$.

$[\text{Ni}(\text{acac})(\text{tftm})]^+$			$[[\text{Ni}(\text{acac})(\text{tftm})^+]]^\ddagger$		
41.511	666.704	1383.742	-396.376	574.171	1368.876
54.75	689.925	1387.966	42.509	607.621	1376.887
58.914	736.478	1390.983	54.09	667.712	1379.101
73.795	753.841	1394.357	60.506	715.11	1381.113
88.841	847.281	1397.617	70.334	743.592	1387.458
102.105	876.08	1409.018	79.16	854.789	1401.52
118.88	896.373	1410.129	91.382	873.243	1419.246
122.34	912.462	1417.977	110.972	891.283	1422.315
132.321	934.56	1421.588	120.806	891.624	1528.214
146.549	937.931	1423.634	128.161	896.147	1446.351
189.975	939.62	1428.685	131.984	915.355	1474.258
201.715	959.814	1457.912	156.512	923.464	1480.525
225.962	963.442	1470.336	166.985	935.551	1489.024
233.582	970.19	1543.442	175.079	952.918	1549.796
244.545	972.75	1573.218	193.268	953.489	1570.516
259.568	977.216	1578.302	211.6	968.307	1582.43
271.816	985.056	1593.597	217.303	975.799	1590.493
278.007	995.863	1600.743	230.784	977.87	1609.233
282.364	1012.409	1610.798	238.758	994.195	1642.697
299.778	1015.66	2958.241	262.597	994.863	2970.416
324.101	1021.798	2969.764	295.74	1001.183	2978.824
344.262	1029.641	3052.649	305.051	1015.481	3042.834
350.978	1047.677	3053.31	324.88	1017.162	3049.852
380.89	1109.803	3068.974	336.036	1047.429	3051.374
387.69	1175.03	3072.743	353.647	1074.312	3053.124
405.227	1187.975	3073.936	370.918	1105.613	3056.387
415.209	1235.927	3075.238	393.259	1171.46	3070.834
420.644	1284.309	3075.991	400.829	1258.037	3073.764
473.362	1303.519	3080.518	407.8	1311.781	3075.441
481.356	1329.693	3083.866	418.167	1322.809	3076.457
487.053	1338.5	3085.44	436.4	1329.78	3079.27
511.044	1350.739	3150.199	471.597	1336.605	3149.599
546.802	1355.09	3151.09	474.779	1354.238	3153.966
561.018	1356.599	3169.039	484.622	1354.395	3159.666
581.646	1368.879	3174.752	543.518	1362.374	3160.97
611.434	1374.777	3177.451	555.974	1367.898	3165.233

Table C.42: Vibrational frequencies (cm^{-1}) for the loss of *t*Bu from $[\text{Zn(acac)(tftm)}]^+$.

$[\text{Zn(acac)(tftm)}]^+$			$[[\text{Zn(acac)(tftm)}]^+]^\ddagger$		
27.26	597.656	1374.6	-337.936	539.677	1374.024
39.198	679.752	1388.407	21.4	540.061	1375.541
41.1	703.445	1389.971	37.095	595.199	1380.834
42.213	714.309	1392.303	40.483	694.563	1381.683
54.792	745.194	1392.748	41.159	704.752	1383.517
98.252	885.122	1398.174	45.119	747.811	1386.934
99.325	914.702	1404.209	71.698	890.139	1387.706
108.236	928.684	1412.254	77.676	893.673	1389.69
113.869	933.809	1413.907	96.825	899.314	1427.091
147.695	937.724	1434.201	108.244	912.22	1477.356
157.638	945.183	1440.345	131.001	918.779	1483.664
174.927	963.146	1491.7	137.541	930.343	1484.149
177.887	964.163	1496.975	144.185	939.117	1492.782
186.572	965.156	1559.296	153.576	946.326	1558.329
194.843	968.823	1578.866	162.47	949.751	1576.025
208.027	984.972	1635.975	163.71	965.235	1651.214
220.29	993.604	1756.37	173.066	985.225	1753.135
242.079	1012.296	1763.015	179.682	995.08	1794.48
267.768	1016.405	1818.536	182.005	996.334	1819.993
270.422	1028.295	3003.196	200.393	997.112	3012.364
278.614	1035.505	3013.877	201.556	1012.905	3023.898
287.501	1066.758	3046.922	222.999	1017.573	3047.643
298.856	1077.515	3048.778	265.735	1037.043	3048.012
325.971	1081.561	3062.8	278.328	1072.371	3053.161
355.268	1155.327	3063.281	287.645	1083.555	3053.285
362.587	1215.744	3075.245	307.047	1103.521	3054.11
373.372	1242.972	3075.488	335.721	1155.397	3063.814
401.569	1284.468	3076.95	373.195	1215.643	3064.142
416.177	1294.187	3086.651	374.409	1312.412	3074.778
428.406	1318.596	3087.576	416.615	1315.533	3075.764
480.093	1336.226	3089.042	424.542	1318.327	3078.379
487.357	1346.11	3145.332	424.691	1336.102	3146.63
494.149	1349.823	3147.019	462.253	1349.298	3147.445
539.861	1361.002	3177.425	482.173	1361.665	3162.663
545.197	1362.52	3179.536	523.709	1361.793	3162.84
570.898	1373.798	3180.98	526.648	1365.764	3164.589

Appendix D: RRKM Calculated Data

Table D.1: Calculated data for $[\text{Ni}(\text{acac})_2]^+$, loss of 1st CH_3 .

E(kJ)	E'	E' [‡]	α	α^{\ddagger}	$\frac{(E^{\ddagger} + a^{\ddagger} E_z^{\ddagger})^s}{(E + aE_z)^{s-1}}$	$\frac{1}{[1 - \beta \frac{dw}{dE'} E']}$	k(E) (sec ⁻¹)
337.582	0.5606	0.5808	0.8950	0.8868	1.83E-16	1.163685	5.221E+18
362.582	0.6021	0.6238	0.8909	0.8824	7.63E-16	1.149949	2.145E+19
387.582	0.6437	0.6668	0.8871	0.8783	2.92E-15	1.138058	8.129E+19
412.582	0.6852	0.7098	0.8834	0.8744	1.04E-14	1.127672	2.859E+20
437.582	0.7267	0.7529	0.8799	0.8707	3.43E-14	1.11853	9.379E+20
462.582	0.7682	0.7959	0.8766	0.8672	1.06E-13	1.110428	2.887E+21
487.582	0.8097	0.8389	0.8723	0.8628	3.04E-13	1.114596	8.294E+21
512.582	0.8512	0.8819	0.8696	0.8599	8.47E-13	1.106454	2.294E+22
537.582	0.8928	0.9249	0.8670	0.8571	2.24E-12	1.09925	6.021E+22
562.582	0.9343	0.9679	0.8645	0.8545	5.63E-12	1.092835	1.506E+23
587.582	0.9758	1.0109	0.8621	0.8520	1.35E-11	1.087091	3.601E+23
612.582	1.0173	1.0539	0.8598	0.8495	3.12E-11	1.081921	8.26E+23
637.582	1.0588	1.0969	0.8576	0.8472	6.92E-11	1.077247	1.822E+24
662.582	1.1003	1.1400	0.8555	0.8450	1.48E-10	1.073004	3.877E+24
687.582	1.1419	1.1830	0.8534	0.8428	3.05E-10	1.069136	7.972E+24
712.582	1.1834	1.2260	0.8515	0.8407	6.09E-10	1.065598	1.588E+25
737.582	1.2249	1.2690	0.8496	0.8388	1.18E-09	1.062351	3.072E+25
762.582	1.2664	1.3120	0.8477	0.8368	2.23E-09	1.059363	5.777E+25
787.582	1.3079	1.3550	0.8460	0.8350	4.1E-09	1.056605	1.059E+26
812.582	1.3494	1.3980	0.8443	0.8332	7.34E-09	1.054052	1.893E+26
837.582	1.3910	1.4410	0.8427	0.8315	1.29E-08	1.051684	3.306E+26
862.582	1.4325	1.4841	0.8411	0.8298	2.2E-08	1.049482	5.651E+26
887.582	1.4740	1.5271	0.8395	0.8282	3.69E-08	1.04743	9.463E+26
912.582	1.5155	1.5701	0.8381	0.8266	6.08E-08	1.045514	1.554E+27
937.582	1.5570	1.6131	0.8366	0.8251	9.82E-08	1.043721	2.506E+27
962.582	1.5985	1.6561	0.8352	0.8237	1.56E-07	1.042041	3.972E+27
987.582	1.6401	1.6991	0.8339	0.8222	2.43E-07	1.040464	6.192E+27
1012.582	1.6816	1.7421	0.8326	0.8209	3.74E-07	1.038981	9.504E+27
1037.582	1.7231	1.7851	0.8313	0.8195	5.66E-07	1.037584	1.437E+28
1062.582	1.7646	1.8282	0.8301	0.8182	8.46E-07	1.036267	2.144E+28
1087.582	1.8061	1.8712	0.8289	0.8170	1.25E-06	1.035023	3.155E+28
1112.582	1.8477	1.9142	0.8277	0.8158	1.81E-06	1.033847	4.585E+28
1137.582	1.8892	1.9572	0.8266	0.8146	2.61E-06	1.032733	6.582E+28
1162.582	1.9307	2.0002	0.8255	0.8135	3.7E-06	1.031678	9.343E+28
1187.582	1.9722	2.0432	0.8244	0.8124	5.2E-06	1.030676	1.312E+29
1212.582	2.0137	2.0862	0.8234	0.8113	7.24E-06	1.029724	1.822E+29
1237.582	2.0552	2.1292	0.8224	0.8102	9.96E-06	1.028819	2.507E+29
1262.582	2.0968	2.1722	0.8214	0.8092	1.36E-05	1.027957	3.416E+29
1287.582	2.1383	2.2153	0.8205	0.8082	1.84E-05	1.027136	4.613E+29

Table D.2: Calculated data for $[\text{Cu}(\text{acac})_2]^+$, loss of 1st CH_3 .

E(kJ)	E'	E'^\ddagger	α	α^\ddagger	$\frac{(E^\ddagger + a^\ddagger E_z^\ddagger)^s}{(E + aE_z)^{s-1}}$	$\frac{1}{[1 - \beta \frac{dw}{dE'} E']}$	k(E) (sec ⁻¹)
548.93	0.9116	0.9444	0.8652	0.8551	1.44E-24	1.088431	1.78E+11
573.93	0.9531	0.9874	0.8625	0.8521	1.02E-23	1.083377	1.26E+12
598.93	0.9946	1.0304	0.8599	0.8496	6.71E-23	1.084678	8.26E+12
623.93	1.0362	1.0735	0.8576	0.8472	3.88E-22	1.079742	4.76E+13
648.93	1.0777	1.1165	0.8554	0.8449	2.03E-21	1.075271	2.48E+14
673.93	1.1192	1.1595	0.8533	0.8426	9.68E-21	1.071204	1.18E+15
698.93	1.1607	1.2025	0.8513	0.8405	4.24E-20	1.067491	5.14E+15
723.93	1.2022	1.2455	0.8494	0.8385	1.72E-19	1.06409	2.08E+16
748.93	1.2437	1.2885	0.8475	0.8365	6.48E-19	1.060965	7.8E+16
773.93	1.2853	1.3315	0.8457	0.8346	2.29E-18	1.058084	2.75E+17
798.93	1.3268	1.3745	0.8439	0.8327	7.59E-18	1.055422	9.09E+17
823.93	1.3683	1.4176	0.8422	0.8310	2.38E-17	1.052955	2.84E+18
848.93	1.4098	1.4606	0.8406	0.8292	7.07E-17	1.050665	8.43E+18
873.93	1.4513	1.5036	0.8390	0.8276	2E-16	1.048533	2.38E+19
898.93	1.4928	1.5466	0.8375	0.8260	5.4E-16	1.046544	6.42E+19
923.93	1.5344	1.5896	0.8360	0.8244	1.4E-15	1.044685	1.66E+20
948.93	1.5759	1.6326	0.8346	0.8229	3.47E-15	1.042945	4.11E+20
973.93	1.6174	1.6756	0.8332	0.8215	8.32E-15	1.041313	9.83E+20
998.93	1.6589	1.7186	0.8319	0.8201	1.92E-14	1.039779	2.27E+21
1023.93	1.7004	1.7617	0.8306	0.8187	4.29E-14	1.038337	5.06E+21
1048.93	1.7419	1.8047	0.8293	0.8174	9.3E-14	1.036977	1.09E+22
1073.93	1.7835	1.8477	0.8281	0.8161	1.96E-13	1.035694	2.3E+22
1098.93	1.8250	1.8907	0.8269	0.8149	4E-13	1.034481	4.69E+22
1123.93	1.8665	1.9337	0.8258	0.8137	7.96E-13	1.033334	9.34E+22
1148.93	1.9080	1.9767	0.8247	0.8125	1.55E-12	1.032247	1.81E+23
1173.93	1.9495	2.0197	0.8236	0.8113	2.94E-12	1.031216	3.44E+23
1198.93	1.9910	2.0627	0.8225	0.8102	5.45E-12	1.030238	6.37E+23
1223.93	2.0326	2.1057	0.8215	0.8092	9.9E-12	1.029308	1.16E+24
1248.93	2.0741	2.1488	0.8205	0.8081	1.76E-11	1.028423	2.06E+24
1273.93	2.1156	2.1918	0.8195	0.8071	3.08E-11	1.02758	3.59E+24
1298.93	2.1571	2.2348	0.8186	0.8061	5.29E-11	1.026776	6.16E+24
1323.93	2.1986	2.2778	0.8176	0.8052	8.92E-11	1.02601	1.04E+25
1348.93	2.2402	2.3208	0.8167	0.8042	1.48E-10	1.025277	1.72E+25
1373.93	2.2817	2.3638	0.8159	0.8033	2.42E-10	1.024578	2.81E+25
1398.93	2.3232	2.4068	0.8150	0.8024	3.89E-10	1.023908	4.52E+25
1423.93	2.3647	2.4498	0.8142	0.8016	6.17E-10	1.023268	7.17E+25
1448.93	2.4062	2.4929	0.8134	0.8007	9.66E-10	1.022654	1.12E+26
1473.93	2.4477	2.5359	0.8126	0.7999	1.49E-09	1.022065	1.73E+26
1498.93	2.4893	2.5789	0.8118	0.7991	2.28E-09	1.021501	2.64E+26

Table D.3: Calculated data for $[\text{Zn}(\text{acac})_2]^+$, loss of 1st CH_3 .

E(kJ)	E'	E'^\ddagger	α	α^\ddagger	$\frac{(E^\ddagger + a^\ddagger E_z^\ddagger)^s}{(E + aE_z)^{s-1}}$	$\frac{1}{[1 - \beta \frac{dw}{dE'} E']}$	k(E) (sec ⁻¹)
292.867	0.4895	0.5032	0.9003	0.8939	2.67E-14	1.1929	9.05E+18
317.867	0.5313	0.5461	0.8956	0.8890	9.48E-14	1.1747	3.16E+19
342.867	0.5731	0.5891	0.8912	0.8843	3.13E-13	1.1593	1.03E+20
367.867	0.6149	0.6320	0.8871	0.8800	9.68E-13	1.1461	3.15E+20
392.867	0.6567	0.6750	0.8832	0.8759	2.81E-12	1.1346	9.06E+20
417.867	0.6985	0.7179	0.8795	0.8720	7.73E-12	1.1246	2.47E+21
442.867	0.7403	0.7609	0.8760	0.8683	2.01E-11	1.1158	6.37E+21
467.867	0.7821	0.8038	0.8712	0.8634	4.87E-11	1.1206	1.55E+22
492.867	0.8238	0.8468	0.8683	0.8604	1.16E-10	1.1117	3.67E+22
517.867	0.8656	0.8898	0.8655	0.8575	2.66E-10	1.1039	8.33E+22
542.867	0.9074	0.9327	0.8629	0.8547	5.84E-10	1.0969	1.82E+23
567.867	0.9492	0.9757	0.8604	0.8520	1.23E-09	1.0907	3.82E+23
592.867	0.9910	1.0186	0.8579	0.8495	2.51E-09	1.0851	7.74E+23
617.867	1.0328	1.0616	0.8556	0.8471	4.96E-09	1.0801	1.52E+24
642.867	1.0746	1.1045	0.8534	0.8447	9.5E-09	1.0756	2.90E+24
667.867	1.1164	1.1475	0.8512	0.8425	1.77E-08	1.0715	5.37E+24
692.867	1.1581	1.1904	0.8492	0.8403	3.2E-08	1.0677	9.68E+24
717.867	1.1999	1.2334	0.8472	0.8382	5.64E-08	1.0643	1.70E+25
742.867	1.2417	1.2763	0.8452	0.8362	9.72E-08	1.0611	2.93E+25
767.867	1.2835	1.3193	0.8434	0.8343	1.64E-07	1.0582	4.92E+25
792.867	1.3253	1.3622	0.8416	0.8324	2.71E-07	1.0555	8.10E+25
817.867	1.3671	1.4052	0.8399	0.8306	4.38E-07	1.0530	1.31E+26
842.867	1.4089	1.4481	0.8382	0.8289	6.96E-07	1.0507	2.07E+26
867.867	1.4507	1.4911	0.8366	0.8272	1.09E-06	1.0486	3.23E+26
892.867	1.4925	1.5340	0.8351	0.8256	1.67E-06	1.0466	4.95E+26
917.867	1.5342	1.5770	0.8335	0.8240	2.52E-06	1.0447	7.47E+26
942.867	1.5760	1.6199	0.8321	0.8225	3.75E-06	1.0429	1.11E+27
967.867	1.6178	1.6629	0.8307	0.8210	5.51E-06	1.0413	1.63E+27
992.867	1.6596	1.7059	0.8293	0.8196	7.98E-06	1.0398	2.36E+27
1017.867	1.7014	1.7488	0.8280	0.8182	1.14E-05	1.0383	3.37E+27
1042.867	1.7432	1.7918	0.8267	0.8169	1.61E-05	1.0369	4.75E+27
1067.867	1.7850	1.8347	0.8254	0.8156	2.26E-05	1.0356	6.63E+27
1092.867	1.8268	1.8777	0.8242	0.8143	3.12E-05	1.0344	9.16E+27
1117.867	1.8685	1.9206	0.8231	0.8131	4.27E-05	1.0333	1.25E+28
1142.867	1.9103	1.9636	0.8219	0.8119	5.78E-05	1.0322	1.69E+28
1167.867	1.9521	2.0065	0.8208	0.8108	7.76E-05	1.0312	2.27E+28
1192.867	1.9939	2.0495	0.8197	0.8096	1.03E-04	1.0302	3.02E+28
1217.867	2.0357	2.0924	0.8187	0.8085	1.36E-04	1.0292	3.98E+28
1242.867	2.0775	2.1354	0.8177	0.8075	1.78E-04	1.0284	5.20E+28

Table D.4: Calculated Data for $[\text{Cu}(\text{acac})(\text{acac-CH}_3)]^+$ loss of CH_3 .

E(kJ)	E'	E'^\ddagger	α	α^\ddagger	$\frac{(E^\ddagger + a^\ddagger E_z^\ddagger)^s}{(E + aE_z)^{s-1}}$	$\frac{1}{[1 - \beta \frac{dw}{dE'} E']}$	k(E) (sec ⁻¹)
328.46	0.6580	0.6933	0.8844	0.8708	1.55E-16	1.1343	5.10E+20
353.46	0.7081	0.7460	0.8801	0.8713	1.28E-15	1.1225	4.15E+21
378.46	0.7582	0.7988	0.8760	0.8670	6.24E-15	1.1123	2.01E+22
403.46	0.8083	0.8516	0.8721	0.8619	2.56E-14	1.1034	8.16E+22
428.46	0.8584	0.9043	0.8676	0.8585	1.08E-13	1.1052	3.44E+23
453.46	0.9084	0.9571	0.8644	0.8552	3.93E-13	1.0967	1.24E+24
478.46	0.9585	1.0099	0.8614	0.8520	1.32E-12	1.0894	4.16E+24
503.46	1.0086	1.0626	0.8586	0.8491	4.11E-12	1.0830	1.29E+25
528.46	1.0587	1.1154	0.8559	0.8462	1.20E-11	1.0773	3.72E+25
553.46	1.1088	1.1681	0.8533	0.8436	3.27E-11	1.0722	1.01E+26
578.46	1.1589	1.2209	0.8509	0.8410	8.43E-11	1.0677	2.60E+26
603.46	1.2089	1.2737	0.8485	0.8385	2.06E-10	1.0636	6.34E+26
628.46	1.2590	1.3264	0.8463	0.8362	4.81E-10	1.0599	1.47E+27
653.46	1.3091	1.3792	0.8441	0.8340	1.07E-09	1.0565	3.28E+27
678.46	1.3592	1.4320	0.8421	0.8318	2.30E-09	1.0535	6.99E+27
703.46	1.4093	1.4847	0.8401	0.8298	4.73E-09	1.0507	1.44E+28
728.46	1.4594	1.5375	0.8382	0.8278	9.40E-09	1.0481	2.85E+28
753.46	1.5094	1.5903	0.8364	0.8259	1.81E-08	1.0458	5.47E+28
778.46	1.5595	1.6430	0.8346	0.8241	3.38E-08	1.0436	1.02E+29
803.46	1.6096	1.6958	0.8329	0.8223	6.13E-08	1.0416	1.85E+29
828.46	1.6597	1.7486	0.8313	0.8207	1.08E-07	1.0398	3.25E+29
853.46	1.7098	1.8013	0.8297	0.8190	1.87E-07	1.0380	5.60E+29
878.46	1.7599	1.8541	0.8282	0.8175	3.14E-07	1.0364	9.42E+29
903.46	1.8099	1.9069	0.8267	0.8160	5.18E-07	1.0349	1.55E+30
928.46	1.8600	1.9596	0.8253	0.8145	8.36E-07	1.0335	2.50E+30
953.46	1.9101	2.0124	0.8240	0.8131	1.32E-06	1.0322	3.95E+30
978.46	1.9602	2.0652	0.8227	0.8118	2.06E-06	1.0310	6.14E+30
1003.46	2.0103	2.1179	0.8214	0.8105	3.15E-06	1.0298	9.38E+30
1028.46	2.0604	2.1707	0.8202	0.8092	4.74E-06	1.0287	1.41E+31
1053.46	2.1104	2.2235	0.8190	0.8080	7.03E-06	1.0277	2.09E+31
1078.46	2.1605	2.2762	0.8179	0.8069	1.03E-05	1.0267	3.05E+31
1103.46	2.2106	2.3290	0.8167	0.8057	1.48E-05	1.0258	4.39E+31
1128.46	2.2607	2.3818	0.8157	0.8046	2.11E-05	1.0249	6.25E+31
1153.46	2.3108	2.4345	0.8146	0.8036	2.96E-05	1.0241	8.78E+31
1178.46	2.3609	2.4873	0.8136	0.8026	4.12E-05	1.0233	1.22E+32
1203.46	2.4109	2.5401	0.8127	0.8016	5.67E-05	1.0226	1.67E+32
1228.46	2.4610	2.5928	0.8117	0.8006	7.71E-05	1.0219	2.28E+32
1253.46	2.5111	2.6456	0.8108	0.7997	1.04E-04	1.0212	3.07E+32
1278.46	2.5612	2.6984	0.8099	0.7988	1.39E-04	1.0206	4.09E+32

Table D.5: Calculated Data for $[\text{Cu}(\text{acac})]^+$ loss of CH_3 .

E(kJ)	E'	E'^\ddagger	α	α^\ddagger	$\frac{(E^\ddagger + a^\ddagger E_z^\ddagger)^s}{(E + aE_z)^{s-1}}$	$\frac{1}{[1 - \beta \frac{dw}{dE'} E']}$	k(E) (sec ⁻¹)
110.403	0.3827	0.3968	0.9064	0.9060	9.68E-05	1.2580	1.91E+29
135.403	0.4694	0.4867	0.8943	0.8941	2.85E-04	1.2028	5.38E+29
160.403	0.5560	0.5765	0.8838	0.8837	7.46E-04	1.1653	1.37E+30
185.403	0.6427	0.6664	0.8745	0.8745	1.77E-03	1.1383	3.16E+30
210.403	0.7293	0.7562	0.8662	0.8663	3.84E-03	1.1180	6.74E+30
235.403	0.8160	0.8461	0.8588	0.8590	7.73E-03	1.1022	1.34E+31
260.403	0.9027	0.9359	0.8521	0.8524	1.46E-02	1.0896	2.49E+31
285.403	0.9893	1.0258	0.8459	0.8464	2.60E-02	1.0793	4.41E+31
310.403	1.0760	1.1156	0.8406	0.8414	4.42E-02	1.0754	7.46E+31
335.403	1.1627	1.2055	0.8359	0.8368	7.16E-02	1.0673	1.20E+32
360.403	1.2493	1.2953	0.8315	0.8325	1.12E-01	1.0606	1.86E+32
385.403	1.3360	1.3852	0.8275	0.8285	1.68E-01	1.0549	2.79E+32
410.403	1.4226	1.4750	0.8237	0.8248	2.45E-01	1.0500	4.05E+32
435.403	1.5093	1.5649	0.8202	0.8214	3.49E-01	1.0458	5.73E+32
460.403	1.5960	1.6547	0.8169	0.8182	4.83E-01	1.0421	7.91E+32
485.403	1.6826	1.7446	0.8138	0.8152	6.55E-01	1.0389	1.07E+33
510.403	1.7693	1.8344	0.8109	0.8123	8.71E-01	1.0361	1.42E+33
535.403	1.8559	1.9243	0.8082	0.8097	1.14E+00	1.0336	1.85E+33
560.403	1.9426	2.0142	0.8056	0.8072	1.46E+00	1.0314	2.37E+33
585.403	2.0293	2.1040	0.8032	0.8049	1.85E+00	1.0294	2.99E+33
610.403	2.1159	2.1939	0.8009	0.8027	2.31E+00	1.0276	3.72E+33
635.403	2.2026	2.2837	0.7988	0.8006	2.85E+00	1.0259	4.59E+33
660.403	2.2892	2.3736	0.7968	0.7987	3.47E+00	1.0245	5.58E+33
685.403	2.3759	2.4634	0.7949	0.7968	4.19E+00	1.0231	6.73E+33
710.403	2.4626	2.5533	0.7930	0.7951	5.01E+00	1.0219	8.04E+33
735.403	2.5492	2.6431	0.7913	0.7934	5.93E+00	1.0207	9.51E+33
760.403	2.6359	2.7330	0.7897	0.7919	6.97E+00	1.0197	1.12E+34
785.403	2.7226	2.8228	0.7881	0.7904	8.13E+00	1.0187	1.30E+34
810.403	2.8092	2.9127	0.7867	0.7890	9.41E+00	1.0178	1.51E+34
835.403	2.8959	3.0025	0.7853	0.7876	1.08E+01	1.0170	1.73E+34
860.403	2.9825	3.0924	0.7840	0.7864	1.24E+01	1.0162	1.98E+34
885.403	3.0692	3.1822	0.7827	0.7852	1.41E+01	1.0155	2.25E+34
910.403	3.1559	3.2721	0.7815	0.7841	1.59E+01	1.0148	2.54E+34
935.403	3.2425	3.3619	0.7804	0.7830	1.79E+01	1.0142	2.86E+34
960.403	3.3292	3.4518	0.7793	0.7820	2.01E+01	1.0136	3.20E+34
985.403	3.4158	3.5417	0.7783	0.7810	2.24E+01	1.0131	3.57E+34
1010.403	3.5025	3.6315	0.7773	0.7801	2.49E+01	1.0126	3.96E+34
1035.403	3.5892	3.7214	0.7764	0.7792	2.75E+01	1.0121	4.38E+34
1060.403	3.6758	3.8112	0.7755	0.7783	3.04E+01	1.0116	4.83E+34
1085.403	3.7625	3.9011	0.7747	0.7776	3.34E+01	1.0112	5.30E+34

Table D.6: Calculated Data for $[\text{Ni}(\text{acac})]^+$ loss of CH_3 .

E(kJ)	E'	E'^\ddagger	α	α^\ddagger	$\frac{(E^\ddagger + a^\ddagger E_z^\ddagger)^s}{(E + aE_z)^{s-1}}$	$\frac{1}{[1 - \beta \frac{dw}{dE'}]}$	k(E) (sec ⁻¹)
431.09	1.4480	1.5467	0.8455	0.8233	2.31E-16	1.0487	4.12E+19
456.09	1.5319	1.6364	0.8425	0.8201	3.04E-15	1.044791	5.40E+20
481.09	1.6159	1.7261	0.8398	0.8170	2.95E-14	1.04137	5.21E+21
506.09	1.6999	1.8158	0.8372	0.8142	2.22E-13	1.038356	3.92E+22
531.09	1.7838	1.9055	0.8348	0.8116	1.36E-12	1.035683	2.39E+23
556.09	1.8678	1.9952	0.8326	0.8091	6.98E-12	1.033299	1.23E+24
581.09	1.9518	2.0849	0.8304	0.8067	3.08E-11	1.031162	5.40E+24
606.09	2.0357	2.1746	0.8284	0.8045	1.19E-10	1.029238	2.09E+25
631.09	2.1197	2.2643	0.8265	0.8025	4.14E-10	1.027498	7.22E+25
656.09	2.2037	2.3540	0.8247	0.8005	1.30E-09	1.025919	2.26E+26
681.09	2.2877	2.4437	0.8230	0.7986	3.73E-09	1.024479	6.50E+26
706.09	2.3716	2.5334	0.8213	0.7969	9.93E-09	1.023163	1.73E+27
731.09	2.4556	2.6231	0.8198	0.7952	2.47E-08	1.021957	4.29E+27
756.09	2.5396	2.7128	0.8183	0.7937	5.77E-08	1.020847	1.00E+28
781.09	2.6235	2.8025	0.8170	0.7922	1.28E-07	1.019823	2.21E+28
806.09	2.7075	2.8922	0.8156	0.7908	2.69E-07	1.018877	4.65E+28
831.09	2.7915	2.9819	0.8144	0.7894	5.40E-07	1.018001	9.35E+28
856.09	2.8754	3.0716	0.8132	0.7882	1.04E-06	1.017187	1.80E+29
881.09	2.9594	3.1613	0.8121	0.7870	1.94E-06	1.016429	3.35E+29
906.09	3.0434	3.2510	0.8110	0.7858	3.49E-06	1.015723	6.02E+29
931.09	3.1274	3.3407	0.8100	0.7847	6.07E-06	1.015063	1.05E+30
956.09	3.2113	3.4304	0.8090	0.7837	1.03E-05	1.014445	1.77E+30
981.09	3.2953	3.5201	0.8081	0.7827	1.69E-05	1.013866	2.91E+30
1006.09	3.3793	3.6097	0.8072	0.7818	2.72E-05	1.013323	4.68E+30
1031.09	3.4632	3.6994	0.8063	0.7809	4.27E-05	1.012812	7.35E+30
1056.09	3.5472	3.7891	0.8055	0.7801	6.57E-05	1.012331	1.13E+31
1081.09	3.6312	3.8788	0.8048	0.7793	9.91E-05	1.011877	1.70E+31
1106.09	3.7152	3.9685	0.8041	0.7785	1.47E-04	1.011449	2.52E+31
1131.09	3.7991	4.0582	0.8034	0.7778	2.14E-04	1.011045	3.67E+31
1156.09	3.8831	4.1479	0.8027	0.7772	3.06E-04	1.010662	5.26E+31
1181.09	3.9671	4.2376	0.8021	0.7765	4.32E-04	1.010299	7.42E+31
1206.09	4.0510	4.3273	0.8015	0.7759	6.02E-04	1.009955	1.03E+32
1231.09	4.1350	4.4170	0.8009	0.7753	8.27E-04	1.009628	1.42E+32
1256.09	4.2190	4.5067	0.8004	0.7748	1.12E-03	1.009318	1.92E+32
1281.09	4.3029	4.5964	0.7998	0.7743	1.51E-03	1.009023	2.58E+32
1306.09	4.3869	4.6861	0.7993	0.7738	2.00E-03	1.008742	3.42E+32
1331.09	4.4709	4.7758	0.7989	0.7733	2.62E-03	1.008474	4.49E+32
1356.09	4.5549	4.8655	0.7984	0.7729	3.41E-03	1.008218	5.84E+32
1381.09	4.6388	4.9552	0.7980	0.7725	4.39E-03	1.007975	7.53E+32
1406.09	4.7228	5.0449	0.7976	0.7721	5.61E-03	1.007742	9.61E+32

Table D.7: Calculated Data for $[\text{Zn}(\text{acac})]^+$ loss of CH_3 .

E(kJ)	E'	E'‡	α	α‡	$\frac{(E^‡ + a^‡ E_z^‡)^s}{(E + aE_z)^{s-1}}$	$\frac{1}{[1 - \beta \frac{dw}{dE'} E']}$	k(E) (sec ⁻¹)
456.225	1.5324	1.6369	0.8433	0.8211	5.74E-17	1.047012	3.75E+18
481.225	1.6163	1.7266	0.8406	0.8181	7.98E-16	1.043415	5.19E+19
506.225	1.7003	1.8163	0.8380	0.8153	8.13E-15	1.040247	5.27E+20
531.225	1.7843	1.9060	0.8356	0.8127	6.42E-14	1.037438	4.16E+21
556.225	1.8683	1.9957	0.8334	0.8102	4.10E-13	1.034934	2.65E+22
581.225	1.9522	2.0854	0.8312	0.8079	2.19E-12	1.032689	1.41E+23
606.225	2.0362	2.1751	0.8292	0.8057	1.00E-11	1.030669	6.44E+23
631.225	2.1202	2.2648	0.8273	0.8036	4.02E-11	1.028841	2.58E+24
656.225	2.2041	2.3545	0.8255	0.8017	1.44E-10	1.027183	9.20E+24
681.225	2.2881	2.4442	0.8238	0.7998	4.64E-10	1.025672	2.97E+25
706.225	2.3721	2.5339	0.8222	0.7981	1.37E-09	1.02429	8.76E+25
731.225	2.4561	2.6236	0.8207	0.7965	3.75E-09	1.023024	2.39E+26
756.225	2.5400	2.7133	0.8192	0.7949	9.56E-09	1.021859	6.09E+26
781.225	2.6240	2.8030	0.8179	0.7934	2.29E-08	1.020785	1.46E+27
806.225	2.7080	2.8927	0.8165	0.7920	5.17E-08	1.019792	3.29E+27
831.225	2.7919	2.9824	0.8153	0.7907	1.11E-07	1.018873	7.06E+27
856.225	2.8759	3.0720	0.8141	0.7894	2.28E-07	1.018019	1.45E+28
881.225	2.9599	3.1617	0.8130	0.7882	4.49E-07	1.017224	2.85E+28
906.225	3.0438	3.2514	0.8119	0.7871	8.51E-07	1.016483	5.39E+28
931.225	3.1278	3.3411	0.8109	0.7860	1.56E-06	1.01579	9.86E+28
956.225	3.2118	3.4308	0.8099	0.7850	2.76E-06	1.015143	1.75E+29
981.225	3.2958	3.5205	0.8090	0.7840	4.74E-06	1.014536	3.00E+29
1006.225	3.3797	3.6102	0.8081	0.7831	7.93E-06	1.013966	5.02E+29
1031.225	3.4637	3.6999	0.8073	0.7823	1.29E-05	1.01343	8.18E+29
1056.225	3.5477	3.7896	0.8065	0.7814	2.06E-05	1.012925	1.30E+30
1081.225	3.6316	3.8793	0.8057	0.7806	3.22E-05	1.01245	2.03E+30
1106.225	3.7156	3.9690	0.8050	0.7799	4.92E-05	1.012001	3.10E+30
1131.225	3.7996	4.0587	0.8043	0.7792	7.38E-05	1.011577	4.65E+30
1156.225	3.8835	4.1484	0.8037	0.7785	1.09E-04	1.011175	6.86E+30
1181.225	3.9675	4.2381	0.8030	0.7779	1.58E-04	1.010795	9.94E+30
1206.225	4.0515	4.3278	0.8025	0.7773	2.25E-04	1.010434	1.42E+31
1231.225	4.1355	4.4175	0.8019	0.7767	3.17E-04	1.010092	2.00E+31
1256.225	4.2194	4.5072	0.8013	0.7761	4.40E-04	1.009766	2.77E+31
1281.225	4.3034	4.5969	0.8008	0.7756	6.04E-04	1.009457	3.80E+31
1306.225	4.3874	4.6866	0.8003	0.7751	8.18E-04	1.009162	5.15E+31
1331.225	4.4713	4.7763	0.7999	0.7747	1.10E-03	1.008881	6.89E+31
1356.225	4.5553	4.8660	0.7994	0.7742	1.45E-03	1.008613	9.13E+31
1381.225	4.6393	4.9557	0.7990	0.7738	1.91E-03	1.008358	1.20E+32
1406.225	4.7233	5.0454	0.7986	0.7734	2.48E-03	1.008113	1.56E+32
1431.225	4.8072	5.1351	0.7982	0.7731	3.19E-03	1.00788	2.01E+32

Table D.8: Calculated Data for $[\text{Cu}(\text{acac})_2]^+$ loss of acac.

E(kJ)	E'	E'‡	α	α‡	$\frac{(E^‡ + a^‡ E_z^‡)^s}{(E + aE_z)^{s-1}}$	$\frac{1}{[1 - \beta \frac{dw}{dE'} E']}$	k(E) (sec ⁻¹)
721.916	1.1972	1.2268	0.8496	0.8402	8.11E-30	1.064485	1.63E+02
746.916	1.2387	1.2693	0.8477	0.8382	7.95E-29	1.061332	1.59E+03
771.916	1.2801	1.3118	0.8459	0.8363	6.77E-28	1.058427	1.35E+04
796.916	1.3216	1.3542	0.8441	0.8344	5.09E-27	1.055743	1.01E+05
821.916	1.3631	1.3967	0.8425	0.8327	3.41E-26	1.053257	6.77E+05
846.916	1.4045	1.4392	0.8408	0.8310	2.06E-25	1.050948	4.07E+06
871.916	1.4460	1.4817	0.8392	0.8293	1.13E-24	1.048799	2.23E+07
896.916	1.4874	1.5242	0.8377	0.8277	5.65E-24	1.046795	1.11E+08
921.916	1.5289	1.5667	0.8362	0.8261	2.61E-23	1.044923	5.14E+08
946.916	1.5703	1.6091	0.8348	0.8246	1.12E-22	1.04317	2.20E+09
971.916	1.6118	1.6516	0.8334	0.8232	4.47E-22	1.041526	8.78E+09
996.916	1.6533	1.6941	0.8321	0.8218	1.68E-21	1.039982	3.29E+10
1021.916	1.6947	1.7366	0.8308	0.8204	5.92E-21	1.03853	1.16E+11
1046.916	1.7362	1.7791	0.8295	0.8191	1.97E-20	1.037161	3.86E+11
1071.916	1.7776	1.8216	0.8283	0.8178	6.25E-20	1.035869	1.22E+12
1096.916	1.8191	1.8640	0.8271	0.8166	1.89E-19	1.034649	3.68E+12
1121.916	1.8606	1.9065	0.8259	0.8154	5.44E-19	1.033494	1.06E+13
1146.916	1.9020	1.9490	0.8248	0.8142	1.5E-18	1.0324	2.92E+13
1171.916	1.9435	1.9915	0.8237	0.8131	3.98E-18	1.031363	7.74E+13
1196.916	1.9849	2.0340	0.8227	0.8119	1.02E-17	1.030379	1.97E+14
1221.916	2.0264	2.0765	0.8216	0.8109	2.5E-17	1.029443	4.86E+14
1246.916	2.0679	2.1190	0.8206	0.8098	5.96E-17	1.028552	1.16E+15
1271.916	2.1093	2.1614	0.8197	0.8088	1.38E-16	1.027705	2.67E+15
1296.916	2.1508	2.2039	0.8187	0.8078	3.08E-16	1.026896	5.97E+15
1321.916	2.1922	2.2464	0.8178	0.8069	6.71E-16	1.026125	1.30E+16
1346.916	2.2337	2.2889	0.8169	0.8059	1.42E-15	1.025389	2.75E+16
1371.916	2.2752	2.3314	0.8160	0.8050	2.94E-15	1.024685	5.68E+16
1396.916	2.3166	2.3739	0.8152	0.8041	5.93E-15	1.024012	1.14E+17
1421.916	2.3581	2.4163	0.8143	0.8033	1.17E-14	1.023368	2.25E+17
1446.916	2.3995	2.4588	0.8135	0.8024	2.25E-14	1.022751	4.34E+17
1471.916	2.4410	2.5013	0.8127	0.8016	4.25E-14	1.022159	8.20E+17
1496.916	2.4825	2.5438	0.8120	0.8008	7.87E-14	1.021592	1.52E+18
1521.916	2.5239	2.5863	0.8112	0.8000	1.43E-13	1.021047	2.75E+18
1546.916	2.5654	2.6288	0.8105	0.7993	2.55E-13	1.020524	4.91E+18
1571.916	2.6068	2.6712	0.8098	0.7985	4.48E-13	1.020021	8.61E+18
1596.916	2.6483	2.7137	0.8091	0.7978	7.73E-13	1.019537	1.49E+19
1621.916	2.6898	2.7562	0.8084	0.7971	1.31E-12	1.019071	2.52E+19
1646.916	2.7312	2.7987	0.8078	0.7964	2.2E-12	1.018623	4.22E+19
1671.916	2.7727	2.8412	0.8071	0.7958	3.62E-12	1.018191	6.95E+19
1696.916	2.8141	2.8837	0.8065	0.7951	5.89E-12	1.017775	1.13E+20

Table D.9: Calculated Data for $[\text{Ni}(\text{acac})_2]^+$ loss of acac.

E(kJ)	E'	E'‡	α	α‡	$\frac{(E^‡ + a^‡ E_z^‡)^s}{(E + aE_z)^{s-1}}$	$\frac{1}{[1 - \beta \frac{dw}{dE'} E']}$	k(E) (sec ⁻¹)
680.557	1.1302	1.1709	0.8540	0.8448	2.4E-28	1.076752	5.72E+06
705.557	1.1717	1.2139	0.8520	0.8427	2.15E-27	1.072764	5.09E+07
730.557	1.2132	1.2569	0.8501	0.8407	1.68E-26	1.069109	3.97E+08
755.557	1.2547	1.2999	0.8483	0.8388	1.16E-25	1.06575	2.74E+09
780.557	1.2963	1.3429	0.8465	0.8369	7.22E-25	1.062653	1.70E+10
805.557	1.3378	1.3859	0.8448	0.8351	4.05E-24	1.05979	9.50E+10
830.557	1.3793	1.4290	0.8431	0.8334	2.07E-23	1.057137	4.85E+11
855.557	1.4208	1.4720	0.8415	0.8317	9.75E-23	1.054673	2.27E+12
880.557	1.4623	1.5150	0.8400	0.8301	4.24E-22	1.052379	9.87E+12
905.557	1.5038	1.5580	0.8385	0.8286	1.71E-21	1.050239	3.98E+13
930.557	1.5454	1.6010	0.8370	0.8271	6.49E-21	1.048239	1.50E+14
955.557	1.5869	1.6440	0.8356	0.8256	2.31E-20	1.046365	5.33E+14
980.557	1.6284	1.6870	0.8343	0.8242	7.73E-20	1.044608	1.79E+15
1005.557	1.6699	1.7300	0.8329	0.8228	2.46E-19	1.042957	5.67E+15
1030.557	1.7114	1.7731	0.8317	0.8215	7.43E-19	1.041403	1.71E+16
1055.557	1.7530	1.8161	0.8304	0.8202	2.14E-18	1.039938	4.93E+16
1080.557	1.7945	1.8591	0.8292	0.8189	5.92E-18	1.038556	1.36E+17
1105.557	1.8360	1.9021	0.8280	0.8177	1.57E-17	1.03725	3.60E+17
1130.557	1.8775	1.9451	0.8269	0.8166	4E-17	1.036014	9.15E+17
1155.557	1.9190	1.9881	0.8258	0.8154	9.82E-17	1.034842	2.25E+18
1180.557	1.9605	2.0311	0.8247	0.8143	2.33E-16	1.033732	5.33E+18
1205.557	2.0021	2.0741	0.8237	0.8132	5.36E-16	1.032677	1.22E+19
1230.557	2.0436	2.1172	0.8227	0.8122	1.19E-15	1.031674	2.72E+19
1255.557	2.0851	2.1602	0.8217	0.8112	2.59E-15	1.03072	5.90E+19
1280.557	2.1266	2.2032	0.8207	0.8102	5.45E-15	1.029811	1.24E+20
1305.557	2.1681	2.2462	0.8198	0.8092	1.12E-14	1.028944	2.55E+20
1330.557	2.2096	2.2892	0.8189	0.8083	2.25E-14	1.028117	5.10E+20
1355.557	2.2512	2.3322	0.8180	0.8074	4.4E-14	1.027328	9.99E+20
1380.557	2.2927	2.3752	0.8172	0.8065	8.42E-14	1.026573	1.91E+21
1405.557	2.3342	2.4182	0.8163	0.8056	1.58E-13	1.025851	3.58E+21
1430.557	2.3757	2.4612	0.8155	0.8048	2.9E-13	1.02516	6.58E+21
1455.557	2.4172	2.5043	0.8147	0.8040	5.24E-13	1.024497	1.19E+22
1480.557	2.4587	2.5473	0.8140	0.8032	9.28E-13	1.023862	2.10E+22
1505.557	2.5003	2.5903	0.8132	0.8024	1.62E-12	1.023253	3.66E+22
1530.557	2.5418	2.6333	0.8125	0.8016	2.77E-12	1.022668	6.26E+22
1555.557	2.5833	2.6763	0.8118	0.8009	4.66E-12	1.022106	1.05E+23
1580.557	2.6248	2.7193	0.8111	0.8002	7.74E-12	1.021566	1.75E+23
1605.557	2.6663	2.7623	0.8104	0.7995	1.27E-11	1.021047	2.86E+23
1630.557	2.7078	2.8053	0.8097	0.7988	2.05E-11	1.020547	4.62E+23
1655.557	2.7494	2.8484	0.8091	0.7982	3.26E-11	1.020065	7.35E+23

Table D.10: Calculated Data for $[\text{Zn}(\text{acac})_2]^+$ loss of acac.

E(kJ)	E'	E'‡	α	α‡	$\frac{(E^‡ + a^‡ E_z^‡)^s}{(E + aE_z)^{s-1}}$	$\frac{1}{[1 - \beta \frac{dw}{dE'}]}$	k(E) (sec ⁻¹)
447.239	0.7470	0.7616	0.8755	0.8683	2.04E-20	1.128896	5.10E+14
472.239	0.7888	0.8042	0.8722	0.8648	1.11E-19	1.120123	2.75E+15
497.239	0.8305	0.8468	0.8690	0.8615	5.47E-19	1.112298	1.35E+16
522.239	0.8723	0.8894	0.8660	0.8583	2.45E-18	1.105279	6.00E+16
547.239	0.9140	0.9319	0.8631	0.8553	1.01E-17	1.098953	2.46E+17
572.239	0.9558	0.9745	0.8604	0.8524	3.86E-17	1.093226	9.32E+17
597.239	0.9976	1.0171	0.8577	0.8497	1.37E-16	1.088021	3.30E+18
622.239	1.0393	1.0597	0.8553	0.8472	4.61E-16	1.089058	1.11E+19
647.239	1.0811	1.1022	0.8531	0.8449	1.45E-15	1.084009	3.47E+19
672.239	1.1228	1.1448	0.8510	0.8427	4.3E-15	1.079422	1.03E+20
697.239	1.1646	1.1874	0.8489	0.8405	1.21E-14	1.075239	2.88E+20
722.239	1.2063	1.2300	0.8470	0.8385	3.24E-14	1.071411	7.68E+20
747.239	1.2481	1.2725	0.8451	0.8365	8.3E-14	1.067897	1.96E+21
772.239	1.2898	1.3151	0.8432	0.8346	2.03E-13	1.06466	4.79E+21
797.239	1.3316	1.3577	0.8415	0.8327	4.79E-13	1.061672	1.12E+22
822.239	1.3734	1.4003	0.8397	0.8309	1.09E-12	1.058905	2.54E+22
847.239	1.4151	1.4428	0.8381	0.8292	2.38E-12	1.056337	5.56E+22
872.239	1.4569	1.4854	0.8365	0.8275	5.04E-12	1.053948	1.18E+23
897.239	1.4986	1.5280	0.8349	0.8259	1.04E-11	1.051721	2.41E+23
922.239	1.5404	1.5706	0.8334	0.8243	2.07E-11	1.049641	4.80E+23
947.239	1.5821	1.6131	0.8320	0.8228	4.02E-11	1.047695	9.31E+23
972.239	1.6239	1.6557	0.8306	0.8213	7.62E-11	1.04587	1.76E+24
997.239	1.6657	1.6983	0.8292	0.8199	1.41E-10	1.044157	3.25E+24
1022.239	1.7074	1.7409	0.8279	0.8186	2.54E-10	1.042545	5.86E+24
1047.239	1.7492	1.7834	0.8266	0.8172	4.5E-10	1.041027	1.04E+25
1072.239	1.7909	1.8260	0.8254	0.8159	7.79E-10	1.039595	1.79E+25
1097.239	1.8327	1.8686	0.8242	0.8147	1.32E-09	1.038243	3.04E+25
1122.239	1.8744	1.9112	0.8230	0.8135	2.21E-09	1.036963	5.07E+25
1147.239	1.9162	1.9537	0.8219	0.8123	3.62E-09	1.035752	8.30E+25
1172.239	1.9580	1.9963	0.8208	0.8111	5.84E-09	1.034603	1.34E+26
1197.239	1.9997	2.0389	0.8197	0.8100	9.28E-09	1.033513	2.12E+26
1222.239	2.0415	2.0815	0.8187	0.8089	1.45E-08	1.032476	3.31E+26
1247.239	2.0832	2.1241	0.8176	0.8079	2.24E-08	1.031491	5.10E+26
1272.239	2.1250	2.1666	0.8167	0.8068	3.4E-08	1.030553	7.76E+26
1297.239	2.1667	2.2092	0.8157	0.8058	5.11E-08	1.029658	1.16E+27
1322.239	2.2085	2.2518	0.8148	0.8049	7.58E-08	1.028805	1.72E+27
1347.239	2.2503	2.2944	0.8139	0.8039	1.11E-07	1.027991	2.53E+27
1372.239	2.2920	2.3369	0.8130	0.8030	1.61E-07	1.027213	3.66E+27
1397.239	2.3338	2.3795	0.8121	0.8021	2.31E-07	1.026468	5.24E+27
1422.239	2.3755	2.4221	0.8113	0.8012	3.28E-07	1.025756	7.44E+27

Table D.11: Calculated Data for $[\text{Cu}(\text{acac})(\text{acac-CH}_3)]^+$ loss of acac.

E(kJ)	E'	E'‡	α	α‡	$\frac{(E^\ddagger + a^\ddagger E_z^\ddagger)^s}{(E + aE_z)^{s-1}}$	$\frac{1}{[1 - \beta \frac{dw}{dE'} E']}$	k(E) (sec ⁻¹)
467.694	0.9370	0.9708	0.8627	0.8502	2.62E-21	1.103595	8.38E+15
492.694	0.9871	1.0227	0.8598	0.8471	2.12E-20	1.095894	6.72E+16
517.694	1.0372	1.0746	0.8570	0.8441	1.47E-19	1.089112	4.63E+17
542.694	1.0873	1.1265	0.8544	0.8413	8.88E-19	1.083099	2.79E+18
567.694	1.1374	1.1784	0.8519	0.8386	4.75E-18	1.077736	1.48E+19
592.694	1.1874	1.2303	0.8495	0.8360	2.28E-17	1.072927	7.09E+19
617.694	1.2375	1.2822	0.8472	0.8336	9.9E-17	1.068594	3.06E+20
642.694	1.2876	1.3341	0.8450	0.8312	3.93E-16	1.064673	1.21E+21
667.694	1.3377	1.3860	0.8429	0.8290	1.44E-15	1.06111	4.42E+21
692.694	1.3878	1.4379	0.8409	0.8268	4.88E-15	1.057859	1.49E+22
717.694	1.4379	1.4898	0.8390	0.8248	1.55E-14	1.054884	4.73E+22
742.694	1.4880	1.5417	0.8371	0.8228	4.6E-14	1.052153	1.40E+23
767.694	1.5381	1.5936	0.8353	0.8209	1.29E-13	1.049638	3.94E+23
792.694	1.5881	1.6455	0.8336	0.8190	3.45E-13	1.047315	1.05E+24
817.694	1.6382	1.6974	0.8320	0.8173	8.75E-13	1.045165	2.65E+24
842.694	1.6883	1.7493	0.8304	0.8156	2.12E-12	1.04317	6.42E+24
867.694	1.7384	1.8012	0.8288	0.8139	4.94E-12	1.041314	1.49E+25
892.694	1.7885	1.8531	0.8274	0.8124	1.1E-11	1.039585	3.32E+25
917.694	1.8386	1.9050	0.8259	0.8108	2.38E-11	1.03797	7.15E+25
942.694	1.8887	1.9569	0.8246	0.8094	4.96E-11	1.036459	1.49E+26
967.694	1.9388	2.0088	0.8232	0.8080	1E-10	1.035043	3.00E+26
992.694	1.9888	2.0607	0.8219	0.8066	1.96E-10	1.033714	5.87E+26
1017.694	2.0389	2.1125	0.8207	0.8053	3.73E-10	1.032464	1.12E+27
1042.694	2.0890	2.1644	0.8195	0.8040	6.93E-10	1.031286	2.07E+27
1067.694	2.1391	2.2163	0.8183	0.8028	1.25E-09	1.030176	3.74E+27
1092.694	2.1892	2.2682	0.8172	0.8016	2.22E-09	1.029128	6.62E+27
1117.694	2.2393	2.3201	0.8161	0.8004	3.84E-09	1.028137	1.14E+28
1142.694	2.2894	2.3720	0.8151	0.7993	6.52E-09	1.027199	1.94E+28
1167.694	2.3394	2.4239	0.8141	0.7982	1.08E-08	1.02631	3.23E+28
1192.694	2.3895	2.4758	0.8131	0.7972	1.77E-08	1.025466	5.26E+28
1217.694	2.4396	2.5277	0.8121	0.7962	2.84E-08	1.024664	8.44E+28
1242.694	2.4897	2.5796	0.8112	0.7952	4.49E-08	1.023902	1.33E+29
1267.694	2.5398	2.6315	0.8103	0.7943	6.98E-08	1.023177	2.07E+29
1292.694	2.5899	2.6834	0.8094	0.7933	1.07E-07	1.022486	3.17E+29
1317.694	2.6400	2.7353	0.8086	0.7924	1.62E-07	1.021827	4.78E+29
1342.694	2.6901	2.7872	0.8077	0.7916	2.41E-07	1.021198	7.12E+29
1367.694	2.7401	2.8391	0.8070	0.7908	3.54E-07	1.020597	1.05E+30
1392.694	2.7902	2.8910	0.8062	0.7899	5.15E-07	1.020023	1.52E+30
1417.694	2.8403	2.9429	0.8054	0.7892	7.4E-07	1.019474	2.19E+30
1442.694	2.8904	2.9948	0.8047	0.7884	1.05E-06	1.018948	3.11E+30

Table C.12: Calculated Data for $[\text{Ni}(\text{acac})(\text{acac-CH}_3)]^+$ loss of *acac*.

E(kJ)	E'	E'‡	α	α‡	$\frac{(E^\ddagger + a^\ddagger E_z^\ddagger)^s}{(E + aE_z)^{s-1}}$	$\frac{1}{[1 - \beta \frac{dw}{dE'} E']}$	k(E) (sec ⁻¹)
527.105	1.0659	1.0816	0.8540	0.8466	1.01E-22	1.085699	9.14E+09
552.105	1.1165	1.1329	0.8514	0.8439	8.82E-22	1.080013	7.9E+10
577.105	1.1671	1.1842	0.8490	0.8413	6.61E-21	1.074932	5.84E+11
602.105	1.2176	1.2355	0.8466	0.8388	4.31E-20	1.070366	3.75E+12
627.105	1.2682	1.2868	0.8443	0.8365	2.47E-19	1.066246	2.12E+13
652.105	1.3187	1.3381	0.8421	0.8342	1.27E-18	1.06251	1.07E+14
677.105	1.3693	1.3895	0.8400	0.8320	5.86E-18	1.059111	4.89E+14
702.105	1.4198	1.4408	0.8380	0.8299	2.47E-17	1.056006	2.04E+15
727.105	1.4704	1.4921	0.8361	0.8279	9.56E-17	1.053161	7.78E+15
752.105	1.5210	1.5434	0.8343	0.8260	3.43E-16	1.050545	2.76E+16
777.105	1.5715	1.5947	0.8325	0.8241	1.15E-15	1.048134	9.09E+16
802.105	1.6221	1.6460	0.8308	0.8224	3.59E-15	1.045906	2.81E+17
827.105	1.6726	1.6973	0.8292	0.8207	1.06E-14	1.043841	8.2E+17
852.105	1.7232	1.7486	0.8276	0.8190	2.95E-14	1.041923	2.26E+18
877.105	1.7737	1.7999	0.8260	0.8174	7.84E-14	1.040138	5.93E+18
902.105	1.8243	1.8512	0.8246	0.8159	1.98E-13	1.038473	1.48E+19
927.105	1.8748	1.9025	0.8232	0.8144	4.81E-13	1.036918	3.56E+19
952.105	1.9254	1.9538	0.8218	0.8130	1.12E-12	1.035461	8.18E+19
977.105	1.9760	2.0051	0.8205	0.8116	2.51E-12	1.034095	1.81E+20
1002.105	2.0265	2.0564	0.8192	0.8103	5.42E-12	1.032812	3.88E+20
1027.105	2.0771	2.1077	0.8180	0.8090	1.13E-11	1.031605	8.02E+20
1052.105	2.1276	2.1590	0.8168	0.8078	2.3E-11	1.030467	1.61E+21
1077.105	2.1782	2.2103	0.8156	0.8066	4.54E-11	1.029394	3.14E+21
1102.105	2.2287	2.2616	0.8145	0.8054	8.7E-11	1.02838	5.95E+21
1127.105	2.2793	2.3129	0.8134	0.8043	1.63E-10	1.027421	1.1E+22
1152.105	2.3299	2.3642	0.8124	0.8032	2.97E-10	1.026513	1.99E+22
1177.105	2.3804	2.4155	0.8113	0.8021	5.3E-10	1.025652	3.51E+22
1202.105	2.4310	2.4668	0.8104	0.8011	9.25E-10	1.024834	6.06E+22
1227.105	2.4815	2.5181	0.8094	0.8001	1.58E-09	1.024057	1.03E+23
1252.105	2.5321	2.5694	0.8085	0.7992	2.66E-09	1.023318	1.7E+23
1277.105	2.5826	2.6207	0.8076	0.7983	4.38E-09	1.022615	2.78E+23
1302.105	2.6332	2.6720	0.8067	0.7974	7.1E-09	1.021944	4.45E+23
1327.105	2.6837	2.7233	0.8059	0.7965	1.13E-08	1.021305	7.03E+23
1352.105	2.7343	2.7746	0.8051	0.7957	1.78E-08	1.020694	1.09E+24
1377.105	2.7849	2.8259	0.8043	0.7948	2.75E-08	1.020111	1.67E+24
1402.105	2.8354	2.8772	0.8035	0.7940	4.19E-08	1.019553	2.52E+24
1427.105	2.8860	2.9285	0.8028	0.7933	6.31E-08	1.019019	3.76E+24
1452.105	2.9365	2.9798	0.8021	0.7925	9.38E-08	1.018508	5.52E+24
1477.105	2.9871	3.0311	0.8014	0.7918	1.38E-07	1.018018	8.02E+24
1502.105	3.0376	3.0824	0.8007	0.7911	2E-07	1.017548	1.15E+25

Table D.13: Calculated Data for $[\text{Zn}(\text{acac})(\text{acac-CH}_3)]^+$ loss of acac.

E(kJ)	E'	E'‡	α	α‡	$\frac{(E^\ddagger + a^\ddagger E_z^\ddagger)^s}{(E + aE_z)^{s-1}}$	$\frac{1}{[1 - \beta \frac{dw}{dE'} E']}$	k(E) (sec ⁻¹)
409.401	0.8245	0.8489	0.8686	0.8590	3.95E-16	1.125324	1.64E+20
434.401	0.8748	0.9007	0.8653	0.8554	1.61E-15	1.114729	6.64E+20
459.401	0.9252	0.9526	0.8622	0.8521	6.03E-15	1.105573	2.47E+21
484.401	0.9755	1.0044	0.8592	0.8490	2.09E-14	1.09759	8.51E+21
509.401	1.0258	1.0563	0.8564	0.8460	6.77E-14	1.090575	2.73E+22
534.401	1.0762	1.1081	0.8537	0.8431	2.05E-13	1.08437	8.23E+22
559.401	1.1265	1.1599	0.8511	0.8404	5.85E-13	1.078845	2.34E+23
584.401	1.1769	1.2118	0.8487	0.8378	1.58E-12	1.0739	6.28E+23
609.401	1.2272	1.2636	0.8463	0.8353	4.05E-12	1.069451	1.60E+24
634.401	1.2776	1.3155	0.8441	0.8329	9.91E-12	1.06543	3.91E+24
659.401	1.3279	1.3673	0.8420	0.8307	2.32E-11	1.06178	9.12E+24
684.401	1.3783	1.4191	0.8399	0.8285	5.22E-11	1.058456	2.04E+25
709.401	1.4286	1.4710	0.8379	0.8264	1.13E-10	1.055416	4.41E+25
734.401	1.4790	1.5228	0.8360	0.8244	2.36E-10	1.052628	9.19E+25
759.401	1.5293	1.5746	0.8342	0.8225	4.77E-10	1.050063	1.85E+26
784.401	1.5796	1.6265	0.8325	0.8206	9.35E-10	1.047697	3.62E+26
809.401	1.6300	1.6783	0.8308	0.8189	1.78E-09	1.045508	6.89E+26
834.401	1.6803	1.7302	0.8291	0.8171	3.3E-09	1.043478	1.27E+27
859.401	1.7307	1.7820	0.8276	0.8155	5.96E-09	1.041592	2.30E+27
884.401	1.7810	1.8338	0.8261	0.8139	1.05E-08	1.039835	4.05E+27
909.401	1.8314	1.8857	0.8246	0.8124	1.81E-08	1.038196	6.97E+27
934.401	1.8817	1.9375	0.8232	0.8109	3.06E-08	1.036663	1.18E+28
959.401	1.9321	1.9893	0.8219	0.8095	5.07E-08	1.035227	1.94E+28
984.401	1.9824	2.0412	0.8205	0.8081	8.24E-08	1.03388	3.15E+28
1009.401	2.0328	2.0930	0.8193	0.8068	1.31E-07	1.032613	5.03E+28
1034.401	2.0831	2.1449	0.8181	0.8055	2.06E-07	1.031422	7.88E+28
1059.401	2.1334	2.1967	0.8169	0.8043	3.19E-07	1.030298	1.22E+29
1084.401	2.1838	2.2485	0.8157	0.8031	4.85E-07	1.029238	1.85E+29
1109.401	2.2341	2.3004	0.8146	0.8019	7.27E-07	1.028236	2.77E+29
1134.401	2.2845	2.3522	0.8135	0.8008	1.08E-06	1.027288	4.09E+29
1159.401	2.3348	2.4041	0.8125	0.7997	1.57E-06	1.02639	5.97E+29
1184.401	2.3852	2.4559	0.8115	0.7986	2.27E-06	1.025537	8.60E+29
1209.401	2.4355	2.5077	0.8105	0.7976	3.23E-06	1.024728	1.23E+30
1234.401	2.4859	2.5596	0.8096	0.7966	4.55E-06	1.023959	1.73E+30
1259.401	2.5362	2.6114	0.8087	0.7957	6.35E-06	1.023228	2.41E+30
1284.401	2.5866	2.6632	0.8078	0.7948	8.77E-06	1.022531	3.32E+30
1309.401	2.6369	2.7151	0.8069	0.7939	1.2E-05	1.021866	4.54E+30
1334.401	2.6873	2.7669	0.8061	0.7930	1.63E-05	1.021233	6.15E+30
1359.401	2.7376	2.8188	0.8053	0.7922	2.18E-05	1.020627	8.25E+30
1384.401	2.7879	2.8706	0.8045	0.7914	2.91E-05	1.020049	1.10E+31

Table D.14: Cu(hfac)₂⁺ loss of 1st CF₃, Calculated Data.

E(kJ)	E'	E' [‡]	α	α^{\ddagger}	$\frac{(E^{\ddagger} + a^{\ddagger} E_z^{\ddagger})^s}{(E + aE_z)^{s-1}}$	$\frac{1}{[1 - \beta \frac{dw}{dE'} E']}$	k(E) (sec ⁻¹)
360.9155	0.9450	0.9651	0.8631	0.8495	3.37E-25	1.08433	4.82E+09
385.9155	1.0104	1.0319	0.8590	0.8452	7.36E-24	1.08274	1.04E+11
410.9155	1.0759	1.0988	0.8555	0.8414	1.22E-22	1.075453	1.69E+12
435.9155	1.1414	1.1656	0.8522	0.8378	1.57E-21	1.06918	2.15E+13
460.9155	1.2068	1.2324	0.8491	0.8345	1.64E-20	1.063732	2.2E+14
485.9155	1.2723	1.2993	0.8462	0.8313	1.41E-19	1.05896	1.87E+15
510.9155	1.3377	1.3661	0.8435	0.8283	1.03E-18	1.054753	1.35E+16
535.9155	1.4032	1.4330	0.8409	0.8255	6.47E-18	1.051019	8.35E+16
560.9155	1.4686	1.4998	0.8384	0.8228	3.57E-17	1.047686	4.54E+17
585.9155	1.5341	1.5667	0.8361	0.8203	1.75E-16	1.044696	2.2E+18
610.9155	1.5996	1.6335	0.8338	0.8178	7.71E-16	1.042001	9.57E+18
635.9155	1.6650	1.7004	0.8317	0.8155	3.09E-15	1.039562	3.79E+19
660.9155	1.7305	1.7672	0.8297	0.8134	1.13E-14	1.037345	1.37E+20
685.9155	1.7959	1.8341	0.8278	0.8113	3.85E-14	1.035322	4.61E+20
710.9155	1.8614	1.9009	0.8259	0.8093	1.22E-13	1.033472	1.44E+21
735.9155	1.9268	1.9678	0.8242	0.8074	3.61E-13	1.031773	4.21E+21
760.9155	1.9923	2.0346	0.8225	0.8056	1.01E-12	1.030209	1.16E+22
785.9155	2.0578	2.1015	0.8209	0.8038	2.65E-12	1.028765	3.03E+22
810.9155	2.1232	2.1683	0.8193	0.8022	6.66E-12	1.027429	7.52E+22
835.9155	2.1887	2.2352	0.8179	0.8006	1.59E-11	1.02619	1.78E+23
860.9155	2.2541	2.3020	0.8165	0.7991	3.65E-11	1.025038	4.03E+23
885.9155	2.3196	2.3689	0.8151	0.7976	8.05E-11	1.023965	8.79E+23
910.9155	2.3850	2.4357	0.8138	0.7962	1.71E-10	1.022964	1.84E+24
935.9155	2.4505	2.5026	0.8126	0.7949	3.5E-10	1.022027	3.74E+24
960.9155	2.5160	2.5694	0.8114	0.7936	6.95E-10	1.02115	7.33E+24
985.9155	2.5814	2.6363	0.8102	0.7924	1.34E-09	1.020327	1.4E+25
1010.9155	2.6469	2.7031	0.8091	0.7912	2.5E-09	1.019553	2.59E+25
1035.9155	2.7123	2.7700	0.8081	0.7900	4.56E-09	1.018825	4.67E+25
1060.9155	2.7778	2.8368	0.8070	0.7889	8.12E-09	1.018139	8.21E+25
1085.9155	2.8432	2.9036	0.8061	0.7879	1.41E-08	1.017492	1.41E+26
1110.9155	2.9087	2.9705	0.8051	0.7869	2.4E-08	1.01688	2.37E+26
1135.9155	2.9742	3.0373	0.8042	0.7859	3.99E-08	1.016301	3.91E+26
1160.9155	3.0396	3.1042	0.8034	0.7850	6.53E-08	1.015753	6.32E+26
1185.9155	3.1051	3.1710	0.8025	0.7841	1.05E-07	1.015233	1E+27
1210.9155	3.1705	3.2379	0.8017	0.7832	1.65E-07	1.01474	1.57E+27
1235.9155	3.2360	3.3047	0.8009	0.7824	2.56E-07	1.014271	2.4E+27
1260.9155	3.3015	3.3716	0.8002	0.7816	3.91E-07	1.013825	3.63E+27
1285.9155	3.3669	3.4384	0.7995	0.7808	5.89E-07	1.013401	5.41E+27
1310.9155	3.4324	3.5053	0.7988	0.7801	8.74E-07	1.012996	7.95E+27
1335.9155	3.4978	3.5721	0.7981	0.7794	1.28E-06	1.01261	1.15E+28

Table D.15: Calculated data for $[\text{Ni}(\text{hfac})_2]^+$, loss of 1st CF_3 .

E(kJ)	E'	E'^\ddagger	α	α^\ddagger	$\frac{(E^\ddagger + a^\ddagger E_z^\ddagger)^s}{(E + aE_z)^{s-1}}$	$\frac{1}{[1 - \beta \frac{dw}{dE'}]}$	k(E) (sec ⁻¹)
309.6578	0.8081	0.8359	0.8718	0.8583	9.85E-23	1.103471	1.39E+16
334.6578	0.8733	0.9034	0.8671	0.8531	1.7E-21	1.093547	2.38E+17
359.6578	0.9386	0.9709	0.8623	0.8481	2.26E-20	1.09221	3.16E+18
384.6578	1.0038	1.0384	0.8585	0.8440	2.43E-19	1.083543	3.37E+19
409.6578	1.0691	1.1059	0.8550	0.8402	2.14E-18	1.076163	2.95E+20
434.6578	1.1343	1.1734	0.8517	0.8366	1.58E-17	1.069814	2.16E+21
459.6578	1.1995	1.2409	0.8486	0.8332	9.95E-17	1.064301	1.36E+22
484.6578	1.2648	1.3084	0.8457	0.8301	5.47E-16	1.059476	7.42E+22
509.6578	1.3300	1.3759	0.8429	0.8270	2.66E-15	1.055222	3.59E+23
534.6578	1.3953	1.4433	0.8403	0.8242	1.16E-14	1.051448	1.56E+24
559.6578	1.4605	1.5108	0.8378	0.8215	4.55E-14	1.048081	6.11E+24
584.6578	1.5257	1.5783	0.8354	0.8189	1.64E-13	1.045061	2.19E+25
609.6578	1.5910	1.6458	0.8332	0.8165	5.44E-13	1.042339	7.27E+25
634.6578	1.6562	1.7133	0.8310	0.8142	1.68E-12	1.039876	2.24E+26
659.6578	1.7215	1.7808	0.8290	0.8120	4.85E-12	1.037637	6.44E+26
684.6578	1.7867	1.8483	0.8270	0.8099	1.32E-11	1.035596	1.75E+27
709.6578	1.8520	1.9158	0.8252	0.8079	3.38E-11	1.033729	4.48E+27
734.6578	1.9172	1.9833	0.8234	0.8060	8.25E-11	1.032015	1.09E+28
759.6578	1.9824	2.0507	0.8217	0.8042	1.92E-10	1.030437	2.53E+28
784.6578	2.0477	2.1182	0.8201	0.8024	4.28E-10	1.02898	5.64E+28
809.6578	2.1129	2.1857	0.8185	0.8008	9.15E-10	1.027633	1.20E+29
834.6578	2.1782	2.2532	0.8171	0.7992	1.89E-09	1.026383	2.48E+29
859.6578	2.2434	2.3207	0.8156	0.7976	3.76E-09	1.025221	4.93E+29
884.6578	2.3086	2.3882	0.8143	0.7962	7.24E-09	1.024139	9.50E+29
909.6578	2.3739	2.4557	0.8130	0.7948	1.36E-08	1.02313	1.78E+30
934.6578	2.4391	2.5232	0.8117	0.7934	2.47E-08	1.022185	3.23E+30
959.6578	2.5044	2.5907	0.8105	0.7922	4.38E-08	1.021301	5.72E+30
984.6578	2.5696	2.6581	0.8093	0.7909	7.57E-08	1.020471	9.90E+30
1009.6578	2.6348	2.7256	0.8082	0.7897	1.28E-07	1.019692	1.67E+31
1034.6578	2.7001	2.7931	0.8072	0.7886	2.12E-07	1.018958	2.77E+31
1059.6578	2.7653	2.8606	0.8061	0.7875	3.44E-07	1.018267	4.49E+31
1084.6578	2.8306	2.9281	0.8051	0.7865	5.48E-07	1.017614	7.14E+31
1109.6578	2.8958	2.9956	0.8042	0.7854	8.56E-07	1.016998	1.12E+32
1134.6578	2.9611	3.0631	0.8033	0.7845	1.32E-06	1.016415	1.71E+32
1159.6578	3.0263	3.1306	0.8024	0.7835	1.99E-06	1.015862	2.59E+32
1184.6578	3.0915	3.1981	0.8016	0.7827	2.97E-06	1.015339	3.86E+32
1209.6578	3.1568	3.2655	0.8007	0.7818	4.37E-06	1.014842	5.68E+32
1234.6578	3.2220	3.3330	0.8000	0.7810	6.33E-06	1.014369	8.23E+32
1259.6578	3.2873	3.4005	0.7992	0.7802	9.07E-06	1.01392	1.18E+33
1284.6578	3.3525	3.4680	0.7985	0.7794	1.28E-05	1.013492	1.66E+33

Table D.16: Calculated data for $[\text{Zn}(\text{hfac})_2]^+$, loss of 1st CF_3 .

E(kJ)	E'	E^\ddagger	α	α^\ddagger	$\frac{(E^\ddagger + a^\ddagger E_z^\ddagger)^s}{(E + aE_z)^{s-1}}$	$\frac{1}{[1 - \beta \frac{dw}{dE'}]}$	k(E) (sec ⁻¹)
182.796	0.4837	0.4974	0.8969	0.8898	1.91E-14	1.195652	4.06E+19
207.796	0.5499	0.5655	0.8892	0.8817	1.35E-13	1.167601	2.82E+20
232.796	0.6160	0.6335	0.8823	0.8744	8.12E-13	1.14579	1.66E+21
257.796	0.6822	0.7015	0.8759	0.8677	4.19E-12	1.12838	8.44E+21
282.796	0.7483	0.7696	0.8684	0.8599	1.83E-11	1.128767	3.69E+22
307.796	0.8145	0.8376	0.8635	0.8547	7.46E-11	1.113613	1.48E+23
332.796	0.8806	0.9056	0.8589	0.8499	2.72E-10	1.101268	5.34E+23
357.796	0.9468	0.9737	0.8547	0.8454	8.97E-10	1.09104	1.75E+24
382.796	1.0129	1.0417	0.8507	0.8413	2.72E-09	1.082442	5.24E+24
407.796	1.0791	1.1097	0.8470	0.8374	7.59E-09	1.075127	1.46E+25
432.796	1.1452	1.1778	0.8435	0.8337	1.98E-08	1.068837	3.77E+25
457.796	1.2114	1.2458	0.8402	0.8303	4.84E-08	1.063378	9.17E+25
482.796	1.2775	1.3138	0.8371	0.8270	1.12E-07	1.058603	2.11E+26
507.796	1.3437	1.3819	0.8342	0.8239	2.44E-07	1.054395	4.59E+26
532.796	1.4098	1.4499	0.8314	0.8210	5.10E-07	1.050663	9.55E+26
557.796	1.4760	1.5179	0.8288	0.8183	1.02E-06	1.047334	1.90E+27
582.796	1.5421	1.5860	0.8263	0.8157	1.95E-06	1.04435	3.64E+27
607.796	1.6083	1.6540	0.8240	0.8132	3.62E-06	1.041662	6.72E+27
632.796	1.6745	1.7220	0.8217	0.8108	6.48E-06	1.039229	1.20E+28
657.796	1.7406	1.7901	0.8196	0.8086	1.12E-05	1.037019	2.08E+28
682.796	1.8068	1.8581	0.8175	0.8065	1.90E-05	1.035005	3.50E+28
707.796	1.8729	1.9261	0.8156	0.8044	3.11E-05	1.033162	5.74E+28
732.796	1.9391	1.9942	0.8137	0.8025	4.99E-05	1.031471	9.19E+28
757.796	2.0052	2.0622	0.8119	0.8006	7.82E-05	1.029915	1.44E+29
782.796	2.0714	2.1302	0.8102	0.7989	1.20E-04	1.028479	2.20E+29
807.796	2.1375	2.1983	0.8086	0.7972	1.81E-04	1.027151	3.31E+29
832.796	2.2037	2.2663	0.8070	0.7956	2.67E-04	1.025919	4.88E+29
857.796	2.2698	2.3343	0.8055	0.7940	3.88E-04	1.024774	7.09E+29
882.796	2.3360	2.4024	0.8041	0.7925	5.54E-04	1.023708	1.01E+30
907.796	2.4021	2.4704	0.8027	0.7911	7.80E-04	1.022713	1.42E+30
932.796	2.4683	2.5384	0.8014	0.7897	1.08E-03	1.021783	1.97E+30
957.796	2.5344	2.6064	0.8002	0.7884	1.48E-03	1.020912	2.70E+30
982.796	2.6006	2.6745	0.7990	0.7872	2.01E-03	1.020095	3.66E+30
1007.796	2.6667	2.7425	0.7978	0.7860	2.69E-03	1.019327	4.89E+30
1032.796	2.7329	2.8105	0.7967	0.7848	3.56E-03	1.018605	6.46E+30
1057.796	2.7991	2.8786	0.7956	0.7837	4.66E-03	1.017925	8.46E+30
1082.796	2.8652	2.9466	0.7946	0.7827	6.04E-03	1.017283	1.10E+31
1107.796	2.9314	3.0146	0.7936	0.7816	7.76E-03	1.016676	1.41E+31
1132.796	2.9975	3.0827	0.7926	0.7807	9.88E-03	1.016102	1.79E+31
1157.796	3.0637	3.1507	0.7917	0.7797	1.25E-02	1.015559	2.26E+31

Table D.17: Calculated data for $[\text{Cu(hfac)}(\text{hfac-CF}_3)]^+$ loss of CF_3 .

E(kJ)	E'	E'^\ddagger	α	α^\ddagger	$\frac{(E^\ddagger + a^\ddagger E_z^\ddagger)^s}{(E + aE_z)^{s-1}}$	$\frac{1}{[1 - \beta \frac{dw}{dE'} E']}$	k(E) (sec ⁻¹)
213.05	0.6363	0.6626	0.8829	0.8730	7.81E-16	1.140052	1.00E+21
238.05	0.7109	0.7403	0.8761	0.8657	8.49E-15	1.121865	1.08E+22
263.05	0.7856	0.8181	0.8699	0.8591	7.25E-14	1.107302	9.06E+22
288.05	0.8603	0.8958	0.8633	0.8524	4.97E-13	1.104814	6.20E+23
313.05	0.9349	0.9736	0.8585	0.8473	2.91E-12	1.092739	3.59E+24
338.05	1.0096	1.0513	0.8541	0.8426	1.45E-11	1.082842	1.78E+25
363.05	1.0843	1.1290	0.8500	0.8383	6.31E-11	1.074601	7.65E+25
388.05	1.1589	1.2068	0.8462	0.8342	2.42E-10	1.067645	2.92E+26
413.05	1.2336	1.2845	0.8426	0.8304	8.35E-10	1.061706	1.00E+27
438.05	1.3082	1.3623	0.8393	0.8269	2.61E-09	1.056585	3.12E+27
463.05	1.3829	1.4400	0.8361	0.8236	7.52E-09	1.05213	8.93E+27
488.05	1.4576	1.5178	0.8332	0.8205	2.01E-08	1.048225	2.37E+28
513.05	1.5322	1.5955	0.8304	0.8175	5.00E-08	1.044778	5.90E+28
538.05	1.6069	1.6733	0.8278	0.8148	1.17E-07	1.041716	1.38E+29
563.05	1.6816	1.7510	0.8253	0.8122	2.60E-07	1.038982	3.05E+29
588.05	1.7562	1.8288	0.8229	0.8097	5.48E-07	1.036527	6.41E+29
613.05	1.8309	1.9065	0.8207	0.8073	1.10E-06	1.034314	1.29E+30
638.05	1.9055	1.9843	0.8186	0.8051	2.14E-06	1.03231	2.49E+30
663.05	1.9802	2.0620	0.8166	0.8030	3.98E-06	1.030489	4.63E+30
688.05	2.0549	2.1398	0.8147	0.8010	7.16E-06	1.028827	8.31E+30
713.05	2.1295	2.2175	0.8129	0.7991	1.25E-05	1.027306	1.45E+31
738.05	2.2042	2.2953	0.8112	0.7973	2.11E-05	1.025909	2.44E+31
763.05	2.2789	2.3730	0.8095	0.7956	3.47E-05	1.024624	4.02E+31
788.05	2.3535	2.4507	0.8079	0.7940	5.58E-05	1.023437	6.44E+31
813.05	2.4282	2.5285	0.8065	0.7925	8.76E-05	1.022339	1.01E+32
838.05	2.5028	2.6062	0.8050	0.7910	1.34E-04	1.021321	1.55E+32
863.05	2.5775	2.6840	0.8037	0.7896	2.03E-04	1.020374	2.33E+32
888.05	2.6522	2.7617	0.8024	0.7882	2.99E-04	1.019493	3.44E+32
913.05	2.7268	2.8395	0.8011	0.7869	4.35E-04	1.01867	5.00E+32
938.05	2.8015	2.9172	0.7999	0.7857	6.21E-04	1.0179	7.14E+32
963.05	2.8762	2.9950	0.7988	0.7845	8.75E-04	1.01718	1.00E+33
988.05	2.9508	3.0727	0.7977	0.7834	1.21E-03	1.016504	1.39E+33
1013.05	3.0255	3.1505	0.7967	0.7824	1.66E-03	1.015869	1.91E+33
1038.05	3.1002	3.2282	0.7957	0.7813	2.25E-03	1.015272	2.58E+33
1063.05	3.1748	3.3060	0.7947	0.7804	3.01E-03	1.014709	3.44E+33
1088.05	3.2495	3.3837	0.7938	0.7794	3.98E-03	1.014178	4.55E+33
1113.05	3.3241	3.4615	0.7930	0.7785	5.20E-03	1.013676	5.95E+33
1138.05	3.3988	3.5392	0.7921	0.7777	6.74E-03	1.013201	7.70E+33
1163.05	3.4735	3.6170	0.7913	0.7769	8.65E-03	1.012752	9.88E+33
1188.05	3.5481	3.6947	0.7906	0.7761	1.10E-02	1.012326	1.26E+34

Table D.18: Calculated data for $[\text{Cu(hfac)}]^+$ loss of CF_3 .

E(kJ)	E'	E'‡	α	α‡	$\frac{(E^‡ + a^‡ E_z^‡)^s}{(E + aE_z)^{s-1}}$	$\frac{1}{[1 - \beta \frac{dw}{dE'} E']}$	k(E) (sec ⁻¹)
178.944	0.9608	1.0204	0.8604	0.8418	2.75E-12	1.089092	1.82E+22
203.944	1.0950	1.1630	0.8531	0.8337	6.88E-11	1.073523	4.50E+23
228.944	1.2293	1.3056	0.8466	0.8266	9.77E-10	1.062024	6.31E+24
253.944	1.3635	1.4481	0.8409	0.8202	9.06E-09	1.05323	5.80E+25
278.944	1.4977	1.5907	0.8357	0.8146	6.04E-08	1.046318	3.85E+26
303.944	1.6320	1.7333	0.8311	0.8096	3.11E-07	1.040763	1.97E+27
328.944	1.7662	1.8758	0.8269	0.8050	1.30E-06	1.036218	8.18E+27
353.944	1.9005	2.0184	0.8231	0.8009	4.57E-06	1.032441	2.87E+28
378.944	2.0347	2.1610	0.8196	0.7971	1.40E-05	1.029261	8.74E+28
403.944	2.1689	2.3035	0.8165	0.7937	3.79E-05	1.026555	2.37E+29
428.944	2.3032	2.4461	0.8136	0.7906	9.31E-05	1.024228	5.80E+29
453.944	2.4374	2.5886	0.8109	0.7878	2.10E-04	1.02221	1.30E+30
478.944	2.5716	2.7312	0.8085	0.7852	4.40E-04	1.020447	2.73E+30
503.944	2.7059	2.8738	0.8062	0.7828	8.64E-04	1.018895	5.35E+30
528.944	2.8401	3.0163	0.8042	0.7806	1.60E-03	1.017522	9.93E+30
553.944	2.9743	3.1589	0.8023	0.7786	2.84E-03	1.0163	1.75E+31
578.944	3.1086	3.3015	0.8005	0.7767	4.81E-03	1.015207	2.97E+31
603.944	3.2428	3.4440	0.7989	0.7750	7.84E-03	1.014224	4.84E+31
628.944	3.3770	3.5866	0.7973	0.7734	1.24E-02	1.013337	7.61E+31
653.944	3.5113	3.7292	0.7960	0.7720	1.89E-02	1.012533	1.16E+32
678.944	3.6455	3.8717	0.7947	0.7706	2.80E-02	1.011803	1.73E+32
703.944	3.7797	4.0143	0.7935	0.7694	4.06E-02	1.011136	2.50E+32
728.944	3.9140	4.1569	0.7924	0.7683	5.76E-02	1.010526	3.54E+32
753.944	4.0482	4.2994	0.7913	0.7672	7.99E-02	1.009966	4.91E+32
778.944	4.1824	4.4420	0.7904	0.7663	1.09E-01	1.009451	6.68E+32
803.944	4.3167	4.5846	0.7895	0.7654	1.46E-01	1.008976	8.95E+32
828.944	4.4509	4.7271	0.7887	0.7646	1.92E-01	1.008537	1.18E+33
853.944	4.5851	4.8697	0.7880	0.7639	2.50E-01	1.008129	1.53E+33
878.944	4.7194	5.0122	0.7873	0.7632	3.20E-01	1.007751	1.96E+33
903.944	4.8536	5.1548	0.7866	0.7626	4.06E-01	1.007399	2.48E+33
928.944	4.9878	5.2974	0.7861	0.7620	5.08E-01	1.007071	3.11E+33
953.944	5.1221	5.4399	0.7855	0.7615	6.29E-01	1.006764	3.85E+33
978.944	5.2563	5.5825	0.7851	0.7611	7.72E-01	1.006478	4.73E+33
1003.944	5.3905	5.7251	0.7846	0.7607	9.39E-01	1.006209	5.75E+33
1028.944	5.5248	5.8676	0.7842	0.7603	1.13E+00	1.005957	6.93E+33
1053.944	5.6590	6.0102	0.7838	0.7600	1.35E+00	1.00572	8.28E+33
1078.944	5.7932	6.1528	0.7835	0.7597	1.61E+00	1.005498	9.83E+33
1103.944	5.9275	6.2953	0.7832	0.7594	1.89E+00	1.005288	1.16E+34
1128.944	6.0617	6.4379	0.7830	0.7592	2.22E+00	1.005089	1.36E+34
1153.944	6.1959	6.5805	0.7827	0.7590	2.58E+00	1.004902	1.58E+34

Table D.19: Calculated data for $[\text{Ni}(\text{hfac})]^+$ loss of CF_3 .

E(kJ)	E'	E^\ddagger	α	α^\ddagger	$\frac{(E^\ddagger + a^\ddagger E_z^\ddagger)^s}{(E + aE_z)^{s-1}}$	$\frac{1}{[1 - \beta \frac{dw}{dE'}]}$	k(E) (sec ⁻¹)
252.464	1.3397	1.3975	0.8421	0.8237	2.51E-15	1.060732	2.96E+19
277.464	1.4723	1.5359	0.8369	0.8181	9.85E-14	1.05277	1.15E+21
302.464	1.6050	1.6743	0.8322	0.8130	2.06E-12	1.046389	2.39E+22
327.464	1.7377	1.8127	0.8280	0.8084	2.67E-11	1.041179	3.09E+23
352.464	1.8703	1.9511	0.8242	0.8042	2.41E-10	1.036856	2.78E+24
377.464	2.0030	2.0895	0.8207	0.8005	1.62E-09	1.033223	1.86E+25
402.464	2.1356	2.2279	0.8175	0.7970	8.63E-09	1.030133	9.89E+25
427.464	2.2683	2.3663	0.8146	0.7939	3.79E-08	1.02748	4.33E+26
452.464	2.4010	2.5046	0.8119	0.7910	1.42E-07	1.025181	1.62E+27
477.464	2.5336	2.6430	0.8094	0.7883	4.63E-07	1.023174	5.27E+27
502.464	2.6663	2.7814	0.8072	0.7859	1.35E-06	1.02141	1.53E+28
527.464	2.7989	2.9198	0.8051	0.7837	3.57E-06	1.019849	4.04E+28
552.464	2.9316	3.0582	0.8031	0.7816	8.65E-06	1.01846	9.80E+28
577.464	3.0643	3.1966	0.8014	0.7797	1.95E-05	1.017219	2.20E+29
602.464	3.1969	3.3350	0.7997	0.7780	4.11E-05	1.016103	4.65E+29
627.464	3.3296	3.4734	0.7982	0.7763	8.20E-05	1.015097	9.25E+29
652.464	3.4623	3.6118	0.7968	0.7748	1.55E-04	1.014185	1.75E+30
677.464	3.5949	3.7501	0.7954	0.7735	2.81E-04	1.013357	3.17E+30
702.464	3.7276	3.8885	0.7942	0.7722	4.89E-04	1.012601	5.51E+30
727.464	3.8602	4.0269	0.7931	0.7710	8.20E-04	1.01191	9.22E+30
752.464	3.9929	4.1653	0.7921	0.7699	1.33E-03	1.011276	1.50E+31
777.464	4.1256	4.3037	0.7911	0.7689	2.10E-03	1.010692	2.35E+31
802.464	4.2582	4.4421	0.7902	0.7680	3.21E-03	1.010154	3.61E+31
827.464	4.3909	4.5805	0.7894	0.7672	4.80E-03	1.009656	5.39E+31
852.464	4.5235	4.7189	0.7886	0.7664	7.03E-03	1.009195	7.88E+31
877.464	4.6562	4.8573	0.7879	0.7657	1.01E-02	1.008767	1.13E+32
902.464	4.7889	4.9956	0.7873	0.7650	1.41E-02	1.008368	1.59E+32
927.464	4.9215	5.1340	0.7867	0.7644	1.95E-02	1.007997	2.19E+32
952.464	5.0542	5.2724	0.7861	0.7639	2.66E-02	1.00765	2.98E+32
977.464	5.1868	5.4108	0.7856	0.7634	3.56E-02	1.007326	3.98E+32
1002.464	5.3195	5.5492	0.7852	0.7629	4.70E-02	1.007022	5.26E+32
1027.464	5.4522	5.6876	0.7848	0.7625	6.13E-02	1.006737	6.86E+32
1052.464	5.5848	5.8260	0.7844	0.7622	7.90E-02	1.006469	8.84E+32
1077.464	5.7175	5.9644	0.7840	0.7619	1.01E-01	1.006217	1.13E+33
1102.464	5.8501	6.1028	0.7837	0.7616	1.27E-01	1.005979	1.42E+33
1127.464	5.9828	6.2412	0.7835	0.7613	1.59E-01	1.005755	1.77E+33
1152.464	6.1155	6.3795	0.7832	0.7611	1.96E-01	1.005544	2.19E+33
1177.464	6.2481	6.5179	0.7830	0.7609	2.41E-01	1.005344	2.69E+33
1202.464	6.3808	6.6563	0.7828	0.7608	2.93E-01	1.005154	3.28E+33
1227.464	6.5134	6.7947	0.7826	0.7606	3.54E-01	1.004975	3.96E+33

Table D.20: Calculated data for $[\text{Zn}(\text{hfac})]^+$ loss of CF_3 .

E(kJ)	E'	E^\ddagger	α	α^\ddagger	$\frac{(E^\ddagger + a^\ddagger E_z^\ddagger)^s}{(E + aE_z)^{s-1}}$	$\frac{1}{[1 - \beta \frac{dw}{dE'}]}$	k(E) (sec ⁻¹)
268.952	1.4246	1.4928	0.8409	0.8220	4.66E-16	1.054632	4.77E+18
293.952	1.5570	1.6316	0.8362	0.8168	2.06E-14	1.047853	2.10E+20
318.952	1.6894	1.7703	0.8319	0.8122	4.75E-13	1.042348	4.81E+21
343.952	1.8218	1.9091	0.8280	0.8079	6.73E-12	1.037805	6.78E+22
368.952	1.9542	2.0478	0.8244	0.8041	6.53E-11	1.034002	6.56E+23
393.952	2.0867	2.1866	0.8212	0.8006	4.70E-10	1.03078	4.70E+24
418.952	2.2191	2.3254	0.8182	0.7974	2.65E-09	1.028021	2.65E+25
443.952	2.3515	2.4641	0.8155	0.7944	1.23E-08	1.025638	1.22E+26
468.952	2.4839	2.6029	0.8130	0.7917	4.82E-08	1.023562	4.80E+26
493.952	2.6163	2.7416	0.8107	0.7893	1.65E-07	1.021742	1.64E+27
518.952	2.7488	2.8804	0.8085	0.7870	5.00E-07	1.020134	4.95E+27
543.952	2.8812	3.0192	0.8066	0.7849	1.37E-06	1.018706	1.36E+28
568.952	3.0136	3.1579	0.8048	0.7830	3.44E-06	1.017432	3.40E+28
593.952	3.1460	3.2967	0.8031	0.7812	8.00E-06	1.016289	7.90E+28
618.952	3.2784	3.4355	0.8015	0.7796	1.74E-05	1.015259	1.72E+29
643.952	3.4109	3.5742	0.8001	0.7781	3.57E-05	1.014327	3.52E+29
668.952	3.5433	3.7130	0.7988	0.7767	6.94E-05	1.013481	6.83E+29
693.952	3.6757	3.8517	0.7975	0.7754	1.29E-04	1.012711	1.27E+30
718.952	3.8081	3.9905	0.7964	0.7742	2.29E-04	1.012006	2.25E+30
743.952	3.9405	4.1293	0.7953	0.7731	3.92E-04	1.011361	3.85E+30
768.952	4.0729	4.2680	0.7944	0.7721	6.50E-04	1.010767	6.38E+30
793.952	4.2054	4.4068	0.7935	0.7712	1.04E-03	1.01022	1.02E+31
818.952	4.3378	4.5455	0.7926	0.7703	1.63E-03	1.009715	1.60E+31
843.952	4.4702	4.6843	0.7918	0.7695	2.48E-03	1.009247	2.43E+31
868.952	4.6026	4.8231	0.7911	0.7688	3.69E-03	1.008813	3.61E+31
893.952	4.7350	4.9618	0.7905	0.7681	5.36E-03	1.008409	5.25E+31
918.952	4.8675	5.1006	0.7899	0.7675	7.65E-03	1.008033	7.49E+31
943.952	4.9999	5.2393	0.7893	0.7670	1.07E-02	1.007682	1.05E+32
968.952	5.1323	5.3781	0.7888	0.7665	1.48E-02	1.007354	1.45E+32
993.952	5.2647	5.5169	0.7883	0.7660	2.00E-02	1.007047	1.96E+32
1018.952	5.3971	5.6556	0.7879	0.7656	2.68E-02	1.006759	2.62E+32
1043.952	5.5296	5.7944	0.7875	0.7653	3.54E-02	1.006488	3.46E+32
1068.952	5.6620	5.9331	0.7872	0.7649	4.61E-02	1.006234	4.51E+32
1093.952	5.7944	6.0719	0.7868	0.7646	5.94E-02	1.005994	5.81E+32
1118.952	5.9268	6.2107	0.7866	0.7644	7.57E-02	1.005768	7.40E+32
1143.952	6.0592	6.3494	0.7863	0.7642	9.56E-02	1.005555	9.33E+32
1168.952	6.1917	6.4882	0.7861	0.7640	1.19E-01	1.005353	1.17E+33
1193.952	6.3241	6.6269	0.7859	0.7638	1.48E-01	1.005162	1.44E+33
1218.952	6.4565	6.7657	0.7857	0.7637	1.82E-01	1.004981	1.77E+33
1243.952	6.5889	6.9045	0.7856	0.7636	2.21E-01	1.00481	2.16E+33

Table D.21: Calculated data for $[\text{Cu}(\text{hfac})_2]^+$ loss of hfac .

E(kJ)	E'	E'^\ddagger	α	α^\ddagger	$\frac{(E^\ddagger + a^\ddagger E_z^\ddagger)^s}{(E + aE_z)^{s-1}}$	$\frac{1}{[1 - \beta \frac{dw}{dE'} E']}$	k(E) (sec ⁻¹)
674.99	1.7673	1.8437	0.8203	0.8050	2.69E-40	1.041786	7.25E-08
699.99	1.8328	1.9120	0.8184	0.8029	2.33E-38	1.039554	6.27E-06
724.99	1.8982	1.9803	0.8165	0.8009	1.33E-36	1.037509	3.58E-04
749.99	1.9637	2.0486	0.8147	0.7990	5.32E-35	1.035629	1.43E-02
774.99	2.0292	2.1168	0.8130	0.7972	1.56E-33	1.033897	4.18E-01
799.99	2.0946	2.1851	0.8113	0.7955	3.5E-32	1.032296	9.35E+00
824.99	2.1601	2.2534	0.8098	0.7938	6.2E-31	1.030814	1.65E+02
849.99	2.2255	2.3217	0.8083	0.7922	8.9E-30	1.029437	2.37E+03
874.99	2.2910	2.3900	0.8068	0.7907	1.06E-28	1.028157	2.83E+04
899.99	2.3564	2.4583	0.8054	0.7893	1.07E-27	1.026963	2.85E+05
924.99	2.4219	2.5266	0.8041	0.7879	9.35E-27	1.025848	2.48E+06
949.99	2.4874	2.5948	0.8028	0.7865	7.12E-26	1.024804	1.89E+07
974.99	2.5528	2.6631	0.8016	0.7853	4.8E-25	1.023826	1.27E+08
999.99	2.6183	2.7314	0.8004	0.7840	2.9E-24	1.022908	7.67E+08
1024.99	2.6837	2.7997	0.7993	0.7829	1.58E-23	1.022045	4.18E+09
1049.99	2.7492	2.8680	0.7982	0.7817	7.86E-23	1.021232	2.08E+10
1074.99	2.8146	2.9363	0.7972	0.7806	3.59E-22	1.020465	9.49E+10
1099.99	2.8801	3.0046	0.7962	0.7796	1.52E-21	1.019741	4.01E+11
1124.99	2.9456	3.0729	0.7952	0.7786	5.97E-21	1.019057	1.58E+12
1149.99	3.0110	3.1411	0.7943	0.7776	2.2E-20	1.018409	5.80E+12
1174.99	3.0765	3.2094	0.7934	0.7767	7.61E-20	1.017795	2.01E+13
1199.99	3.1419	3.2777	0.7925	0.7758	2.49E-19	1.017213	6.55E+13
1224.99	3.2074	3.3460	0.7917	0.7750	7.71E-19	1.01666	2.03E+14
1249.99	3.2728	3.4143	0.7909	0.7742	2.28E-18	1.016134	5.99E+14
1274.99	3.3383	3.4826	0.7901	0.7734	6.41E-18	1.015634	1.68E+15
1299.99	3.4038	3.5509	0.7894	0.7726	1.73E-17	1.015158	4.54E+15
1324.99	3.4692	3.6191	0.7887	0.7719	4.47E-17	1.014704	1.18E+16
1349.99	3.5347	3.6874	0.7880	0.7712	1.12E-16	1.01427	2.93E+16
1374.99	3.6001	3.7557	0.7874	0.7705	2.68E-16	1.013857	7.04E+16
1399.99	3.6656	3.8240	0.7867	0.7699	6.23E-16	1.013461	1.64E+17
1424.99	3.7310	3.8923	0.7861	0.7692	1.4E-15	1.013083	3.68E+17
1449.99	3.7965	3.9606	0.7855	0.7686	3.07E-15	1.012721	8.05E+17
1474.99	3.8620	4.0289	0.7850	0.7681	6.52E-15	1.012375	1.71E+18
1499.99	3.9274	4.0971	0.7844	0.7675	1.35E-14	1.012042	3.54E+18
1524.99	3.9929	4.1654	0.7839	0.7670	2.72E-14	1.011724	7.13E+18
1549.99	4.0583	4.2337	0.7834	0.7665	5.36E-14	1.011418	1.40E+19
1574.99	4.1238	4.3020	0.7829	0.7660	1.03E-13	1.011124	2.70E+19
1599.99	4.1892	4.3703	0.7824	0.7655	1.94E-13	1.010842	5.09E+19
1624.99	4.2547	4.4386	0.7820	0.7651	3.59E-13	1.010571	9.39E+19
1649.99	4.3202	4.5069	0.7816	0.7646	6.49E-13	1.01031	1.70E+20

Table D.22: Calculated data for $[\text{Ni}(\text{hfac})_2]^+$ loss of hfac .

E(kJ)	E'	E [‡]	α	α^{\ddagger}	$\frac{(E^{\ddagger} + \alpha^{\ddagger} E_z^{\ddagger})^s}{(E + aE_z)^{s-1}}$	$\frac{1}{[1 - \beta \frac{dw}{dE'}]}$	k(E) (sec ⁻¹)
938.331	2.4487	2.5542	0.8115	0.7856	3.55E-49	1.02436	3.25E-12
963.331	2.5140	2.6222	0.8103	0.7842	5.52E-47	1.02339	5.05E-10
988.331	2.5792	2.6903	0.8092	0.7830	5.4E-45	1.02248	4.94E-08
1013.331	2.6444	2.7583	0.8081	0.7818	3.55E-43	1.021625	3.24E-06
1038.331	2.7097	2.8264	0.8070	0.7806	1.66E-41	1.02082	1.51E-04
1063.331	2.7749	2.8944	0.8060	0.7795	5.74E-40	1.020062	5.24E-03
1088.331	2.8402	2.9625	0.8050	0.7784	1.53E-38	1.019346	1.39E-01
1113.331	2.9054	3.0305	0.8041	0.7774	3.24E-37	1.01867	2.95E+00
1138.331	2.9706	3.0986	0.8032	0.7764	5.57E-36	1.01803	5.07E+01
1163.331	3.0359	3.1666	0.8023	0.7754	7.97E-35	1.017424	7.24E+02
1188.331	3.1011	3.2347	0.8014	0.7745	9.66E-34	1.01685	8.78E+03
1213.331	3.1664	3.3027	0.8006	0.7736	1.01E-32	1.016304	9.16E+04
1238.331	3.2316	3.3708	0.7998	0.7728	9.19E-32	1.015786	8.35E+05
1263.331	3.2968	3.4388	0.7991	0.7720	7.4E-31	1.015293	6.72E+06
1288.331	3.3621	3.5069	0.7984	0.7712	5.33E-30	1.014824	4.84E+07
1313.331	3.4273	3.5749	0.7977	0.7705	3.46E-29	1.014377	3.14E+08
1338.331	3.4926	3.6430	0.7970	0.7697	2.04E-28	1.01395	1.85E+09
1363.331	3.5578	3.7110	0.7964	0.7690	1.1E-27	1.013543	1.00E+10
1388.331	3.6231	3.7791	0.7957	0.7684	5.51E-27	1.013154	4.99E+10
1413.331	3.6883	3.8471	0.7951	0.7677	2.55E-26	1.012782	2.31E+11
1438.331	3.7535	3.9152	0.7946	0.7671	1.1E-25	1.012426	9.96E+11
1463.331	3.8188	3.9832	0.7940	0.7665	4.45E-25	1.012086	4.03E+12
1488.331	3.8840	4.0513	0.7935	0.7660	1.7E-24	1.011759	1.53E+13
1513.331	3.9493	4.1194	0.7930	0.7654	6.11E-24	1.011446	5.53E+13
1538.331	4.0145	4.1874	0.7925	0.7649	2.09E-23	1.011146	1.89E+14
1563.331	4.0797	4.2555	0.7920	0.7644	6.79E-23	1.010858	6.14E+14
1588.331	4.1450	4.3235	0.7915	0.7639	2.11E-22	1.010581	1.90E+15
1613.331	4.2102	4.3916	0.7911	0.7634	6.27E-22	1.010315	5.66E+15
1638.331	4.2755	4.4596	0.7907	0.7630	1.79E-21	1.010059	1.61E+16
1663.331	4.3407	4.5277	0.7903	0.7626	4.91E-21	1.009812	4.43E+16
1688.331	4.4059	4.5957	0.7899	0.7621	1.3E-20	1.009575	1.17E+17
1713.331	4.4712	4.6638	0.7895	0.7617	3.32E-20	1.009347	3.00E+17
1738.331	4.5364	4.7318	0.7891	0.7614	8.22E-20	1.009126	7.42E+17
1763.331	4.6017	4.7999	0.7888	0.7610	1.97E-19	1.008914	1.78E+18
1788.331	4.6669	4.8679	0.7884	0.7607	4.6E-19	1.008709	4.15E+18
1813.331	4.7322	4.9360	0.7881	0.7603	1.04E-18	1.008511	9.40E+18
1838.331	4.7974	5.0040	0.7878	0.7600	2.3E-18	1.00832	2.07E+19
1863.331	4.8626	5.0721	0.7875	0.7597	4.96E-18	1.008136	4.47E+19
1888.331	4.9279	5.1401	0.7872	0.7594	1.04E-17	1.007958	9.39E+19
1913.331	4.9931	5.2082	0.7870	0.7591	2.14E-17	1.007785	1.93E+20

Table D.23: Calculated data for $[\text{Zn}(\text{hfac})_2]^+$ loss of hfac .

E(kJ)	E'	E [‡]	α	α^{\ddagger}	$\frac{(E^{\ddagger} + \alpha^{\ddagger} E_z^{\ddagger})^s}{(E + aE_z)^{s-1}}$	$\frac{1}{[1 - \beta \frac{dw}{dE'}]}$	k(E) (sec ⁻¹)
428.976	1.1351	1.1709	0.8440	0.8345	2.54E-29	1.081731	1.67E+06
453.976	1.2013	1.2391	0.8407	0.8310	8.86E-28	1.07513	5.80E+07
478.976	1.2674	1.3074	0.8376	0.8278	2.21E-26	1.069372	1.44E+09
503.976	1.3336	1.3756	0.8347	0.8247	4.14E-25	1.06431	2.68E+10
528.976	1.3997	1.4438	0.8319	0.8218	6.04E-24	1.059832	3.89E+11
553.976	1.4659	1.5121	0.8292	0.8190	7.07E-23	1.055845	4.54E+12
578.976	1.5320	1.5803	0.8267	0.8164	6.83E-22	1.052277	4.37E+13
603.976	1.5982	1.6485	0.8243	0.8139	5.57E-21	1.049068	3.55E+14
628.976	1.6643	1.7168	0.8220	0.8115	3.9E-20	1.046168	2.48E+15
653.976	1.7305	1.7850	0.8199	0.8093	2.39E-19	1.043538	1.52E+16
678.976	1.7967	1.8532	0.8178	0.8071	1.3E-18	1.041143	8.20E+16
703.976	1.8628	1.9215	0.8159	0.8051	6.3E-18	1.038955	3.98E+17
728.976	1.9290	1.9897	0.8140	0.8032	2.77E-17	1.036949	1.75E+18
753.976	1.9951	2.0580	0.8122	0.8013	1.12E-16	1.035105	7.04E+18
778.976	2.0613	2.1262	0.8105	0.7995	4.15E-16	1.033404	2.61E+19
803.976	2.1274	2.1944	0.8088	0.7978	1.43E-15	1.031833	8.98E+19
828.976	2.1936	2.2627	0.8073	0.7962	4.6E-15	1.030376	2.88E+20
853.976	2.2597	2.3309	0.8058	0.7947	1.39E-14	1.029024	8.71E+20
878.976	2.3259	2.3991	0.8043	0.7932	3.97E-14	1.027765	2.48E+21
903.976	2.3920	2.4674	0.8029	0.7917	1.07E-13	1.026591	6.71E+21
928.976	2.4582	2.5356	0.8016	0.7904	2.77E-13	1.025494	1.73E+22
953.976	2.5243	2.6039	0.8004	0.7891	6.81E-13	1.024468	4.24E+22
978.976	2.5905	2.6721	0.7991	0.7878	1.61E-12	1.023506	1.00E+23
1003.976	2.6566	2.7403	0.7980	0.7866	3.64E-12	1.022602	2.27E+23
1028.976	2.7228	2.8086	0.7968	0.7855	7.97E-12	1.021752	4.95E+23
1053.976	2.7889	2.8768	0.7958	0.7843	1.68E-11	1.020952	1.04E+24
1078.976	2.8551	2.9450	0.7947	0.7833	3.44E-11	1.020197	2.14E+24
1103.976	2.9213	3.0133	0.7937	0.7823	6.83E-11	1.019484	4.24E+24
1128.976	2.9874	3.0815	0.7928	0.7813	1.32E-10	1.01881	8.17E+24
1153.976	3.0536	3.1497	0.7918	0.7803	2.48E-10	1.018172	1.54E+25
1178.976	3.1197	3.2180	0.7910	0.7794	4.55E-10	1.017567	2.81E+25
1203.976	3.1859	3.2862	0.7901	0.7786	8.15E-10	1.016993	5.04E+25
1228.976	3.2520	3.3545	0.7893	0.7777	1.43E-09	1.016448	8.83E+25
1253.976	3.3182	3.4227	0.7885	0.7769	2.45E-09	1.01593	1.51E+26
1278.976	3.3843	3.4909	0.7877	0.7761	4.12E-09	1.015437	2.55E+26
1303.976	3.4505	3.5592	0.7870	0.7754	6.81E-09	1.014967	4.21E+26
1328.976	3.5166	3.6274	0.7863	0.7747	1.11E-08	1.014519	6.83E+26
1353.976	3.5828	3.6956	0.7856	0.7740	1.77E-08	1.014092	1.09E+27
1378.976	3.6489	3.7639	0.7850	0.7733	2.77E-08	1.013684	1.71E+27
1403.976	3.7151	3.8321	0.7843	0.7727	4.29E-08	1.013294	2.65E+27

Table D.24: Calculated data for $[\text{Cu}(\text{hfac}-\text{CF}_3)(\text{hfac})]^+$ loss of *hfac*.

E(kJ)	E'	E [‡]	α	α^{\ddagger}	$\frac{(E^{\ddagger} + a^{\ddagger} E_z^{\ddagger})^s}{(E + aE_z)^{s-1}}$	$\frac{1}{[1 - \beta \frac{dw}{dE'}]}$	k(E) (sec ⁻¹)
324.924	0.9703	1.0109	0.8564	0.8433	2.5E-22	1.100744	7.05E+11
349.924	1.0450	1.0886	0.8522	0.8388	5.97E-21	1.090242	1.67E+13
374.924	1.1197	1.1664	0.8482	0.8345	1.02E-19	1.081458	2.82E+14
399.924	1.1943	1.2442	0.8445	0.8305	1.31E-18	1.074016	3.60E+15
424.924	1.2690	1.3220	0.8411	0.8268	1.32E-17	1.067642	3.60E+16
449.924	1.3436	1.3997	0.8378	0.8234	1.08E-16	1.062129	2.93E+17
474.924	1.4183	1.4775	0.8348	0.8201	7.35E-16	1.057321	1.99E+18
499.924	1.4930	1.5553	0.8319	0.8171	4.28E-15	1.053097	1.15E+19
524.924	1.5676	1.6331	0.8292	0.8142	2.17E-14	1.04936	5.83E+19
549.924	1.6423	1.7109	0.8266	0.8115	9.7E-14	1.046035	2.60E+20
574.924	1.7169	1.7886	0.8242	0.8089	3.89E-13	1.04306	1.04E+21
599.924	1.7916	1.8664	0.8219	0.8065	1.42E-12	1.040386	3.78E+21
624.924	1.8663	1.9442	0.8197	0.8041	4.72E-12	1.037971	1.26E+22
649.924	1.9409	2.0220	0.8177	0.8020	1.45E-11	1.035782	3.86E+22
674.924	2.0156	2.0997	0.8157	0.7999	4.17E-11	1.033789	1.11E+23
699.924	2.0902	2.1775	0.8139	0.7979	1.12E-10	1.031969	2.97E+23
724.924	2.1649	2.2553	0.8121	0.7961	2.84E-10	1.030301	7.51E+23
749.924	2.2396	2.3331	0.8104	0.7943	6.83E-10	1.028769	1.80E+24
774.924	2.3142	2.4108	0.8088	0.7926	1.56E-09	1.027357	4.12E+24
799.924	2.3889	2.4886	0.8073	0.7910	3.42E-09	1.026052	8.99E+24
824.924	2.4635	2.5664	0.8058	0.7895	7.17E-09	1.024844	1.88E+25
849.924	2.5382	2.6442	0.8044	0.7880	1.45E-08	1.023723	3.80E+25
874.924	2.6129	2.7220	0.8031	0.7866	2.82E-08	1.022679	7.40E+25
899.924	2.6875	2.7997	0.8018	0.7853	5.32E-08	1.021707	1.39E+26
924.924	2.7622	2.8775	0.8006	0.7840	9.74E-08	1.020799	2.55E+26
949.924	2.8368	2.9553	0.7995	0.7828	1.73E-07	1.01995	4.53E+26
974.924	2.9115	3.0331	0.7983	0.7816	3.01E-07	1.019153	7.85E+26
999.924	2.9861	3.1108	0.7973	0.7805	5.08E-07	1.018406	1.33E+27
1024.924	3.0608	3.1886	0.7963	0.7795	8.41E-07	1.017704	2.19E+27
1049.924	3.1355	3.2664	0.7953	0.7785	1.36E-06	1.017043	3.55E+27
1074.924	3.2101	3.3442	0.7944	0.7775	2.16E-06	1.01642	5.62E+27
1099.924	3.2848	3.4219	0.7935	0.7766	3.36E-06	1.015831	8.75E+27
1124.924	3.3594	3.4997	0.7926	0.7757	5.14E-06	1.015275	1.34E+28
1149.924	3.4341	3.5775	0.7918	0.7749	7.73E-06	1.014749	2.01E+28
1174.924	3.5088	3.6553	0.7910	0.7741	1.15E-05	1.014251	2.98E+28
1199.924	3.5834	3.7330	0.7903	0.7733	1.67E-05	1.013778	4.35E+28
1224.924	3.6581	3.8108	0.7895	0.7725	2.41E-05	1.013329	6.25E+28
1249.924	3.7327	3.8886	0.7889	0.7718	3.42E-05	1.012903	8.88E+28
1274.924	3.8074	3.9664	0.7882	0.7712	4.8E-05	1.012497	1.25E+29
1299.924	3.8821	4.0442	0.7876	0.7705	6.65E-05	1.012111	1.73E+29

Table D.25: Calculated data for $[\text{Ni}(\text{hfac}-\text{CF}_3)(\text{hfac})]^+$ loss of hfac.

E(kJ)	E'	E [‡]	α	α^{\ddagger}	$\frac{(E^{\ddagger} + a^{\ddagger} E_z^{\ddagger})^s}{(E + aE_z)^{s-1}}$	$\frac{1}{[1 - \beta \frac{dw}{dE'}]}$	k(E) (sec ⁻¹)
336.858	1.0079	1.0267	0.8575	0.8191	3.78E-23	1.092935	4.95E+08
361.858	1.0827	1.1029	0.8534	0.8141	9.41E-22	1.083583	1.22E+10
386.858	1.1575	1.1791	0.8497	0.8093	1.67E-20	1.075708	2.15E+11
411.858	1.2323	1.2553	0.8462	0.8049	2.24E-19	1.068997	2.87E+12
436.858	1.3071	1.3315	0.8429	0.8008	2.35E-18	1.06322	2.99E+13
461.858	1.3819	1.4077	0.8398	0.7969	2E-17	1.058202	2.53E+14
486.858	1.4567	1.4839	0.8369	0.7933	1.42E-16	1.053808	1.79E+15
511.858	1.5315	1.5601	0.8342	0.7899	8.57E-16	1.049934	1.08E+16
536.858	1.6063	1.6363	0.8316	0.7866	4.5E-15	1.046497	5.64E+16
561.858	1.6811	1.7125	0.8292	0.7836	2.09E-14	1.04343	2.61E+17
586.858	1.7559	1.7887	0.8269	0.7807	8.67E-14	1.040679	1.08E+18
611.858	1.8307	1.8649	0.8247	0.7780	3.26E-13	1.038201	4.05E+18
636.858	1.9055	1.9411	0.8226	0.7754	1.12E-12	1.035958	1.39E+19
661.858	1.9803	2.0173	0.8207	0.7729	3.56E-12	1.03392	4.41E+19
686.858	2.0551	2.0935	0.8188	0.7706	1.05E-11	1.032062	1.30E+20
711.858	2.1299	2.1697	0.8170	0.7684	2.91E-11	1.030363	3.59E+20
736.858	2.2047	2.2459	0.8153	0.7663	7.59E-11	1.028803	9.34E+20
761.858	2.2795	2.3221	0.8137	0.7642	1.87E-10	1.027368	2.30E+21
786.858	2.3543	2.3983	0.8122	0.7623	4.39E-10	1.026044	5.39E+21
811.858	2.4291	2.4745	0.8107	0.7605	9.84E-10	1.024819	1.21E+22
836.858	2.5039	2.5507	0.8093	0.7588	2.11E-09	1.023683	2.59E+22
861.858	2.5787	2.6269	0.8080	0.7571	4.37E-09	1.022628	5.34E+22
886.858	2.6535	2.7031	0.8067	0.7555	8.71E-09	1.021645	1.06E+23
911.858	2.7283	2.7793	0.8055	0.7540	1.68E-08	1.020728	2.05E+23
936.858	2.8031	2.8555	0.8044	0.7526	3.14E-08	1.019871	3.83E+23
961.858	2.8779	2.9317	0.8033	0.7512	5.69E-08	1.019069	6.94E+23
986.858	2.9527	3.0079	0.8022	0.7499	1.01E-07	1.018316	1.23E+24
1011.858	3.0275	3.0841	0.8012	0.7486	1.74E-07	1.01761	2.11E+24
1036.858	3.1023	3.1603	0.8002	0.7474	2.92E-07	1.016945	3.55E+24
1061.858	3.1771	3.2365	0.7993	0.7462	4.81E-07	1.016318	5.85E+24
1086.858	3.2519	3.3127	0.7984	0.7451	7.77E-07	1.015728	9.44E+24
1111.858	3.3267	3.3889	0.7975	0.7441	1.23E-06	1.01517	1.49E+25
1136.858	3.4015	3.4651	0.7967	0.7431	1.91E-06	1.014642	2.32E+25
1161.858	3.4763	3.5413	0.7959	0.7421	2.92E-06	1.014142	3.55E+25
1186.858	3.5511	3.6175	0.7952	0.7412	4.4E-06	1.013669	5.33E+25
1211.858	3.6259	3.6937	0.7945	0.7403	6.51E-06	1.013219	7.89E+25
1236.858	3.7007	3.7699	0.7938	0.7395	9.51E-06	1.012792	1.15E+26
1261.858	3.7755	3.8461	0.7931	0.7386	1.37E-05	1.012387	1.66E+26
1286.858	3.8503	3.9223	0.7925	0.7379	1.95E-05	1.012	2.36E+26
1311.858	3.9251	3.9985	0.7919	0.7371	2.74E-05	1.011633	3.31E+26

Table D.26: Calculated data for $[Zn(hfac-CF_3)(hfac)]^+$ loss of *hfac*.

E(kJ)	E'	E [‡]	α	α^{\ddagger}	$\frac{(E^{\ddagger} + a^{\ddagger} E_z^{\ddagger})^s}{(E + aE_z)^{s-1}}$	$\frac{1}{[1 - \beta \frac{dw}{dE'}]}$	k(E) (sec ⁻¹)
398.62	1.2058	1.2596	0.8412	0.8215	1.45E-26	1.074368	5.95E+08
423.62	1.2815	1.3386	0.8377	0.8176	5.78E-25	1.067935	2.35E+10
448.62	1.3571	1.4176	0.8343	0.8139	1.55E-23	1.062375	6.24E+11
473.62	1.4327	1.4966	0.8312	0.8105	2.96E-22	1.057529	1.19E+13
498.62	1.5083	1.5756	0.8283	0.8073	4.28E-21	1.053272	1.71E+14
523.62	1.5840	1.6546	0.8256	0.8043	4.85E-20	1.049509	1.93E+15
548.62	1.6596	1.7336	0.8230	0.8014	4.46E-19	1.046162	1.77E+16
573.62	1.7352	1.8126	0.8205	0.7988	3.41E-18	1.043168	1.35E+17
598.62	1.8108	1.8916	0.8182	0.7962	2.22E-17	1.040478	8.74E+17
623.62	1.8865	1.9706	0.8160	0.7938	1.25E-16	1.03805	4.92E+18
648.62	1.9621	2.0496	0.8139	0.7915	6.24E-16	1.035848	2.45E+19
673.62	2.0377	2.1286	0.8119	0.7894	2.78E-15	1.033845	1.09E+20
698.62	2.1133	2.2076	0.8100	0.7873	1.12E-14	1.032016	4.36E+20
723.62	2.1890	2.2866	0.8082	0.7854	4.11E-14	1.030341	1.60E+21
748.62	2.2646	2.3656	0.8065	0.7835	1.39E-13	1.028802	5.41E+21
773.62	2.3402	2.4446	0.8049	0.7817	4.37E-13	1.027384	1.70E+22
798.62	2.4158	2.5236	0.8033	0.7801	1.28E-12	1.026074	4.98E+22
823.62	2.4915	2.6026	0.8018	0.7785	3.55E-12	1.024861	1.37E+23
848.62	2.5671	2.6816	0.8004	0.7769	9.27E-12	1.023736	3.58E+23
873.62	2.6427	2.7606	0.7991	0.7755	2.3E-11	1.022689	8.87E+23
898.62	2.7183	2.8396	0.7978	0.7741	5.43E-11	1.021713	2.09E+24
923.62	2.7940	2.9186	0.7965	0.7728	1.23E-10	1.020802	4.73E+24
948.62	2.8696	2.9976	0.7954	0.7715	2.67E-10	1.01995	1.03E+25
973.62	2.9452	3.0766	0.7943	0.7703	5.58E-10	1.019152	2.15E+25
998.62	3.0208	3.1556	0.7932	0.7692	1.13E-09	1.018403	4.33E+25
1023.62	3.0965	3.2346	0.7922	0.7681	2.21E-09	1.017699	8.47E+25
1048.62	3.1721	3.3136	0.7912	0.7670	4.19E-09	1.017036	1.61E+26
1073.62	3.2477	3.3926	0.7902	0.7660	7.72E-09	1.016411	2.96E+26
1098.62	3.3233	3.4716	0.7893	0.7651	1.39E-08	1.015822	5.31E+26
1123.62	3.3990	3.5506	0.7885	0.7642	2.43E-08	1.015265	9.31E+26
1148.62	3.4746	3.6296	0.7876	0.7633	4.17E-08	1.014738	1.59E+27
1173.62	3.5502	3.7086	0.7869	0.7625	6.99E-08	1.014238	2.67E+27
1198.62	3.6258	3.7876	0.7861	0.7617	1.15E-07	1.013765	4.38E+27
1223.62	3.7015	3.8666	0.7854	0.7609	1.85E-07	1.013315	7.06E+27
1248.62	3.7771	3.9456	0.7847	0.7602	2.93E-07	1.012888	1.12E+28
1273.62	3.8527	4.0246	0.7840	0.7595	4.55E-07	1.012482	1.74E+28
1298.62	3.9283	4.1036	0.7834	0.7588	6.97E-07	1.012095	2.66E+28
1323.62	4.0040	4.1826	0.7828	0.7582	1.05E-06	1.011727	4.01E+28
1348.62	4.0796	4.2616	0.7822	0.7576	1.56E-06	1.011375	5.95E+28
1373.62	4.1552	4.3406	0.7817	0.7570	2.29E-06	1.01104	8.72E+28

Table D.27: Calculated data for $[\text{Cu}(\text{tfm})_2]^+$ loss of 1st tBu.

E(kJ)	E'	E [‡]	α	α^{\ddagger}	$\frac{(E^{\ddagger} + a^{\ddagger} E_z^{\ddagger})^s}{(E + aE_z)^{s-1}}$	$\frac{1}{[1 - \beta \frac{dw}{dE'}]}$	k(E) (sec ⁻¹)
199.535	0.2123	0.2162	0.9402	0.9382	8.27E-11	1.613946	4.06E+23
224.535	0.2389	0.2432	0.9350	0.9328	1.55E-10	1.531181	7.21E+23
249.535	0.2655	0.2703	0.9302	0.9278	2.85E-10	1.467333	1.27E+24
274.535	0.2921	0.2974	0.9256	0.9231	5.17E-10	1.416508	2.23E+24
299.535	0.3187	0.3245	0.9212	0.9187	9.23E-10	1.375052	3.86E+24
324.535	0.3453	0.3516	0.9171	0.9144	1.62E-09	1.340574	6.61E+24
349.535	0.3719	0.3787	0.9132	0.9104	2.80E-09	1.311442	1.12E+25
374.535	0.3985	0.4057	0.9094	0.9065	4.76E-09	1.286498	1.86E+25
399.535	0.4251	0.4328	0.9058	0.9029	7.97E-09	1.264903	3.06E+25
424.535	0.4517	0.4599	0.9024	0.8994	1.31E-08	1.246025	4.97E+25
449.535	0.4783	0.4870	0.8991	0.8960	2.13E-08	1.229386	7.97E+25
474.535	0.5049	0.5141	0.8960	0.8928	3.41E-08	1.214614	1.26E+26
499.535	0.5315	0.5411	0.8930	0.8897	5.38E-08	1.201416	1.97E+26
524.535	0.5581	0.5682	0.8901	0.8867	8.38E-08	1.189555	3.03E+26
549.535	0.5847	0.5953	0.8873	0.8839	1.29E-07	1.178843	4.61E+26
574.535	0.6113	0.6224	0.8846	0.8811	1.95E-07	1.169123	6.94E+26
599.535	0.6379	0.6495	0.8820	0.8784	2.92E-07	1.160266	1.03E+27
624.535	0.6645	0.6766	0.8795	0.8759	4.33E-07	1.152166	1.52E+27
649.535	0.6911	0.7036	0.8771	0.8734	6.34E-07	1.144733	2.21E+27
674.535	0.7177	0.7307	0.8747	0.8710	9.17E-07	1.137888	3.17E+27
699.535	0.7443	0.7578	0.8725	0.8687	1.31E-06	1.131568	4.52E+27
724.535	0.7709	0.7849	0.8703	0.8665	1.86E-06	1.125716	6.38E+27
749.535	0.7975	0.8120	0.8682	0.8643	2.62E-06	1.120284	8.92E+27
774.535	0.8241	0.8391	0.8661	0.8622	3.64E-06	1.115229	1.23E+28
799.535	0.8507	0.8661	0.8641	0.8601	5.02E-06	1.110517	1.69E+28
824.535	0.8773	0.8932	0.8622	0.8581	6.86E-06	1.106113	2.31E+28
849.535	0.9039	0.9203	0.8603	0.8562	9.29E-06	1.10199	3.11E+28
874.535	0.9305	0.9474	0.8584	0.8543	1.25E-05	1.098124	4.17E+28
899.535	0.9571	0.9745	0.8566	0.8525	1.66E-05	1.094491	5.54E+28
924.535	0.9837	1.0015	0.8549	0.8507	2.19E-05	1.091073	7.28E+28
949.535	1.0103	1.0286	0.8532	0.8491	2.92E-05	1.094306	9.71E+28
974.535	1.0369	1.0557	0.8517	0.8476	3.81E-05	1.090739	1.26E+29
999.535	1.0635	1.0828	0.8503	0.8461	4.95E-05	1.087392	1.64E+29
1024.535	1.0901	1.1099	0.8488	0.8446	6.38E-05	1.084248	2.10E+29
1049.535	1.1167	1.1370	0.8474	0.8432	8.17E-05	1.081289	2.69E+29
1074.535	1.1433	1.1640	0.8461	0.8418	1.04E-04	1.078499	3.41E+29
1099.535	1.1699	1.1911	0.8448	0.8405	1.32E-04	1.075866	4.31E+29
1124.535	1.1965	1.2182	0.8435	0.8392	1.66E-04	1.073377	5.40E+29
1149.535	1.2231	1.2453	0.8422	0.8379	2.07E-04	1.071021	6.75E+29
1174.535	1.2497	1.2724	0.8410	0.8366	2.58E-04	1.068788	8.38E+29

Table D.28: Calculated data for $[\text{Ni}(\text{tftm})_2]^+$ loss of 1st *tBu*.

E(kJ)	E'	E'^\ddagger	α	α^\ddagger	$\frac{(E^\ddagger + a^\ddagger E_z^\ddagger)^s}{(E + aE_z)^{s-1}}$	$\frac{1}{[1 - \beta \frac{dw}{dE'} E']}$	k(E) (sec ⁻¹)
932.41	0.9908	1.0146	0.8561	0.8482	1.70E-44	1.09019	1.15E-08
957.41	1.0174	1.0418	0.8545	0.8467	1.56E-43	1.093331	1.07E-07
982.41	1.0440	1.0690	0.8531	0.8451	1.31E-42	1.089828	8.88E-07
1007.41	1.0705	1.0962	0.8516	0.8436	1.00E-41	1.086541	6.81E-06
1032.41	1.0971	1.1234	0.8502	0.8422	7.14E-41	1.083451	4.83E-05
1057.41	1.1237	1.1506	0.8489	0.8407	4.72E-40	1.080542	3.18E-04
1082.41	1.1502	1.1778	0.8475	0.8393	2.91E-39	1.077798	1.95E-03
1107.41	1.1768	1.2050	0.8462	0.8380	1.68E-38	1.075207	1.12E-02
1132.41	1.2034	1.2322	0.8449	0.8367	9.08E-38	1.072756	6.08E-02
1157.41	1.2299	1.2594	0.8437	0.8354	4.64E-37	1.070436	3.10E-01
1182.41	1.2565	1.2866	0.8425	0.8341	2.24E-36	1.068236	1.49E+00
1207.41	1.2831	1.3138	0.8413	0.8329	1.03E-35	1.066148	6.83E+00
1232.41	1.3096	1.3410	0.8402	0.8317	4.47E-35	1.064163	2.97E+01
1257.41	1.3362	1.3682	0.8390	0.8305	1.86E-34	1.062275	1.23E+02
1282.41	1.3628	1.3954	0.8379	0.8293	7.37E-34	1.060478	4.88E+02
1307.41	1.3893	1.4226	0.8368	0.8282	2.80E-33	1.058764	1.85E+03
1332.41	1.4159	1.4498	0.8358	0.8271	1.02E-32	1.057129	6.74E+03
1357.41	1.4425	1.4770	0.8347	0.8260	3.58E-32	1.055568	2.36E+04
1382.41	1.4690	1.5042	0.8337	0.8250	1.21E-31	1.054075	7.96E+04
1407.41	1.4956	1.5314	0.8327	0.8239	3.94E-31	1.052648	2.59E+05
1432.41	1.5222	1.5586	0.8318	0.8229	1.24E-30	1.051281	8.14E+05
1457.41	1.5487	1.5858	0.8308	0.8219	3.78E-30	1.049971	2.48E+06
1482.41	1.5753	1.6130	0.8299	0.8210	1.12E-29	1.048715	7.30E+06
1507.41	1.6019	1.6402	0.8289	0.8200	3.20E-29	1.04751	2.09E+07
1532.41	1.6284	1.6674	0.8280	0.8191	8.89E-29	1.046353	5.81E+07
1557.41	1.6550	1.6946	0.8272	0.8182	2.41E-28	1.045241	1.57E+08
1582.41	1.6816	1.7218	0.8263	0.8173	6.35E-28	1.044172	4.14E+08
1607.41	1.7081	1.7490	0.8255	0.8164	1.63E-27	1.043144	1.06E+09
1632.41	1.7347	1.7762	0.8246	0.8155	4.09E-27	1.042154	2.66E+09
1657.41	1.7613	1.8035	0.8238	0.8147	1.00E-26	1.0412	6.51E+09
1682.41	1.7878	1.8307	0.8230	0.8139	2.40E-26	1.040281	1.56E+10
1707.41	1.8144	1.8579	0.8222	0.8130	5.62E-26	1.039395	3.65E+10
1732.41	1.8410	1.8851	0.8215	0.8122	1.29E-25	1.038539	8.36E+10
1757.41	1.8675	1.9123	0.8207	0.8115	2.90E-25	1.037714	1.88E+11
1782.41	1.8941	1.9395	0.8200	0.8107	6.40E-25	1.036917	4.14E+11
1807.41	1.9207	1.9667	0.8192	0.8099	1.38E-24	1.036146	8.96E+11
1832.41	1.9472	1.9939	0.8185	0.8092	2.94E-24	1.035401	1.90E+12
1857.41	1.9738	2.0211	0.8178	0.8085	6.15E-24	1.034681	3.97E+12
1882.41	2.0004	2.0483	0.8171	0.8078	1.26E-23	1.033984	8.15E+12
1907.41	2.0269	2.0755	0.8165	0.8071	2.55E-23	1.03331	1.65E+13

Table D.29: Calculated data for $[Zn(tftm)_2]^+$ loss of 1st *tBu*.

E(kJ)	E'	E'^\ddagger	α	α^\ddagger	$\frac{(E^\ddagger + a^\ddagger E_z^\ddagger)^s}{(E + aE_z)^{s-1}}$	$\frac{1}{[1 - \beta \frac{dw}{dE'} E']}$	k(E) (sec ⁻¹)
127.77	0.1365	0.1387	0.9566	0.9554	1.52E-06	2.090638	7.84E+27
152.77	0.1633	0.1659	0.9503	0.9489	2.29E-06	1.856725	1.05E+28
177.77	0.1900	0.1930	0.9444	0.9429	3.44E-06	1.705254	1.45E+28
202.77	0.2167	0.2202	0.9389	0.9372	5.12E-06	1.598623	2.02E+28
227.77	0.2434	0.2473	0.9338	0.9319	7.56E-06	1.519227	2.83E+28
252.77	0.2701	0.2744	0.9289	0.9270	1.11E-05	1.457683	3.98E+28
277.77	0.2968	0.3016	0.9243	0.9223	1.60E-05	1.408511	5.58E+28
302.77	0.3236	0.3287	0.9199	0.9178	2.31E-05	1.368287	7.78E+28
327.77	0.3503	0.3559	0.9158	0.9136	3.28E-05	1.334756	1.08E+29
352.77	0.3770	0.3830	0.9119	0.9096	4.62E-05	1.30637	1.49E+29
377.77	0.4037	0.4102	0.9081	0.9057	6.45E-05	1.282026	2.04E+29
402.77	0.4304	0.4373	0.9045	0.9021	8.93E-05	1.26092	2.78E+29
427.77	0.4571	0.4644	0.9011	0.8986	1.22E-04	1.24245	3.75E+29
452.77	0.4839	0.4916	0.8978	0.8952	1.66E-04	1.226153	5.03E+29
477.77	0.5106	0.5187	0.8947	0.8920	2.24E-04	1.211673	6.69E+29
502.77	0.5373	0.5459	0.8917	0.8889	2.99E-04	1.198724	8.84E+29
527.77	0.5640	0.5730	0.8888	0.8827	2.83E-04	1.18708	8.28E+29
552.77	0.5907	0.6002	0.8829	0.8801	5.07E-04	1.211765	1.52E+30
577.77	0.6175	0.6273	0.8805	0.8776	6.64E-04	1.19777	1.96E+30
602.77	0.6442	0.6545	0.8781	0.8752	8.62E-04	1.185314	2.52E+30
627.77	0.6709	0.6816	0.8758	0.8729	1.11E-03	1.174162	3.22E+30
652.77	0.6976	0.7087	0.8736	0.8706	1.42E-03	1.164126	4.08E+30
677.77	0.7243	0.7359	0.8715	0.8685	1.81E-03	1.155051	5.15E+30
702.77	0.7510	0.7630	0.8694	0.8664	2.28E-03	1.146808	6.45E+30
727.77	0.7778	0.7902	0.8674	0.8643	2.86E-03	1.139291	8.04E+30
752.77	0.8045	0.8173	0.8655	0.8624	3.56E-03	1.132411	9.95E+30
777.77	0.8312	0.8445	0.8636	0.8605	4.41E-03	1.126094	1.23E+31
802.77	0.8579	0.8716	0.8618	0.8586	5.44E-03	1.120274	1.50E+31
827.77	0.8846	0.8987	0.8600	0.8568	6.66E-03	1.114898	1.83E+31
852.77	0.9113	0.9259	0.8583	0.8550	8.11E-03	1.109918	2.22E+31
877.77	0.9381	0.9530	0.8566	0.8533	9.83E-03	1.105294	2.68E+31
902.77	0.9648	0.9802	0.8550	0.8517	1.19E-02	1.10099	3.22E+31
927.77	0.9915	1.0073	0.8534	0.8501	1.42E-02	1.096975	3.85E+31
952.77	1.0182	1.0345	0.8518	0.8485	1.70E-02	1.093222	4.59E+31
977.77	1.0449	1.0616	0.8503	0.8470	2.02E-02	1.089707	5.44E+31
1002.77	1.0716	1.0887	0.8489	0.8455	2.40E-02	1.086409	6.42E+31
1027.77	1.0984	1.1159	0.8474	0.8440	2.83E-02	1.08331	7.56E+31
1052.77	1.1251	1.1430	0.8460	0.8426	3.32E-02	1.080393	8.85E+31
1077.77	1.1518	1.1702	0.8447	0.8412	3.89E-02	1.077642	1.03E+32
1102.77	1.1785	1.1973	0.8434	0.8399	4.53E-02	1.075045	1.20E+32

Table D.30: Calculated data for $[\text{Cu}(\text{tfm})(\text{tfm}-t\text{Bu})]^+$ loss of 2nd *t*Bu.

E(kJ)	E'	E'^\ddagger	α	α^\ddagger	$\frac{(E^\ddagger + a^\ddagger E_z^\ddagger)^s}{(E + aE_z)^{s-1}}$	$\frac{1}{[1 - \beta \frac{dw}{dE'} E']}$	k(E) (sec ⁻¹)
187.61	0.3060	0.3178	0.9221	0.9170	1.32E-11	1.39378	1.86E+25
212.61	0.3468	0.3602	0.9156	0.9102	3.70E-11	1.33877	5.00E+25
237.61	0.3876	0.4026	0.9096	0.9038	9.89E-11	1.296263	1.29E+26
262.61	0.4284	0.4449	0.9040	0.8980	2.52E-10	1.262429	3.21E+26
287.61	0.4692	0.4873	0.8987	0.8925	6.14E-10	1.234867	7.65E+26
312.61	0.5100	0.5296	0.8938	0.8873	1.43E-09	1.211991	1.75E+27
337.61	0.5507	0.5720	0.8892	0.8825	3.21E-09	1.192714	3.86E+27
362.61	0.5915	0.6143	0.8849	0.8779	6.90E-09	1.17626	8.19E+27
387.61	0.6323	0.6567	0.8808	0.8736	1.43E-08	1.162063	1.68E+28
412.61	0.6731	0.6990	0.8745	0.8674	2.80E-08	1.173294	3.32E+28
437.61	0.7139	0.7414	0.8712	0.8639	5.49E-08	1.158493	6.41E+28
462.61	0.7547	0.7837	0.8680	0.8605	1.04E-07	1.145749	1.20E+29
487.61	0.7954	0.8261	0.8650	0.8574	1.92E-07	1.13467	2.19E+29
512.61	0.8362	0.8685	0.8621	0.8543	3.43E-07	1.124961	3.89E+29
537.61	0.8770	0.9108	0.8593	0.8514	5.99E-07	1.116389	6.74E+29
562.61	0.9178	0.9532	0.8566	0.8487	1.02E-06	1.108771	1.14E+30
587.61	0.9586	0.9955	0.8541	0.8460	1.70E-06	1.101962	1.89E+30
612.61	0.9994	1.0379	0.8516	0.8435	2.76E-06	1.095844	3.05E+30
637.61	1.0401	1.0802	0.8493	0.8411	4.41E-06	1.09032	4.85E+30
662.61	1.0809	1.1226	0.8470	0.8387	6.91E-06	1.085312	7.56E+30
687.61	1.1217	1.1649	0.8449	0.8365	1.06E-05	1.080752	1.16E+31
712.61	1.1625	1.2073	0.8428	0.8343	1.61E-05	1.076585	1.74E+31
737.61	1.2033	1.2496	0.8408	0.8322	2.39E-05	1.072766	2.59E+31
762.61	1.2440	1.2920	0.8388	0.8302	3.50E-05	1.069253	3.78E+31
787.61	1.2848	1.3343	0.8369	0.8282	5.06E-05	1.066013	5.45E+31
812.61	1.3256	1.3767	0.8351	0.8264	7.22E-05	1.063017	7.74E+31
837.61	1.3664	1.4191	0.8334	0.8246	1.02E-04	1.060239	1.09E+32
862.61	1.4072	1.4614	0.8317	0.8228	1.41E-04	1.057658	1.51E+32
887.61	1.4480	1.5038	0.8300	0.8211	1.94E-04	1.055254	2.07E+32
912.61	1.4887	1.5461	0.8285	0.8195	2.64E-04	1.05301	2.81E+32
937.61	1.5295	1.5885	0.8269	0.8179	3.56E-04	1.050912	3.77E+32
962.61	1.5703	1.6308	0.8254	0.8164	4.74E-04	1.048947	5.01E+32
987.61	1.6111	1.6732	0.8240	0.8149	6.26E-04	1.047103	6.61E+32
1012.61	1.6519	1.7155	0.8226	0.8134	8.18E-04	1.04537	8.63E+32
1037.61	1.6927	1.7579	0.8212	0.8120	1.06E-03	1.043738	1.12E+33
1062.61	1.7334	1.8002	0.8199	0.8107	1.37E-03	1.0422	1.44E+33
1087.61	1.7742	1.8426	0.8186	0.8094	1.74E-03	1.040748	1.83E+33
1112.61	1.8150	1.8850	0.8174	0.8081	2.21E-03	1.039375	2.32E+33
1137.61	1.8558	1.9273	0.8162	0.8069	2.78E-03	1.038075	2.91E+33
1162.61	1.8966	1.9697	0.8150	0.8057	3.48E-03	1.036844	3.64E+33

Table D.31: Calculated data for $[\text{Cu}(\text{tftm})]^+$ loss of *t*Bu.

E(kJ)	E'	E^\ddagger	α	α^\ddagger	$\frac{(E^\ddagger + a^\ddagger E_z^\ddagger)^s}{(E + aE_z)^{s-1}}$	$\frac{1}{[1 - \beta \frac{dw}{dE'}]}$	k(E) (sec ⁻¹)
83.894	0.1800	0.1875	0.9461	0.9415	2.62E-04	1.792974	1.29E+32
108.894	0.2336	0.2434	0.9350	0.9296	4.78E-04	1.569714	2.06E+32
133.894	0.2873	0.2993	0.9252	0.9191	8.52E-04	1.442037	3.37E+32
158.894	0.3409	0.3551	0.9164	0.9098	1.48E-03	1.358963	5.50E+32
183.894	0.3946	0.4110	0.9085	0.9013	2.49E-03	1.300488	8.87E+32
208.894	0.4482	0.4669	0.9013	0.8936	4.08E-03	1.257085	1.40E+33
233.894	0.5018	0.5228	0.8947	0.8866	6.50E-03	1.223612	2.18E+33
258.894	0.5555	0.5786	0.8886	0.8801	1.01E-02	1.197039	3.31E+33
283.894	0.6091	0.6345	0.8801	0.8713	1.51E-02	1.208768	4.99E+33
308.894	0.6628	0.6904	0.8753	0.8663	2.24E-02	1.183286	7.28E+33
333.894	0.7164	0.7463	0.8709	0.8616	3.27E-02	1.162764	1.04E+34
358.894	0.7700	0.8021	0.8667	0.8572	4.65E-02	1.145913	1.46E+34
383.894	0.8237	0.8580	0.8628	0.8531	6.51E-02	1.131853	2.02E+34
408.894	0.8773	0.9139	0.8591	0.8492	8.93E-02	1.119962	2.74E+34
433.894	0.9310	0.9698	0.8557	0.8456	1.21E-01	1.109787	3.67E+34
458.894	0.9846	1.0256	0.8524	0.8421	1.60E-01	1.100994	4.84E+34
483.894	1.0382	1.0815	0.8493	0.8388	2.10E-01	1.093328	6.30E+34
508.894	1.0919	1.1374	0.8463	0.8357	2.72E-01	1.086593	8.10E+34
533.894	1.1455	1.1933	0.8435	0.8327	3.48E-01	1.080634	1.03E+35
558.894	1.1992	1.2491	0.8408	0.8299	4.39E-01	1.07533	1.29E+35
583.894	1.2528	1.3050	0.8383	0.8273	5.49E-01	1.070583	1.61E+35
608.894	1.3064	1.3609	0.8358	0.8247	6.79E-01	1.066313	1.98E+35
633.894	1.3601	1.4168	0.8335	0.8223	8.32E-01	1.062454	2.42E+35
658.894	1.4137	1.4726	0.8313	0.8199	1.01E+00	1.058953	2.93E+35
683.894	1.4673	1.5285	0.8291	0.8177	1.22E+00	1.055764	3.52E+35
708.894	1.5210	1.5844	0.8271	0.8156	1.46E+00	1.052848	4.20E+35
733.894	1.5746	1.6403	0.8251	0.8135	1.73E+00	1.050175	4.98E+35
758.894	1.6283	1.6961	0.8233	0.8116	2.04E+00	1.047715	5.85E+35
783.894	1.6819	1.7520	0.8214	0.8097	2.39E+00	1.045447	6.84E+35
808.894	1.7355	1.8079	0.8197	0.8079	2.78E+00	1.043349	7.95E+35
833.894	1.7892	1.8638	0.8180	0.8061	3.22E+00	1.041404	9.19E+35
858.894	1.8428	1.9196	0.8164	0.8044	3.71E+00	1.039597	1.06E+36
883.894	1.8965	1.9755	0.8149	0.8028	4.25E+00	1.037914	1.21E+36
908.894	1.9501	2.0314	0.8134	0.8013	4.84E+00	1.036344	1.38E+36
933.894	2.0037	2.0873	0.8120	0.7998	5.50E+00	1.034876	1.56E+36
958.894	2.0574	2.1431	0.8106	0.7984	6.21E+00	1.033501	1.76E+36
983.894	2.1110	2.1990	0.8092	0.7970	7.00E+00	1.032212	1.98E+36
1008.894	2.1647	2.2549	0.8079	0.7956	7.84E+00	1.031	2.22E+36
1033.894	2.2183	2.3108	0.8067	0.7944	8.76E+00	1.02986	2.47E+36
1058.894	2.2719	2.3666	0.8055	0.7931	9.76E+00	1.028785	2.75E+36

Table D.32: Calculated data for $[\text{Ni}(\text{tftm})]^+$ loss of $t\text{Bu}$.

E(kJ)	E'	E^\ddagger	α	α^\ddagger	$\frac{(E^\ddagger + a^\ddagger E_z^\ddagger)^s}{(E + aE_z)^{s-1}}$	$\frac{1}{[1 - \beta \frac{dw}{dE'}]}$	k(E) (sec ⁻¹)
146.858	0.3181	0.3326	0.9184	0.9111	5.30E-08	1.40168	2.45E+27
171.858	0.3723	0.3892	0.9099	0.9019	1.43E-07	1.331348	6.31E+27
196.858	0.4264	0.4459	0.9022	0.8937	3.65E-07	1.280451	1.55E+28
221.858	0.4806	0.5025	0.8952	0.8861	8.77E-07	1.241922	3.60E+28
246.858	0.5347	0.5591	0.8887	0.8792	1.99E-06	1.21177	7.98E+28
271.858	0.5889	0.6157	0.8827	0.8728	4.30E-06	1.187559	1.69E+29
296.858	0.6430	0.6724	0.8772	0.8669	8.84E-06	1.167717	3.41E+29
321.858	0.6972	0.7290	0.8720	0.8614	1.74E-05	1.151183	6.62E+29
346.858	0.7513	0.7856	0.8672	0.8563	3.29E-05	1.137212	1.24E+30
371.858	0.8055	0.8422	0.8627	0.8515	5.98E-05	1.125268	2.23E+30
396.858	0.8596	0.8988	0.8584	0.8470	1.05E-04	1.114953	3.88E+30
421.858	0.9138	0.9555	0.8544	0.8427	1.79E-04	1.105966	6.54E+30
446.858	0.9679	1.0121	0.8506	0.8387	2.96E-04	1.098076	1.07E+31
471.858	1.0221	1.0687	0.8471	0.8353	4.82E-04	1.091101	1.74E+31
496.858	1.0762	1.1253	0.8440	0.8320	7.56E-04	1.090444	2.73E+31
521.858	1.1304	1.1820	0.8411	0.8289	1.16E-03	1.084067	4.16E+31
546.858	1.1845	1.2386	0.8383	0.8259	1.74E-03	1.078409	6.21E+31
571.858	1.2387	1.2952	0.8356	0.8231	2.56E-03	1.073358	9.08E+31
596.858	1.2929	1.3518	0.8331	0.8204	3.69E-03	1.068826	1.31E+32
621.858	1.3470	1.4084	0.8307	0.8179	5.24E-03	1.06474	1.84E+32
646.858	1.4012	1.4651	0.8284	0.8154	7.30E-03	1.06104	2.56E+32
671.858	1.4553	1.5217	0.8261	0.8131	1.00E-02	1.057677	3.51E+32
696.858	1.5095	1.5783	0.8240	0.8109	1.36E-02	1.054607	4.74E+32
721.858	1.5636	1.6349	0.8220	0.8087	1.82E-02	1.051797	6.32E+32
746.858	1.6178	1.6915	0.8200	0.8067	2.40E-02	1.049216	8.32E+32
771.858	1.6719	1.7482	0.8181	0.8047	3.13E-02	1.046838	1.08E+33
796.858	1.7261	1.8048	0.8163	0.8028	4.04E-02	1.044642	1.39E+33
821.858	1.7802	1.8614	0.8146	0.8010	5.15E-02	1.042609	1.78E+33
846.858	1.8344	1.9180	0.8129	0.7993	6.52E-02	1.040722	2.24E+33
871.858	1.8885	1.9747	0.8113	0.7976	8.17E-02	1.038967	2.81E+33
896.858	1.9427	2.0313	0.8098	0.7960	1.02E-01	1.037331	3.48E+33
921.858	1.9968	2.0879	0.8083	0.7944	1.25E-01	1.035803	4.29E+33
946.858	2.0510	2.1445	0.8069	0.7929	1.53E-01	1.034373	5.24E+33
971.858	2.1051	2.2011	0.8055	0.7915	1.86E-01	1.033033	6.35E+33
996.858	2.1593	2.2578	0.8041	0.7901	2.24E-01	1.031775	7.66E+33
1021.858	2.2134	2.3144	0.8028	0.7888	2.69E-01	1.030592	9.16E+33
1046.858	2.2676	2.3710	0.8016	0.7875	3.20E-01	1.029478	1.09E+34
1071.858	2.3217	2.4276	0.8004	0.7862	3.79E-01	1.028428	1.29E+34
1096.858	2.3759	2.4843	0.7992	0.7850	4.47E-01	1.027436	1.52E+34
1121.858	2.4301	2.5409	0.7981	0.7839	5.23E-01	1.026498	1.78E+34

Table D.33: Calculated data for $[Zn(tftm)]^+$ loss of *t*Bu.

E(kJ)	E'	E^\ddagger	α	α^\ddagger	$\frac{(E^\ddagger + a^\ddagger E_z^\ddagger)^s}{(E + aE_z)^{s-1}}$	$\frac{1}{[1 - \beta \frac{dw}{dE'}]}$	k(E) (sec ⁻¹)
162.189	0.3470	0.3622	0.9154	0.9089	1.34E-08	1.351938	5.97E+26
187.189	0.4005	0.4180	0.9076	0.9006	3.64E-09	1.295557	1.56E+26
212.189	0.4540	0.4738	0.9005	0.8930	1.08E-09	1.253475	4.48E+25
237.189	0.5074	0.5297	0.8939	0.8861	3.46E-10	1.220887	1.39E+25
262.189	0.5609	0.5855	0.8879	0.8797	1.19E-10	1.194932	4.69E+24
287.189	0.6144	0.6413	0.8823	0.8738	4.34E-11	1.173799	1.69E+24
312.189	0.6679	0.6971	0.8771	0.8683	1.69E-11	1.156281	6.46E+23
337.189	0.7214	0.7530	0.8723	0.8632	6.93E-12	1.141545	2.62E+23
362.189	0.7749	0.8088	0.8677	0.8584	2.99E-12	1.128993	1.12E+23
387.189	0.8284	0.8646	0.8635	0.8540	1.35E-12	1.118187	5.01E+22
412.189	0.8818	0.9204	0.8594	0.8497	6.4E-13	1.108799	2.35E+22
437.189	0.9353	0.9763	0.8557	0.8458	3.15E-13	1.100577	1.14E+22
462.189	0.9888	1.0321	0.8521	0.8421	1.62E-13	1.093325	5.85E+21
487.189	1.0423	1.0879	0.8489	0.8389	8.65E-14	1.092914	3.13E+21
512.189	1.0958	1.1437	0.8459	0.8358	4.75E-14	1.08625	1.71E+21
537.189	1.1493	1.1996	0.8431	0.8329	2.69E-14	1.080351	9.61E+20
562.189	1.2027	1.2554	0.8405	0.8301	1.56E-14	1.075096	5.56E+20
587.189	1.2562	1.3112	0.8379	0.8274	9.34E-15	1.070389	3.31E+20
612.189	1.3097	1.3670	0.8355	0.8249	5.71E-15	1.066153	2.01E+20
637.189	1.3632	1.4229	0.8332	0.8225	3.57E-15	1.062322	1.25E+20
662.189	1.4167	1.4787	0.8310	0.8202	2.28E-15	1.058845	7.98E+19
687.189	1.4702	1.5345	0.8288	0.8180	1.49E-15	1.055676	5.18E+19
712.189	1.5237	1.5903	0.8268	0.8158	9.85E-16	1.052778	3.43E+19
737.189	1.5771	1.6462	0.8248	0.8138	6.66E-16	1.05012	2.31E+19
762.189	1.6306	1.7020	0.8230	0.8119	4.57E-16	1.047673	1.58E+19
787.189	1.6841	1.7578	0.8212	0.8100	3.19E-16	1.045416	1.10E+19
812.189	1.7376	1.8136	0.8194	0.8082	2.25E-16	1.043328	7.78E+18
837.189	1.7911	1.8695	0.8178	0.8065	1.62E-16	1.041391	5.57E+18
862.189	1.8446	1.9253	0.8162	0.8048	1.18E-16	1.039591	4.04E+18
887.189	1.8981	1.9811	0.8146	0.8032	8.65E-17	1.037915	2.97E+18
912.189	1.9515	2.0370	0.8131	0.8017	6.44E-17	1.03635	2.21E+18
937.189	2.0050	2.0928	0.8117	0.8002	4.85E-17	1.034887	1.66E+18
962.189	2.0585	2.1486	0.8103	0.7988	3.69E-17	1.033516	1.26E+18
987.189	2.1120	2.2044	0.8090	0.7974	2.84E-17	1.03223	9.68E+17
1012.189	2.1655	2.2603	0.8077	0.7961	2.2E-17	1.031022	7.50E+17
1037.189	2.2190	2.3161	0.8064	0.7948	1.72E-17	1.029884	5.87E+17
1062.189	2.2725	2.3719	0.8052	0.7936	1.36E-17	1.028812	4.63E+17
1087.189	2.3259	2.4277	0.8041	0.7924	1.08E-17	1.0278	3.68E+17
1112.189	2.3794	2.4836	0.8030	0.7912	8.68E-18	1.026843	2.95E+17
1137.189	2.4329	2.5394	0.8019	0.7901	7.02E-18	1.025938	2.38E+17

Table D.34: Calculated data for $[\text{Cu}(\text{tftm})_2]^+$ loss of *tftm*.

E(kJ)	E'	E^\ddagger	α	α^\ddagger	$\frac{(E^\ddagger + a^\ddagger E_z^\ddagger)^s}{(E + aE_z)^{s-1}}$	$\frac{1}{[1 - \beta \frac{dw}{dE'}]}$	k(E) (sec ⁻¹)
692.047	0.7363	0.7497	0.8731	0.8685	9.07E-35	1.135186	4.42E-02
717.047	0.7629	0.7768	0.8709	0.8662	5.41E-34	1.12911	2.62E-01
742.047	0.7895	0.8038	0.8688	0.8640	3.01E-33	1.123475	1.45E+00
767.047	0.8161	0.8309	0.8667	0.8619	1.57E-32	1.118237	7.54E+00
792.047	0.8427	0.8580	0.8647	0.8598	7.70E-32	1.113355	3.68E+01
817.047	0.8693	0.8851	0.8627	0.8578	3.56E-31	1.108798	1.69E+02
842.047	0.8959	0.9122	0.8608	0.8558	1.56E-30	1.104534	7.38E+02
867.047	0.9225	0.9392	0.8590	0.8539	6.46E-30	1.100538	3.05E+03
892.047	0.9491	0.9663	0.8572	0.8521	2.55E-29	1.096785	1.20E+04
917.047	0.9757	0.9934	0.8554	0.8503	9.59E-29	1.093256	4.50E+04
942.047	1.0023	1.0205	0.8537	0.8485	3.45E-28	1.089932	1.62E+05
967.047	1.0289	1.0476	0.8521	0.8468	1.19E-27	1.086797	5.56E+05
992.047	1.0555	1.0747	0.8504	0.8451	3.94E-27	1.083835	1.83E+06
1017.047	1.0821	1.1017	0.8489	0.8435	1.25E-26	1.081034	5.83E+06
1042.047	1.1087	1.1288	0.8473	0.8419	3.85E-26	1.078381	1.78E+07
1067.047	1.1353	1.1559	0.8458	0.8404	1.14E-25	1.075866	5.27E+07
1092.047	1.1619	1.1830	0.8444	0.8389	3.27E-25	1.073479	1.51E+08
1117.047	1.1885	1.2101	0.8429	0.8374	9.07E-25	1.07121	4.17E+08
1142.047	1.2151	1.2371	0.8415	0.8360	2.44E-24	1.069051	1.12E+09
1167.047	1.2417	1.2642	0.8402	0.8346	6.37E-24	1.066996	2.92E+09
1192.047	1.2683	1.2913	0.8388	0.8332	1.62E-23	1.065038	7.41E+09
1217.047	1.2949	1.3184	0.8375	0.8319	4.00E-23	1.063169	1.83E+10
1242.047	1.3215	1.3455	0.8363	0.8306	9.65E-23	1.061385	4.40E+10
1267.047	1.3481	1.3726	0.8350	0.8293	2.27E-22	1.05968	1.03E+11
1292.047	1.3747	1.3996	0.8338	0.8299	6.19E-22	1.058049	2.81E+11
1317.047	1.4013	1.4267	0.8344	0.8288	1.25E-21	1.058737	5.70E+11
1342.047	1.4279	1.4538	0.8334	0.8277	2.76E-21	1.057113	1.25E+12
1367.047	1.4545	1.4809	0.8323	0.8266	5.94E-21	1.055561	2.69E+12
1392.047	1.4811	1.5080	0.8313	0.8256	1.25E-20	1.054078	5.67E+12
1417.047	1.5077	1.5350	0.8303	0.8246	2.59E-20	1.052658	1.17E+13
1442.047	1.5343	1.5621	0.8293	0.8236	5.27E-20	1.051299	2.38E+13
1467.047	1.5609	1.5892	0.8284	0.8226	1.05E-19	1.049996	4.74E+13
1492.047	1.5875	1.6163	0.8274	0.8216	2.06E-19	1.048747	9.29E+13
1517.047	1.6141	1.6434	0.8265	0.8207	3.98E-19	1.047547	1.79E+14
1542.047	1.6407	1.6705	0.8256	0.8198	7.55E-19	1.046395	3.40E+14
1567.047	1.6673	1.6975	0.8247	0.8189	1.41E-18	1.045288	6.34E+14
1592.047	1.6939	1.7246	0.8239	0.8180	2.60E-18	1.044224	1.17E+15
1617.047	1.7205	1.7517	0.8230	0.8171	4.72E-18	1.043199	2.11E+15
1642.047	1.7471	1.7788	0.8222	0.8163	8.44E-18	1.042213	3.78E+15
1667.047	1.7737	1.8059	0.8214	0.8154	1.49E-17	1.041262	6.67E+15

Table D.35: Calculated data for $[\text{Ni}(\text{tftm})_2]^+$ loss of tftm .

E(kJ)	E'	E'^\ddagger	α	α^\ddagger	$\frac{(E^\ddagger + a^\ddagger E_z^\ddagger)^s}{(E + aE_z)^{s-1}}$	$\frac{1}{[1 - \beta \frac{dw}{dE'} E']}$	k(E) (sec ⁻¹)
932.41	0.9908	1.0146	0.8561	0.8482	1.70E-44	1.09019	1.15E-08
957.41	1.0174	1.0418	0.8545	0.8467	1.56E-43	1.093331	1.07E-07
982.41	1.0440	1.0690	0.8531	0.8451	1.31E-42	1.089828	8.88E-07
1007.41	1.0705	1.0962	0.8516	0.8436	1.00E-41	1.086541	6.81E-06
1032.41	1.0971	1.1234	0.8502	0.8422	7.14E-41	1.083451	4.83E-05
1057.41	1.1237	1.1506	0.8489	0.8407	4.72E-40	1.080542	3.18E-04
1082.41	1.1502	1.1778	0.8475	0.8393	2.91E-39	1.077798	1.95E-03
1107.41	1.1768	1.2050	0.8462	0.8380	1.68E-38	1.075207	1.12E-02
1132.41	1.2034	1.2322	0.8449	0.8367	9.08E-38	1.072756	6.08E-02
1157.41	1.2299	1.2594	0.8437	0.8354	4.64E-37	1.070436	3.10E-01
1182.41	1.2565	1.2866	0.8425	0.8341	2.24E-36	1.068236	1.49E+00
1207.41	1.2831	1.3138	0.8413	0.8329	1.03E-35	1.066148	6.83E+00
1232.41	1.3096	1.3410	0.8402	0.8317	4.47E-35	1.064163	2.97E+01
1257.41	1.3362	1.3682	0.8390	0.8305	1.86E-34	1.062275	1.23E+02
1282.41	1.3628	1.3954	0.8379	0.8293	7.37E-34	1.060478	4.88E+02
1307.41	1.3893	1.4226	0.8368	0.8282	2.80E-33	1.058764	1.85E+03
1332.41	1.4159	1.4498	0.8358	0.8271	1.02E-32	1.057129	6.74E+03
1357.41	1.4425	1.4770	0.8347	0.8260	3.58E-32	1.055568	2.36E+04
1382.41	1.4690	1.5042	0.8337	0.8250	1.21E-31	1.054075	7.96E+04
1407.41	1.4956	1.5314	0.8327	0.8239	3.94E-31	1.052648	2.59E+05
1432.41	1.5222	1.5586	0.8318	0.8229	1.24E-30	1.051281	8.14E+05
1457.41	1.5487	1.5858	0.8308	0.8219	3.78E-30	1.049971	2.48E+06
1482.41	1.5753	1.6130	0.8299	0.8210	1.12E-29	1.048715	7.30E+06
1507.41	1.6019	1.6402	0.8289	0.8200	3.20E-29	1.04751	2.09E+07
1532.41	1.6284	1.6674	0.8280	0.8191	8.89E-29	1.046353	5.81E+07
1557.41	1.6550	1.6946	0.8272	0.8182	2.41E-28	1.045241	1.57E+08
1582.41	1.6816	1.7218	0.8263	0.8173	6.35E-28	1.044172	4.14E+08
1607.41	1.7081	1.7490	0.8255	0.8164	1.63E-27	1.043144	1.06E+09
1632.41	1.7347	1.7762	0.8246	0.8155	4.09E-27	1.042154	2.66E+09
1657.41	1.7613	1.8035	0.8238	0.8147	1.00E-26	1.0412	6.51E+09
1682.41	1.7878	1.8307	0.8230	0.8139	2.40E-26	1.040281	1.56E+10
1707.41	1.8144	1.8579	0.8222	0.8130	5.62E-26	1.039395	3.65E+10
1732.41	1.8410	1.8851	0.8215	0.8122	1.29E-25	1.038539	8.36E+10
1757.41	1.8675	1.9123	0.8207	0.8115	2.90E-25	1.037714	1.88E+11
1782.41	1.8941	1.9395	0.8200	0.8107	6.40E-25	1.036917	4.14E+11
1807.41	1.9207	1.9667	0.8192	0.8099	1.38E-24	1.036146	8.96E+11
1832.41	1.9472	1.9939	0.8185	0.8092	2.94E-24	1.035401	1.90E+12
1857.41	1.9738	2.0211	0.8178	0.8085	6.15E-24	1.034681	3.97E+12
1882.41	2.0004	2.0483	0.8171	0.8078	1.26E-23	1.033984	8.15E+12
1907.41	2.0269	2.0755	0.8165	0.8071	2.55E-23	1.03331	1.65E+13

Table D.36: Calculated data for $[\text{Zn}(\text{tftm})_2]^+$ loss of *tftm*.

E(kJ)	E'	E^\ddagger	α	α^\ddagger	$\frac{(E^\ddagger + a^\ddagger E_z^\ddagger)^s}{(E + aE_z)^{s-1}}$	$\frac{1}{[1 - \beta \frac{dw}{dE'}]}$	k(E) (sec ⁻¹)
433.037	0.4628	0.4689	0.9004	0.8975	6.74E-23	1.244223	8.38E+10
458.037	0.4895	0.4960	0.8972	0.8942	2.32E-22	1.227913	2.85E+11
483.037	0.5162	0.5231	0.8940	0.8910	7.66E-22	1.213408	9.29E+11
508.037	0.5429	0.5501	0.8910	0.8879	2.42E-21	1.200428	2.90E+12
533.037	0.5696	0.5772	0.8882	0.8850	7.34E-21	1.188748	8.73E+12
558.037	0.5964	0.6043	0.8854	0.8822	2.14E-20	1.178185	2.52E+13
583.037	0.6231	0.6314	0.8827	0.8794	6.03E-20	1.168591	7.04E+13
608.037	0.6498	0.6584	0.8801	0.8768	1.64E-19	1.15984	1.90E+14
633.037	0.6765	0.6855	0.8776	0.8742	4.29E-19	1.15183	4.94E+14
658.037	0.7032	0.7126	0.8752	0.8718	1.09E-18	1.144472	1.25E+15
683.037	0.7299	0.7397	0.8729	0.8694	2.68E-18	1.137693	3.05E+15
708.037	0.7567	0.7667	0.8706	0.8671	6.42E-18	1.131428	7.26E+15
733.037	0.7834	0.7938	0.8685	0.8648	1.49E-17	1.125624	1.68E+16
758.037	0.8101	0.8209	0.8663	0.8627	3.37E-17	1.120233	3.78E+16
783.037	0.8368	0.8479	0.8643	0.8606	7.44E-17	1.115214	8.29E+16
808.037	0.8635	0.8750	0.8623	0.8585	1.60E-16	1.110532	1.78E+17
833.037	0.8903	0.9021	0.8604	0.8566	3.36E-16	1.106154	3.71E+17
858.037	0.9170	0.9292	0.8585	0.8546	6.90E-16	1.102055	7.60E+17
883.037	0.9437	0.9562	0.8566	0.8528	1.39E-15	1.098208	1.52E+18
908.037	0.9704	0.9833	0.8549	0.8510	2.73E-15	1.094593	2.99E+18
933.037	0.9971	1.0104	0.8531	0.8492	5.27E-15	1.09119	5.74E+18
958.037	1.0238	1.0374	0.8515	0.8476	1.01E-14	1.094292	1.10E+19
983.037	1.0506	1.0645	0.8500	0.8461	1.88E-14	1.09075	2.05E+19
1008.037	1.0773	1.0916	0.8486	0.8446	3.44E-14	1.087427	3.74E+19
1033.037	1.1040	1.1187	0.8471	0.8431	6.19E-14	1.084302	6.71E+19
1058.037	1.1307	1.1457	0.8458	0.8417	1.10E-13	1.08136	1.19E+20
1083.037	1.1574	1.1728	0.8444	0.8403	1.91E-13	1.078586	2.06E+20
1108.037	1.1841	1.1999	0.8431	0.8390	3.29E-13	1.075967	3.53E+20
1133.037	1.2109	1.2270	0.8418	0.8377	5.56E-13	1.073489	5.97E+20
1158.037	1.2376	1.2540	0.8405	0.8364	9.29E-13	1.071144	9.94E+20
1183.037	1.2643	1.2811	0.8393	0.8351	1.53E-12	1.06892	1.63E+21
1208.037	1.2910	1.3082	0.8381	0.8339	2.49E-12	1.066809	2.65E+21
1233.037	1.3177	1.3352	0.8369	0.8327	3.99E-12	1.064803	4.25E+21
1258.037	1.3444	1.3623	0.8358	0.8315	6.34E-12	1.062895	6.73E+21
1283.037	1.3712	1.3894	0.8346	0.8304	9.94E-12	1.061078	1.05E+22
1308.037	1.3979	1.4165	0.8335	0.8293	1.54E-11	1.059346	1.63E+22
1333.037	1.4246	1.4435	0.8325	0.8282	2.37E-11	1.057694	2.50E+22
1358.037	1.4513	1.4706	0.8314	0.8271	3.59E-11	1.056116	3.80E+22
1383.037	1.4780	1.4977	0.8304	0.8260	5.41E-11	1.054607	5.70E+22
1408.037	1.5047	1.5247	0.8294	0.8250	8.05E-11	1.053164	8.48E+22

Table D.37: Calculated data for $[\text{Cu}(\text{tfm}-t\text{Bu})(\text{tfm})]^+$ loss of *tfm*.

E(kJ)	E'	E^\ddagger	α	α^\ddagger	$\frac{(E^\ddagger + a^\ddagger E_z^\ddagger)^s}{(E + aE_z)^{s-1}}$	$\frac{1}{[1 - \beta \frac{dw}{dE'}]}$	k(E) (sec ⁻¹)
447.717	0.7305	0.7515	0.8717	0.8618	5.87E-23	1.138948	3.26E+14
472.717	0.7713	0.7935	0.8683	0.8581	3.63E-24	1.129482	2.00E+13
497.717	0.8121	0.8354	0.8650	0.8546	2.02E-23	1.12104	1.10E+14
522.717	0.8529	0.8774	0.8619	0.8513	1.02E-22	1.113472	5.54E+14
547.717	0.8937	0.9194	0.8589	0.8481	4.73E-22	1.106653	2.55E+15
572.717	0.9345	0.9613	0.8560	0.8451	2.02E-21	1.100482	1.08E+16
597.717	0.9753	1.0033	0.8533	0.8421	7.97E-21	1.094874	4.26E+16
622.717	1.0161	1.0453	0.8507	0.8396	3.00E-20	1.096297	1.61E+17
647.717	1.0569	1.0872	0.8483	0.8371	1.05E-19	1.090821	5.58E+17
672.717	1.0976	1.1292	0.8461	0.8347	3.44E-19	1.085849	1.82E+18
697.717	1.1384	1.1711	0.8440	0.8325	1.07E-18	1.081317	5.63E+18
722.717	1.1792	1.2131	0.8419	0.8303	3.15E-18	1.07717	1.65E+19
747.717	1.2200	1.2551	0.8399	0.8282	8.81E-18	1.073365	4.61E+19
772.717	1.2608	1.2970	0.8380	0.8261	2.36E-17	1.069862	1.23E+20
797.717	1.3016	1.3390	0.8362	0.8242	6.05E-17	1.066628	3.14E+20
822.717	1.3424	1.3810	0.8344	0.8223	1.49E-16	1.063635	7.72E+20
847.717	1.3832	1.4229	0.8327	0.8205	3.53E-16	1.060858	1.83E+21
872.717	1.4240	1.4649	0.8310	0.8187	8.08E-16	1.058275	4.17E+21
897.717	1.4648	1.5069	0.8294	0.8170	1.79E-15	1.055868	9.21E+21
922.717	1.5056	1.5488	0.8278	0.8153	3.84E-15	1.05362	1.97E+22
947.717	1.5464	1.5908	0.8263	0.8137	7.99E-15	1.051516	4.10E+22
972.717	1.5871	1.6327	0.8248	0.8122	1.62E-14	1.049545	8.28E+22
997.717	1.6279	1.6747	0.8234	0.8107	3.19E-14	1.047694	1.63E+23
1022.717	1.6687	1.7167	0.8220	0.8092	6.15E-14	1.045953	3.13E+23
1047.717	1.7095	1.7586	0.8207	0.8078	1.16E-13	1.044313	5.88E+23
1072.717	1.7503	1.8006	0.8194	0.8064	2.12E-13	1.042767	1.08E+24
1097.717	1.7911	1.8426	0.8181	0.8051	3.82E-13	1.041306	1.94E+24
1122.717	1.8319	1.8845	0.8169	0.8038	6.74E-13	1.039925	3.42E+24
1147.717	1.8727	1.9265	0.8157	0.8026	1.17E-12	1.038616	5.91E+24
1172.717	1.9135	1.9685	0.8145	0.8013	1.98E-12	1.037376	1.00E+25
1197.717	1.9543	2.0104	0.8134	0.8002	3.32E-12	1.036199	1.68E+25
1222.717	1.9951	2.0524	0.8123	0.7990	5.45E-12	1.035081	2.75E+25
1247.717	2.0359	2.0943	0.8113	0.7979	8.82E-12	1.034017	4.45E+25
1272.717	2.0766	2.1363	0.8102	0.7968	1.41E-11	1.033004	7.09E+25
1297.717	2.1174	2.1783	0.8092	0.7957	2.21E-11	1.032039	1.11E+26
1322.717	2.1582	2.2202	0.8082	0.7947	3.43E-11	1.031118	1.72E+26
1347.717	2.1990	2.2622	0.8073	0.7937	5.25E-11	1.030239	2.64E+26
1372.717	2.2398	2.3042	0.8063	0.7927	7.94E-11	1.029399	3.98E+26
1397.717	2.2806	2.3461	0.8054	0.7918	1.19E-10	1.028596	5.95E+26
1422.717	2.3214	2.3881	0.8046	0.7909	1.75E-10	1.027827	8.78E+26

Table D.38: Calculated data for $[\text{Ni}(\text{tfm}-t\text{Bu})(\text{tfm})]^+$ loss of *tfm*.

E(kJ)	E'	E^\ddagger	α	α^\ddagger	$\frac{(E^\ddagger + a^\ddagger E_z^\ddagger)^s}{(E + aE_z)^{s-1}}$	$\frac{1}{[1 - \beta \frac{dw}{dE'}]}$	k(E) (sec ⁻¹)
332.474	0.5428	0.5478	0.8913	0.8840	1.01E-17	1.199631	9.43E+16
357.474	0.5836	0.5890	0.8869	0.8794	4.32E-19	1.182325	3.96E+15
382.474	0.6244	0.6302	0.8828	0.8750	1.70E-18	1.167431	1.54E+16
407.474	0.6652	0.6713	0.8789	0.8709	6.24E-18	1.154487	5.59E+16
432.474	0.7061	0.7125	0.8752	0.8669	2.14E-17	1.143143	1.89E+17
457.474	0.7469	0.7537	0.8717	0.8632	6.86E-17	1.133128	6.03E+17
482.474	0.7877	0.7949	0.8684	0.8597	2.08E-16	1.124229	1.81E+18
507.474	0.8285	0.8361	0.8652	0.8563	5.96E-16	1.116274	5.16E+18
532.474	0.8693	0.8773	0.8621	0.8530	1.62E-15	1.109126	1.40E+19
557.474	0.9101	0.9185	0.8592	0.8500	4.21E-15	1.102673	3.60E+19
582.474	0.9510	0.9597	0.8564	0.8470	1.05E-14	1.096823	8.90E+19
607.474	0.9918	1.0009	0.8538	0.8441	2.48E-14	1.091498	2.10E+20
632.474	1.0326	1.0420	0.8513	0.8416	5.75E-14	1.092745	4.87E+20
657.474	1.0734	1.0832	0.8491	0.8392	1.28E-13	1.087555	1.08E+21
682.474	1.1142	1.1244	0.8469	0.8369	2.74E-13	1.082835	2.30E+21
707.474	1.1550	1.1656	0.8448	0.8347	5.68E-13	1.078526	4.75E+21
732.474	1.1958	1.2068	0.8428	0.8326	1.14E-12	1.074578	9.53E+21
757.474	1.2367	1.2480	0.8409	0.8305	2.23E-12	1.07095	1.86E+22
782.474	1.2775	1.2892	0.8390	0.8286	4.25E-12	1.067606	3.52E+22
807.474	1.3183	1.3304	0.8372	0.8266	7.88E-12	1.064516	6.51E+22
832.474	1.3591	1.3716	0.8355	0.8248	1.43E-11	1.061653	1.18E+23
857.474	1.3999	1.4127	0.8338	0.8230	2.53E-11	1.058994	2.08E+23
882.474	1.4407	1.4539	0.8322	0.8213	4.38E-11	1.056518	3.59E+23
907.474	1.4816	1.4951	0.8306	0.8196	7.43E-11	1.054209	6.08E+23
932.474	1.5224	1.5363	0.8290	0.8180	1.24E-10	1.052051	1.01E+24
957.474	1.5632	1.5775	0.8276	0.8164	2.02E-10	1.05003	1.65E+24
982.474	1.6040	1.6187	0.8261	0.8149	3.25E-10	1.048134	2.64E+24
1007.474	1.6448	1.6599	0.8247	0.8134	5.14E-10	1.046353	4.18E+24
1032.474	1.6856	1.7011	0.8234	0.8120	8.01E-10	1.044677	6.49E+24
1057.474	1.7264	1.7423	0.8221	0.8106	1.23E-09	1.043098	9.94E+24
1082.474	1.7673	1.7834	0.8208	0.8093	1.86E-09	1.041607	1.50E+25
1107.474	1.8081	1.8246	0.8196	0.8079	2.77E-09	1.040199	2.24E+25
1132.474	1.8489	1.8658	0.8184	0.8067	4.09E-09	1.038866	3.30E+25
1157.474	1.8897	1.9070	0.8172	0.8054	5.95E-09	1.037603	4.79E+25
1182.474	1.9305	1.9482	0.8161	0.8042	8.57E-09	1.036405	6.89E+25
1207.474	1.9713	1.9894	0.8150	0.8031	1.22E-08	1.035267	9.80E+25
1232.474	2.0122	2.0306	0.8139	0.8019	1.72E-08	1.034186	1.38E+26
1257.474	2.0530	2.0718	0.8129	0.8008	2.40E-08	1.033157	1.92E+26
1282.474	2.0938	2.1130	0.8118	0.7998	3.31E-08	1.032177	2.65E+26
1307.474	2.1346	2.1541	0.8109	0.7987	4.53E-08	1.031243	3.63E+26

Table D.39: Calculated data for $[Zn(tftm-tBu)(tftm)]^+$ loss of *tftm*.

E(kJ)	E'	E [‡]	α	α^{\ddagger}	$\frac{(E^{\ddagger} + a^{\ddagger} E_z^{\ddagger})^s}{(E + aE_z)^{s-1}}$	$\frac{1}{[1 - \beta \frac{dw}{dE'}]}$	k(E) (sec ⁻¹)
391.929	0.6428	0.6609	0.8765	0.8684	2.00E-20	1.168852	3.07E+14
416.929	0.6838	0.7031	0.8725	0.8642	1.05E-21	1.155972	1.59E+13
441.929	0.7248	0.7452	0.8688	0.8603	5.00E-21	1.144662	7.51E+13
466.929	0.7658	0.7874	0.8652	0.8565	2.19E-20	1.134659	3.26E+14
491.929	0.8068	0.8295	0.8618	0.8529	8.84E-20	1.125757	1.31E+15
516.929	0.8479	0.8717	0.8586	0.8495	3.32E-19	1.117788	4.87E+15
541.929	0.8889	0.9138	0.8554	0.8462	1.17E-18	1.11062	1.70E+16
566.929	0.9299	0.9560	0.8525	0.8431	3.84E-18	1.104142	5.56E+16
591.929	0.9709	0.9982	0.8496	0.8401	1.19E-17	1.098262	1.72E+17
616.929	1.0119	1.0403	0.8469	0.8374	3.55E-17	1.099745	5.13E+17
641.929	1.0529	1.0825	0.8445	0.8349	9.99E-17	1.094008	1.43E+18
666.929	1.0939	1.1246	0.8422	0.8325	2.68E-16	1.088805	3.82E+18
691.929	1.1349	1.1668	0.8400	0.8301	6.85E-16	1.084067	9.75E+18
716.929	1.1759	1.2089	0.8379	0.8279	1.68E-15	1.079738	2.38E+19
741.929	1.2169	1.2511	0.8358	0.8258	3.97E-15	1.075768	5.61E+19
766.929	1.2579	1.2933	0.8338	0.8237	9.03E-15	1.072116	1.27E+20
791.929	1.2989	1.3354	0.8319	0.8217	1.98E-14	1.068748	2.78E+20
816.929	1.3399	1.3776	0.8301	0.8197	4.22E-14	1.065632	5.90E+20
841.929	1.3809	1.4197	0.8283	0.8179	8.70E-14	1.062744	1.21E+21
866.929	1.4219	1.4619	0.8265	0.8161	1.74E-13	1.060059	2.43E+21
891.929	1.4629	1.5040	0.8249	0.8143	3.40E-13	1.057559	4.72E+21
916.929	1.5039	1.5462	0.8233	0.8126	6.46E-13	1.055225	8.95E+21
941.929	1.5449	1.5884	0.8217	0.8110	1.20E-12	1.053042	1.66E+22
966.929	1.5859	1.6305	0.8202	0.8094	2.18E-12	1.050998	3.00E+22
991.929	1.6269	1.6727	0.8187	0.8079	3.86E-12	1.049079	5.32E+22
1016.929	1.6679	1.7148	0.8173	0.8064	6.72E-12	1.047275	9.23E+22
1041.929	1.7089	1.7570	0.8159	0.8049	1.15E-11	1.045577	1.57E+23
1066.929	1.7499	1.7991	0.8145	0.8035	1.92E-11	1.043976	2.63E+23
1091.929	1.7910	1.8413	0.8132	0.8022	3.16E-11	1.042465	4.32E+23
1116.929	1.8320	1.8835	0.8120	0.8009	5.11E-11	1.041035	6.98E+23
1141.929	1.8730	1.9256	0.8108	0.7996	8.14E-11	1.039683	1.11E+24
1166.929	1.9140	1.9678	0.8096	0.7983	1.28E-10	1.038401	1.74E+24
1191.929	1.9550	2.0099	0.8084	0.7971	1.98E-10	1.037184	2.69E+24
1216.929	1.9960	2.0521	0.8073	0.7959	3.02E-10	1.036029	4.11E+24
1241.929	2.0370	2.0942	0.8062	0.7948	4.55E-10	1.03493	6.18E+24
1266.929	2.0780	2.1364	0.8051	0.7937	6.77E-10	1.033885	9.19E+24
1291.929	2.1190	2.1785	0.8041	0.7926	9.95E-10	1.032888	1.35E+25
1316.929	2.1600	2.2207	0.8031	0.7916	1.45E-09	1.031938	1.96E+25
1341.929	2.2010	2.2629	0.8021	0.7905	2.08E-09	1.031031	2.82E+25
1366.929	2.2420	2.3050	0.8011	0.7895	2.96E-09	1.030165	4.01E+25

Table C.40: Calculated data for $[\text{Cu}(\text{acac})(\text{tfm})]^+$ loss of $t\text{Bu}$.

E(kJ)	E'	E [‡]	α	α^{\ddagger}	$\frac{(E^{\ddagger} + a^{\ddagger} E_z^{\ddagger})^s}{(E + aE_z)^{s-1}}$	$\frac{1}{[1 - \beta \frac{dw}{dE'}]}$	k(E) (sec ⁻¹)
210.601	0.2728	0.2788	0.9124	0.9088	3.07E-11	1.634564	2.59E+23
235.601	0.3051	0.3118	0.9056	0.9018	6.63E-11	1.545717	5.23E+23
260.601	0.3375	0.3449	0.8993	0.8952	1.40E-10	1.477497	1.04E+24
285.601	0.3699	0.3780	0.8934	0.8891	2.88E-10	1.423437	2.05E+24
310.601	0.4023	0.4111	0.8878	0.8833	5.79E-10	1.379537	3.96E+24
335.601	0.4347	0.4442	0.8825	0.8778	1.14E-09	1.343179	7.48E+24
360.601	0.4670	0.4773	0.8774	0.8726	2.18E-09	1.312582	1.39E+25
385.601	0.4994	0.5104	0.8727	0.8677	4.09E-09	1.286484	2.53E+25
410.601	0.5318	0.5435	0.8681	0.8630	7.49E-09	1.263972	4.5E+25
435.601	0.5642	0.5766	0.8638	0.8586	1.34E-08	1.244362	7.87E+25
460.601	0.5966	0.6097	0.8597	0.8543	2.36E-08	1.227136	1.35E+26
485.601	0.6289	0.6427	0.8557	0.8502	4.07E-08	1.211891	2.27E+26
510.601	0.6613	0.6758	0.8519	0.8463	6.87E-08	1.198312	3.76E+26
535.601	0.6937	0.7089	0.8483	0.8426	1.14E-07	1.186145	6.12E+26
560.601	0.7261	0.7420	0.8448	0.8390	1.86E-07	1.175187	9.78E+26
585.601	0.7584	0.7751	0.8414	0.8356	2.98E-07	1.165271	1.54E+27
610.601	0.7908	0.8082	0.8382	0.8322	4.70E-07	1.15626	2.38E+27
635.601	0.8232	0.8413	0.8351	0.8290	7.29E-07	1.14804	3.64E+27
660.601	0.8556	0.8744	0.8321	0.8260	1.12E-06	1.140513	5.47E+27
685.601	0.8880	0.9075	0.8292	0.8230	1.68E-06	1.1336	8.12E+27
710.601	0.9203	0.9406	0.8264	0.8201	2.50E-06	1.12723	1.19E+28
735.601	0.9527	0.9736	0.8238	0.8174	3.68E-06	1.121346	1.72E+28
760.601	0.9851	1.0067	0.8211	0.8147	5.33E-06	1.115895	2.46E+28
785.601	1.0175	1.0398	0.8187	0.8123	7.74E-06	1.119055	3.54E+28
810.601	1.0499	1.0729	0.8164	0.8100	1.10E-05	1.113526	4.95E+28
835.601	1.0822	1.1060	0.8143	0.8078	1.54E-05	1.108417	6.86E+28
860.601	1.1146	1.1391	0.8122	0.8056	2.15E-05	1.103684	9.4E+28
885.601	1.1470	1.1722	0.8101	0.8036	2.96E-05	1.099288	1.28E+29
910.601	1.1794	1.2053	0.8082	0.8015	4.03E-05	1.095195	1.71E+29
935.601	1.2118	1.2384	0.8062	0.7996	5.44E-05	1.091377	2.28E+29
960.601	1.2441	1.2714	0.8044	0.7977	7.28E-05	1.087808	3.02E+29
985.601	1.2765	1.3045	0.8026	0.7958	9.66E-05	1.084466	3.95E+29
1010.601	1.3089	1.3376	0.8008	0.7940	1.27E-04	1.08133	5.14E+29
1035.601	1.3413	1.3707	0.7991	0.7922	1.66E-04	1.078382	6.62E+29
1060.601	1.3736	1.4038	0.7974	0.7905	2.15E-04	1.075608	8.48E+29
1085.601	1.4060	1.4369	0.7958	0.7889	2.77E-04	1.072992	1.08E+30
1110.601	1.4384	1.4700	0.7942	0.7872	3.54E-04	1.070523	1.36E+30
1135.601	1.4708	1.5031	0.7927	0.7857	4.50E-04	1.068188	1.71E+30
1160.601	1.5032	1.5362	0.7912	0.7841	5.68E-04	1.065978	2.13E+30
1185.601	1.5355	1.5693	0.7897	0.7826	7.12E-04	1.063884	2.64E+30

Table C.41: Calculated data for $[\text{Ni}(\text{acac})(\text{tfm})]^+$ loss of $t\text{Bu}$.

E(kJ)	E'	E^\ddagger	α	α^\ddagger	$\frac{(E^\ddagger + a^\ddagger E_z^\ddagger)^s}{(E + aE_z)^{s-1}}$	$\frac{1}{[1 - \beta \frac{dw}{dE'}]}$	k(E) (sec ⁻¹)
237.243	0.3063	0.3138	0.9064	0.9024	2.24E-11	1.534486	4.57E+22
262.243	0.3386	0.3468	0.9001	0.8959	4.86E-11	1.468426	9.50E+22
287.243	0.3709	0.3799	0.8943	0.8899	1.03E-10	1.415929	1.94E+23
312.243	0.4031	0.4129	0.8888	0.8842	2.13E-10	1.3732	3.90E+23
337.243	0.4354	0.4460	0.8835	0.8788	4.30E-10	1.337746	7.66E+23
362.243	0.4677	0.4791	0.8786	0.8737	8.46E-10	1.307863	1.47E+24
387.243	0.5000	0.5121	0.8739	0.8688	1.63E-09	1.282341	2.78E+24
412.243	0.5322	0.5452	0.8694	0.8642	3.05E-09	1.2603	5.12E+24
437.243	0.5645	0.5782	0.8651	0.8598	5.61E-09	1.241082	9.26E+24
462.243	0.5968	0.6113	0.8611	0.8556	1.01E-08	1.224186	1.64E+25
487.243	0.6291	0.6444	0.8572	0.8516	1.77E-08	1.209221	2.85E+25
512.243	0.6613	0.6774	0.8534	0.8477	3.05E-08	1.195882	4.86E+25
537.243	0.6936	0.7105	0.8498	0.8440	5.16E-08	1.183924	8.14E+25
562.243	0.7259	0.7436	0.8464	0.8405	8.57E-08	1.173147	1.34E+26
587.243	0.7582	0.7766	0.8431	0.8371	1.40E-07	1.163391	2.17E+26
612.243	0.7905	0.8097	0.8399	0.8338	2.24E-07	1.154521	3.45E+26
637.243	0.8227	0.8427	0.8368	0.8306	3.54E-07	1.146425	5.40E+26
662.243	0.8550	0.8758	0.8339	0.8276	5.50E-07	1.13901	8.33E+26
687.243	0.8873	0.9089	0.8310	0.8247	8.41E-07	1.132197	1.27E+27
712.243	0.9196	0.9419	0.8283	0.8219	1.27E-06	1.125917	1.90E+27
737.243	0.9518	0.9750	0.8256	0.8191	1.89E-06	1.120114	2.82E+27
762.243	0.9841	1.0081	0.8230	0.8165	2.78E-06	1.114737	4.12E+27
787.243	1.0164	1.0411	0.8206	0.8141	4.09E-06	1.11789	6.08E+27
812.243	1.0487	1.0742	0.8184	0.8119	5.88E-06	1.112433	8.71E+27
837.243	1.0810	1.1072	0.8163	0.8097	8.36E-06	1.107388	1.23E+28
862.243	1.1132	1.1403	0.8142	0.8075	1.18E-05	1.102713	1.73E+28
887.243	1.1455	1.1734	0.8122	0.8055	1.64E-05	1.098371	2.39E+28
912.243	1.1778	1.2064	0.8102	0.8035	2.26E-05	1.094327	3.29E+28
937.243	1.2101	1.2395	0.8083	0.8015	3.08E-05	1.090554	4.47E+28
962.243	1.2423	1.2726	0.8065	0.7997	4.16E-05	1.087026	6.02E+28
987.243	1.2746	1.3056	0.8047	0.7978	5.58E-05	1.083722	8.05E+28
1012.243	1.3069	1.3387	0.8029	0.7960	7.41E-05	1.080621	1.07E+29
1037.243	1.3392	1.3717	0.8012	0.7943	9.77E-05	1.077706	1.40E+29
1062.243	1.3714	1.4048	0.7996	0.7926	1.28E-04	1.074962	1.83E+29
1087.243	1.4037	1.4379	0.7980	0.7910	1.66E-04	1.072375	2.37E+29
1112.243	1.4360	1.4709	0.7964	0.7894	2.14E-04	1.069931	3.04E+29
1137.243	1.4683	1.5040	0.7949	0.7878	2.74E-04	1.067622	3.89E+29
1162.243	1.5006	1.5370	0.7934	0.7863	3.48E-04	1.065435	4.93E+29
1187.243	1.5328	1.5701	0.7919	0.7848	4.39E-04	1.063362	6.22E+29
1212.243	1.5651	1.6032	0.7905	0.7833	5.52E-04	1.061394	7.80E+29

Table C.42: Calculated data for $[\text{Zn}(\text{acac})(\text{tfm})]^+$ loss of $t\text{Bu}$.

E(kJ)	E'	E [‡]	α	α^{\ddagger}	$\frac{(E^{\ddagger} + a^{\ddagger} E_z^{\ddagger})^s}{(E + aE_z)^{s-1}}$	$\frac{1}{[1 - \beta \frac{dw}{dE'}]}$	k(E) (sec ⁻¹)
214.239	0.2789	0.2853	0.9105	0.9065	1.45E-11	1.621714	2.31E+23
239.239	0.3115	0.3186	0.9038	0.8995	3.19E-11	1.535966	4.83E+23
264.239	0.3440	0.3519	0.8975	0.8929	6.86E-11	1.469824	9.95E+23
289.239	0.3766	0.3852	0.8915	0.8867	1.44E-10	1.417228	2.01E+24
314.239	0.4091	0.4185	0.8859	0.8809	2.95E-10	1.374399	4.00E+24
339.239	0.4417	0.4518	0.8806	0.8754	5.90E-10	1.338851	7.79E+24
364.239	0.4742	0.4850	0.8756	0.8702	1.15E-09	1.30888	1.49E+25
389.239	0.5068	0.5183	0.8708	0.8653	2.19E-09	1.283279	2.78E+25
414.239	0.5394	0.5516	0.8663	0.8606	4.08E-09	1.261166	5.08E+25
439.239	0.5719	0.5849	0.8619	0.8561	7.44E-09	1.241883	9.12E+25
464.239	0.6045	0.6182	0.8578	0.8518	1.33E-08	1.224928	1.60E+26
489.239	0.6370	0.6515	0.8539	0.8477	2.32E-08	1.209911	2.77E+26
514.239	0.6696	0.6848	0.8501	0.8438	3.97E-08	1.196524	4.68E+26
539.239	0.7021	0.7181	0.8464	0.8401	6.66E-08	1.184522	7.79E+26
564.239	0.7347	0.7514	0.8429	0.8365	1.10E-07	1.173706	1.27E+27
589.239	0.7672	0.7847	0.8396	0.8330	1.78E-07	1.163914	2.05E+27
614.239	0.7998	0.8180	0.8364	0.8297	2.84E-07	1.155011	3.24E+27
639.239	0.8323	0.8513	0.8332	0.8265	4.46E-07	1.146886	5.05E+27
664.239	0.8649	0.8846	0.8303	0.8234	6.90E-07	1.139444	7.76E+27
689.239	0.8974	0.9178	0.8274	0.8204	1.05E-06	1.132605	1.17E+28
714.239	0.9300	0.9511	0.8246	0.8175	1.58E-06	1.126303	1.75E+28
739.239	0.9625	0.9844	0.8219	0.8145	2.31E-06	1.120479	2.55E+28
764.239	0.9951	1.0177	0.8192	0.8121	3.46E-06	1.124006	3.84E+28
789.239	1.0276	1.0510	0.8168	0.8097	5.01E-06	1.118083	5.53E+28
814.239	1.0602	1.0843	0.8146	0.8074	7.18E-06	1.112622	7.89E+28
839.239	1.0927	1.1176	0.8124	0.8052	1.02E-05	1.107574	1.11E+29
864.239	1.1253	1.1509	0.8103	0.8030	1.43E-05	1.102896	1.55E+29
889.239	1.1578	1.1842	0.8083	0.8009	1.98E-05	1.098549	2.14E+29
914.239	1.1904	1.2175	0.8063	0.7989	2.71E-05	1.094501	2.93E+29
939.239	1.2229	1.2508	0.8044	0.7969	3.69E-05	1.090724	3.97E+29
964.239	1.2555	1.2841	0.8025	0.7950	4.97E-05	1.087192	5.34E+29
989.239	1.2880	1.3174	0.8007	0.7931	6.65E-05	1.083884	7.11E+29
1014.239	1.3206	1.3506	0.7990	0.7913	8.80E-05	1.080779	9.39E+29
1039.239	1.3531	1.3839	0.7972	0.7895	1.16E-04	1.07786	1.23E+30
1064.239	1.3857	1.4172	0.7956	0.7878	1.51E-04	1.075112	1.60E+30
1089.239	1.4182	1.4505	0.7939	0.7862	1.95E-04	1.072521	2.07E+30
1114.239	1.4508	1.4838	0.7923	0.7845	2.51E-04	1.070074	2.65E+30
1139.239	1.4833	1.5171	0.7908	0.7829	3.20E-04	1.06776	3.38E+30
1164.239	1.5159	1.5504	0.7893	0.7814	4.06E-04	1.06557	4.28E+30
1189.239	1.5484	1.5837	0.7878	0.7799	5.12E-04	1.063493	5.38E+30

Appendix E: NMR Data

Part of the study of metal β -diketonate complexes involved examining their NMR spectra. Due to difficulties in solvating these complexes as well as a lack of variety in deuterated solvents, this area of study was not pursued more. The ^1H NMR spectra of metal β -diketonate complexes that proved to be soluble in deuterated chloroform are included in this appendix. All complexes reported here were synthesized in the research lab by Jennifer Pekar and Dominic Silvestri.

Figure E.1: ^1H NMR Spectrum of $\text{Al}(\text{acac})_3$.

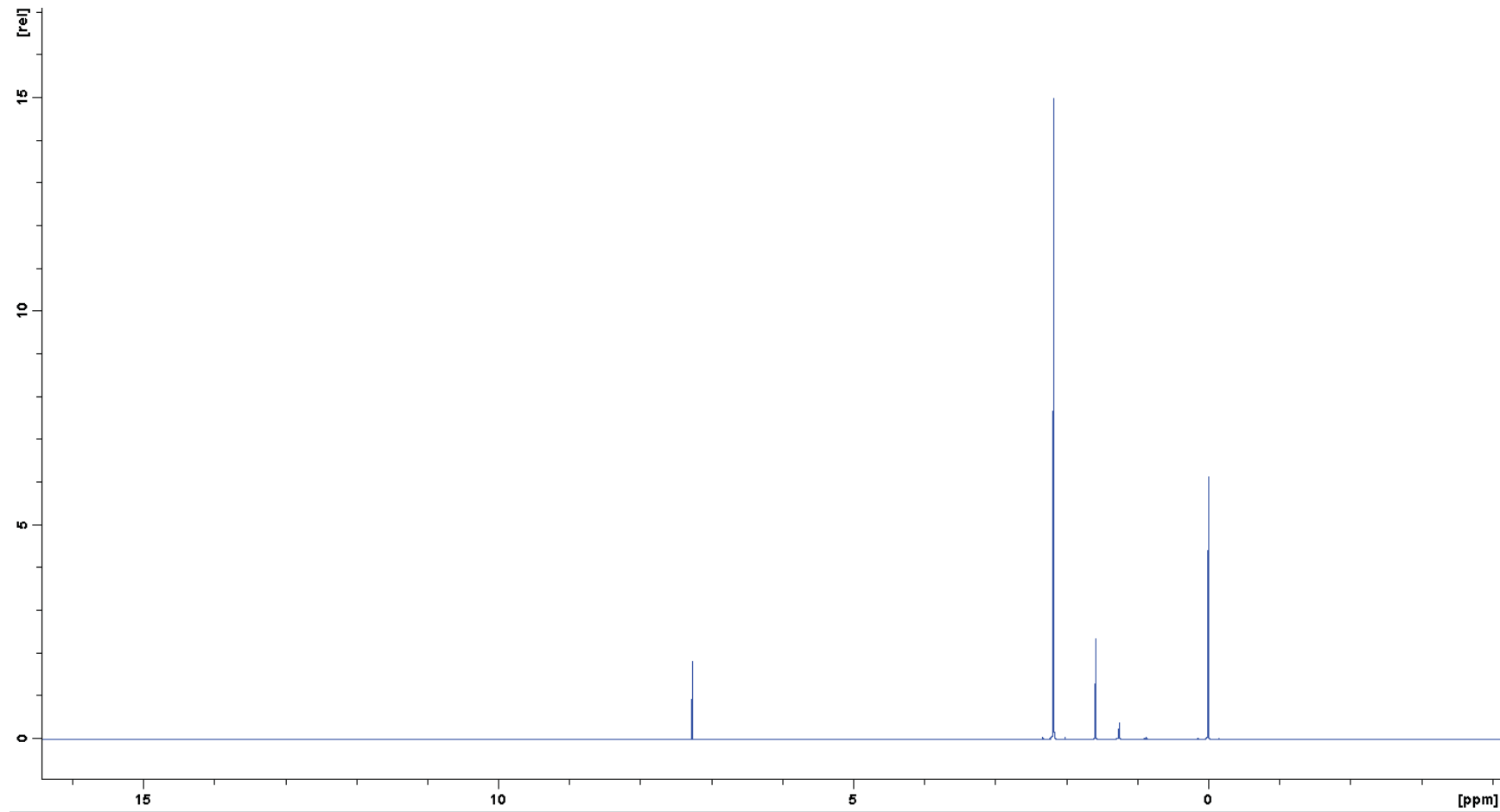


Figure E.2: ^1H NMR Spectrum of $\text{Cu}(\text{acac})_2$.

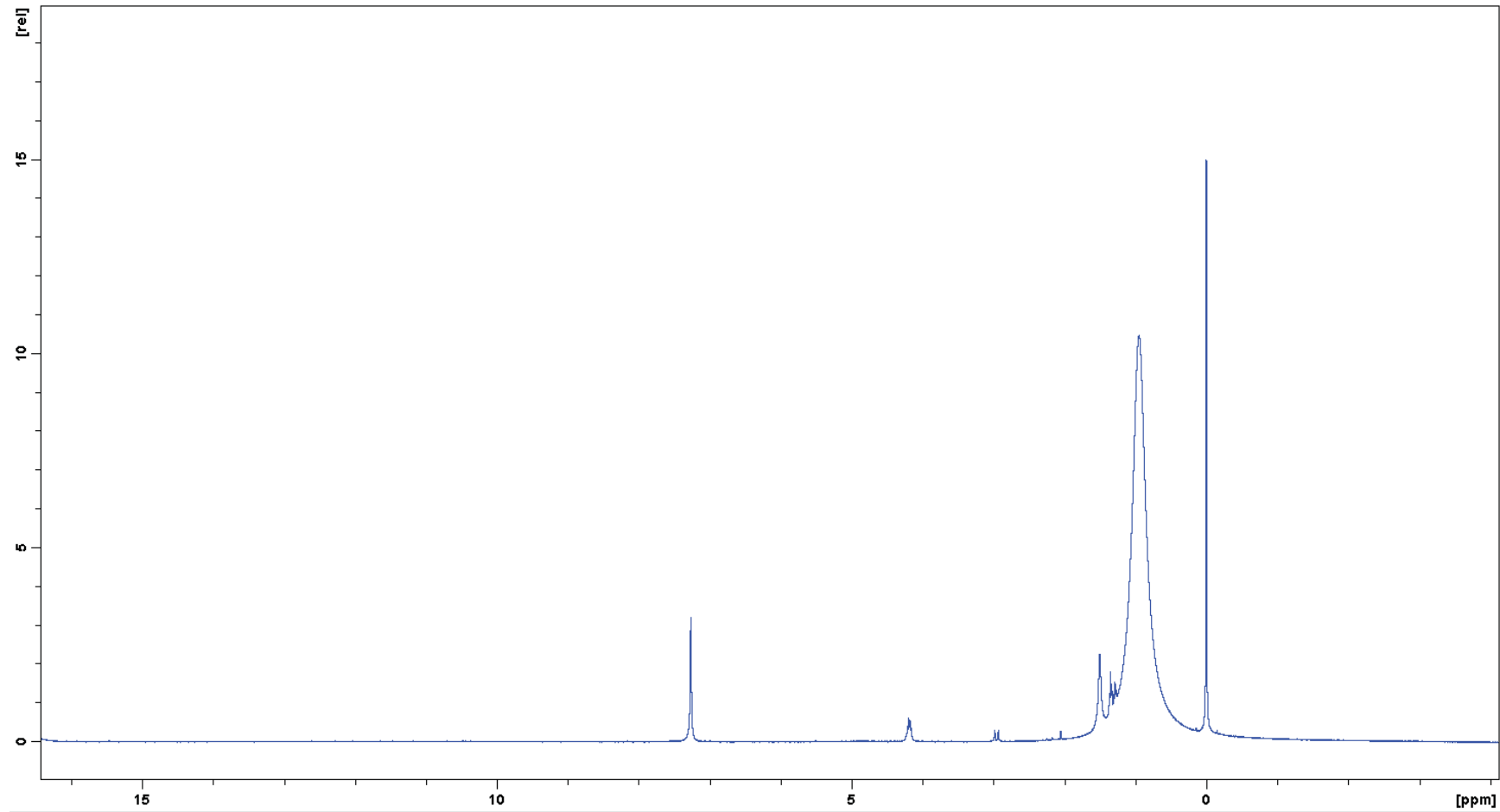


Figure E.3: ^1H NMR Spectrum of $\text{Ni}(\text{acac})_2$.

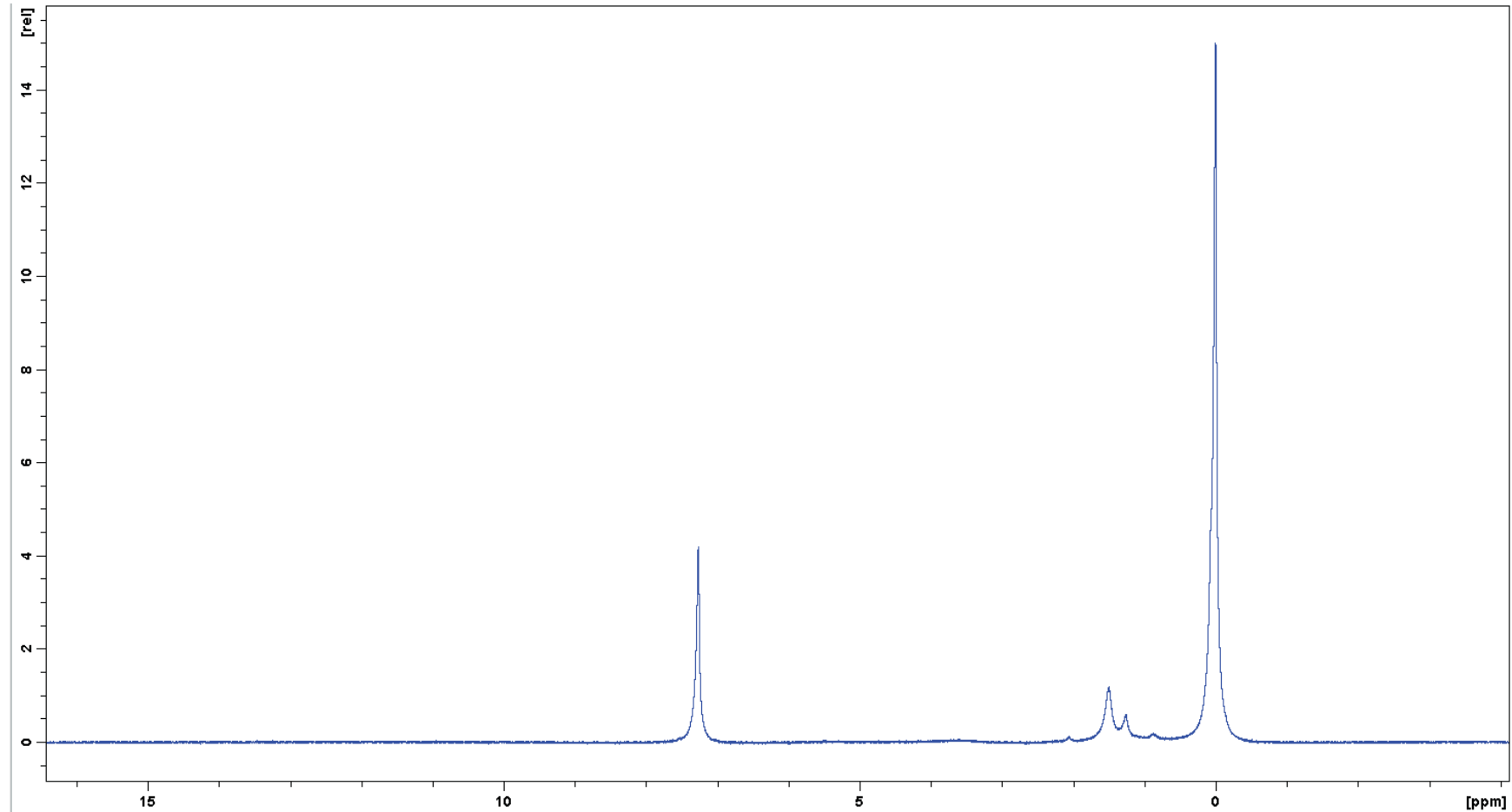


Figure E.4: ^1H NMR Spectrum of $\text{Al}(\text{tftm})_3$.

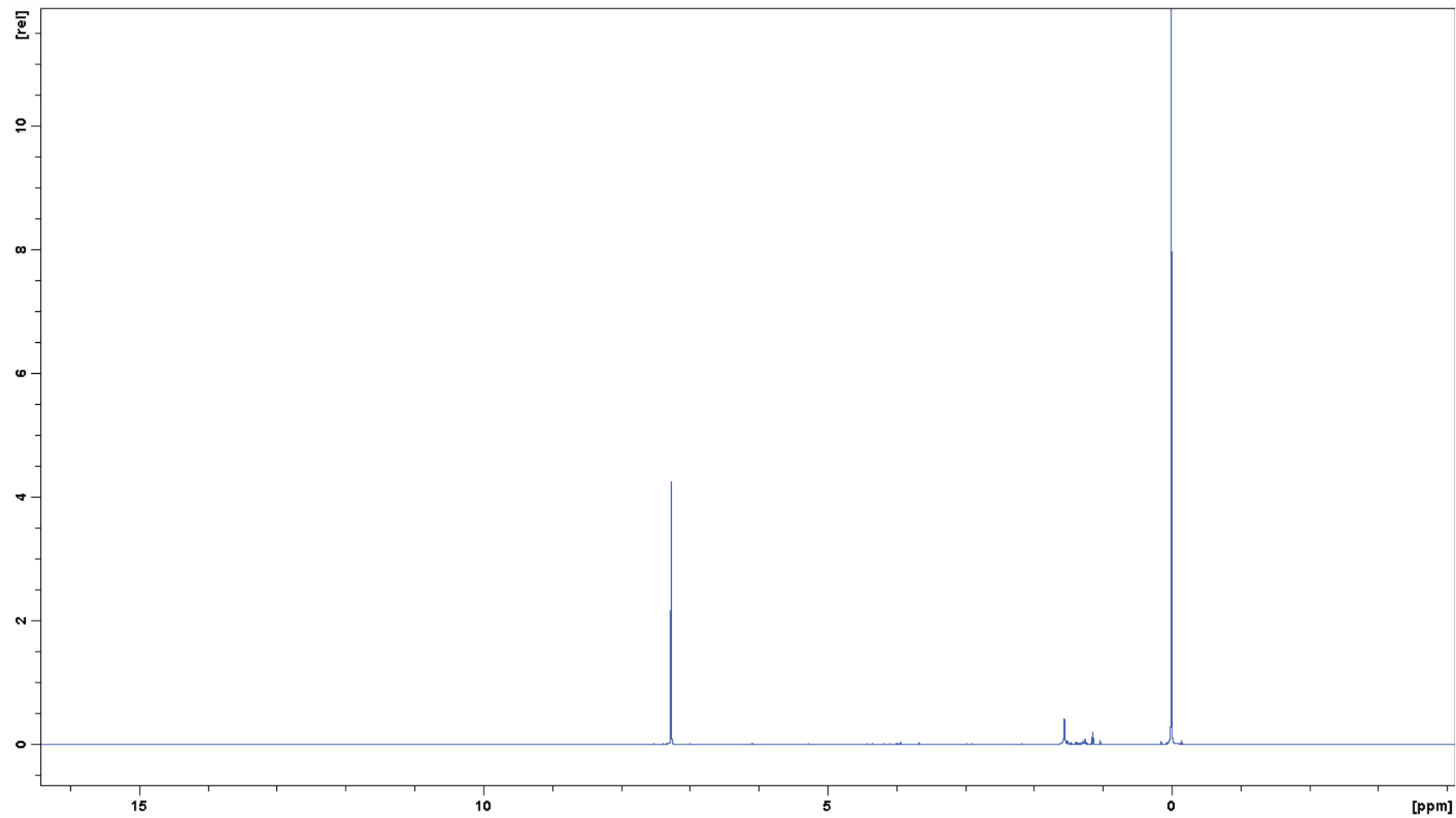


Figure E.5: ^1H NMR Spectrum of $\text{Mg}(\text{tftm})_2$.

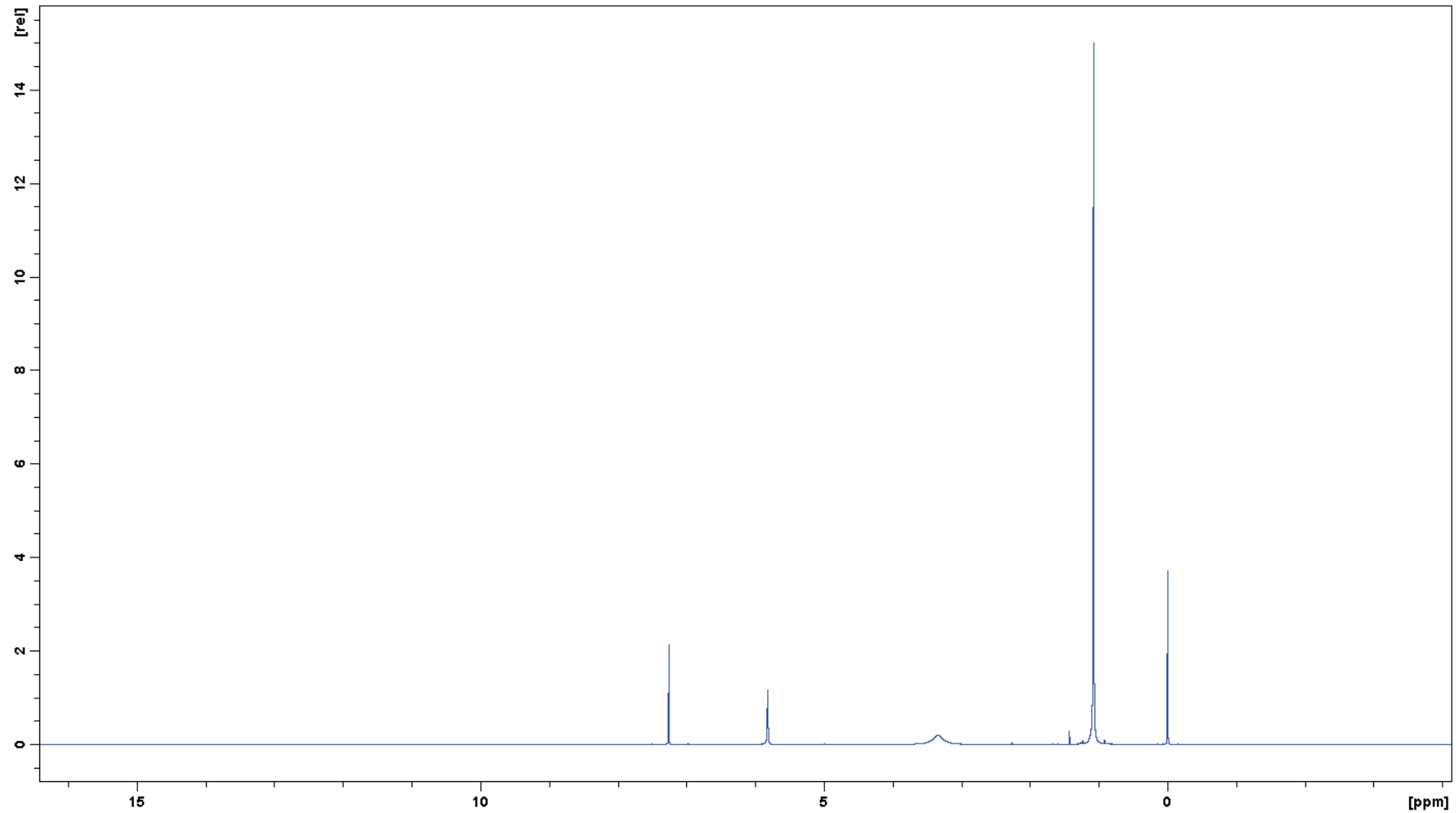


Figure E.6: ^1H NMR Spectrum of $\text{Pd}(\text{tftm})_2$.

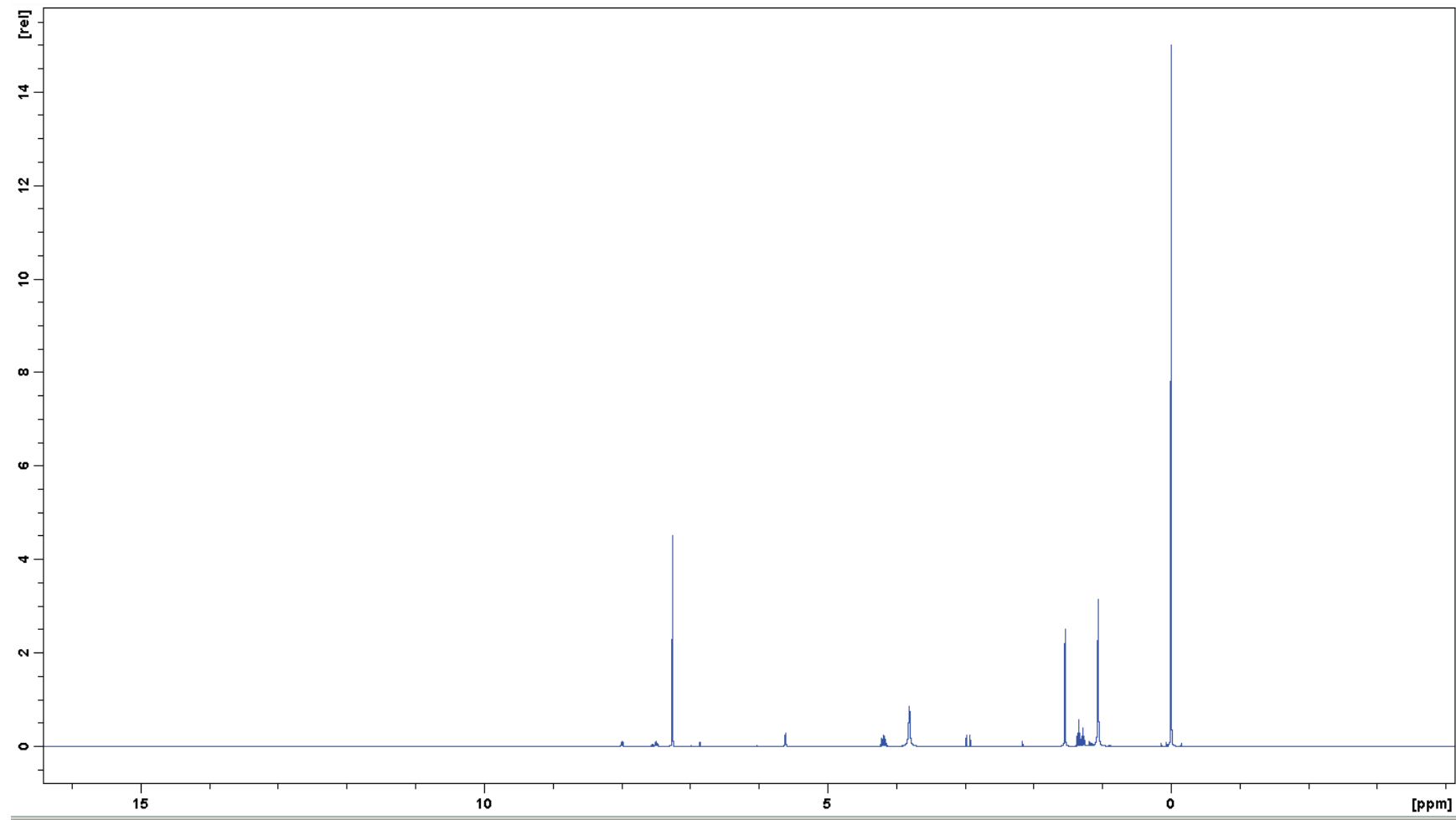


Figure E.7: ^1H NMR Spectrum of Cu(DBM)₂.

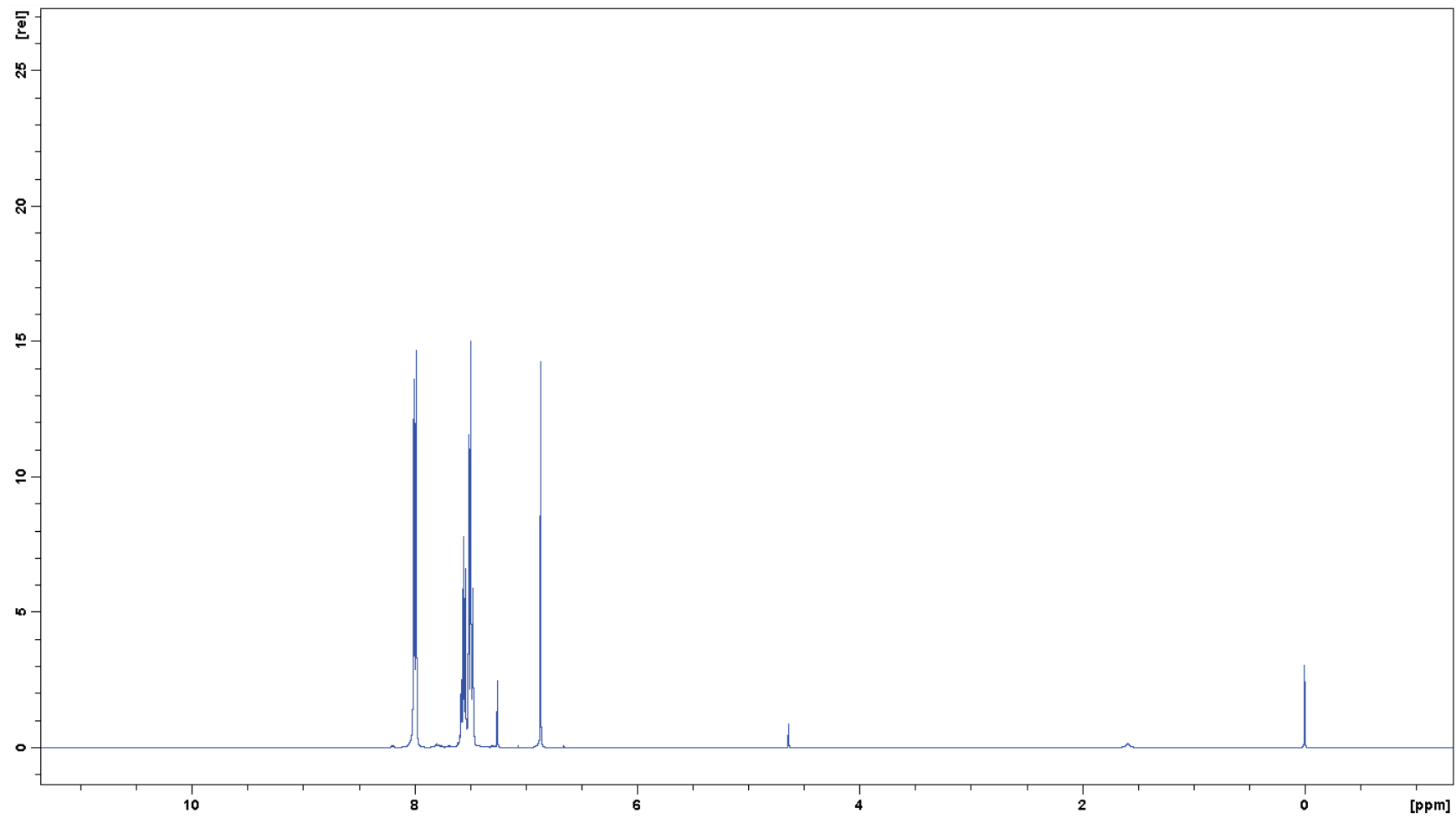


Figure E.8: ^1H NMR Spectrum of Li(DBM).

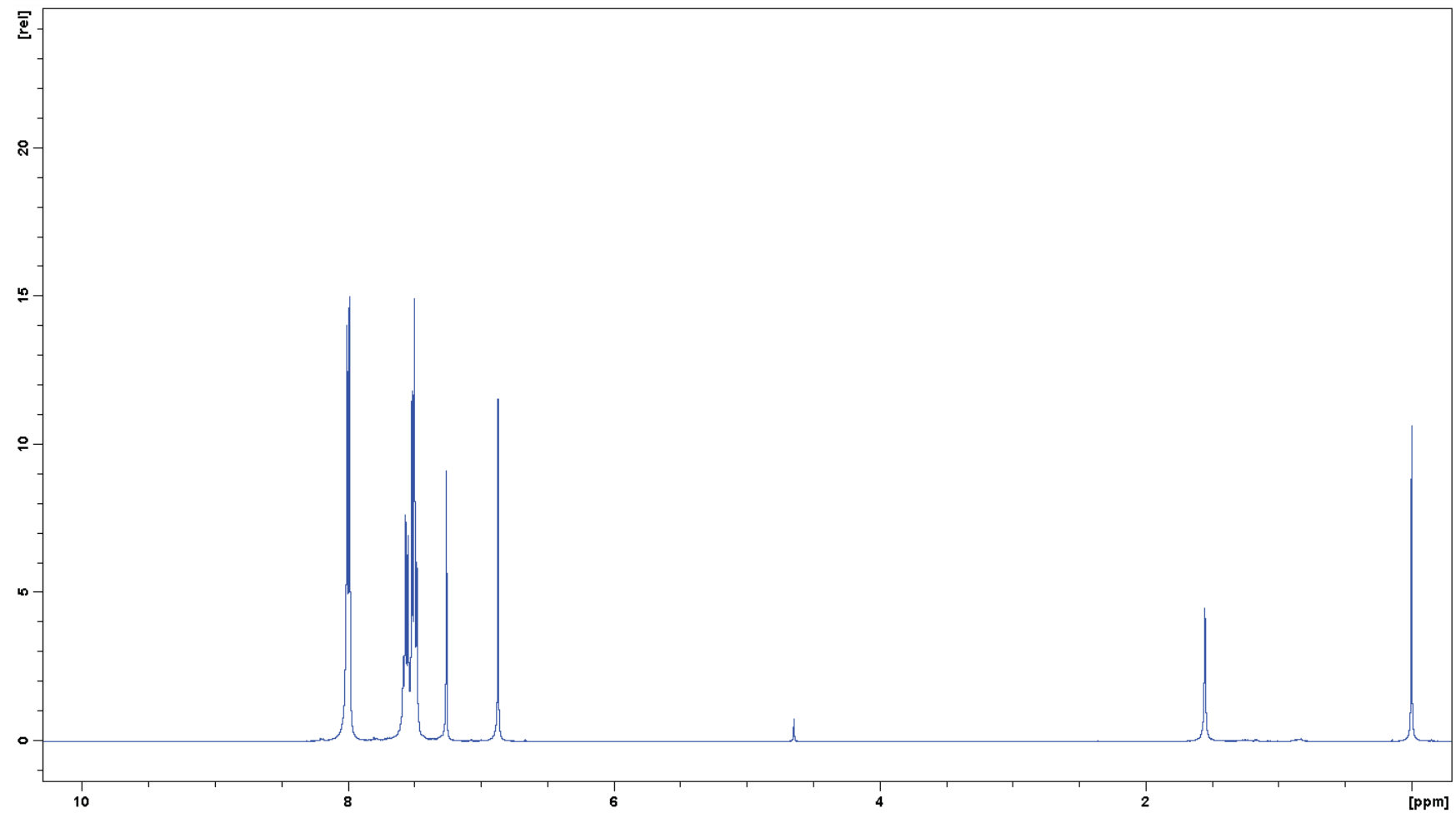


Figure E.9: ^1H NMR Spectrum of $\text{Mg}(\text{DBM})_2$.

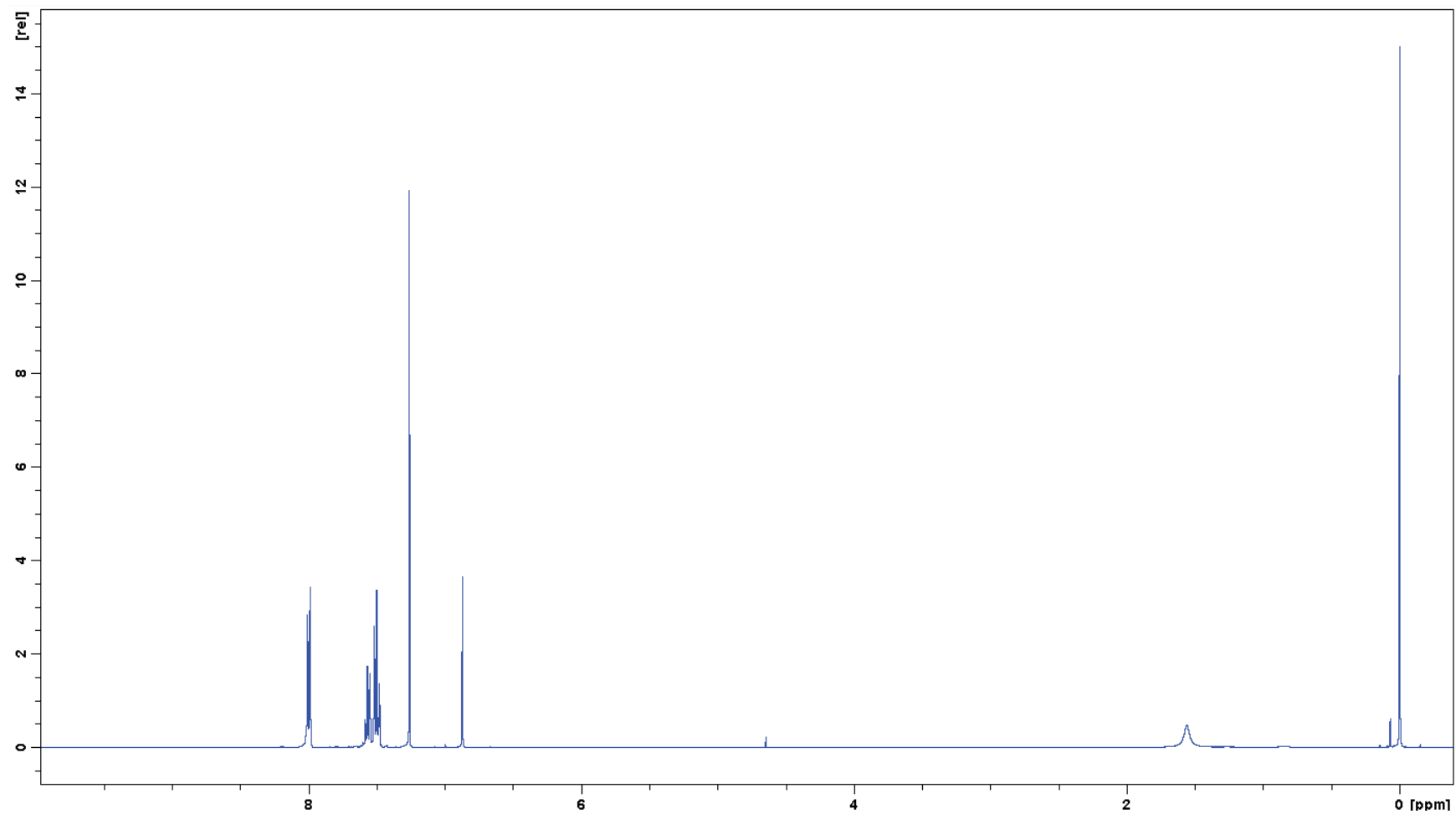
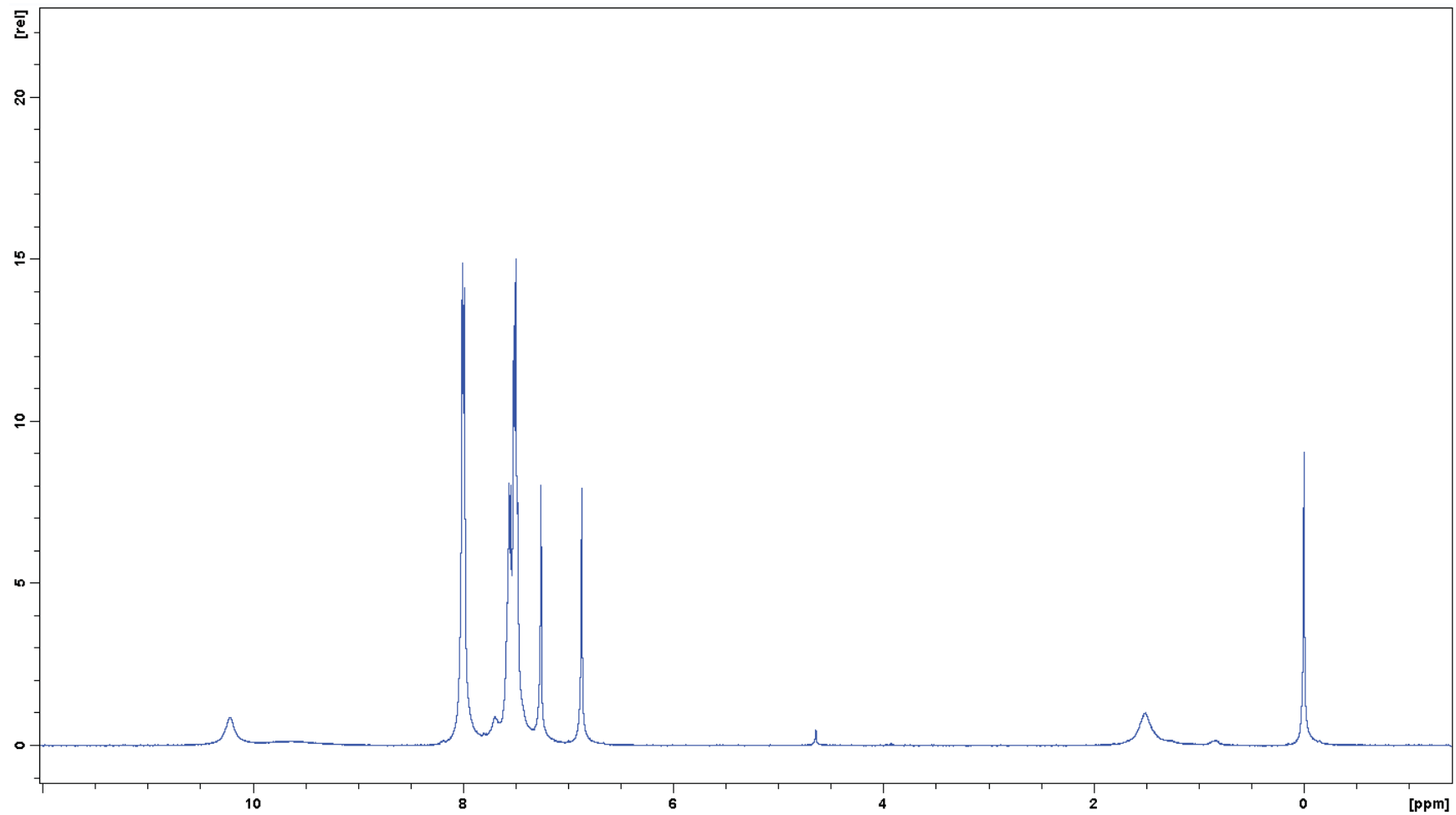
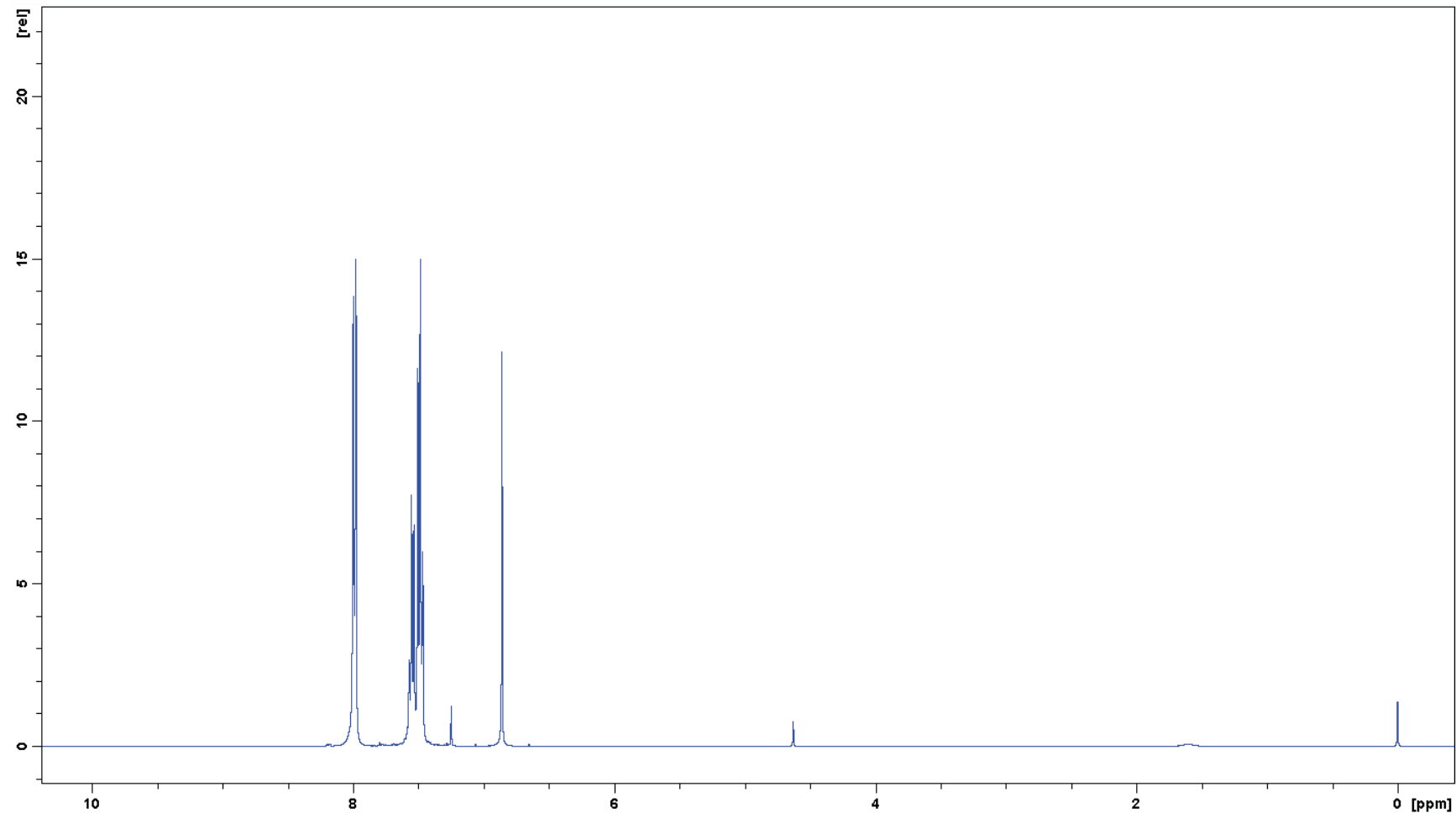


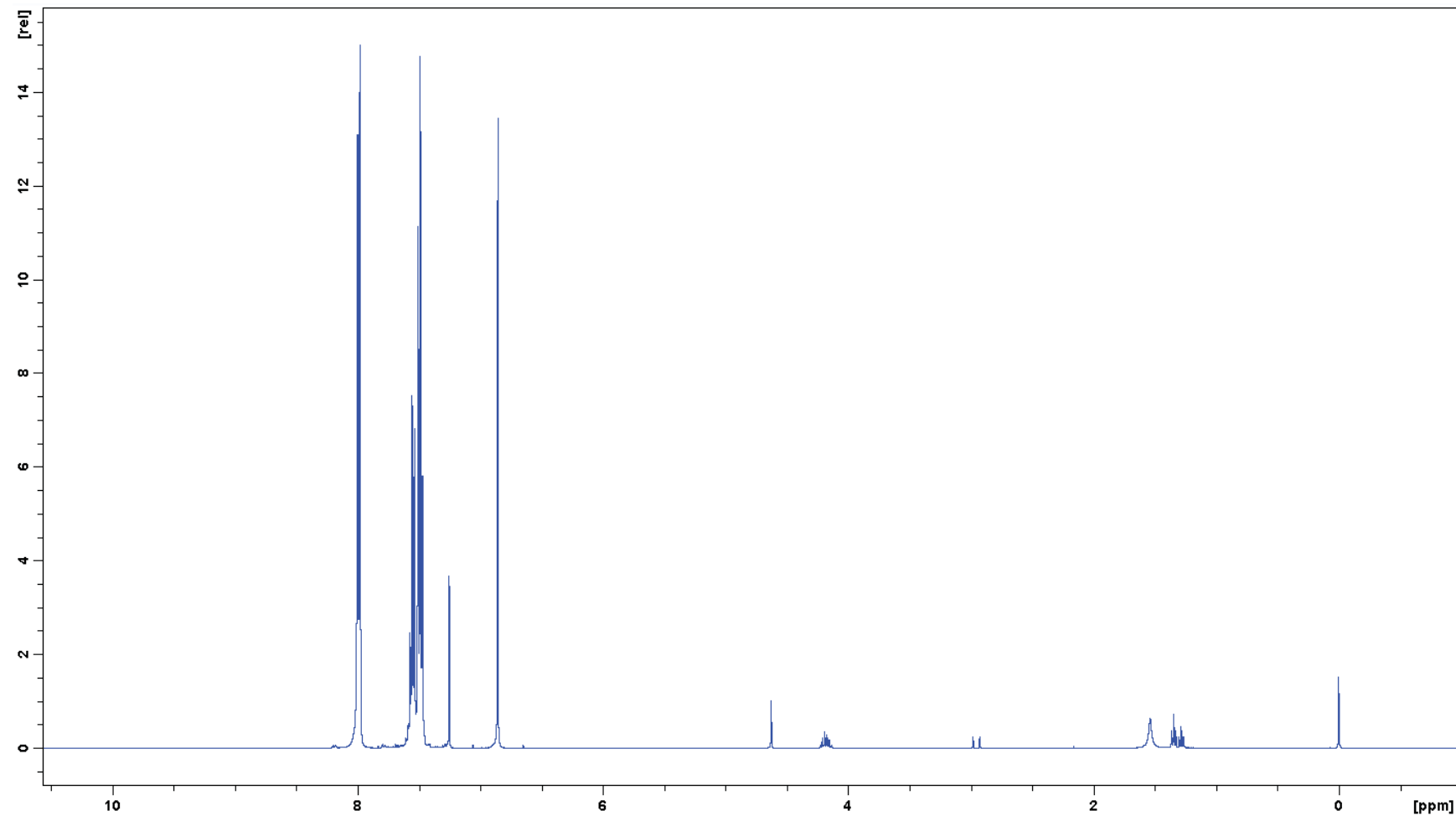
Figure E.10: ^1H NMR Spectrum of $\text{Ni}(\text{DBM})_2$.



E.11: ^1H NMR Spectrum of $\text{Pb}(\text{DBM})_2$.



E.12: ^1H NMR Spectrum of $\text{Pd}(\text{DBM})_2$.



E.13: ^1H NMR Spectrum of $\text{Zn}(\text{DBM})_2$.

